The influence of Low Impact Development on rainfall-runoff relationships at catchment scale

Xinxin Sui

TU Delft

NUS National University of Singapore

The influence of Low Impact Development on rainfall-runoff relationships at catchment scale

by

Xinxin Sui

to obtain the degree of Master of Science
at the Delft University of Technology,
to be defended publicly on Thursday August 29, 2019 at 10:30 AM.

Student number:	4691326	
Project duration:	November 1, 2018 – August 29, 2019	
Thesis committee:	Dr. ir. Frans van de Ven,	TU Delft, supervisor
	Dr. Vladan Babovic,	NUS
	Dr. Markus Hrachowitz,	TU Delft
	Ir. Rikkert, S.J.H.,	TU Delft

This thesis is confidential and cannot be made public until August 29, 2019.

TU Delft

NUS National University of Singapore

Abstract

With the rapid urbanization all over the world, Low Impact Development (LID) is promoted as an alternative to Conventional Drainage (CD), seeking a natural solution for current urban water problems such as water logging and urban flood. The positive effects of LID were the main theme of recent LID research, but this project aims to deeply investigate the impact of LID implementation on extreme peak runoffs on catchment scale including the potential problem caused by more overlap (or stacking) of peak flows from urban and rural areas.

In this research, a catchment in San Antonio City, USA, was selected as a case to study these problems. Precipitation, evaporation and discharge 30-minuate time series data of study catchment and two sub-catchments between 2017-04-12 and 2018-12-02 (600 days) were collected, processed and checked. The first 365 days data of study catchment were utilized to calibrate the parameters, and the last 235 days data were used for verification.

The modelling started from one rural and one urban lumped models for two sub-catchments based on the SUPERFLEX model framework. This framework was used because of its low data requirement and flexible character. Based on the general framework of two lumped models, a rural-urban semi-distributed model is constructed to simulate the current rainfall-runoff relationship of the study catchment. Besides, model expressions of 4 most typical LID practices (bioretention cells, vegetated swales, green roofs, and permeable pavements) were developed under the SUPERFLEX framework. Relevant parameters were determined referring to previous field experiments, empirical parameters and official LID documents.

To deal with the prediction uncertainty, three urban development scenarios for 2040 and five LID implementation scenarios were designed for San Antonio City, based on local urban development plans and LID implementation guidelines. Their influences on the urban and basin peak runoffs were quantitatively studied with the model results.

Research result shows that, without larger water retention capacity, forceful evaporation ability and continuous recharge from groundwater to streamflow, the urban runoff tended to swing between extreme flood and extreme drought in the reference situation;

And next, the infill urban development strategy, which means developing the vacant or undeveloped land within an existing community, was more helpful on peak runoff and total runoff volume control than sprawl urban development strategy with the same population growth. In this research, a full infill development plan, which accommodates 0.9 million more populations (based on the 1.5 million current population in 2017), only increased 2.7% of total runoff volume compared to current situation (in 2017). However for a half-infill and half-sprawl development plan, this number was 14.3%. For the peak runoff, the full infill development plan decreased 4.3% of a typical extreme peak runoff. And the half-infill and half-sprawl development plan increased 16.1% of the peak runoff.

Thirdly, the bioretention cells, vegetated swales, and permeable pavements had similar good performance on peak runoff reduction, which can be mainly ascribe to the stormwater infiltration process. As for the retention of total runoff volume, the bioretention cells, permeable pavements, and green roofs perform better than vegetated swales since the rapid water transportation character of vegetated swales decrease the water residence time for infiltration;

The runoff reduction function of LID practices performs effective on the large peaks in dry and normal seasons, but it will be restrained significantly in flood season. Because the large or extreme large peak runoffs in flood season are also contributed by rural and urban green areas, together with urban grey areas. Since the LID practices only influence the rainfall-runoff relationship of urban grey areas, the peak mitigation effect of LID practices is less obvious for the peaks in flood season than dry and normal seasons;

According to model result, the rural peak runoffs happened 6.5 to 15.5 hours after the urban peaks. And for 4 LID implementation scenarios in which 15% of urban grey areas is covered by LID practices, the urban peaks are delayed between 0.5 and 2.5 hours. And for the scenario with the LID cover areas as 50% of the urban grey areas, the time lag of urban peaks varies from 0.5 to 6.5 hours. For this scenario, since the obvious time delay of urban peaks, more stack

of urban and rural peaks is caused by the time approaching of urban and rural peaks, which causes the increases of two total basin peaks in flood season from 3.57 to 3.65 mm/d and from 6.35 to 6.47 mm/d respectively. In conclusion we may say that the stacking effect of LID implementation on total basin runoff is limited in the case of San Antonio basin, partly due to the fact that only a small part of this basin is urbanized.

Preface

The basic idea of this research topic came from a course, Water Management in Urban Areas, lectured by Dr. ir. Frans van de Ven. In that course, the possible negative effect of Low Impact Development implementation was mentioned. This topic caught my attention, since the valuable and meaningful problems are neglected by most LID researchers. And when I worked on a Sponge City (similar to Low impact development) project in China, my colleagues and I never noticed any risks about LID implementation. Therefore, I chose this topic as my Master graduation project, to fill the research gap and also to meet my own curiosity.

My original intention of this research work comes from curiosity, but more qualities, such as patience when encountering failure and persistence on achieving goals, and honest academic attitude, supported me to complete this project. Progressively, I accumulated the basic research experience as a young researcher. For example, this project was not a smooth sailing and more than half of the six research months was used for trial and error. Every knowledge blind spot stored up trouble for the future and every failed attempt took me back to the starting point. But these failure experiences are precious and fundamental, which taught me more than the successful one.

Although happiness and frustration went together along with my research progress, I really enjoyed these relatively independent and wonderful days in the peaceful and graceful Delft, Netherlands and lively and brilliant Singapore. And I would like to show my great appreciation to the people who give me tremendous amount of support and encouragement, inspiration and guidance, during the two years. Firstly, I would like to show my sincere respect to my main supervisor, Frans van de Ven, who supervised me not only on my project but also on the academic attitude. I think he is a very professional and experienced engineer and also a responsible, conscientious and inspiring mentor. I appreciate this opportunity to learn from him and work with him.

Secondly, I would like to explicitly express my gratitude to the other members of my graduation committee: Vladan Babovic for his kind invitation to Singapore, in which I was provided with this priority to perceive the excellent academic environment in NUS; Markus Hrachowitz for his excellent academic work, which enlightened and guided me on the crucial modelling part of this project; Stephan Rikkert for his scientific discussions and feedback, which inspired me with the rigorous academic attitude.

Then, I would like to express my deepest respect to all the professors who taught or inspired me on both the scientific study and research spirit in TUD: Hubert Savenije, Mark Bakker, Astrid Blom, etc. And I would like to thank all my fellow students, who gave me support and company during these two years, especially the other five members in Sponge City group.

Last but not least, I would like to thank my boyfriend, Allen, and my parents for their unconditional support, care, and love. I cannot own my achievement only to myself. It was their support, care and love, that made it possible for me to come this far.

Xinxin Sui
Singapore, July 2019

Contents

List of Acronyms

CD – Conventional Development

IC – Impervious cover

LID – Low impact development

NSE – Nash Sutcliffe Efficiency

PCSWCM – Bexar County Post-Construction Storm Water Control Measures

QQ plot – Quantile-quantile plot

SAWS - San Antonio Water System

WRC - Water recycling centre

1

Introduction

Since 20th century, urbanization has rapidly developed across the world. Until now half of the world's population is living in urban areas. This rapid urbanization comes at the expense of deforestation and land use changes; large areas of pervious surface are replaced by impervious surface. This dense artificial land use in urban areas greatly influence the natural hydrological processes: Evaporation and transpiration are impaired remarkably with less vegetation interception and less water storage in unsaturated zone, which may lead to urban heat problem; Rainwater infiltration and percolation are significantly reduced by the artificial impervious grey surface; And with less rainwater recharge, the groundwater level decreases, which may lead to more problems such as ground subsidence and collapse. These artificial urbanization activities cut off some essential water processes in natural hydrological cycle and lead to series of water quantity problems in urban areas such as water logging and urban flooding in the rain season, and drought and low groundwater level in dry season.

1.1 Brief introduction of Low Impact Development

Low Impact Development (LID) is promoted as a solution to these urban water problems such as water scarcity, urban flooding, water logging and water quality degradation to replace the Conventional urban Development (CD) approach (Gilroy, 2009; Ahiablame, 2012). The CD approach could be recognized as a disturbance to the natural hydrologic system: Less vegetation and more impervious surface diminish the interception and infiltration process, and therefore more intensive overland flow and flood risk are produced. To reduce urban flood risk, rapid water transfer strategy is adopted in CD (Qin, 2013). Urban water drainage systems are built to collect and convey stormwater to nearby water bodies, centralized municipal facilities or downstream rural areas. This CD approach does not solve water problems, but only shifts the water problems to another place to some extent.

Instead of traditional grey infrastructures such as pipelines and reservoirs, Low Impact Development exploits green blue measures such as bioretention cells and green roofs to mimic the natural hydrologic system by promoting natural water detention and consuming processes including interception, transpiration, infiltration and recharge to groundwater. Compared to the traditional centralized drainage infrastructure, LID practices control the rainwater at the source and at the same time decrease and delay the peak runoff of urban areas after large rainfall events and keep the groundwater level relatively stable (Dietz, 2007; Gilroy, 2009; Bedan, 2009; Ahiablame, 2012).

1.2 Problem statement

Low Impact Development is meant to reduce flood risk of urban areas by decreasing and delaying peak runoff. But when it comes to certain catchments in which the urban areas are located at or close to the outlet of the whole catchment, delaying urban runoff process may bring more overlap (or stacking) of peak runoffs of urban and rural areas, causing higher peak flows and more flooding events downstream as shown in Figure 1.

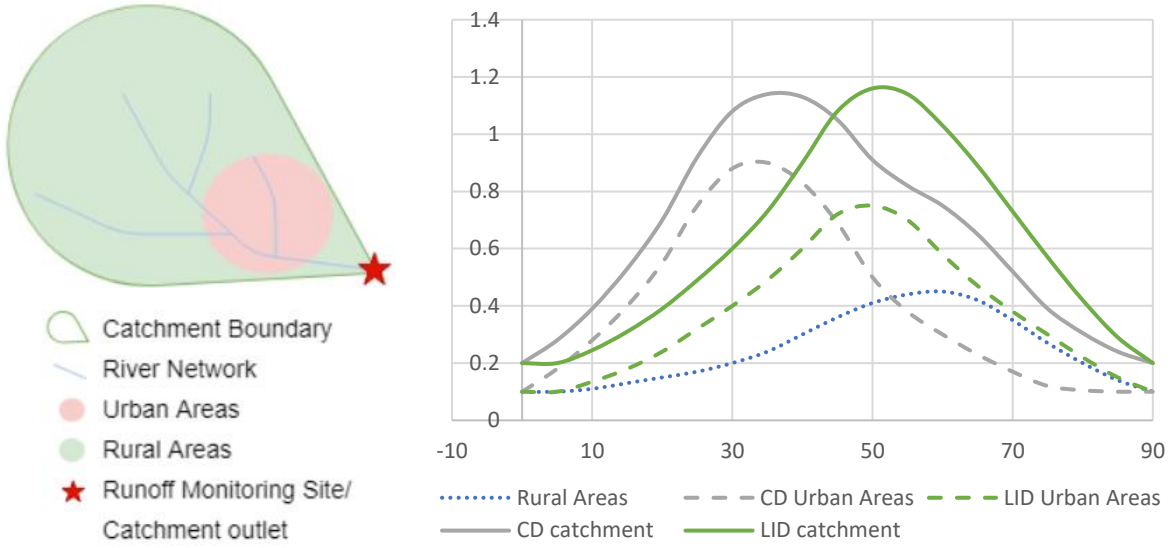

Figure 1. The schematic figures for problem statement. The left figure indicates the type of catchments which may suffer from the delay function of LID implementation. The right figure indicates the runoff progresses of rural, urban and basin areas after one rainfall.

Considering the influence of urbanization, larger urban areas and higher density of impervious surface will bring significant hydrologic influences on the runoff performance with more peak events and higher peak values in the future. Implementation of LID measures is meant to reduce this impact but could lead to stacking of runoff peaks.

The main research problem of this project is to explore the impact of LID implementation with regard to peak runoff value on the catchment scale.

This main question is however followed by several sub-problems:

a. The different hydrologic characters of urban and rural areas;
b. The urbanization influence on rainfall-runoff relationship on catchment scale;
c. The LID implementation influence on rainfall-runoff relationship on catchment scale;
d. The problem caused by the time approaching and stacking of peak flows from urban and rural areas, due to implementation of LID in a partly urbanized drainage basin;

To deal with the prediction uncertainty, scenario analysis of both LID implementation and urban development are to be used to give a reliable answer to the main research question.

1.3 Research approach

In this research, a conceptual semi-distributed model based on SUPERFLEX framework will be exploited to simulate the rainfall-runoff relationship of a study catchment under three different development conditions (a. CD condition; b. Urbanized CD condition; c. Urbanized LID condition).

The case study was introduced in Chapter 2; The conceptual model setup was shown in Chapter 3 and 4; The chapter 5 and 6 focused on scenarios design of urban development condition and LID

implementation; The main research problem and four sub-problems were answered in Chapter 7. The reliability of this research is discussed in Chapter 8. And finally the conclusions and some recommendations are in Chapter 9. The report structure is explained in more detail in Table 1.

Table 1. The storyline of this report

Num.	Heading	Main topics
1	Introduction	The first chapter provides a brief introduction of LID concept, research problems, and research approach.
2	Case study: San Antonio City	The social, natural, and geographical conditions of study catchment are introduced with the urban water management system. And the hydrological data collection is introduced finally.
3	Methodology	In this chapter, three considerations for model selection are states. And then SUPERFLEX framework is introduced. It follows by several important modelling strategies which are the basis of chapter 3.
4	Modelling	The rural and urban lumped models are built for two sub-catchments and then the current rainfall-runoff relationship of study catchment is simulated with the conceptual semi-distributed model. Finally the expressions of four typical LID practices are devised.
5	The urban development forecast and scenario design	The urban development condition of San Antonio City in 2040 is predicted and three urbanization scenarios are designed.
6	The character analysis of LID practises and scenario design	The hydrologic performances of four typical LID practices are analysed and five LID implementation scenarios are designed.
7	Result	Four sub-problems are answered here which answer the main research question together.
8	Discussions	The confidence space and reliable degree of this research are discussed from the aspects of model uncertainty, scenario limitation, and the comparability of this research and literatures.
9	Conclusions and recommendations	The research results are concluded here and several suggestions are supplied for urban development and LID implementation strategies.

2

Case study: San Antonio City

This research used the catchment where San Antonio City (29.424349; -98.491142) locates in to analyse the problems. The background information of research area is introduced here.

The research catchment is part of the catchment of San Antonio River with 4544 km^2. San Antonio City takes around 27% of the whole research catchment with 1209.5 km^2 and located near the outlet of study catchment. Figure 2 shows the locations of study catchment and two sub-catchments. Most areas in these two sub-catchments are rural and urban areas respectively. The river network is also shown in Figure 2. Several rivers and creeks, including San Antonio River, flow through San Antonio downtown and then join with Medina River out of urban area.

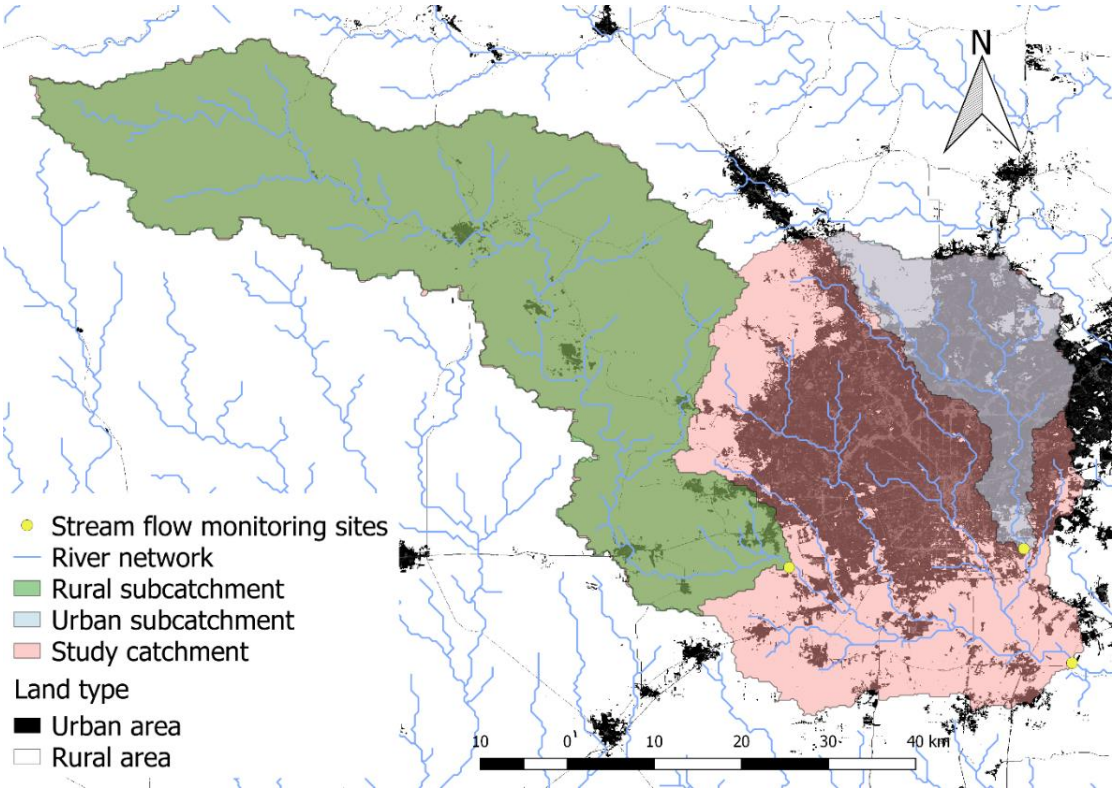

Figure 2. The location of study catchment and two sub-catchments with the stream network

2.1 Social condition

San Antonio city is the seventh most populous city in the U.S., and the second most populous city in Texas state and the Southern United States with more than 1.5 million residents. It was also the fastest-growing of the top ten largest cities in the United States. From 2010 to 2017, San Antonio experienced a population growth rate between 1.5% and 2.0% and still keep a stable growth rate as

shown in Figure 3. With this stable population growth rate of San Antonio City, the urbanization of San Antonio City could be expected to keep in progress.

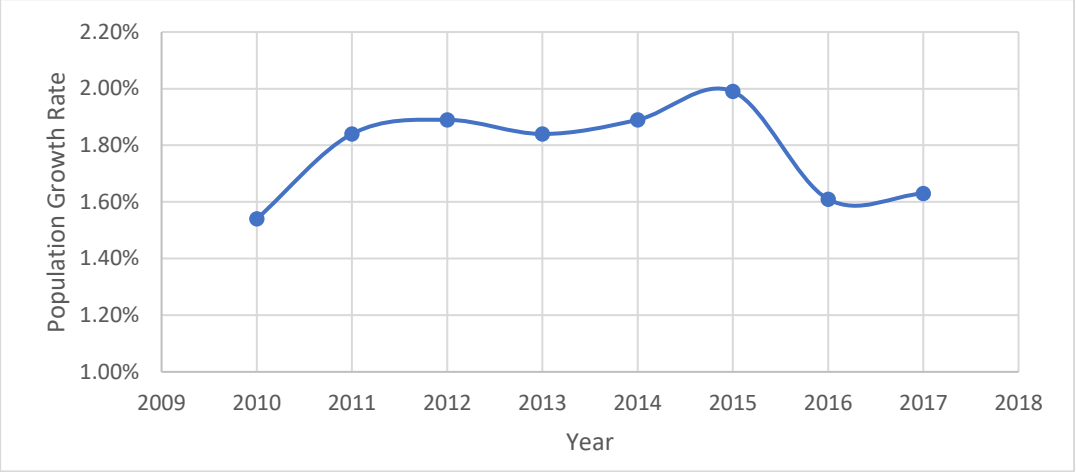

Figure 3. The population growth rate of San Antonio City from 2010 to 2017

Figure 2 shows the urban expansion situation in 2010 which information is provided by NASA. As similar as many other urban centres in the Southwestern United States, most of population concentrates in urban and suburban areas and the areas outside the city limits are sparsely populated.

2.2 Natural and geographical condition

2.2.1 Vegetation

Natural vegetation in the San Antonio area (where undisturbed by development) includes oak-cedar woodland, oak grassland savanna, chaparral brush and riparian (stream) woodland.

2.2.2 Climate

San Antonio has a transitional humid subtropical climate featuring very hot, long, and humid summers and mild to cool winters. San Antonio receives about a dozen subfreezing nights each year, typically seeing snow, sleet, or freezing rain about once every two or three winters, but accumulation and snow itself are very rare. Winters may pass without any frozen precipitation at all, and up to a decade has passed between snowfalls. In San Antonio, July and August tie for the average warmest months, with an average high of 35 °C. The coolest month is January.

May, June, and October have quite a bit of precipitation. Since recording began in 1871, the average annual precipitation has been 737 mm, with a maximum of 1,328 mm and a minimum of 256.8 mm in one year.

2.2.3 Geology

According to the soil survey of Bexar county, the permeability of local soil is moderate. The soil in San Antonio City mainly belong to moderately permeable deep clayey soils and marl. Besides the soil distributes around river bank and occupies bottom lands and low terraces which is deep, calcareous soils in alluvium as shown in Figure 41 in Appendix.

2.2.4 Geohydrology

Edwards Aquifer is the most important groundwater aquifer in study area, which is a prolific aquifer. Edwards Aquifer covers part of the research catchment and provides the urban usage water for people in San Antonio City. It has found that the northwest part of study area is one of the contribution zone to recharge Edwards Aquifer. The distribution area of Edwards Aquifer could be found in Figure 4.

Figure 4. The distribution area of Edwards Aquifer and the location of San Antonio City (Resources: Wikipedia)

2.3 Urban water system

The following information was retrieved from San Antonio Water System (SAWS) website.

SAWS is a public utility owned by the City of San Antonio who responses for city water supply utility and sewage collection and treatment. The water supply of San Antonio City currently dependent on day-to-day pumping from the Edwards Aquifer. To reduce the reliance on the Edwards Aquifer, the diversity of water supply approach is being developed by SAWS.

San Antonio City has separate sewer and stormwater systems. The precipitation collected by stormwater pipeline system in urban areas would be discharged to nearby water body directly without water treatment. And for the wastewater, with a service area of almost 1295 km2, SAWS provides water treatment to people in San Antonio and neighbouring cities. SAWS operates three major water recycling centres (WRCs) in San Antonio, Medio Creek WRC, Leno Creek WRC and Dos Rios WRC, which can be regarded as typical waste water treatment plants. Those treated water is discharged to outfalls on the San Antonio River, Salado Creek, Leon Creek, and Medio Creek. According to the Statistics data shown on SAWS websites, the three WRCs produce a combined volume of tertiary treated recycled water of about 154 km3 per dry year. The wastewater treatment capacity of all SAWS facilities is 338 cubic feet per second with 7563 km sewer lines in the collection system. The plants location, discharge location and service areas of these three Water Recycling Centres are shown in Figure 5.

(All the water discharge locations of the three WRCs are in the study catchment and out of the study urban sub-catchment, which may lead to a water unbalance situation in urban sub-catchment and the inconsistent rainfall-runoff relationships of urban sub-catchment and the whole urban area in study catchment. This problem will be solved by detailed analysis of artificial-caused hydrologic differences

and the adjustment of semi-distributed model structure as explained in 4.2.4 d. The hydrological difference between urban sub-catchment and study catchment)

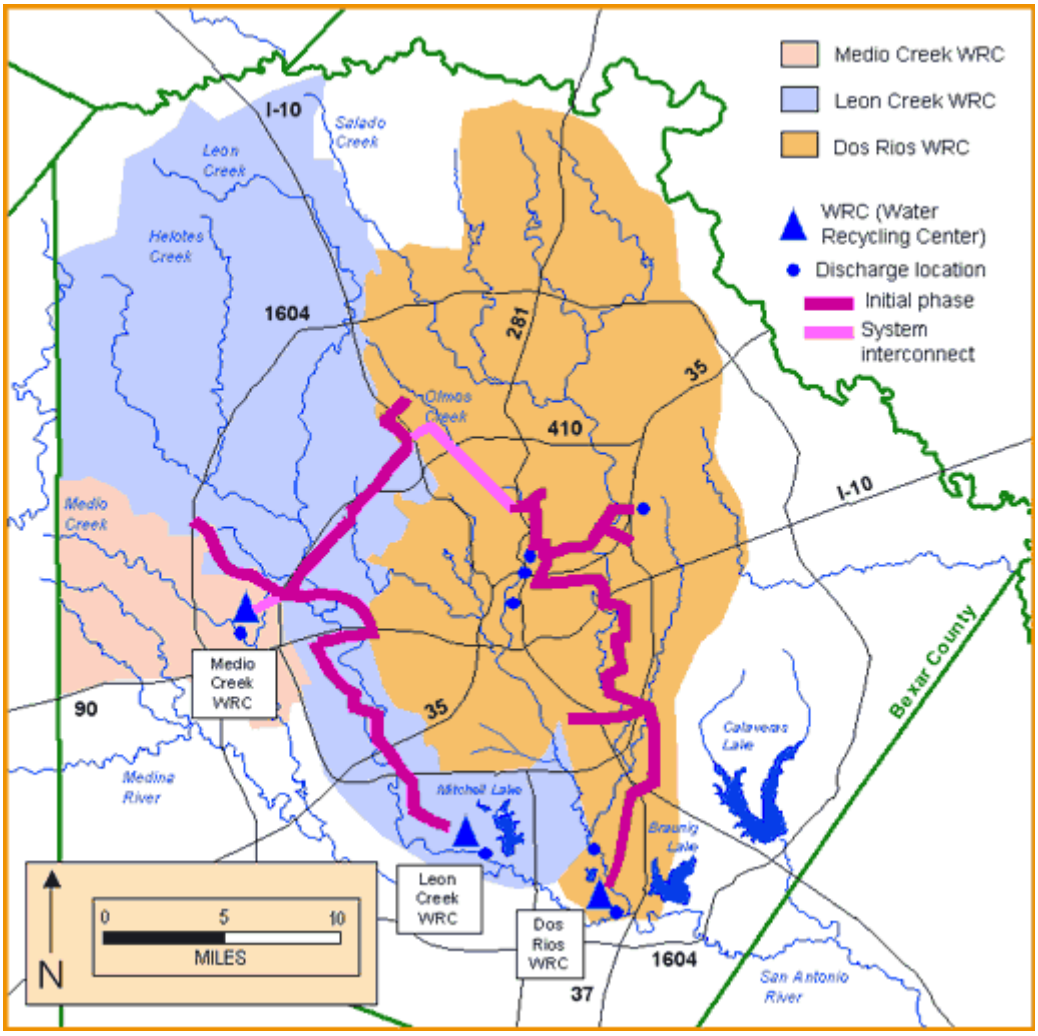

Figure 5. The plants location, discharge location and service areas of three Water Recycling Centres of San Antonio City (Resources: SAWS)

In addition, there is a groundwater recharge project originated with SAWS in north part of San Antonio City. Two types of recharge structures either on or above the recharge zone are exploited in this project. In the contributing zone, storm runoff would be hold back to seep more water into the Edwards Aquifer. And in recharge zone the storm runoff is impounded and allowed to recharge directly into Edwards aquifer.

It's worth noting that in the recharge zone, unofficial infiltration process is restricted in case of groundwater pollution. Since the area of recharge zone is small and most of San Antonio City area locates at the artesian zone, the restriction would not cause a problem when selecting LID practices and the subsoil infiltration of the LID measures is principally allowed in urban areas.

2.4 Hydrological data from the basin

All of the monitoring data come from USGS website.

The available period of the evaporation, precipitation and discharge data is from 2017-04-12 00:00 to 2018-12-02 23:30 (600 days) which is used as the research period. And the available time scale is 30 minutes. Therefore, the total available time-series data number are 28800 (600 days * 24 hours/day * 2/hour) for both calibration and verification period.

2.4.1 Evaporation data

The evaporation data come from a meteorological station (No. 293355098560601) in research area, which is shown as the yellow dot in Figure 6. This meteorological station provides several kinds of necessary raw time-series data to calculate evaporation such as air temperature, wind speed and relative humidity as shown in Figure 7. And the "evapotranspiration" time series data are available to download.

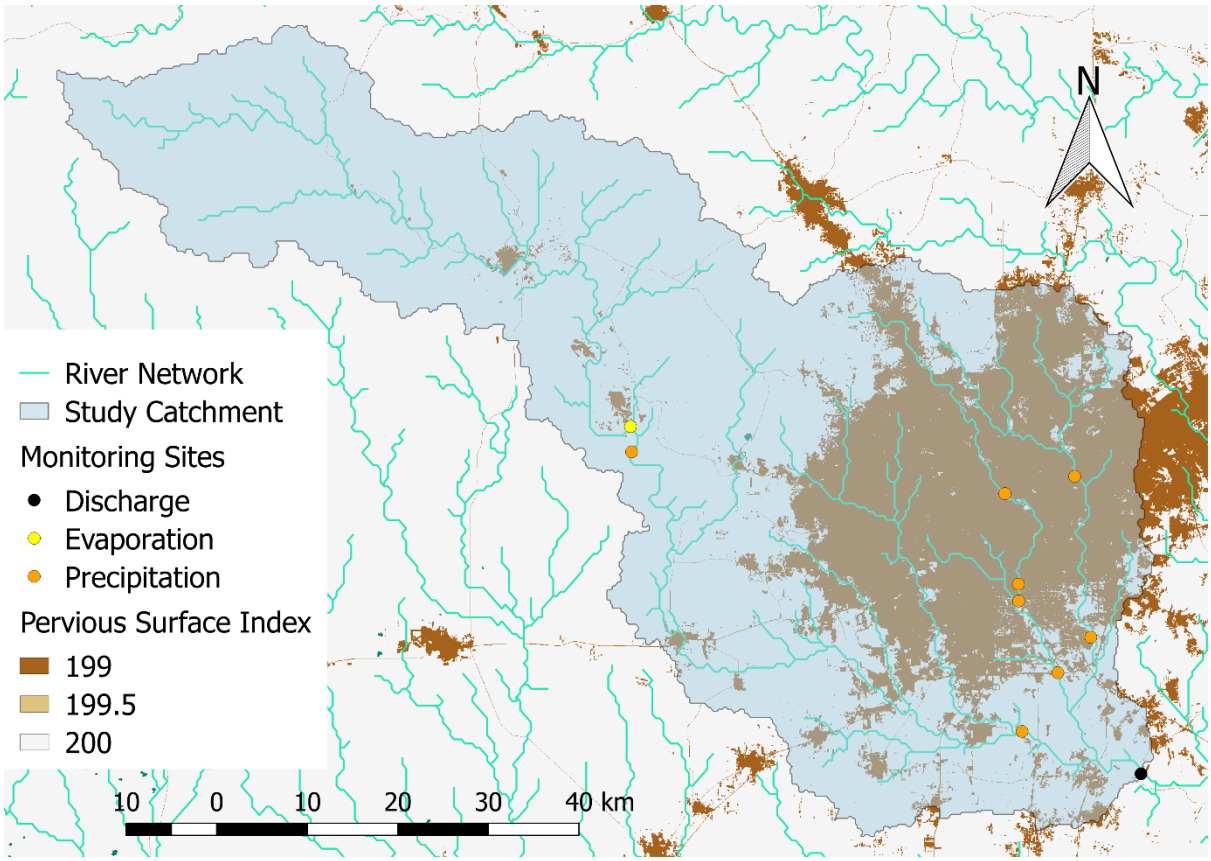

Figure 6. The position of evaporation (yellow dot), precipitation (orange dots) and basin runoff (black) monitoring site

On USGS website, the term "evapotranspiration" is defined as the sum of evaporation and transpiration. But there is no explanation of the estimation method of "evapotranspiration". However, since the latent-heat flux and sensible-heat flux data of this station are also provided, it could be speculated that evapotranspiration is estimated from energy balance equation.

Available Parameters	Available Period
All 11 Available Parameters for this site	
00020 Temperature, air	2017-04-10 2018-12-03
00036 Wind direction	2017-04-11 2018-12-03
00045 Precipitation	2018-10-09 2018-12-03
00052 Relative humidity	2017-04-11 2018-12-03
62607 Atmos. press., uncor	2017-04-11 2018-12-03
62625 Wind speed	2017-04-11 2018-12-03
62968 Latent-heat flux	2017-04-10 2018-12-03
62969 Sensible-heat flux	2017-04-10 2018-12-03
72125 WaterVaporPres, calc	2017-04-11 2018-12-03
72159 Evapotranspiration	2017-04-11 2018-12-03
72192 Precipitation, cumul	2017-04-10 2018-12-03

Figure 7. Available data of meteorological station 293355098560601 on USGS website (Resources: USGS)

2.4.2 Discharge data

The outflow discharge data (in ft^3/s) from three catchments (study catchment and two sub-catchments) are collected from three stream flow monitoring station (No. 08181800, No. 08180700 and No. 08178800) which located at the outlet of the three catchments as the yellow dots in Figure 8. This monitoring station provides discharge data in cubic feet per second since 1986 with 15-minute time scale.

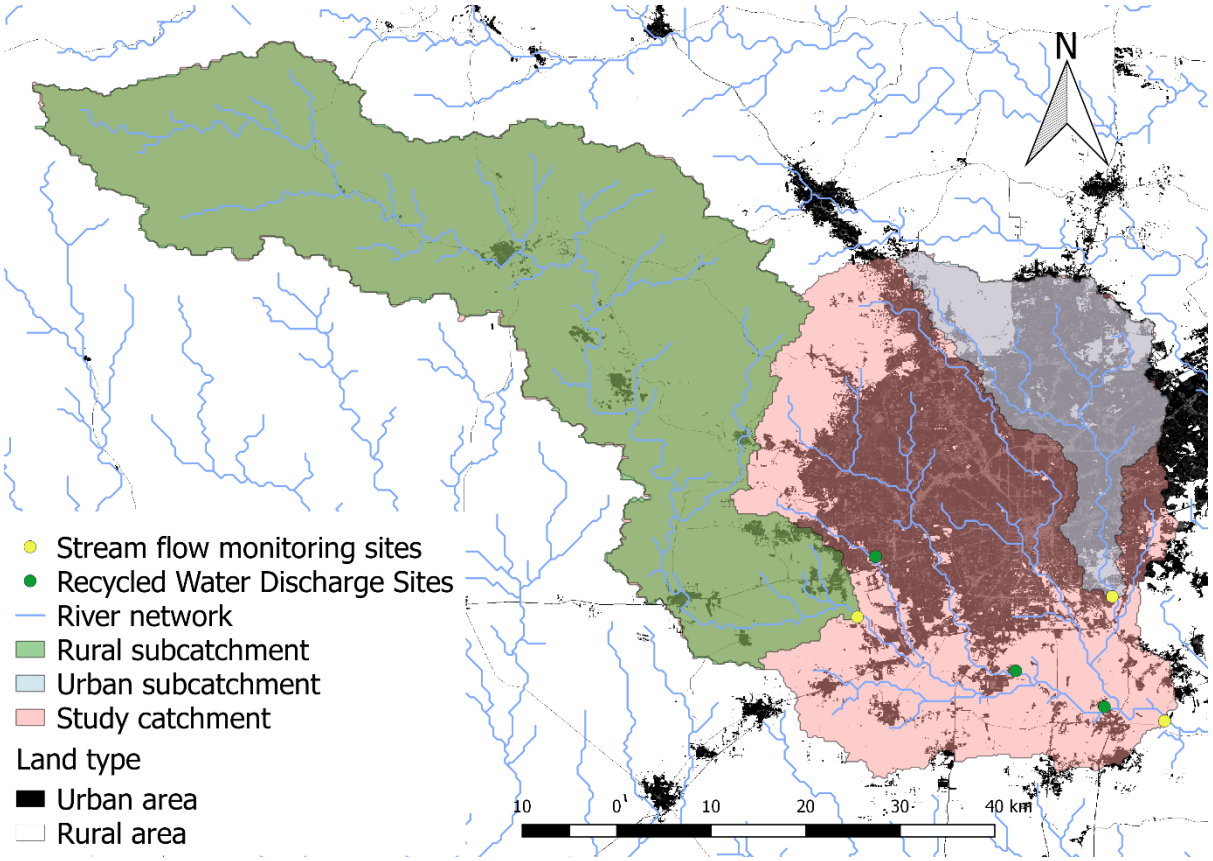

Figure 8. The location of three stream flow monitoring sites

2.4.3 Precipitation data

There are 31 surface water monitoring stations which provide small time-scales (15 minutes) precipitation data in research area. But most of the stations are temporary and only provide for the recent 120 days. Removed these monitoring stations with temporary data, the precipitation data of 10 stations are available during research period, from 2017-04-12 to 2018-12-02. The positions of the 10 stations are shown in Figure 6. And Thiessen polygons are exploited to calculate the weights of each monitoring station to get the total precipitation in this catchment.

The detailed information on the data processing and checking that are used for this study can be found in Appendix C Data processing and checking.

3

Methodology

The first part of this chapter states three considerations when selecting rainfall-runoff model and the reason for selecting SUPERFLEX framework. And then the theoretical development, applications and comments of SUPERFLEX framework are further introduced *in 3.2 The introduction of SUPERFLEX framework*. It follows by three important strategies for model design, parameter calibration and model or model structure selection in this research. Finally the strategy for LID expression under SUPERFLEX framework is shown in *3.4 The expression of LID in model*.

3.1 Rainfall-runoff model selection

Instead of using existing fixed rainfall-runoff models, this research will set up a specific conceptual semi-distributed model by exploiting a relatively novel flexible model framework, SUPERFLEX framework (Fenicia, 2011) to fit the hydrologic condition of study catchment as much as possible. Although SUPERFLEX framework has been used to apply in different topography conditions (eg. plateau, hillslope and wetland), yet this framework has not been exploited to discriminate the hydrologic differences between urban and rural areas.

This conceptual semi-distributed model with SUPERFLEX framework is chosen in this research under three considerations.

3.1.1 Conceptual versus physical-based model:

Since the development of computing power, physical-based models become popular these years with the advantage of representing more realistic hydrological system. However complex model structure and large number of parameters may bring the problems of equifinality and considerable model uncertainty. Besides, the high data requirement of physical-based model is difficult to achieve. Therefore, conceptual model is chosen in this research.

3.1.3 Flexible framework versus fixed model structure:

Flexible framework is chosen in this research to better perform the hydrologic process of study area. Because the flexible framework allows the hydrologist to hypothesize, build, and test different model structures using combinations of generic components to identify the dominant hydrological process in study catchment. Many fixed models are also allowed to add specialized modules to adapt model structure to fit specific catchment conditions. However this interfacing framework is still quiet coarse granularity compared with flexible models which consider hydrological system as a whole (Fenicia, 2011).

3.1.2 Lumped versus distributed model:

Semi-distributed model is used to distinguish the rural and urban areas in this research. Because the main research content is comparing and analysing the rainfall-runoff relationships of urban and rural areas in one catchment. Lumped model cannot distinguish different land use. However semi-distributed model could perform the differences of urban and rural areas effectively. And at the same time it is helpful to reduce the problems (such as equifinality and model uncertainty) caused by too complex distributed models.

3.2 The introduction of SUPERFLEX framework

3.2.1 Theoretical supporting of SUPERFLEX flexible framework

With the development of hydrologic modelling, various of modelling paradigms are developed since last century. The richer model-building paradigms bring a realistic demand of comparing different model structures and parameters (Fenicia et al., 2010). The SUPERFLEX framework (Fenicia et al., 2010) was proposed in 2010, which aims to provide modellers a unified platform to develop, test, compare, specify conceptual model structures. It solves the inflexibility problem of traditional fixed models and can also be used for building tailor-made model structure, testing hypothesis, model evaluation and investigating catchment behaviour.

3.2.2 The foundation and development of SUPERFLEX framework

Fabrizio Fenicia and Hubert H. G. Savenije firstly proposed the concept of FLEX framework in 2006. FLEX (Flux Exchange) model (Fenicia et al., 2006) is more like a relatively complete hydrologic model for direct application rather than an operable framework. FLEX model has mature model structure with four reservoirs: interception reservoir (IR), unsaturated soil reservoir (UR), fast reacting reservoir (FR), and slow reacting reservoir (SR).

In 2008, the Framework for Understanding Structural Errors (FUSE) (Clark et al., 2008) was developed by combining components of 4 existing hydrological models: PRMS, SACRAMENTO, TOPMODEL and ARNO/VIC model. FUSE allows more flexibility in the model architecture but it remain restricted to a two-layer hypothesis of the soil store.

In 2011, SUPERFLEX multi-hypothesis framework was promoted as an extension to the earlier FLEX framework by Fabrizio Fenicia, Dmitri Kavetski and Hubert H. G. Savenije (Fenicia et al., 2010). This systematic and robust platform with flexible generic components shares the same idea of the flexible model paradigm with FUSE and allows broader and more thorough exploration of the model hypothesis space (Fenicia et al., 2010). Dmitri Kavetski examined the potential of SUPERFLEX framework with respect to systematic and stringent hypothesis-testing by applying seven SUPERFLEX configuration models to four hydrologically distinct experimental catchments in a companion paper (Kavetski et al., 2010).

3.2.3 The applications and comments of SUPERFLEX framework

a. Application of SUPERFLEX framework

Although cited many time as an typical example of flexible framework of conceptual model, SUPERFLEX framework is far from being widely used in hydrologic modelling. However among the few relevant articles, several prominent models are designed to fit different field conditions based on SUPERFLEX or FLEX framework:

Savenije promoted FLEX-Topo model which is a semi-distributed model with topography as common control factor (Savenije, H. H. G., 2010). FLEX-Topo is one of the most practical branching models of FLEX model, and is always applicated in European study watershed. Besides, the DYNAMIT (DYNAmic MIxing Tank) model is promoted by Hrachowitz, which is loosely based on FLEX model with the temporal water process dynamics (M.Hrachowitz, 2014). In addition, Structure for Unifying Multiple Modeling Alternatives (SUMMA) model provides a unified approach to process-based hydrologic modelling with the combination of thermodynamics and hydrology (Clark et al., 2015). Furthermore, FLEXG model is a glacier hydrological model, integrated snow and glacier accumulation and ablation processes (Gao et al., 2018). The SUPERFLEX framework-based model sometimes was also combined with hydraulic model as the output of SUPERFLEX model could be the input of a hydraulic model like Lisflood-FP (Hostache, Renaud et al., 2018).

b. Comments of SUPERFLEX framework

There was a high consistency of the positive comments on SUPERFLEX framework: SUPERFLEX framework could provide modellers a platform to develop, test, compare, and specify tailor-made model structures (Hrachowitz et al., 2013; Weiler et al., 2015; Broderick et al., 2016; Beck et al., 2017). And without the inflexible drawback of traditional fixed model, SUPERFLEX framework has the advantage in model evaluation, structural errors explorations and investigating catchment behaviour (Smith et al., 2013; Munyaneza et al., 2014; Futter et al., 2014; Atchley et al., 2015; Bahremand et al., 2016;). Besides, several discussions directly appraised the model performance for reproducing rainfall-runoff relationship (Westhoff et al., 2012; Esse et al., 2013). Only few researchers indicated the limitations and improving directions of SUPERFLEX framework such as improving flexibility with a set of ‘‘nonstationary’’ parameterizations (Westra et al., 2014).

3.3 Modelling Strategy and Method

3.3.1 Strategy of model structure design

To avoid the over-parameterization and equifinality problems, the model will start from two simple lumped models for the rural and urban sub-catchments respectively, rather than build one semi-distributed model directly. In this process, we can analyse and explore the characteristics of rural and urban areas and adapt the lumped models accordingly, and meanwhile the lumped model performance and the parameter distribution would provide a further guidance to adapt the next model generation. After that several lumped model structures with good model performance and its suitable parameter range will be selected as the element components to build the semi-distributed model to simulate the whole study catchment.

3.3.2 Strategy to deal with parameter uncertainty problem

To deal with the parameter uncertainty problem, multi-objective strategy will be exploit in this research: For parameter calibration, multiple objective functions such as Nash Sutcliffe Efficiency (NSE) and correlation coefficient (R^2) will be used to evaluate the modelled time series of basin runoff; For the selection of appropriate parameter set, the model performance of multiple modelled variables such as the urban and rural sub-flow would be considered, and frequency domain analysis such as quantile-quantile plot (QQ plot) would be exploited.

3.3.3 Parameter calibration method

The available period of the evaporation, precipitation and discharge data is from 2017-04-12 00:00 to 2018-12-02 23:30 (600 days) which is used as the research period. And the available time scale is 30 minutes. Therefore, there are 28800 (600 days * 24 hours/day * 2/hour) data sets of 3 catchments (study catchment and two sub-catchments) for both calibration and verification period.

The data of two sub-catchments is used to calibrate two lumped models. And the combined semi-distributed models will be calibrated with the first 365 days data of study catchment. Finally the semi-distributed models will be verified with the last 235 days data.

The modelled discharge time series is compared to observed discharge time series. Since the scope of this project focuses on the flood peak, Nash Sutcliffe Efficiency (NSE) is exploited as main objective function to describe the model performance. And correlation coefficient (R^2) is used as secondary objective function.

In calibration process the parameter range is generally based on expert knowledge and cannot violate the hydrological meaning of parameters. The maximum and minimum limitations of each parameter are firstly given according to empirical values. And random parameter sets are sampled between the maximum and minimum limitation by Monte Carlo method. More complex models with larger numbers of parameters will have larger numbers of parameter samples to ensure the calibration scale

as “fair” as possible. With the variation of NSE, the interval of each parameters will be adjusted to capture better model performance until the interval of parameter sets with satisfactory model performance are founded.

For the semi-distributed models, some constraints on the rural and urban parameters could be exploited to reduce the risk of unrealistic combinations of parameters, based on the analysis about the different hydrological characters of rural and urban areas.

3.3.4 Model components or model selection method

As mentioned before, some model components in two lumped models will be selected to build the semi-distributed model. This model components selection follows these procedures: Firstly, the dominant water processes will be identified by analysing the NSE of model verification result, and the undominant water process will be abandoned. Secondly, among the remained model elements, more effective and efficient (high NSE with less parameters and less buckets) model components or structures would be selected for semi-distributed model design.

And after the design of several semi-distributed models, one near-optimal model with appropriate parameter set will be selected for the further influence analysis of urban development and LID implementation. For the selection of the near-optimal semi-distributed model, the model structure will be firstly determined considering the accuracy and precision. The accuracy of model structure will be revealed by the optimal verified objective functions such as NSE and R^2, and the mean of verified NSE. And the precision of the model structure will be indicated by the variance of verified NSE. After determining the model structure, the appropriate parameter set will be selected considering the performance of rural and urban sub-flows and peak flow simulation. It will be followed by the distribution comparison of observed data and model result with quantile-quantile plot (QQ plot) for a comprehensive assessment.

3.4 The expression of LID in model

The expression of LID could be divided into two parts. Firstly, the qualitative hydrologic routes of LID practices need to be designed to fit in the whole model structure; And next the reasonable values of involved parameters should be given.

The qualitative hydrologic routes design for certain LID practices is relatively easier than the quantitative analysis. The specific configuration of LID practices should be known and their hydrologic characters and functions should be analysed. Then the dominant hydrologic processes of LID practices need to be recognized, and corresponding model components should be devised in conceptual model.

Secondly for the parameters regarding the hydrologic character of specific LID practices, the relevant literature, the realistic field test results and local government files of LID practices could provide a reliable reference for rough parameter range. And the concrete parameter values could be estimated with some reasonable assumptions based on the referred parameter ranges.

4

Modelling

The rural and urban lumped models were built for two sub-catchments in *4.1 Lumped models for rural and urban sub-catchments*. And then based on two lumped model structures, the current rainfall-runoff relationship of study catchment was simulated by the semi-distributed model in *4.2 Semi-distributed model for study catchment*. Finally the expressions of four typical LID practices in the semi-distributed model were devised in *4.3 The expression of LID practices in* model.

4.1 Lumped models for rural and urban sub-catchments

According to *3.3.1 Strategy of model structure design*, two lumped models would be built for rural and urban sub-catchments firstly. The data processing and check processes are shown in *Appendix Data processing and check*.

4.1.1 Rural lumped models

a. Rural lumped model development

Since in most of the research period the runoff from rural sub-catchment kept at base flow and the target of this research focuses on peak flow, the last 150 days of research period from 6/7/2018 to 2/12/2018 with frequent extreme peaks are cut out as modelling period for rural lumped model.

5 generic reservoir elements (Interception Reservoir IR; Unsaturated soil Reservoir UR; Riparian zone Reservoir RR; Fast reacting Reservoir RR; and Slow reacting Reservoir SR) in SUPERFLEX framework were tested here with 6 generations of rural lumped models. The test of model structure started from the first generation of rural lumped models which is a one-bucket model with 3 or 4 parameters and ended at the rural lumped Model 06 with 5 buckets and 12 parameters.

Table 2 shows the basic frameworks of 6 rural lumped model generations. Among the 6 model generations, 5 reservoirs were tested successively. And several other model components such as capillary rise (Cr), discharge exponent (α) and precipitation distribution factor (D) were further tested among different models in one generation. The complete rural lumped model test and parameter calibration progress are shown in *Appendix D.1 Rural lumped model test*.

Table 2. Basic framework of 7 rural lumped model generations

	Schematic figure the basic model framework	Reservoirs	Parameter number
Model 01	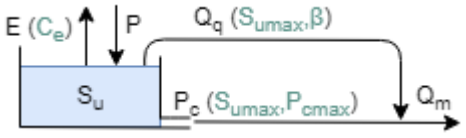	Unsaturated Reservoir UR;	3-4

Model 02	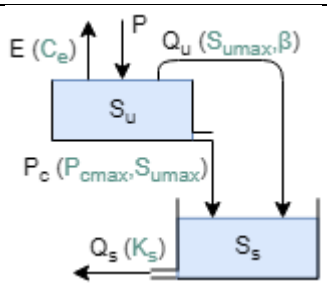	Unsaturated soil Reservoir UR; Slow reacting Reservoir SR;	5
Model 03	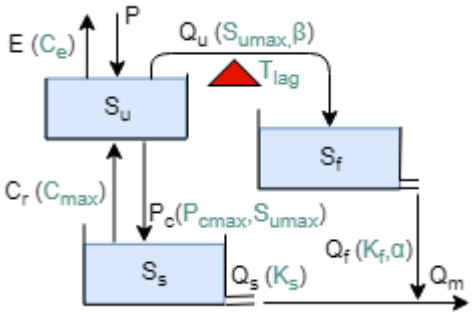	Unsaturated soil Reservoir UR; Slow reacting Reservoir SR; Fast reacting Reservoir RR;	7-10
Model 04	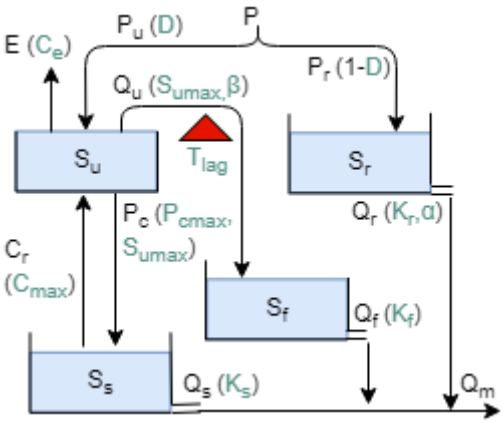	Unsaturated soil Reservoir UR; Slow reacting Reservoir SR; Fast reacting Reservoir RR; Riparian zone Reservoir RR;	10-11
Model 05	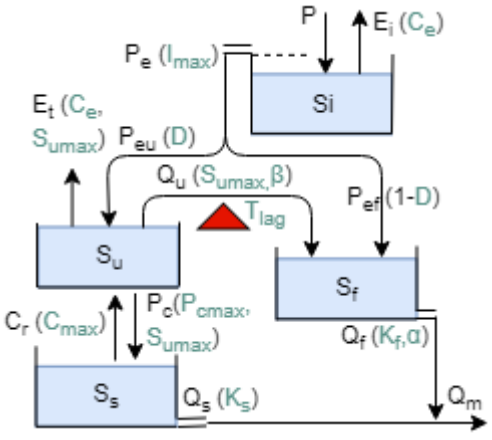	Unsaturated soil Reservoir UR; Slow reacting Reservoir SR; Fast reacting Reservoir RR; Interception Reservoir IR;	10-11

Model 06	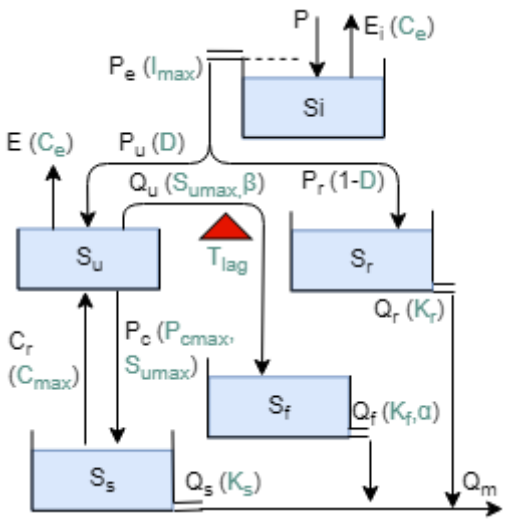	Unsaturated soil Reservoir UR; Slow reacting Reservoir SR; Fast reacting Reservoir RR; Riparian zone Reservoir RR; Interception Reservoir IR;	12

Symbols: the reservoirs with underline indicate the main test reservoir in this model generation

b. Rural lumped model result

Among the test 6 generations of rural lumped model, more complex model structures with more parameters would not always bring better model performance as shown in Figure 9. Among these 6 generations of 18 rural lumped models, Model 04B achieved the highest NSE (0.802) with four buckets (UR, RR, FR and SR) and 11 parameters (including Cr, α and D). The 5th and 6th generations of rural lumped model with additional IR did not get higher NSE. Among the test rural lumped models with high NSE, Model 03A is the most "efficient" model which got acceptable NSE (NSE>0.6) with only three buckets and 7 parameters.

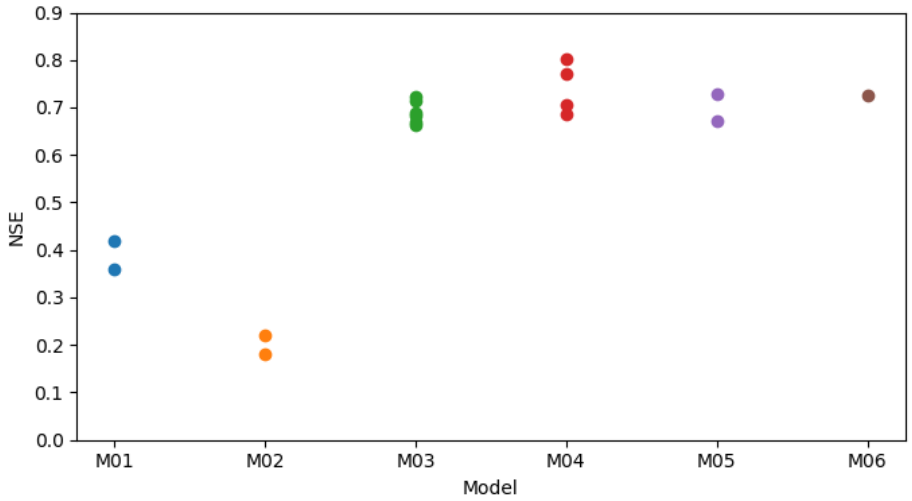

Figure 9. The NSE results of 6 generations of rural lumped model

c. Identification of dominant hydrological processes in rural sub-catchment

By comparing the performance of rural lumped Model 01 to 06, it could be found that almost all the test models with acceptable model performance (NSE > 0.6 and stable model performance) are built based on "UR-SR-FR" three buckets model structure (as the schematic figure of Model 03 as shown in Table 2). It is because that the "UR-SR-FR" model structure provides the basic flexibility of model structure to simulate several dominant water processes in study rural sub-catchment: The Unsaturated Reservoir as one critical separation bucket realizes three dominant water processes, transpiration, percolation and overland flow; The Slow reacting Reservoir simulates the fundamental groundwater storage and dispatch processes in study rural sub-catchment; And the Fast reacting Reservoir is the main resource to generate peak flow.

And then several other model components such as RR, capillary rise (Cr) and discharge exponent (α) also contribute to the improvement of model performance. Firstly, because of the intensive expansion of river network in study rural sub-catchment, the riparian environment is also an important part. According to the result of M04, RR also contribute to the improvement of model performance especially on small peaks simulation, which increase the NSE of Model 04 significantly than Model 03. Secondly, since the favourable vegetation condition of rural area, the capillary rise (Cr) is also one of key water process of study rural sub-catchment. According to the model result, under the same model framework, the models with capillary rise always achieve larger NSE than the models without capillary rise. Thirdly, based on the test results of Model 03 and Model 04, adding one additional discharge exponent (α) on the overflow from FR (Qf) could improve the model performance significantly on simulating peak runoffs, which effect is better than adding the discharge exponent (α) on the overflow from RR (Qr).

To the contrary, according to model results, the IR cannot improve the model performance, which may be not one dominant water process in rural sub-catchment.

d. Model component selection for semi-distributed model from rural lumped model
When selecting the model elements to further build the semi-distributed model, the "UR-SR-FR" three buckets model structure will be exploited as the basic model framework for rural part of semi-distributed model. And other effective model components such as RR, discharge exponent (α) and capillary rise (Cr) would also be kept in semi-distributed model and the other non-dominant or ineffective model components like IR would not be considered.

e. Parameter calibration of rural lumped model and parameter interval in semi-distributed model
All parameter sets with the objective function (NSE) larger than 0.6 were retained and then the ranges of these retained calibrated parameters were used to determine the initial parameter interval in semi-distributed model rather than specific parameter values. The parameter calibration results of rural lumped M04B are shown in Figure 10 as an example. The retained parameter intervals of rural lumped model are shown in Table 4 (page 26).

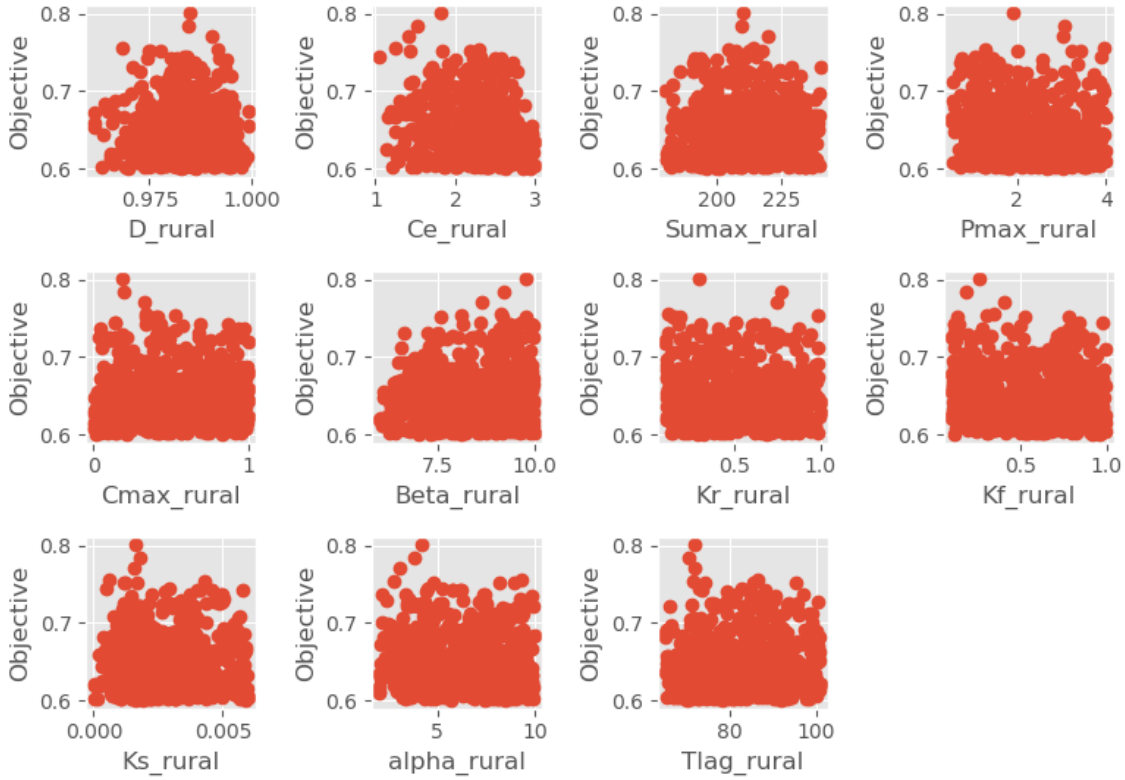

Figure 10. Parameter Calibration Result of M04B. The parameter intervals, which could capture the objective function larger than 0.6, were reserved and used to determine the initial parameter interval in semi-distributed model.

4.1.2 Urban lumped models

a. Urban lumped model development

The structure test of urban lumped f model or urban sub-catchment follows the similar procedures as the rural lumped model. 5 generic reservoir elements (Interception Reservoir IR; Unsaturated soil Reservoir UR; Fast reacting Reservoir FR; Human impact Reservoir HR; and Slow reacting Reservoir SR) were tested here with 5 generations of urban lumped models.

Table 3 shows the basic framework of 5 urban lumped model generations. Among the 5 model generations, the 5 reservoirs was tested successively. And several model components such as capillary rise (Cr), discharge exponent (α) and precipitation distribution factor (D) were further tested among different models in one generation. The complete urban lumped model test and parameter calibration progress are shown in *Appendix D.2 Urban lumped model test*.

Table 3. Basic framework of 5 urban lumped model generations

	Schematic figure the basic model framework	Reservoirs	Parameter number
Model 01	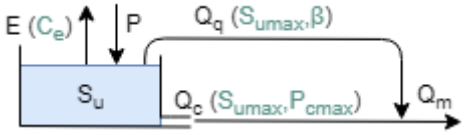	Unsaturated soil Reservoir UR;	3-4
Model 02	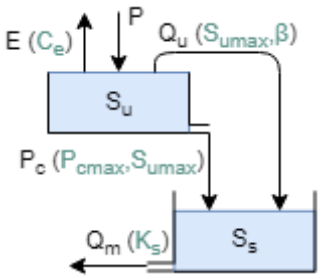	Unsaturated soil Reservoir UR; Slow reacting Reservoir SR;	5
Model 03	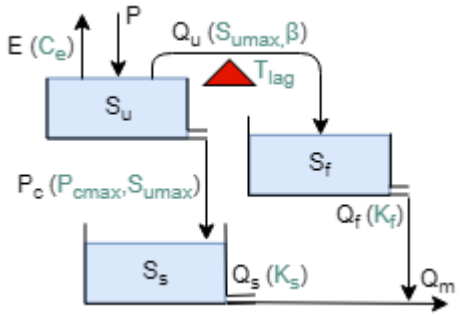	Unsaturated soil Reservoir UR; Slow reacting Reservoir SR; Fast reacting Reservoir SR;	7
Model 04	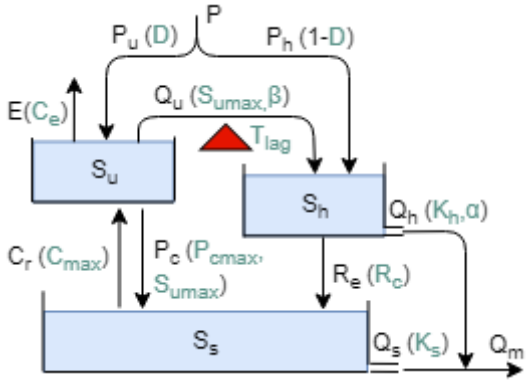	Unsaturated soil Reservoir UR; Slow reacting Reservoir SR; Human impact Reservoir RR;	8-11

Model 05	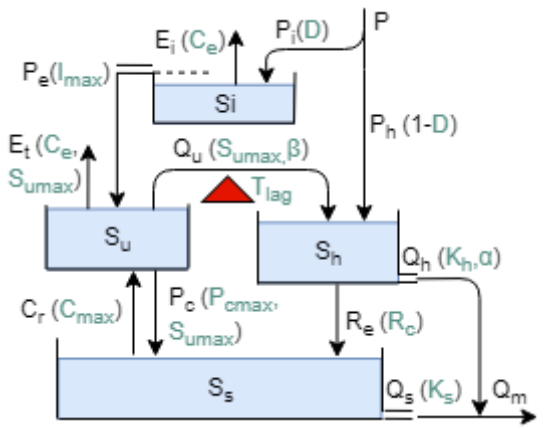	Unsaturated soil Reservoir UR; Slow reacting Reservoir SR; Human impact Reservoir RR; <u>Interception Reservoir IR;</u>	11-12

Symbols: the <u>reservoirs</u> with underline indicate the main test reservoir in this model generation

b. Urban lumped model result

Similarly as the rural lumped models, more complex model structures with more parameters will not always bring better model performance as the NSE results of urban lumped models shown in Figure 11.

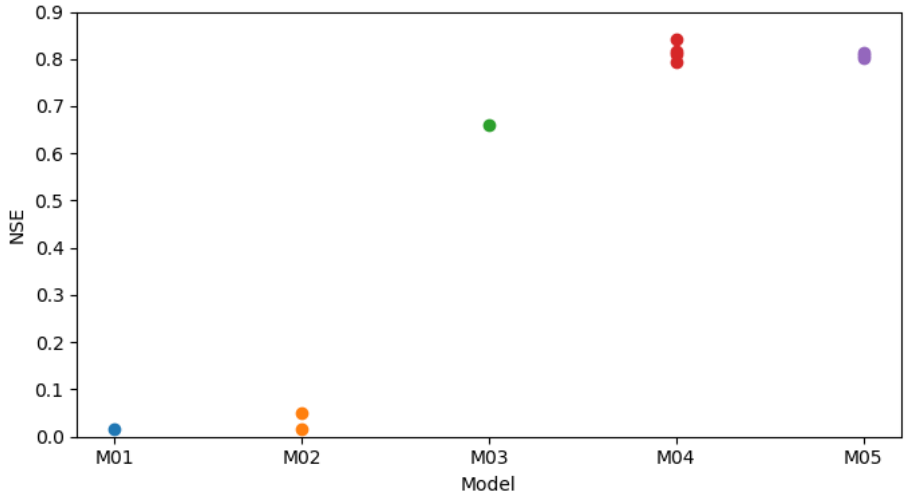

Figure 11. The NSE results of 5 generations of urban lumped model

As Figure 11 shows, none of urban lumped M01 and M02 have acceptable model performance since the over-simple model structure cannot reproduce the complex hydrologic processes in urban sub-catchment. And then M03 with three buckets (Unsaturated Reservoir, Slow reacting Reservoir and Fast reacting Reservoir) could preliminary reproduce the hydrological condition of urban sub-catchment with acceptable NSE result. However according to the parameter calibration result, the parameter, the maximum percolation velocity (Pmax), in M03 is far more than real natural percolation level because of an artificial groundwater recharge program in urban sub-catchment.

Therefore, in M04 one Human impact Reservoir (HR) was designed to replace the FR in M03, which aims to simulate these artificial hydrological processes such as groundwater recharge and fast stormwater conveyance process. Model 04 got the highest NSE among the test 5 generations of urban lumped models. Among the 5 generations of 13 urban lumped models, M04D with three buckets (UR, HR, and SR) and 11 parameters (including Cr, α and D) achieved the highest NSE as 0.842. Finally, the last generation, M05, with one additional IR did not attain higher NSE than M04D, but the model performance of M05 on peak runoff simulation was improved as shown in Figure 12.

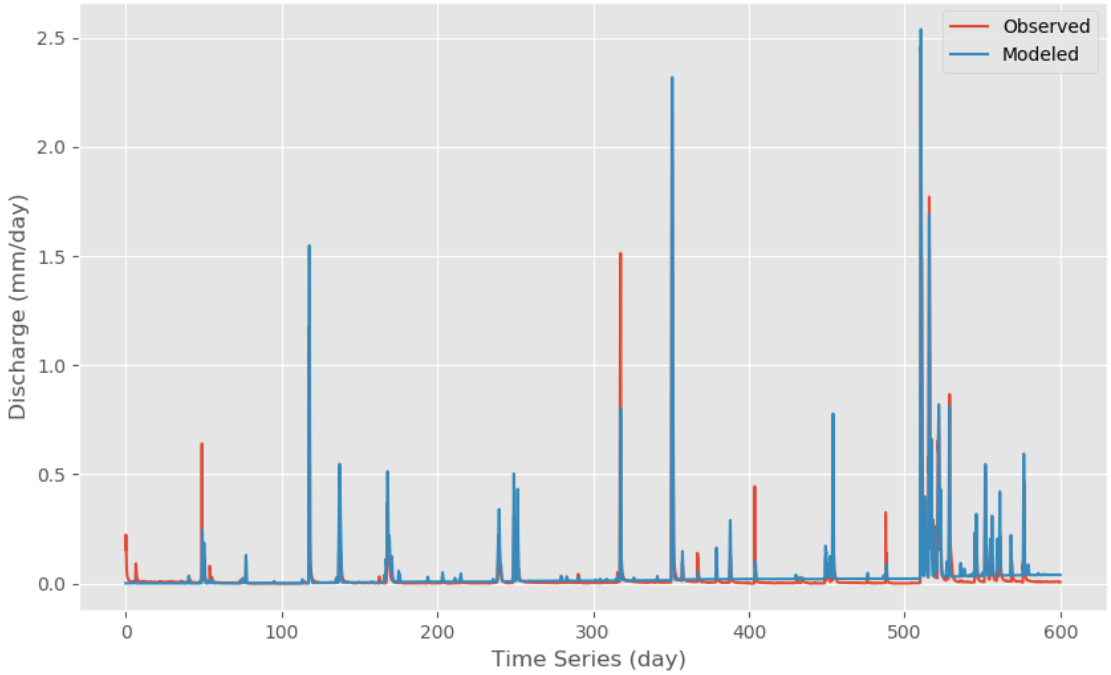

Figure 12. Model Result of Urban Lumped M05B

c. Identification of dominant processes in urban sub-catchment
By comparing the performance of urban lumped Model 01 to 05, it could be found that almost all the test models with acceptable model performance (NSE > 0.6 and stable model performance) are built based on "UR-SR-HR" model structure (as the schematic figure of Model 04 as shown in Table 3. It is because the "UR-SR-HR" model structure provides the fundamental flexibility of model structure to simulate several dominant water processes in study urban sub-catchment: The Unsaturated Reservoir as one critical separation bucket realizes three dominant water processes, transpiration, percolation and overland flow; And the Slow Response Reservoir could realize the fundamental groundwater storage and dispatch processes in study urban sub-catchment; And the Human impact Reservoir simulates the artificial groundwater recharge and fast stormwater discharge processes, which is also the main resource for peak flow generation.

Based on the "UR-SR-HR" three bucket model framework, the capillary rise (Cr), discharge exponent (α), and precipitation distribution factor (D) all contribute to NSE improvement. Although additional IR does not have obvious positive effect on the NSE, the model performance on peak runoff simulation is improved.

Therefore when developing the semi-distributed models, the "UR-SR-HR" three bucket model framework will be used as the basic model framework for urban part of semi-distributed models and other effective model components such as IR, the capillary rise (Cr), discharge exponent (α), and precipitation distribution factor (D) could also be kept in semi-distributed models.

d. The hydrological difference between urban sub-catchment and study catchment
Since human activities are varies a lot by region, the artificial caused hydrologic differences of urban sub-catchment and study catchment may be considerable. Therefore, the model components and parameter intervals in urban lumped model cannot be used in semi-distributed model directly. More artificial influences should be considered when converting the urban lumped model to the semi-distributed model.

Firstly, as the background information of San Antonio City, there is a groundwater recharge project in north part of San Antonio City. And two different types of recharge structures are exploited in this project for the contributing and recharge zone respectively. Therefore, the groundwater recharge

process will not happen evenly within the whole San Antonio City area. Secondly, a part of groundwater is pumped out as domestic water. After used, this water would be collected by wastewater sewer system and then be conveyed to the three Water Recycling Centres in San Antonio City and finally be discharged to surface water bodies. However the water discharge locations of three WRCs are out of the urban sub-catchment and locates in the research catchment. Therefore in urban sub-catchment these urban sewage processes would not be observed, which should be reproduced in semi-distributed model.

In semi-distributed model, a more complete human activity component with groundwater recharge, groundwater pumping, and fast water discharge processes would be further designed based on the prototype of HR tested in urban lumped model. More information about the human activity component could be found in *b. Human activity module for urban area.*

Not only the model structure, these considerable artificial caused hydrological differences would also lead to the discrepancy of the parameter intervals in lumped model and semi-distributed model. For example, with different construction degree, the precipitation distribution factor (D) between UR and HR will be different; Besides, with the different layouts of urban stormwater sewer system, the urban rainwater conveyance efficiency will be different by region and correspondingly the discharge coefficient of HR (Kh) will be changed; Thirdly, the uneven groundwater recharge process must influence the value of recharge coefficient (Rc) in model. And then with different groundwater recharge extents, the groundwater stock in SR will be different and correspondingly the discharge coefficient of SR (Ks) have to be changed.

Therefore the calibrated parameter intervals of urban lumped model will not be used in semi-distributed model directly. The calibrated parameter intervals of urban lumped model are shown in Table 4.

Table 4. Calibrated parameter intervals of rural and urban lumped models

Para. range		Imax [mm]	D [-]	Ce [-]	Sumax [mm]	Pmax [mm/d]	Cmax [mm/d]
Rural	Min	-	0.97	1	150	0	0
	Max	-	1	3	250	5	1
Urban	Min	0	0.985	0.5	30	0	0
	Max	5	1	3	375	5	1
Para. range		beta [-]	Kr/Kh [1/mm*d]	Kf/Rc [1/mm*d]	Ks [1/mm*d]	alpha [-]	Tlag [-]
Rural	Min	5	0	0	0	1	41
	Max	10	1	1	0.006	10	101
Urban	Min	0.5	0	1	0	1	21
	Max	5	0.5	15	0.0002	2	85

Symbols: the shadowed parameter intervals would be modified in semi-distributed model

4.2 Semi-distributed model for study catchment

In this part, the semi-distributed model is built to simulate the whole study catchment. Three key elements in semi-distributed models are introduced in *4.2.1 Key elements in semi-distributed model*. In *4.2.2 Model structure generation of Semi-distributed model*, the generation of three semi-distributed models is explained. Finally, in *4.2.3 Selection of Semi-distributed model*, one near-optimal model is selected for the scenarios modelling.

4.2.1 Key elements in semi-distributed model

Considering some realistic conditions of study catchment such as the positions of rural and urban area, the domestic water supply for urban population, and urban wastewater treatment system, some key elements are exploited in semi-distributed model to improve the model.

a. Time lag for rural area

Firstly since the rural areas are located at the upstream part within the whole study catchment, a triangular time lag function is added on the rural runoff to simulate the time delay caused by the long hydrological distance of rural areas. The schematic figure and time lag function is shown below:

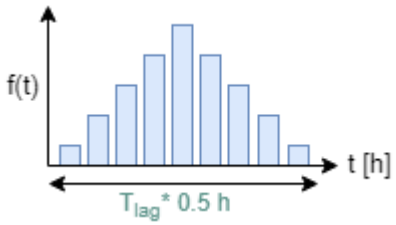

Figure 13. Schematic figure of Time Lag function

$$T = T_{lag} * 0.5h$$

$$f = \begin{cases} \dfrac{4t}{(T)^2}, 0 < t < \dfrac{T}{2} \\ \dfrac{4(T-t)}{(T)^2}, \dfrac{T}{2} < t < T \\ 0, t > T \end{cases}$$

In which:

T: the scale of total delayed time [h]

Tlag: the number of delayed time interval [-]

t: time [min]

There is one dimensionless parameter in time lag function, Tlag, which indicate the number of delayed time interval. The initial parameter interval for Tlag is determined by the rough estimation of the time difference between the peak runoffs from rural sub-catchment and the whole study catchment as shown in Figure 14. The calibration interval of Tlag is determined as from 6 to 41, which indicate a peak delay from 1.25 hours to 10 hours.

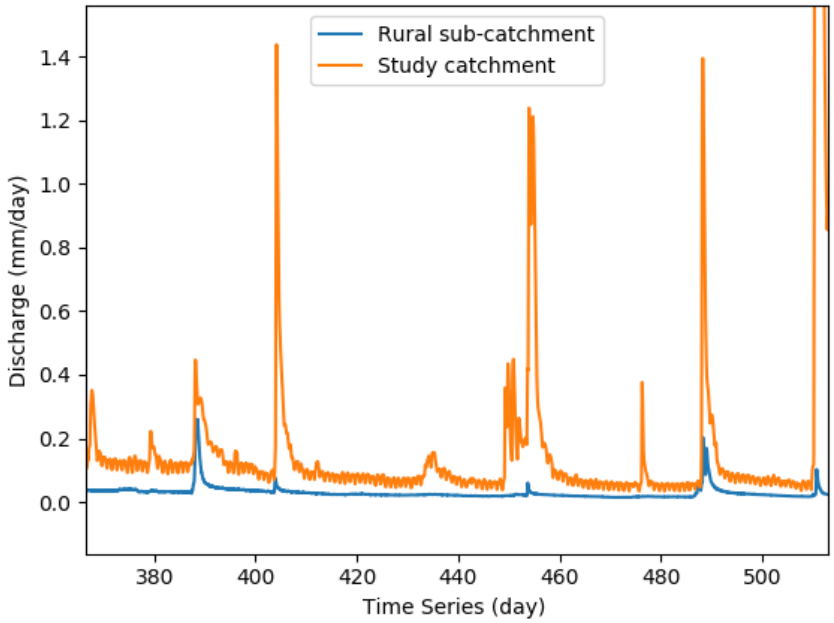

Figure 14. The time difference between the peak runoffs of rural sub-catchment and study catchment

b. Human activity module for urban area

As mentioned in *d. The hydrological difference between urban sub-catchment and study catchment*, a human activity module is designed in semi-distributed model based on the prototype of HR tested in urban lumped model.

The human activity module should contain four essential human impact elements:

(1) Because lots of soil and vegetation are removed in urban area, large areas of impervious surface are constructed, which accelerate and promote the runoff generation. Therefore, in human activity module, a HR is created to collect part of precipitation, which indicates the urban impervious surface or grey surface. And the remaining water is collected by UR which indicates the urban green areas with soil layer such as parks or greenbelts. The precipitation distribution ratio between HR and UR is determined by precipitation distribution factor, D. The position of HR in human impact module is shown in Figure 17.

(2) Since the CD seeks to route water off-site as fast as possible, most of urban grey areas are connected to urban stormwater sewer system. The collected precipitation by urban stormwater sewer system would be discharged to nearby water bodies, which would significantly accelerate the natural water discharge process. Therefore the hydrologic response time from rainfall to runoff would be quite short for HR. In this human activity module, the fast hydrological response rate will be simulated by a large value of discharge coefficient of HR (Kh>Ks).

(3) There is a groundwater recharge project in north part of San Antonio City. Two types of recharge structures either on or above the recharge zone are exploited in this project. Therefore a fast groundwater recharge process from HR to SR should be added in human activity module with a recharge coefficient (Rc).

(4) Because of the daily water usage fluctuation of urban population, an obvious daily fluctuation of water discharge could be found as shown in Figure 15. Most of the urban water supply comes from the underground Edwards Aquifer. The water is pumped out from Edwards Aquifer and conveyed to the households by pipeline system continuously. After use, the waste water will be collected and conveyed to the three WRCs in San Antonio City. Finally the treated water will be discharged to surface streams within research catchment.

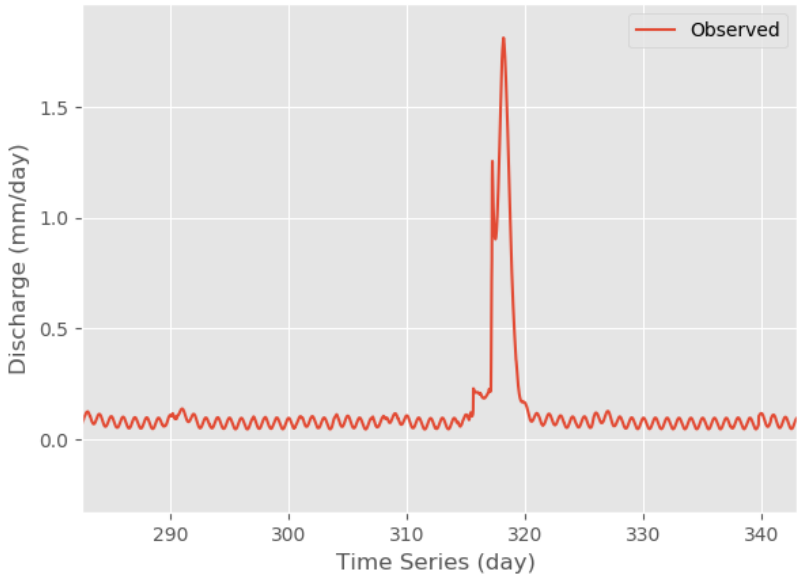

Figure 15 Daily fluctuation of runoff of research catchment

Since all of the water discharge locations of the three WRCs are out of the urban sub-catchment, the runoff from urban sub-catchment does not show a daily fluctuation and the urban lumped model does not contain the urban domestic water usage process, which should be further considered and added in human activity module.

In human activity module, urban water supply is achieved by pumping groundwater from SR to HR. Because of the shape of daily urban water usage fluctuation, sine function is used to simulate the groundwater pumping process (Qp).

$$Q_p = A * \sin\left(\frac{2\pi}{T}t + \varphi\right) + A + Q_{pmin}$$

In which:

Qp: water pumping rate in mm/d (the pumped water volume in unit of time divided by urban area);

A: the amplitude of water pumping use rate in mm;

T: the cycle period of water pumping rate, which is 1 day;

t: timestep in 1/48 day (30min);

ϕ: phase of water pumping rate in day (between 0 and 2π);

Qpmin: the minimum water pumping rate in mm/d;

There are three parameters, A, ϕ and Qpmin in the water pumping function. Since the magnitude of daily water discharge variation is quite small compared to the total discharge, these three parameters could not be calibrated with other parameters together. Therefore a pre-calibration method is exploited with a 10 days base flow.

As the calibration result, the phase parameter ϕ has an obvious near-optimal solution as 2.2. And the calibration result showns that Qpmin is closed to zero, which means the minimum water usage rate of urban people in one day could be neglected. The amplitude parameter A is closed to 0.65 mm/d. The calibration result is shown in Figure 16.

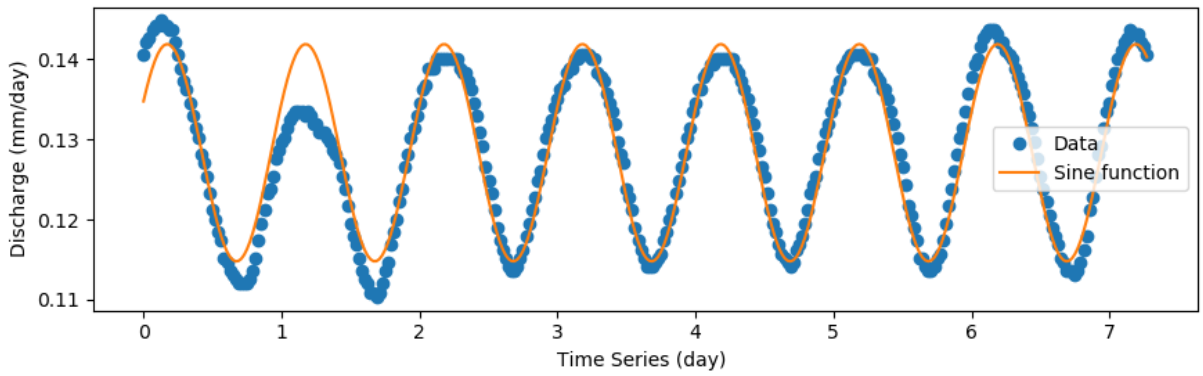

Figure 16. The calibration result of water pumping process

After determining the three parameters, the water pumping process could be exploited in every semi-distributed model as a complete model component without calibration process. Since the water pumping process follows a stable daily fluctuation and it is decided by fixed habit of human water usage, which will not be significantly changed under the similar model framework.

The final schematic figure of human impact module is shown in Figure 17.

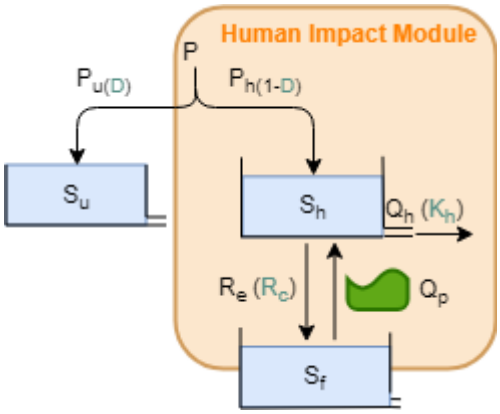

Figure 17. Schematic figure of designed Human Impact Module

In which:

Mathematical expression	Parameter	Description
$Q_p = 0.65 * \sin(2\pi t + 2.2) + 0.65$	t [d]	Time
$Q_h = K_h S_h$	Kh [1/d]	Discharge coefficient
$R_e = R_c S_h$	Rc [1/d]	Recharge coefficient

c. Constraints on parameter limitation

Some constraints of parameters based on expert knowledge and parameter analysis above are exploited for parameter calibration in semi-distributed model. Firstly, the maximum percolation velocity in urban areas is assumed to be smaller than it in rural areas ($P_{max,R} > P_{max,U}$). And then the water storage depth in unsaturated zone in urban areas is assumed to be smaller than it in rural areas ($S_{umax,R} > S_{umax,U}$).

4.2.2 Model structure generation of Semi-distributed model

Four generations of semi-distributed model are created as shown in Table 5, all of which are based on the 6 buckets model framework: “UR-SR-FR” three buckets model framework for rural module and

"UR-SR-HR" three buckets model framework for urban module. The rural and urban modules of all the 4 generations of semi-distributed models are all come from the test lumped models. And in urban module, UR, HR and SR indicate the urban green, grey surface and underground part respectively. As shown in the schematic figures in Table 5, part of precipitation on urban area is collected by UR which indicate the urban green surface with soil layer such as greenbelts and parks, and the last precipitation would be collected by HR which indicate the urban grey (impervious) surface. Both of UR and HR have hydrological connections with Slow groundwater Reservoir.

Table 5. Basic framework of 3 semi-distributed model generations

	Schematic figure the basic model framework	Para. Num.	Bucket Num.
M01	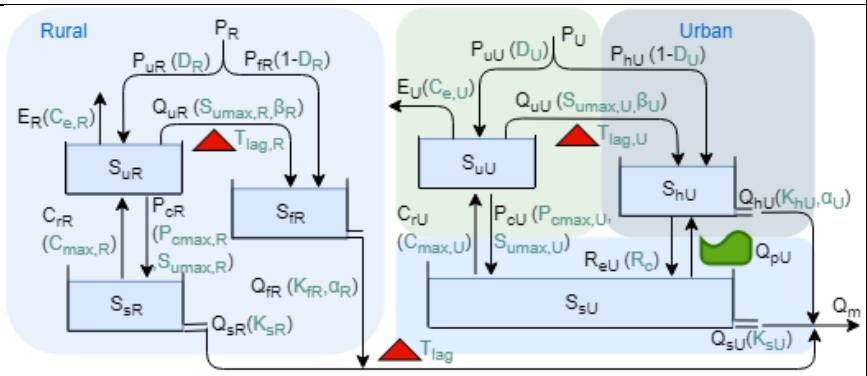	21-22	6
M02	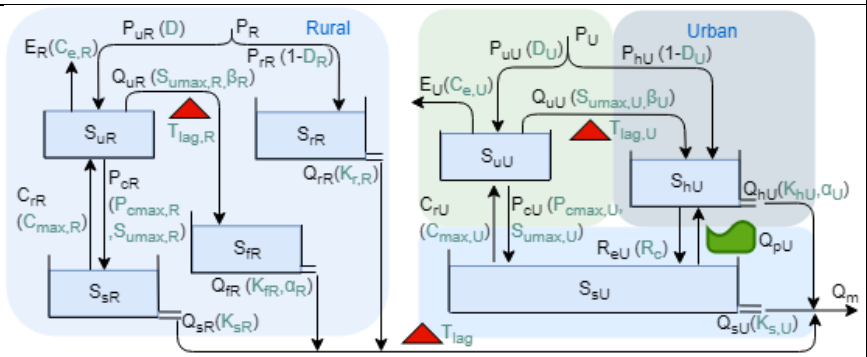	23	7
M03	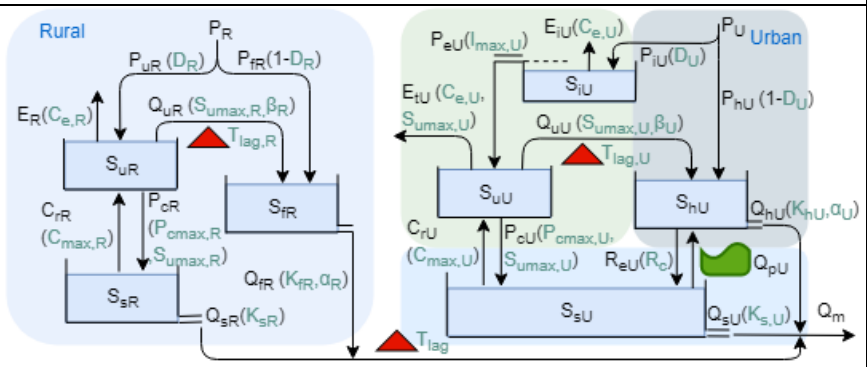	22-23	7

M04	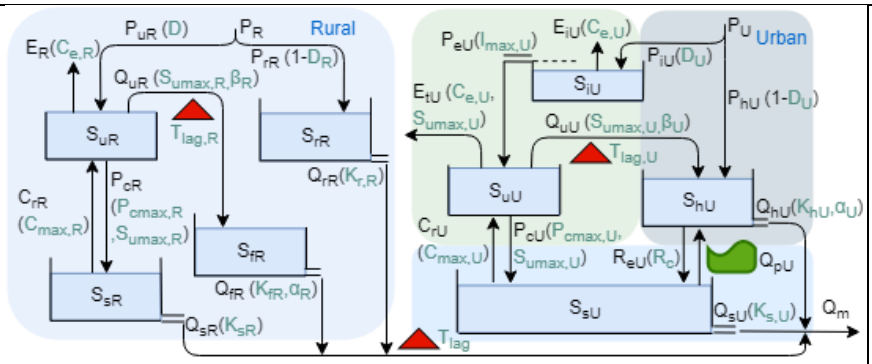	24	8

The first generation of semi-distributed model 01 (M01) is designed based on the simplest 6 buckets model framework. And there are 7 buckets in M02, in which one more RR is added and tested in rural module based on M01. For M03, there are also 7 bucket with an additional IR in urban module based on M01. Finally, M03 describes a relatively full hydrologic picture with 8 buckets, including a RR in rural module and a IR in urban module.

The complete semi-distributed model test progress is shown in *Appendix D.3 Semi-distributed model test.*

4.2.3 Selection of Semi-distributed model

One near-optimal model with appropriate parameter set will be selected from those 4 generations of semi-distributed model for the further influence analysis of urban development and LID implementation.

a. The selection of model structure

Firstly, the model structure will be determined considering the accuracy and precision: The accuracy of model structure is revealed by the optimal verified objective functions such as NSE and R^2 and also the mean of NSE; And the precision of the model structure is indicated by the variance of NSE. The relevant information is shown in Table 6.

It could be found that the accuracy performances of all the Model 01B, Model 02 and M04 are outstanding, but considering the model precision M01B performs better than M02 and M04: M01B gets one of the largest verified NSE and R^2 among the 6 tested semi-distributed models and it achieve the largest mean value of NSE and the least variance of NSE. Secondly the model structure of M01B is also efficient with 6 buckets and 22 parameters. Therefore the effective and efficient model structure of M01B is selected for further modelling work.

Table 6. The model performance of 12 semi-distributed models

	Accuracy index					Precision index
Model Num.	*The R^2 of calibration*	Optimal verified R^2	*The NSE of calibration*	Optimal verified NSE	Mean of verified NSE	Variance of verified NSE
M01A	*0.882*	0.865	*0.723*	0.735	0.117	0.399
M01B	***0.897***	**0.873**	***0.673***	**0.748**	**0.297**	**0.240**
M02	*0.863*	0.871	*0.712*	0.749	0.155	0.424
M03A	*0.902*	0.850	*0.721*	0.706	-0.056	0.758
M03B	*0.815*	0.855	*0.656*	0.730	0.039	0.587
M04	*0.878*	0.883	*0.714*	0.744	0.036	0.606

Symbols: Boldface row indicates the selected model structure; Italic columns indicate the calibration results.

b. The determination of propriate parameter set

After determining the model structure, the propriate parameter set will be selected considering the performance of rural and urban sub-flows and the extreme peaks simulation. It will be followed by the distribution comparison of observed peaks and modelled peaks with quantile-quantile plot (QQ plot) for a comprehensive assessment.

Firstly, the optimal 20 parameter sets with the largest verified NSE among the 23000 samples of parameter set are preliminary selected. Then the modelling rural and urban sub-flows of these 10 parameter sets are drawn. One example is shown in Figure 18.

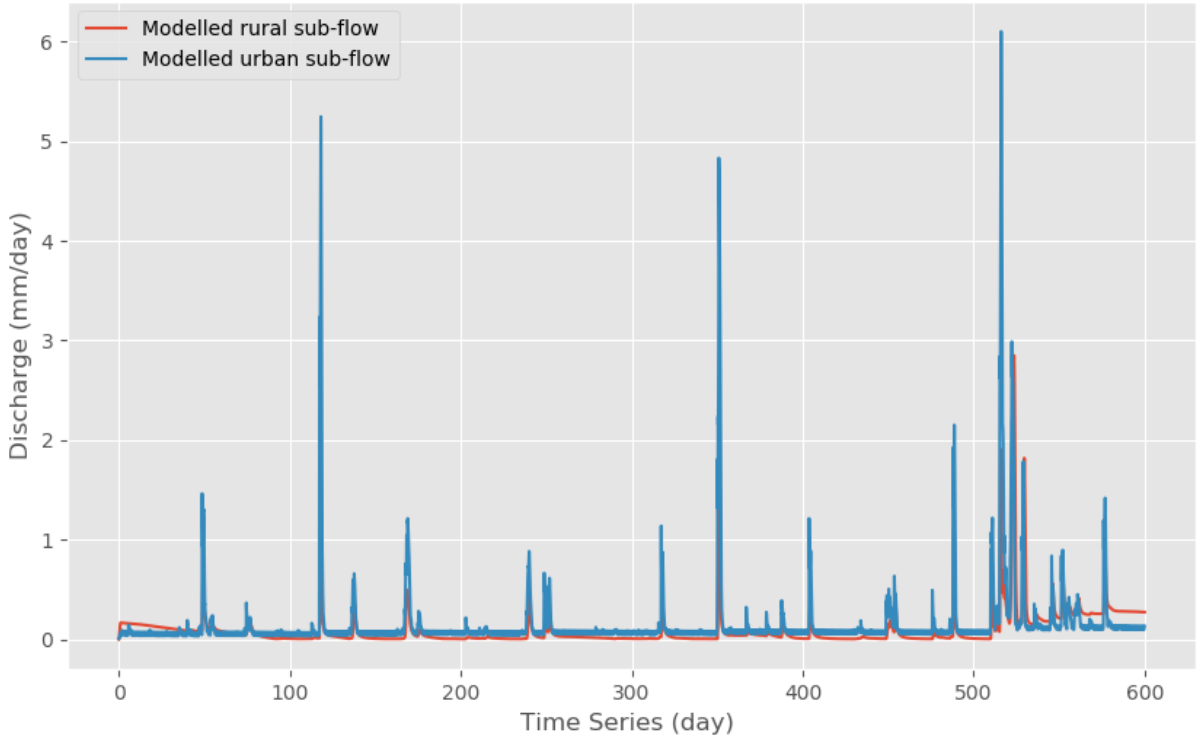

Figure 18. The modelled rural and urban sub-flows with one of the 20 optimal parameter sets

These 20 sub-flow figures all perform similar satisfactory urban sub-flows but the performances of rural sub-flows are far different. Some of the modelling rural sub-flows still keep the character of rural runoff as in lumped model: sufficient base flow and less and small peaks. But other parameter sets cannot capture these characters and present unrealistic rural sub-flow with frequent high peaks. These parameter sets with unrealistic sub-flow performance are removed. After the cleaning of models with unrealistic performance on sub-flows, 9 parameter sets are left out of the 20 optimal parameter sets.

Secondly, since this research focuses on the extreme peak flows, 2 parameter sets with outstanding performance on extreme peak flow simulation are selected out of the 9 parameter sets.

Finally, since the time corresponding model performance has already been assessed with the objective functions of NSE and R^2. Another distribution analysis is exploited here to assess the possibility corresponding model performance for a comprehensive assessment. The distribution comparison of observed peak values and modelled peak values is developed with the quantile-quantile plots (QQ plots). The runoff values larger than 0.5 mm/d are saved for the distribution analysis for peak flows. The QQ plots of 2 parameter sets are shown in Figure 19.

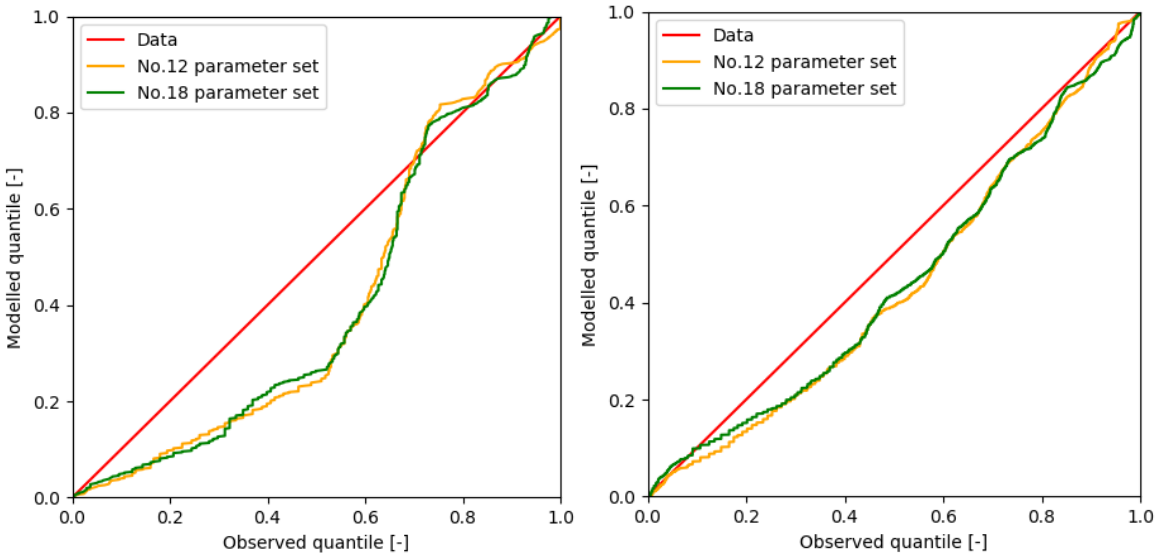

Figure 19. QQ plots of peak runoff values for calibration (left) and verification (right) result

The QQ plots show the statistical difference between observed peak values and modelled peak values. Every point on the QQ line indicates one specific runoff value, which horizontal and vertical coordinates mean the quantile number of the specific runoff value in observed data set and modelled runoff set respectively. For example, if the observed runoff data is seen as one extreme near-optimal model result and this model could simulate the runoff exactly the same as observed runoff data, the QQ line of this model should be the exactly located at the diagonal of this QQ plot with the same modelled and observed runoff value sets and the same corresponding relationship of every runoff value and its quantile number.

It could be found from Figure 19 that, these two parameter sets share similar distribution character. And because the low flow values smaller than 0.5 mm/d are removed, both the QQ lines of observed data and model result start from 0.5 mm/d at coordinate (0, 0) as shown in Figure 19. As for the high flow, it could be found that the upper right end points of QQ lines for both two parameter sets are closed to the coordinate (1, 1) since the second screening of extreme peak simulation.

The areas (α) between the QQ lines and the diagonal, and the standard deviations (σ) of QQ lines and the diagonal are calculated, which are shown in Figure 20. The area index (α) between the QQ line and the diagonal could quantify the predictive reliability of model, and predictive precision could be quantified by the standard deviation (σ) (Kavetski., 2011).

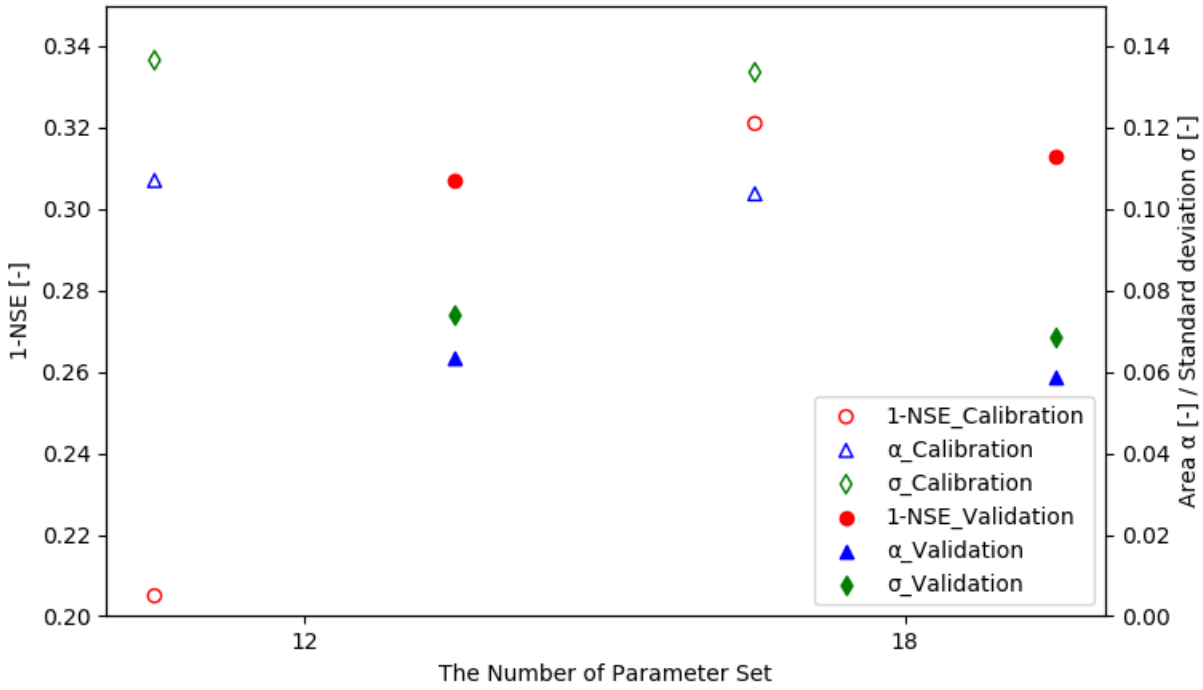

Figure 20. The comparison of model performances with the NSE, the area indexes (α) and the standard deviation (σ) of QQ lines and the diagonal in Figure 19

As shown in Figure 20, the distribution difference between two parameter sets is small and the verification performances of the two parameter sets are better than the calibration performances with smaller numbers of area index (α) and standard deviation (σ).

Since the No.18 parameter set has slightly better model reliability and precision performance of both the calibration and verification results, the No.18 parameter set is selected for further analysis about urban development and LID implementation.

4.2.4 The final selection of rainfall-runoff semi-distributed model for current condition

The final selection of semi-distributed model structure is Model 01B, and the schematic figure is shown in Figure 21.

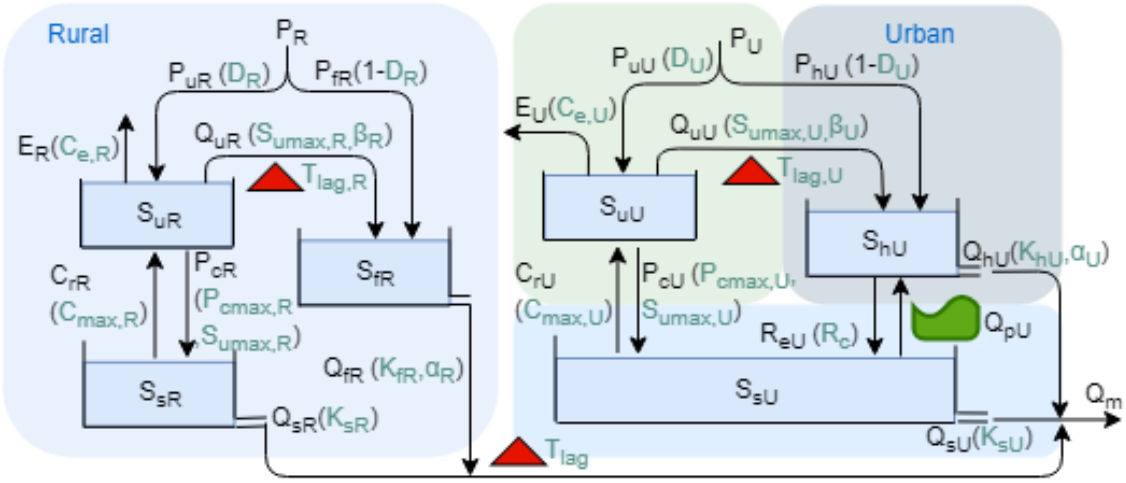

Figure 21. Schematic figure of current model structure (The capital letters R or U in subscript in model structure schematic figure indicate Rural or Urban areas which would not be distinguished in the annotation table below.)

In which:

Parameter	Description	Model Components	Description
D [-]	Precipitation distribution factor	Su (mm)	Storage in UR
Ce [-]	Evaporation correction coefficient	Sh (mm)	Storage in HR
Sumax [mm]	Maximum unsaturated storage	Ss (mm)	Storage in SR
β [-]	Discharge exponent	Sf (mm)	Storage in FR
Pmax [mm/d]	Maximum percolation velocity	Re (mm/d)	Groundwater recharge
Cmax [mm/d]	Maximum capillary rise velocity	Qu (mm/d)	Overflow from UR
Rc [1/mm*d]	Recharge coefficient	Pc (mm/d)	Percolation
Kh [1/mm*d]	Human impact reservoir coefficient	Cr (mm/d)	Capillary rise
Ks [1/mm*d]	Slow reservoir coefficient	Qp (mm/d)	Groundwater pumping
Kf [1/mm*d]	Fast reservoir coefficient	Qs (mm/d)	Discharge from SR
α [-]	Discharge exponent	Qh (mm/d)	Discharge from HR
Tlag [-]	Time lag coefficient	Qf (mm/d)	Discharge from FR

In the rural module, there are three buckets as Unsaturated Reservoir (UR), Fast reacting reservoir (FR) and Slow reacting Reservoir (SR) with one time lag function and 10 parameters. The rural module depicts a fully natural hydrological picture with several dominant water processes, precipitation (P_R), evaporation (E_R), overflow from unsaturated zone (Q_{uR}), percolation (P_{cR}), capillary rise (C_{rR}), and fast and slow groundwater flow (Q_{fR} and Q_{sR}).

The urban module can be divided into three parts, urban green surface, urban grey surface and groundwater part, corresponding with three reservoirs, Unsaturated Reservoir (UR), Human impact Reservoir (HR) and Slow reacting Reservoir (SR). The green model components focuses on the natural water processes in urban park or greenbelt areas such as precipitation on soil layer (P_{uU}), overflow from unsaturated zone (Q_{uU}), percolation (P_{cU}) and capillary rise (C_{rU}); The grey model components replicates the artificial water processes such as precipitation on impervious surface (P_{hU}), groundwater water pumping (Q_{pU}), groundwater recharge (R_{eU}), and rapid urban water conveyance and discharge process (Q_{hU}). The outflow from the urban module is composed by two part: discharge from urban drainage system and groundwater discharge.

The selected parameter set is shown in Table 7. And the runoff simulation result for current rainfall-runoff relationship is shown in Figure 22 with NSEs as 0.679 in calibration period (the first 365 days) and as 0.687 in verification period (the last 235 days).

Table 7. Parameter values in current model

Para.	D	Ce	Sumax	Pcmax	Cmax	Rc
Unit	[-]	[-]	[mm]	[mm/d]	[mm/d]	[1/d]
Rural	0.983	2.70	186	4.94	0.70	-
Urban	0.830	1.08	51.1	4.79	0.99	1.47
Para.	beta	Kf/Kh	Ks	alpha	Tlag	Tlag for rural sub-flow
Unit	[-]	[1/d]	[1/d]	[-]	[-]	[-]
Rural	6.49	0.875	0.0036	8.04	83.7	39.5
Urban	1.60	0.510	0.0017	1.45	83.9	-

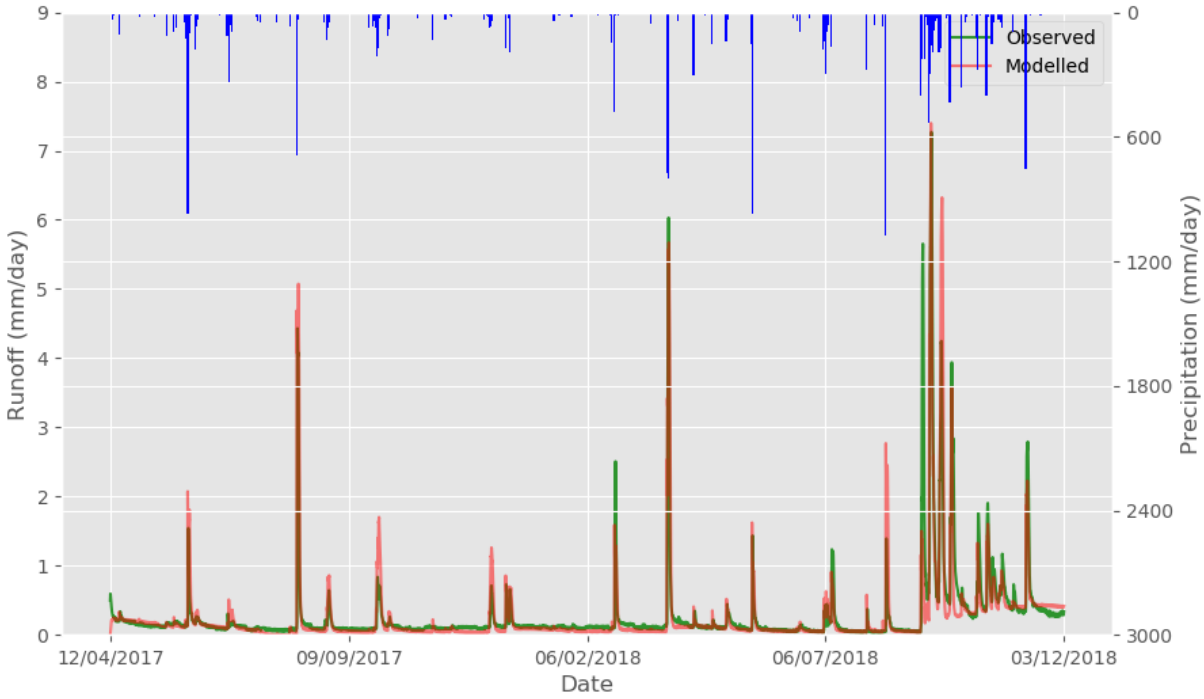

Figure 22. Semi-distributed model result for current simulation. (The blue histogram indicates rainfall intensity; green and red lines indicate the observed and modelled runoff time series)

4.3 The expression of LID practices in model

In this part, the hydrological meaning of current model structure is analysed. And based on the hydrologic meaning behind current model structure, the hydrologic routes for four representative LID practises are designed here for further analysis.

4.3.1 The expression of Bioretention

Since offline and online configuration of bioretention exploit different drainage methods, the configuration of bioretention needs to be discussed here. According to the "*SARA LID Guidance Manual"*, if the subsoil infiltration rate is less than 12.7 mm/hour (0.5 inch/hour), online configuration should be installed with an additional underdrain instead of offline configuration. However in "*Soil Survey of Bexar County, Texas"*, most of the soil in San Antonio City is labelled as moderately permeable which generally meet the requirement for offline configuration. Therefore, considering the financial aspect, offline configuration of bioretention is exploited in this project.

From a hydrologic perspective, bioretention is one of the most effective LID practices to capture runoff with thick layer of soil and lush vegetation, which could mimic nearly all water processes in a complete natural system. The main hydrologic functions of an offline bioretention could be summarized as:

(1) Interception. The interception is mainly realized by lush green land canopies in a bioretention. The interception capacity changes with different vegetation condition in a wide range.
(2) Transpiration. Transpiration is the biological water consumption by plants, which is mainly influenced by vegetation condition and the water retention capacity of the soil layer.
(3) Infiltration/Percolation. The infiltration/percolation function refers in particular to the water infiltration or percolation from subsoil into deep groundwater. The infiltration capacity could be seen as a relatively stubborn parameter depends on the local soil characteristics.
(4) Delay. All of the above three water processes consume runoff volume essentially. However except the quantitative water consumption, the delay function is also realized in the slow soil

soaking process. The runoff delay process is also one important hydrologic process to extend the flooding time and reduce peak flow.

(5) Storage. The water storage function of bioretention is mainly realized by soil layer and vegetation interception.

In the model, two additional Interception Reservoir (IR) and Unsaturated Reservoir (UR) are designed to simulate the interception, transpiration and percolation routes of the bioretention. And a symmetric time lag function is exploited to simulate the delay function of bioretention cells. And because of the offline configuration, there is no need to build an additional artificial underdrain to connect bioretention and urban drainage system. The schematic figure of updated urban model components for the bioretention scenario is shown as Figure 23.

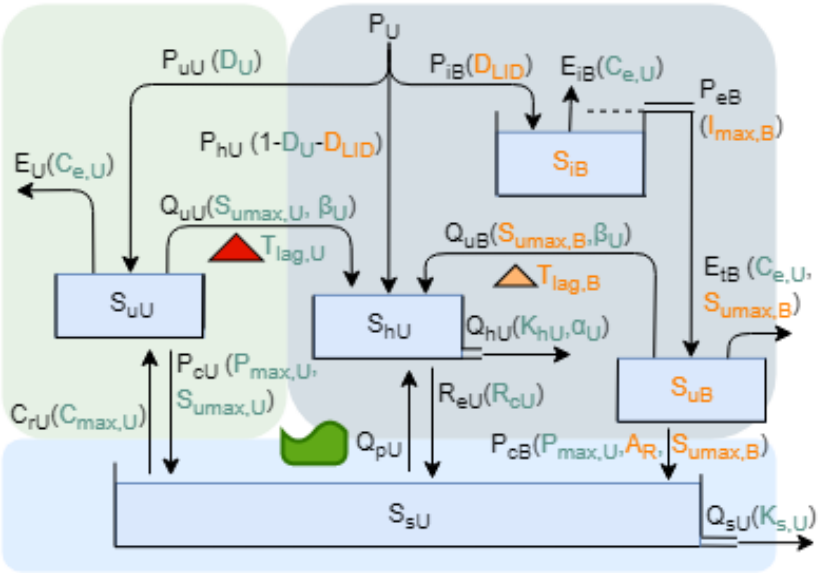

Figure 23. Schematic figure of updated urban model components for bioretention scenario

With the mathematical expressions of hydrologic routes relating to the bioretention:

Water process	Mathematical expression
Precipitation on bioretention cells	$P_{iB} = D_{\mathrm{LID}} * P$
Evaporation (Interception)	$E_{iB} = C_e E_r * D_{\mathrm{LID}}/A_R$
Effective precipitation after interception	$P_{eB} = S_{iB} - I_{max,B}$
Transpiration from bioretention cells	$E_{tB} = (C_e E_r - E_{iB}) * D_{\mathrm{LID}}/A_R * (\frac{S_{uB}}{S_{umax,B}})$
Overflow from bioretention cells	$Q_{uB} = P_{eB} * \left(\frac{S_{uB}}{S_{umax,B}}\right)^{\beta_U}$
Percolation from bioretention cells to groundwater	$P_{cB} = \frac{P_{cmax} * D_{\mathrm{LID}}}{A_R} * \frac{S_{uB}}{S_{umax,B}}$
Time lag of overflow from bioretention cells	$f = \begin{cases} \frac{4t}{(T_{lagB})^2}, 0 < t < \frac{T_{lagB}}{2} \\ \frac{4(T_{lagB}-t)}{(T_{lagB})^2}, \frac{T_{lagB}}{2} < t < T_{lagB} \\ 0, t > T_{lagB} \end{cases}$

In which:

Parameter and Model Components	Description
D_{LID} [-]	Precipitation distribution factor for bioretention cells
A_R [-]	The ratio of construction area to drainage area

C_e [mm]	Evaporation coefficient
E_r [mm/d]	Reference Evaporation
$I_{max,B}$ [mm]	Maximum interception depth on bioretention cells
$S_{umax,B}$ [mm/d]	Maximum water storage depth in subsoil layer of bioretention cells
P_{cmax} [mm/d]	Maximum percolation velocity
S_{iB} [mm]	The depth of water storage in IR of bioretention cells
S_{uB} [mm]	The depth of water storage in UR of bioretention cells
T_{lagB} [-]	Time lag coefficient of bioretention cells

There are five parameters in the bioretention model component, the precipitation distribution factor (D_{LID}), the ratio of drainage area to construction area (A_R), the maximum interception depth ($I_{max,B}$), the maximum water storage depth in soil layer (S_{umax}), and time lag coefficient of bioretention cells (T_{lagB}).

Both of the precipitation distribution factor (D_{LID}) and the ratio of construction area to drainage area (A_R) depends on the concrete LID implementation plan, which two could be adjusted to fit the LID scenario. The parameter, D_{LID}, indicates the proportion of the drainage areas of bioretention cells to the whole urban grey (impervious) area.

And then the maximum interception depth ($I_{max,B}$) indicated the interception capacity of bioretention cells. Li et al. (2009) found that the intercept depths for six bioretention facilities ranged from 0.6 to 4.6 mm in Maryland, U.S. A relatively good vegetation condition of the bioretention is assumed in this project with the 3.5 mm interception capacity. To adapt this parameter into the urban module, the assumed interception capacity should be multiplied by the precipitation distribution factor (D_{LID}) and be divided by the ratio of construction area to drainage area (A_R), which is the final parameter, $I_{max,B}$;

As for the maximum water storage depth $S_{umax,B,}$, according to "*SARA LID Guidance Manual"*, 0.6 to 1.2 m (2 to 5 feet) soil media depth is recommended for the bioretention design and the average soil media depth of the six typical bioretention facilities in the Maryland is referred as 0.84 m (Li et al. 2009). Considering these two recommended values, the depth of soil media layer is presumed as 0.85 m in this project, and an empirical soil porosity is chosen as 0.35 since the moderately permeable condition of local soil. Therefore, the water storage capacity for the bioretention is supposed as 300 mm. Then the water storage capacity should multiply with the precipitation distribution factor (D_{LID}) and be divided by the ratio of construction area to drainage area (A_R), which is the estimated value of parameter $S_{umax,B}$;

Finally, according to a field test by Hunt. (2008), the peak flow of the bioretention cell could be delayed by 3 hours. Therefore according to the mathematical expression, the reference of time lag coefficient (T_{lagB}) is assumed to be 13 without dimension for bioretention cells.

4.3.2 The expression of Vegetated swales

The main function of vegetated swales is water transportation rather than water retention as bioretention cells. Therefore although vegetated swales share a similar configuration as bioretention, with far smaller size of vegetation and far thinner soil layer, the transpiration capacity of most vegetated swales is small and only a small volume of rainfall would be intercepted by vegetation in the early water transportation process compared to the bioretention cells. In general, the evaporation function (both of the transpiration and interception) of vegetated swales is weak and it could be neglected compared to the other two important hydrologic processes:

(1) Delay. As mentioned before, the bioretention cells realize the delay function by slow soil soaking process. Different from the delay function of the bioretention cells, vegetated swales

realize the runoff delay in water conveyance process. With the rough vegetation surface, vegetated swales extend the water transportation time greatly compared to traditional urban water conveyance measures like concrete gutters and curbs, which is helpful to reduce peak flow.

(2) Infiltration/Percolation. With the runoff delay function, the time for infiltration is also extended in water conveyance process by vegetated swales.

In the model, an additional Vegetated Swales Reservoir (VSR) would be designed to simulate vegetated swales. Part of precipitation in impervious grey areas would be collected and conveyed by VSR with a precipitation distribution factor D_2. The value of D_2 depends on the contribution area of vegetated swales.

As for the configuration regulation, the same minimum infiltration capacity for offline vegetated swales is required as 12.7 mm/hour (0.5 inch/hour). Although most of the soil in San Antonio City meet the requirement for offline configuration, to improve the diversity of LID configuration and to distinguish from the offline bioretention designed above, the online configuration of vegetated swales is exploited in this project. Therefore an additional artificial underdrain from VSR to HR should be designed for the online configuration. A linear drainage system is assumed for vegetated swales with a discharge coefficient (Kvs). To simulate the runoff delay function, the discharge coefficient of vegetated swales (Kvs) should far smaller than the discharge coefficient of traditional water conveyance system (Kr).

In addition, since the percolation capacity mainly depends on the local soil characteristics and the moisture condition of the soil, there should be large similarity of percolation velocity between the green surface and vegetated swales. Therefore the percolation velocity (P_{cVR}) of vegetated swales could be assumed as the same as the percolation velocity of other green surface (P_{cU}) in urban area. The schematic figure of updated urban model components for vegetated swales scenario is shown as Figure 24.

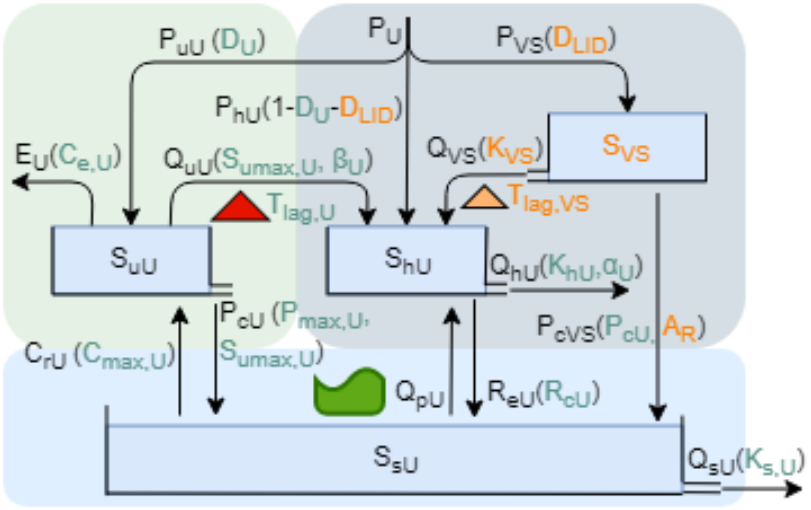

Figure 24. Schematic figure of updated urban model components for Vegetated Swales scenario

With the mathematical expression of hydrologic routes relating to vegetated swales:

Water process	Mathematical expression
Precipitation flow through vegetated swales	$P_{VS} = D_{\mathrm{LID}} * P$
Discharge from vegetated swales	$Q_{VS} = K_{VS} * S_{VS}$
Percolation from vegetated swales to groundwater	$P_{cVS} = \frac{P_{cU}}{A_R} * D_{\mathrm{LID}}$

Time lag of runoff from vegetated swales

$$f = \begin{cases} \frac{4t}{(T_{lagVS})^2}, 0 < t < \frac{T_{lagVS}}{2} \\ \frac{4(T_{lagVS}-t)}{(T_{lagVS})^2}, \frac{T_{lagVS}}{2} < t < T_{lagVS} \\ 0, t > T_{lagVS} \end{cases}$$

In which:

Parameter and Model Components	Description
D_{LID} [-]	Precipitation distribution factor for vegetated swales
A_R [-]	The ratio of construction area to drainage area
K_{VS} [mm]	Discharge coefficient of vegetated swales
S_{VS} [mm]	Water storage depth in vegetated swales
P_{cU} [mm/d]	Percolation velocity of urban green areas
T_{lagVS} [-]	Time lag coefficient of vegetated swales

There are four parameters in the vegetated swales model component, precipitation distribution factor (D_{LID}), the ratio of drainage area to construction area (A_R), time lag coefficient (T_{lagVS}) and discharge coefficient (K_{VS}).

Both of the precipitation distribution factor (D_{LID}) and the ratio of construction area to drainage area (A_R) depends on the concrete LID implementation plan, which two could be adjusted to fit the LID scenario. The parameter, D_{LID}, indicates the proportion of the drainage areas of bioretention cells to the whole urban grey (impervious) area.

According to a field monitoring result in King City, Ontario (Van Seters, 2006), the peak flow of the vegetated swales could be delayed by 2.5 h. Therefore according to the mathematical expression, the reference of time lag coefficient (T_{lagVS}) is assumed as 11 for vegetated swales;

Different from other volume-based LID practices, the vegetated swales are flow-based control practices (more information could be found *in Flow-based control practices in Appendix*). Therefore hydraulic calculation equation is considered here for the estimation of K_{VS}. The discharge coefficient (K_{VS}) is determined by the hydrologic characteristic of vegetated swales such as the vegetation condition, the slope and the shape of cross section. Manning-Strickler formula is used to estimate the K_{VS} parameter:

$$V = \frac{k}{n} R_h^{2/3} S^{1/2}$$

where:

Character	Description
V [L/T]	The cross-sectional average velocity
n [-]	The Gauckler–Manning coefficient
R_h [L]	The hydraulic radius
k [$L_{1/3}$/T]	The conversion factor
S [L/L]	The slope of the hydraulic grade line or the linear hydraulic head loss

It is assumed that there is no obvious difference of the conduit configurations between the reformed vegetated swales and traditional concrete gutters and curbs, and therefore the factors relating to

conduit configuration, R_h and S, would keep the same value. The main influencing factor of discharge is Manning coefficient which depends on the roughness of channel surface.

The normal n value is exploited to compare the water transportation velocity of vegetated swales and concrete gutters in Table 8. And the discharge coefficient k should be directly proportional to Manning's n values. With the known discharge coefficient of conventional water conveyance system (K_h) as 0.51, the discharge coefficient of vegetated swales (K_{VS}) could be speculated as 0.34.

Table 8. Empirical Manning's n Values Table (Chow, 1959)

Type of Channel and Description	Minimum	Normal	Maximum
Shotcrete, good section	0.016	0.019	0.023
Grass, some weeds	0.025	0.030	0.033

4.3.3 The expression of Green roof

As the introduction below, all the green roof have underdrain system in case of the oversaturation of soil layer and the overweight load on roof. There are three dominant hydrologic functions of green roofs:

(1) Interception. A large proportion of water consumption of the green roof is created by plant interception. The specific interception capacity of intensive and extensive green roofs varies a lot.
(2) Transpiration. Transpiration is the biological water consumption by plants. Similarly as the interception process, the transpiration capacity of green roofs depends on both of the vegetation type and the thickness of soil layer.
(3) Storage. Similarly as the bioretention, the water storage function of green roofs is mainly realized by soil layer, which could also be seen as an accessory function of soil layer.
(4) Delay. The delay function of green roof is realized in slow soil soaking process, which could be seen as an accessory function of soil layer.

Since the high requirement of roof structure and the prerequisite of drip irrigation device, the intensive green roof may be not an attractive option for San Antonio Citizens. Extensive green roofs are designed here.

In the model, two additional Interception Reservoir (IR) and Unsaturated Reservoir (UR) are designed to simulate the interception and transpiration routes of extensive green roofs as shown in Figure 25.

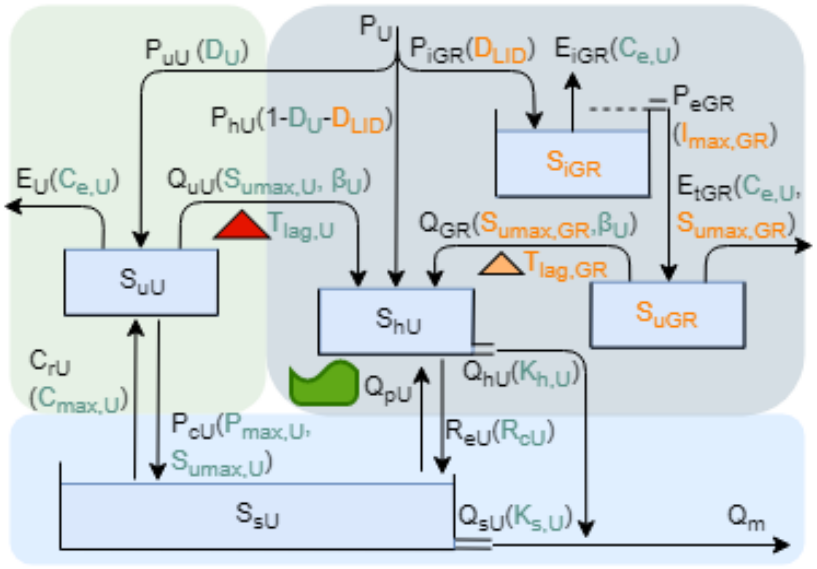

Figure 25. Schematic figure of updated urban model components for Green Roofs scenario

With the mathematical expression of hydrologic routes relating to Green roofs:

Water process	Mathematical expression
Precipitation on green roofs	$P_{iGR} = D_{\mathrm{LID}} * P$
Evaporation (Interception)	$E_{iGR} = C_e E_r * D_{\mathrm{LID}}$
Effective precipitation after interception	$P_{eGR} = S_{iGR} - I_{max,GR}$
Transpiration from green roofs	$E_{tGR} = (C_e E_r - E_{iGR}) * D_{\mathrm{LID}} * (\frac{S_{uGR}}{S_{umax,GR}})$
Overflow from green roofs	$Q_{GR} = P_{eGR} * \left(\frac{S_{uGR}}{S_{umax,GR}}\right)^{\beta_U}$
Time lag of runoff from green roofs	$f = \begin{cases} \frac{4t}{(T_{lagGR})^2}, 0 < t < \frac{T_{lagGR}}{2} \\ \frac{4(T_{lagGR}-t)}{(T_{lagGR})^2}, \frac{T_{lagGR}}{2} < t < T_{lagGR} \\ 0, t > T_{lagGR} \end{cases}$

In which:

Parameter and Model Components	Description
D_{LID} [-]	Precipitation distribution factor for green roofs
C_e [mm]	Evaporation coefficient
E_r [mm/d]	Reference Evaporation
$I_{max,GR}$ [mm]	Maximum interception depth on green roofs
$S_{umax,GR}$ [mm/d]	Maximum water storage in subsoil layer of green roofs
S_{iGR} [mm]	Water storage depth in IR of green roofs
S_{uGR} [mm]	Water storage depth in UR of green roofs
T_{lagGR} [-]	Time lag coefficient of green roofs

Four parameters involved in the green roofs model component need to be adjust to simulate the green roofs scenario, the precipitation distribution factor (D_{LID}), the maximum interception depth ($I_{max,GR}$), the maximum water storage in soil layer ($S_{umax,GR}$) and the time lag coefficient (T_{lagGR}).

The precipitation distribution factor (D_{LID}) depends on the ratio of the covered urban area by green roofs and the total urban impervious area, which could be adjusted to fit the designed LID implementation scenario;

Besides, similar to the bioretention, the maximum interception depth parameter ($I_{max,GR}$) depends on the interception capacity of green roofs and the area distribution factor. Different from the bioretention, the area distribution factor of green roofs is always equal to the precipitation distribution factor (D_2), since no additional rainfall would be discharged to green roofs. And the interception capacity of green roofs could be estimated as 3.1 mm based on the studies of green roofs interception by Carter and Jackson (2007); Therefore the parameter, $I_{max,GR}$, would be $3.1*D_{LID}$ (mm);

And the soil layer depths of most of the extensive green roofs are smaller than 15 cm and in "*SARA LID Guidance Manual"* 10 to 15 cm (4 to 6 inches) media depths are recommended for extensive green roofs. In this project, 12 cm is selected as media depth of green roofs with 0.35 porosity. Therefore the maximum water storage capacity for green roofs is assumed as 42 mm. Then the precipitation distribution factor (D_{LID}) should be exploited to multiply with the storage capacity, which is the estimated value of parameter $S_{umax,GR}$;

Finally, according to Carter (2006), average runoff lag times is 34.9 minutes for the green roof. Therefore, the time lag of peak runoff is assumed as 30 min and correspondingly the time lag coefficient (T_{lagGR}) is 3 for the green roof here.

4.3.4 The expression of Permeable pavement

Although permeable pavements have various configurations such as the porous asphalt, the pervious concrete, and permeable interlocking concrete pavers, the hydrologic functions of these pervious pavements could be ordinary summarized into three points:

(1) Infiltration/Percolation. The infiltration capacity of permeable pavements depends largely on the soil characteristic. For very high permeable soil, the infiltration efficiency of permeable pavements could reach one hundred percent (Bean et al. 2007). As for the soil without sufficient infiltration capacity, additional underground detention facility could be operated to promote infiltration.
(2) Storage/Interception. Most of LID measures realize the water storage function with the porosity between soil particles. However the permeable pavements provide water storage space not only in the subsoil layer, but also in the porous pavement media. This retaining water by porous pavements could also be seen as interception.
(3) Delay. The delay function of permeable pavements usually come with the rainwater infiltration and storage processes.

In the model, one additional Permeable Pavement Reservoir (PPR) is designed to qualitative describe the relevant hydrologic routes of pervious pavements as shown in Figure 26.

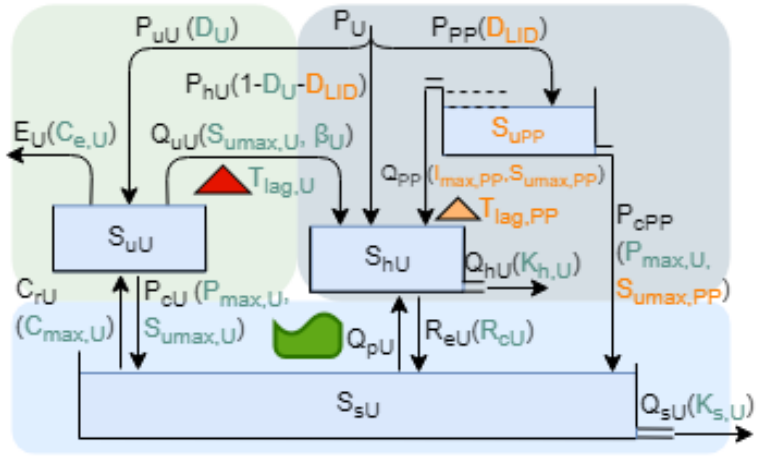

Figure 26. Schematic figure of updated urban model components for Pervious Pavements scenario

With the mathematical expression of hydrologic routes relating to pervious pavements:

Water process	Mathematical expression
Precipitation on permeable pavements	$P_{PP} = D_{\mathrm{LID}} * P$
Overflow from permeable pavements	$Q_{PP} = S_{PP} - (I_{max,PP} + S_{umax,PP})$
Percolation from permeable pavements to groundwater	$P_{cPP} = \begin{cases} P_{cmax} * D_{\mathrm{LID}} * \frac{S_{PP}}{S_{umax,PP}}, S_{PP} < S_{umax,PP} \\ P_{cmax} * D_{\mathrm{LID}}, S_{PP} > S_{umax,PP} \end{cases}$
Time lag of runoff from permeable pavement	$f = \begin{cases} \frac{4t}{(T_{lagPP})^2}, 0 < t < \frac{T_{lagPP}}{2} \\ \frac{4(T_{lagPP}-t)}{(T_{lagPP})^2}, \frac{T_{lagPP}}{2} < t < T_{lagPP} \\ 0, t > T_{lagPP} \end{cases}$

In which:

Parameter and Model Components	Description
D_{LID} [-]	Precipitation distribution factor for pervious pavements
$S_{umax,PP}$ [mm]	Maximum water storage in subsoil layer of pervious pavements
$I_{max,PP}$ [mm]	Maximum interception depth on permeable pavements
P_{cmax} [mm/d]	Maximum percolation velocity
S_{PP} [mm]	Water storage depth in PPR
T_{lagPP} [-]	Time lag coefficient of permeable pavements

Four involved parameters in permeable pavement model component need to be adjust to simulate the green roofs scenario, the precipitation distribution factor (D_{LID}), the maximum interception depth ($I_{max,PP}$), the maximum water storage depth ($S_{umax,PP}$), and time lag coefficient (T_{lagPP}).

Since the ratio of drainage area to construction area of permeable pavements is recommended as 1:1 in "*SARA LID Guidance Manual"*, the contribution area is exact the covered area of permeable pavements. And the precipitation distribution factor (D_{LID}) will depend on the ratio of the covered area by permeable pavements to the total urban grey surface area. The parameter D_{LID} would be adjusted to fit the designed LID implementation scenario;

Besides, as for the maximum interception depth ($I_{max,PP}$), Collins et al. (2008) found that concrete grid paver and permeable interlocking concrete pavements could retain 6 mm of rainfall with no runoff, which number may be less for the porous asphalt and the pervious concrete. In this project, 4 mm is

selected as the normal interception capacity for all kinds of permeable pavements. This number would be multiplied by area/precipitation distribution factor (D_{LID}) as the parameter $I_{max,PP}$;

In addition, in "*SARA LID Guidance Manual"* the minimum 30 cm (12 inches) subsoil is recommended for offline permeable pavements. In this project, 35 cm is selected as the subsoil depth of permeable pavements with 0.35 porosity. Therefore the maximum water storage capacity for permeable pavements is presumed as 120 mm. And then the factor D_{LID} should be used to multiply with the storage capacity, which is the estimated value of parameter $S_{umax,PP}$;

Finally, according to a field monitoring result in King City, Ontario (Van Seters, 2006), the peak flow of the permeable pavements could be delayed by 2.5 h. Therefore according to the mathematical expression, the reference of time lag coefficient (T_{lagPP}) is assumed to be 11 for permeable pavements.

4.3.5 Hydrological comparison of LID measures

The hydrologic functions of four representative LID practises analysed before could be summarized in Table 9. In summary, bioretention cells, as the most effective LID practice among these four LID practises, could mimic nearly all water processes in a complete natural system. And the other three LID practices all have their own drawbacks.

Table 9. The hydrologic functions of four representative LID practises

	Interception	Transpiration	Infiltration	Storage	Delay
Bioretention	++	++	++	++	++
Vegetated swales	+	+	++	+	++
Green roof	++	++	-	-	+
Permeable Pavement	++	-	++	+	++

Symbols: ++ major function; + accessory function; - insignificant function;

And the quantitative comparison of the parameter values and their physical meaning are shown in Table 10. The parameters shown here denote a favourable LID implementation condition.

Table 10. The comparison of physical processes and their parameter expression in model

Physical Meaning	Prec. dist. factor [-]	Drainage area / Construction area [-]	Max intercept. Capacity [mm]	Max. storage capacity [mm]	Time lag of peak runoff [h]	Discharge coefficient [-]
Urban green area	0.779	1	-	51	-	-
Bioretention cell	D_B	$A_{R,B} \geq 1$	3.5	300	3	-
Vegetated swale	D_{VS}	$A_{R,VS} \geq 1$	-	-	2.5	0.34
Green roof	D_{GR}	1	3.1	42	0.5	-
Permeable Pavement	D_{PP}	1	4	120	2.5	-
Parameters	D [-]	A_R [-]	Imax [mm]	Sumax [mm]	Tlag [-]	K [-]
Urban green area	0.779	-	-	51	-	-
Bioretention cell	D_B	$A_{R,B} \geq 1$	$3.5/A_R*D_B$	$300/A_R*D_B$	13	-
Vegetated swale	D_{VS}	$A_{R,VS} \geq 1$	-	-	11	0.34
Green roof	D_{GR}	-	$3.1*D_{GR}$	$42*D_{GR}$	3	-
Permeable Pavement	D_{PP}	-	$4* D_{PP}$	$120*D_{PP}$	11	-

Symbols: - non-exist; The parameters, D and A_R, depend on the concrete LID implementation scenarios

5

The urban development forecast and scenario design

To deal with the prediction uncertainty, scenario analysis is exploited for the influence study of urban development on rainfall-runoff relationship. In this Chapter, the development plan of San Antonio is analysed and three urbanized CD scenarios in 2040 are designed in *0 5.1 Urban development forecast* scenarios. In *5.2 The expression of urban development in model*, the expression of urban development in model is explained.

5.1 Urban development forecast scenarios

5.1.1 Development plan of San Antonio City

The following information was retrieved from the *City of San Antonio: Comprehensive Plan* issued in 2016.

According to 2014 US Census, San Antonio, with a total population of 1.44 million, had become the seventh largest city in the US and still keeps a stable growth rate. Projected growth for Bexar County is expected to add up to 1.1 million new residents, with 500,000 new jobs, and 500,000 new dwelling units between 2010 and 2040. An updated developing plan needs to be proposed to deal with the opportunities and challenges driven by the new growth for the San Antonio region.

Over the past few decades, due to sufficient land resources in Bexar County, San Antonio City was experiencing the unconstrained outward growth. The continued outward urban expansion has led to the perception of disinvestment in the urban core and the heavy pressure of high cost of infrastructure and utility service. Therefore instead of the former oversupply of land in underutilized commercial and industrial zones, the strategic infill and retrofit of the existing suburban fabric offers the best way forward.

In the aspect of land use type, a Land and Development Capacity Study of San Antonio City found that the current residential zoned land cannot afford the forecasted demand for housing particularly within the north part of the city by 2040. To release the housing pressure, the residentially-focused, mixed-use neighbourhoods would be repositioned in the areas with large concentrations of vacant and underutilized commercial and industrial-zoned parcels. Besides, in several targeted locations the slightly higher density of neighbourhoods would be invested and the multi-family residential areas would be developed instead of the single-family residential area.

5.1.2 Scenarios design of urban development

According to the projected growth information provided by "*City of San Antonio: Comprehensive Plan"*, there will be 1.1 million new residents and 500,000 new dwelling units between 2010 and 2040, which could be used as the basis to predict the future development scenarios of San Antonio City. In this project the time of current situation could be defined as 2017 with relatively complete statistical data. Therefore from 2017 there would be 0.9 million new residents by 2040. In addition,

the development strategy of San Antonio City could be ascribed to two points, less expansion and higher density.

Based on the projected growth information above, three urban development scenarios in 2040 could be designed between the fully infill and partly sprawl development strategy as shown in Table 11. The first scenario offers a fully infill development situation. In this scenario the urban areas would keep the same number as 1,209 km2 (data in 2017) in 2040 and the space for all the new population and dwelling would be provided in the urban area. The second scenario presents a partial infill and partial sprawl development situation. In this scenario 70% of the new dwelling would be developed in urban areas and the last 30% dwelling would be developed in sprawling suburban areas with a certain extent of urban expansion. In the last scenario, 50% of the new residents are assumed to stay in sprawling suburban areas and the other 50% would infill current vacant and underutilized urban areas for the next 23 year (2017-2040).

Table 11. Urban development scenarios between 2017 and 2040

Scenarios	New residents follows infill development [%]	Total residents in current urban areas (million)	New residents follows sprawl development [%]	New residents in urban expansion areas (million)
Current (2017)	-	1.5	-	-
A (2040)	100	2.4	0	0
B (2040)	70	2.13	30	0.27
C (2040)	50	1.95	50	0.45

5.2 The expression of urban development in model

In the hydrological model the sprawl development strategy could be expressed with larger proportion of urban areas and smaller proportion of rural areas in the study catchment; And the higher-density infill development strategy could be reflected with larger distribution factor of grey areas within a relatively stable urban areas (1-D). The concrete mathematical expressions of the three urban development scenarios are shown in Table 12, which are under the premise of several assumptions:

1. The level of urban construction and water drainage system are assumed to be roughly consistent in the whole urban areas (including the current urban areas and future urban expansion area).
2. Since the infill development strategy may bring the compact of people living space, per capita urban grey areas for scenario A is assumed to be 0.85 times of the current per capita urban grey area; and for scenario B, this number would increase to 0.9; the scenario C is assumed to keep the same level of per capita grey areas as current situation.

Table 12. Parameter calculation table of Urbanization Scenarios

	Num.	*Calculating formula*	**Current (2017)**	**A (2040)**	**B (2040)**	**C (2040)**
Total residents (million)	*(1)*	*Known*	1.5	2.4	2.4	2.4
The residents in current urban areas (million)	*(2)*	*From Table 11*	1.5	2.4	2.13	1.95
The residents in urban expansion areas (million)	*(3)*	*From Table 11*	0	0	0.27	0.45
Per capita urban areas (m2)	*(4)*	*1209.5 km2 /(2)*	806.3	504.0	567.8	620.3
Expansion areas (km2)	*(5)*	*(3)*(4)*	0	0	153.3	279.1

Total urban areas after expansion (km2)	*(6)*	*1209.5 km2 +(5)*	1209.5	1209.5	1362.8	1488.6
The proportion of urban areas in study catchment	*(7)*	*(6)/4544.3 km2*	0.266	0.266	0.300	0.328
Distribution factor of grey areas (1-D)	*(8)*	*Model result; (9)/(6)*	0.170	0.232	0.218	0.221
Total urban grey areas (km2)	*(9)*	*(8)*(6); (10)*(1)*	206	280	297	330
Per capita urban grey areas (m2)	*(10)*	*(9)/(1); (10_current)*(11)*	137	117	124	137
Compact factor of Per capita urban grey areas (-)	*(11)*	*Assumption*	1	0.85	0.9	1

**The shaded numbers are used to adapt current model to urban developed model*

6

The character analysis of LID practises and scenario design

Since the promotion of LID concept during the 1990's, plenty of LID practices are designed and introduced to incorporated in different field conditions and to realize different functions. Besides, relevant technical guidance and guideline are also developed by different government institutions and technical companies these years, which describe a relatively full picture of these LID practises and provide a reliable and operable design manual for LID implementation. A basic local LID implementation criteria and assessment method are described in *Appendix E Relevant LID implementation criteria and assessment.*

In this chapter, 4 widely applied LID practices are selected and analysed here as examples for further analysis. The brief introductions of the 4 LID practices are presented in *6.1 A brief introduction of 4 representative* LID practices. And their expression methods in model are designed respectively in *0.* Five LID implementation scenarios are designed in *6.2 LID implementation* scenarios.

6.1 A brief introduction of 4 representative LID practices

6.1.1 Introduction for bioretention cells

The bioretention is also known as rain garden or depressed green. It is one of the most effective LID practice which mimic the natural system before the city development very well. Bioretention is a shallow depressed green area which could integrated into highly developed city areas and also increase the aesthetic feeling for urban people. Therefore it is also one of the most common LID practises.

There are 4 components for a typical bioretention (San Antonio River Authority, 2015):

1. pre-treatment system: The pre-treatment could be a forebay which is helpful to retain the sediment and prevent the structure erosion;
2. surface ponding area: The surface ponding area provide a small space to retain water temporary;
3. mulch layer: The mulch layer protects the small or medium size plant;
4. planting soil media: The planting soil layer provides most moisture for vegetation;

The bioretention cells could be designed as an online or offline measures. For online designs, there should be an underdrain connecting the bioretention cells to urban water collection system. For offline designs, no underdrain system is needed. If large water retention capacity is needed, more ponding space and thicker soil layer could be designed and larger size of plant could be grown. An example of a bioretention cell is shown in Figure 27.

Figure 27. Bioretention cell (left) and Vegetated Swales (right) (Resources: NACTO and Susdrain)

6.1.2 Introduction for Vegetated Swales

Vegetated swales are shallow and narrow open channels to convey the rainfall which could be a favourable alternative LID practice of traditional concrete gutters and curbs. Vegetated swales share a similar configuration as the bioretention with the same depressed green area and small or medium size plants. However the vegetated swales focus more on the runoff conveyance rather than water storage and consumption function.

The vegetated swales could be designed as an online or offline measures. For online designs, the outlet of vegetated swale should be connected to urban water collection system. For offline designs, a diversion or bypass structure could be installed for high flows. An example of a vegetated swales is shown in Figure 27.

6.1.3 Introduction for Green roof

Green roof is also one of the most popular LID practises because of its multiple advantages. The configuration of green roof varies from extensive green roof to intensive green roof according to the thickness of soil media. The intensive green roof with greater depth of soil layer allows larger size and number of vegetations. More rainwater could be intercept by the canopy of vegetations, and excepted the hydrological benefit the intensive green roof could also be helpful to keep the house in a stable temperature by reducing the heat flux.

But the cost of intensive green roof is higher than extensive green roof. The stability requirement of roof structure is higher for intensive green roof to support the heavier soil media than extensive green roof. And according to the introduction of the LID technical design guidance manual of San Antonio River Authority, intensive green roofs in the San Antonio region may require drip irrigation to sustain vegetation through hot summer months.

The hydrological performance of different green roofs varies a lot, which is also a hot research topic these years. For example, as the brief description above, different depths of by soil layer lead to a difference on water retention capacity (Berndtsson, 2010; Bianchini, 2012). Different species of vegetation also cause a different interception capacity (Berndtsson, 2010; Dvorak, 2010). And different slopes of roof lead to different delay time of peak runoff (Vanwoert, 2005; Getter, 2007; Berndtsson, 2010).

In case of the oversaturation of soil layer, a drainage system should be designed on the roof, which means that except the water consumed by evaporation (including interception on canopy and

transpiration by plants), every drop of runoff will be discharged to urban pipeline system at last. The example of extensive and intensive green roof are shown in Figure 28.

Figure 28. Extensive (left) and intensive (right) green roof (Resources: 2030 PALETTE and Skyluxe)

6.1.4 Introduction for Permeable Pavement

Permeable pavements could be seen as a multifunction LID practice which could enjoy the hydrologic benefit of high infiltration and storage capacity and at the same time it could also be flexibly incorporated in different pavement-needed surroundings.

Different materials of permeable pavements are provided in the market for selecting according to varies field conditions. For example the porous asphalt could be utilized for parking lots; The low traffic roads could be paved with the pervious concrete; And permeable interlocking concrete pavers could be used for walkway. The example of permeable interlocking pavers and porous asphalt are shown in Figure 29.

Figure 29. Permeable interlocking pavers (left) and Porous asphalt (right) (Resources: MASONRY DESIGN and NCAT Auburn University)

Most of the water volume reduction function of permeable pavements is realized by infiltration. At some places with high permeable soil, the infiltration efficiency could reach one hundred percent (Bean et al. 2007).

6.2 LID implementation scenarios

The local LID implementation regulation is studied as shown in *E.2 LID* implementation assessment in Appendix. It is found that the implementation of LID measures is not strictly mandatory for every development/redevelopment project in Bexar County and there is a great flexibility of LID measure selection for project managers. Therefore the designed LID implementation scenario in this project

would not focus on the forecast of real local LID implementation condition of San Antonio City in 2040, and alternatively an idealized LID implementation scenario would be designed in this project.

Five scenarios are formulated and tested based on the urban development scenario C. The first four scenarios with single LID practice are designed to compare the different hydrologic performances of different LID practices, and the last mixed LID scenario is aimed to provide a practical LID implementation plan:

(1) Bioretention scenario: In this scenario, the contribution area of bioretention cells is assumed as the same as the drainage area. 15% of the precipitation on urban impervious grey surface would be collected and discharged to the offline bioretention.
(2) Vegetated swales scenario: In this scenario, 15% of the precipitation on urban impervious grey surface would be conveyed by vegetated swales.
(3) Extensive green roof scenario: In this scenario, 15% of the precipitation on urban impervious grey surface would be retained by extensive green roofs.
(4) Permeable pavement scenario: In this scenario, 15% of the urban impervious grey surface would be replaced by permeable pavement.
(5) Mixed LID scenario: In this scenario, 5% of the urban impervious grey surface would be covered by green roofs; 15% of the precipitation on urban impervious grey surface would be discharged to the offline bioretention and the construction area of bioretention would take 10% of the urban impervious grey surface; 15% of the precipitation would be conveyed by vegetated swales and the construction area of vegetated swales would take 5% of the urban impervious grey surface; 15% of the urban impervious grey surface would be replaced by permeable pavement.

As similar as the scenarios for urban development, the level of LID implementation is assumed to be roughly consistent in the whole urban areas (including the current urban areas and future urban expansion area).

And for the final mixed LID scenario, the cascade connections among these LID practices were designed as shown in Figure 30. In this cascade connection design, the overflow from green roof (Q_{GR}) would be conveyed to the UR of bioretention cells (S_{uB}), and then the overflow from bioretention cells (Q_{uB}) would be transported by vegetated swales (S_{VS}), and finally collected by HR (S_{hU}) which indicates urban drainage system. And for the permeable pavement, the overflow (S_{uPP}) is assumed to be collected by HR directly, considering the construction condition of permeable pavements in reality.

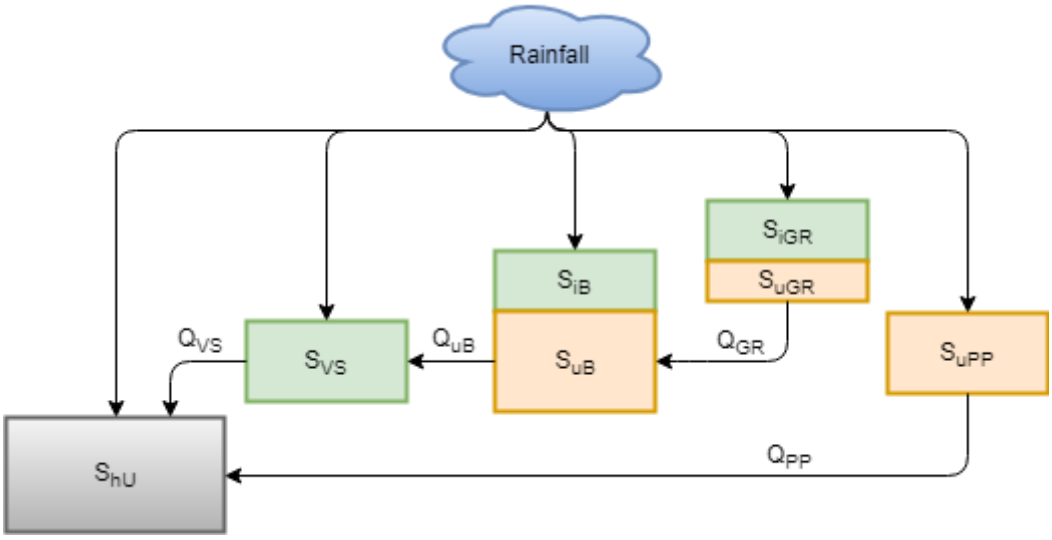

Figure 30. Cascade connection methods between different LID practices in the mixed LID scenario

7

Result

The research problem would be answered in this chapter with the results of four sub-problems corresponding to the four parts of this chapter.

7.1 The different hydrological characters of rural and urban areas

7.1.1 Parameters comparison of rural and urban lumped models

The different hydrological characters of rural and urban areas could be partly indicated by the different parameter intervals in rural and urban lumped models according to the parameter calibration results. The parameters which exist in both the rural and urban lumped models are compared and shown in Table 13.

It could be found from Table 13 that some parameters have different intervals between urban and rural areas: Firstly influenced by the favourable evaporation condition in rural areas, evaporation correction coefficient (Ce) for rural sub-catchment is larger than it for urban sub-catchment; Secondly, the groundwater discharge coefficient (Ks) for urban sub-catchment is far less than it for rural sub-catchment, which denotes a more drought condition with less base flow of urban sub-catchment in dry seasons; Thirdly, for the maximum unsaturated storage depth (Sumax), this parameter for urban sub-catchment has more uncertainty with larger interval than it for rural sub-catchment. And the minimum limitation of Sumax for urban areas is far less than it for rural areas since there is less soil media in urban areas than rural areas; Finally, the time lag (Tlag) for rural sub-catchment is larger than it for urban sub-catchment, which reveals the response time of rural areas is larger than it of urban areas.

And some parameters have similar interval between urban and rural areas: the maximum percolation velocity (Pmax) and the maximum capillary rise velocity (Cmax). One explanation could be that the test rural and urban sub-catchments have similar soil media, therefore the percolation and capillary rise abilities of rural and urban sub-catchments are similar. The other reason could be that the magnitudes of percolation and capillary rise are small compared to other forceful water processes, therefore the sensitivities of these two parameters are weak and it is difficult to distinguish the parameter preference.

Table 13. The comparison of parameter intervals in rural and urban lumped models

Para. range		Ce [-]	Sumax [mm]	Pmax [mm/d]	Cmax [mm/d]	Ks [1/mm*d]	Tlag [-]
Rural	Min	1	150	0	0	0	41
	Max	3	250	5	1	0.006	101
Urban	Min	0.5	30	0	0	0	21
	Max	3	375	5	1	0.0002	85

7.1.2 The different rainfall-runoff relationship of urban and rural area

Based on the parameter comparison of rural and urban lumped model above, it could be speculated that with smaller numbers of evaporation correction coefficient (Ce) and maximum unsaturated storage (Sumax), the evaporation process and water retention capacity in urban areas are undermined, which would bring more frequent peak flows as shown in Figure 31.

And with small value of groundwater discharge coefficient (Ks), the recharge capacity from groundwater to streamflow is extreme small in urban area, and therefore most of the base flow values in urban sub-catchment are close to zero.

In conclusion, the rainfall-runoff relationship of rural areas performs more moderate than it in urban areas. The character of the urban rainfall-runoff relationship varies between extreme flood and extreme drought.

For rural areas, the peak flows seldom happen since the large water retention capacity, especially in dry seasons. However when it comes to flood season, if the water retention capacity is exhausted, the peak flows will happen and the magnitude of peaks may be great. And the presence of peak runoff is always accompanied with the increase of base flow caused by large groundwater stock.

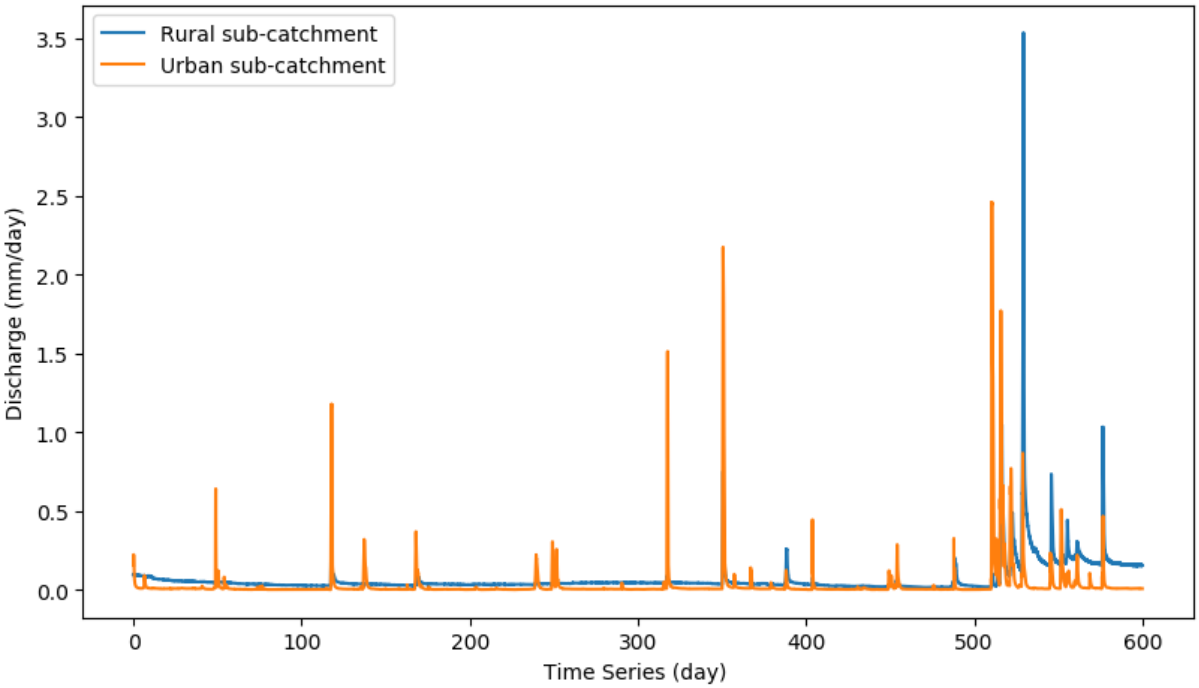

Figure 31. The runoff character comparison of rural and urban sub-catchments

7.2 The scenario analysis of urbanization influence on rainfall-runoff relationship

The model results and the histograms of the runoff values for the three urban developed scenarios are shown in Figure 32 and Figure 33. It could be found that the infill development strategy is more helpful to control peak runoffs than the sprawl development strategy.

Among the three urban development scenarios, scenario C always brought the largest runoff peak values which is also the most sprawl developed scenario. Particularly, the most extreme peak runoff in research period significantly raised by 16% from 7.4 mm/d to 8.6 mm/d. And for scenario B which depicts a 30%-sprawl and 70%-infill development picture, the peak flow increased by 7.5% from 7.4 mm/d to 8.0 mm/d.

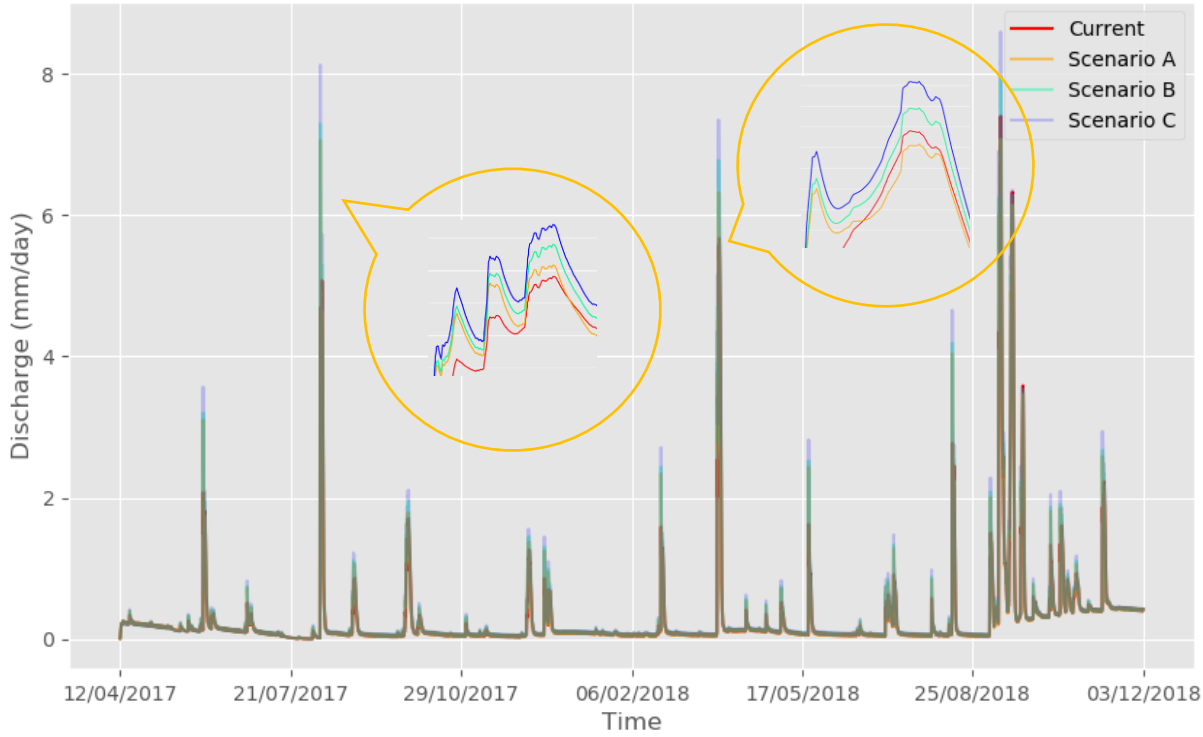

Figure 32. The total basin runoffs of the three urban developed scenarios

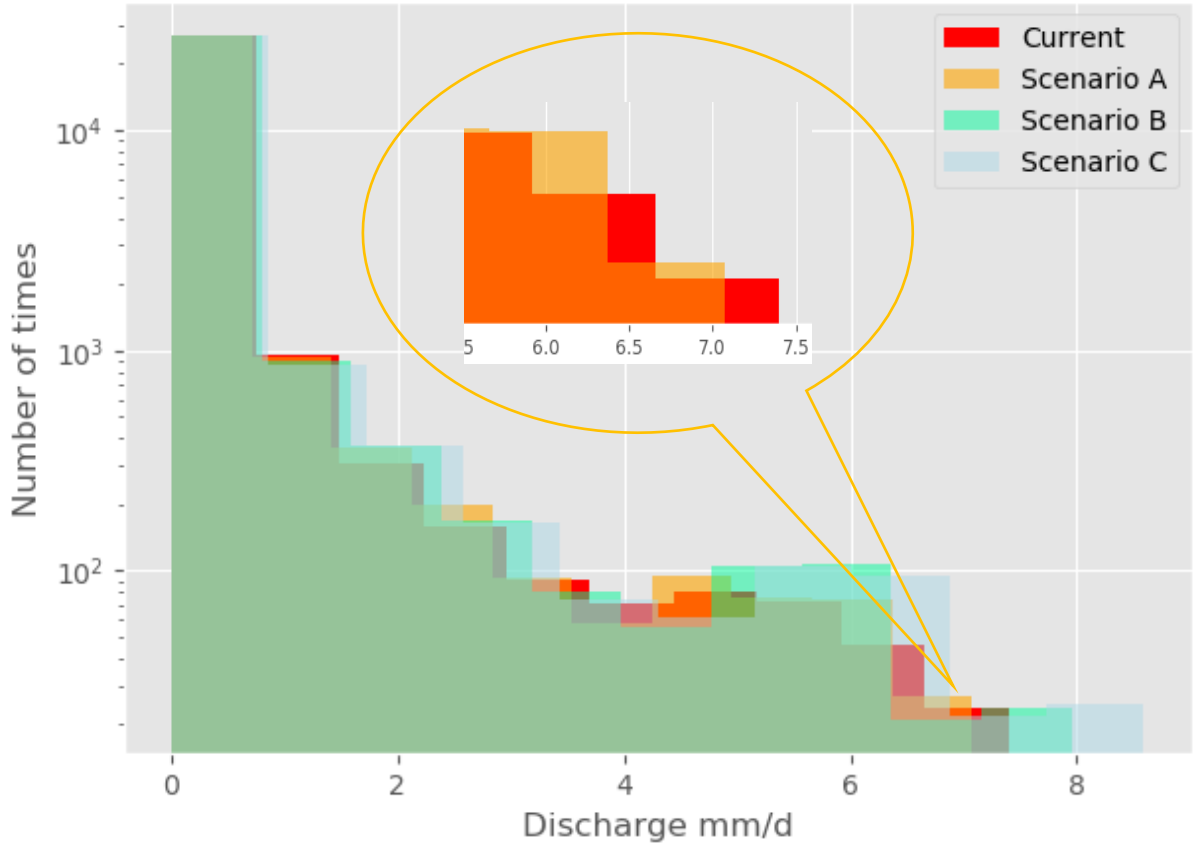

Figure 33. The histogram of the total basin runoff values of the three urban developed scenarios

As for the scenario A, there were also obvious increases for the small to medium peaks, but the most extreme peak runoffs are well controlled by scenario A as shown in Figure 33. This is because the

small to medium peaks are mostly generated from the rapid runoffs from urban grey areas and the extreme peak flows are always contributed by the large runoff volume from broad urban green surface. And with more urban grey areas and less urban green surface in scenario A, the small to medium peak runoffs from grey areas increase but the most extreme peak runoffs from green surface decline.

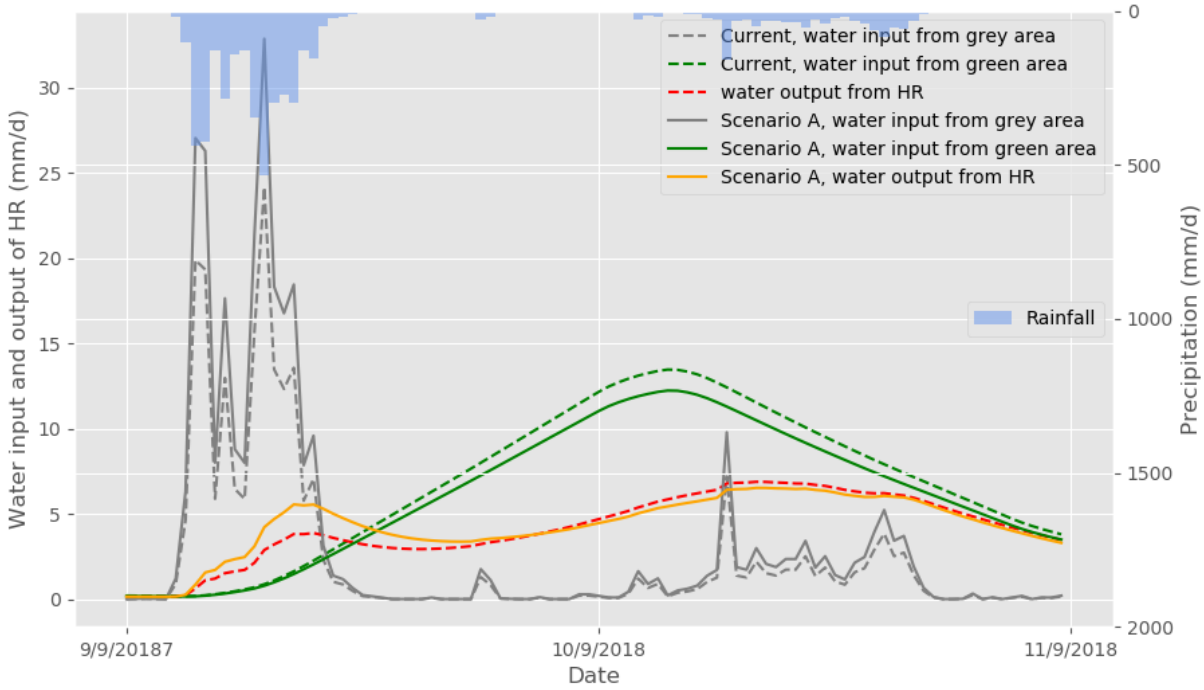

Figure 34. The water input and output of urban drainage system (HR) in current situation and urban development scenario A

Figure 34 shows the water input and output from urban drainage system (HR). The orange solid line and red dashed line indicate the outflow from HR for scenario A and for current situation respectively. It could be found that the water output lines experienced two peaks in succession. The first smaller peak is contributed by the fast input from urban grey surface (grey lines) and the second larger peak is generated from the slow input from urban green surface (green lines).

If comparing the scenario A (solid lines) and current situation (dashed lines), it could be found that there are more water input from urban grey areas and less input from urban green areas for scenario A. And correspondingly the first peak contributed by grey areas increased and the second peak generated from green areas declines.

In conclusion, similarly as rural areas, the peak runoff from urban green areas happens infrequently, but once it happens, the magnitude of peaks will be great. Therefore the most extreme peak flows are always contributed by the urban green surface. And the urban development scenario A cuts down the urban green areas which diminishes the value of extreme peak runoff.

The statistical information of the modelled runoff for three urban development scenarios is shown in Table 14. It could be found that all the three urban development scenarios brought the growth of total runoff volume. For the most critical scenario C, the total runoff will rise by 14.3% compared to current situation. For scenario B, this number falls to 8.7% and the scenario A has the least total runoff gain as 2.7%.

Table 14. The statistical analysis of modelled runoff results for three urban development scenarios

	Current	Scenario A	Scenario B	Scenario C
Total runoff volume in research period [mm]	159.6	163.9	173.5	182.5
Increase proportion of the total runoff [-]	-	2.7%	8.7%	14.3%
The maximum peak runoff [mm/d]	7.40	7.08	7.95	8.59
Increase proportion of the maximum peak runoff [-]	-	-4.3%	7.5%	16.1%

7.3 The scenario analysis of LID implementation influence on rainfall-runoff relationship

All the designed LID scenarios below were built based on the urban development Scenario C (called as “CD scenario forecast” below).

The model results of 5 LID scenarios and the CD scenario forecast are shown in Figure 35.

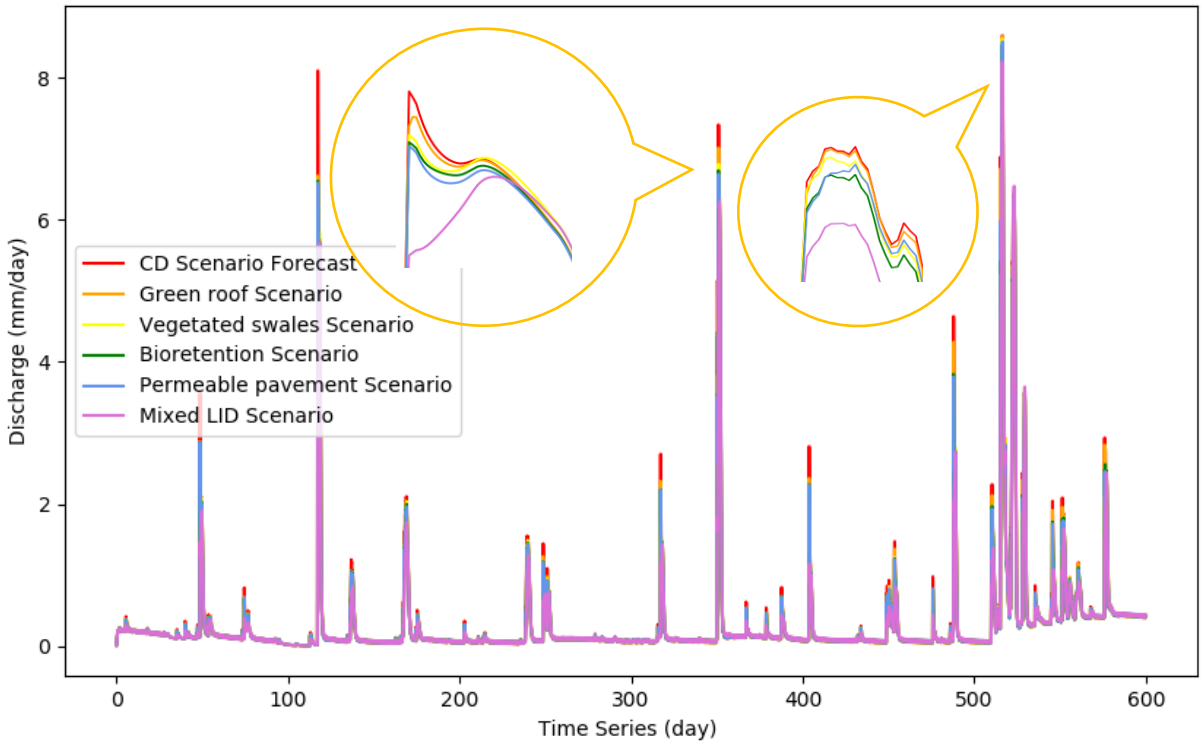

Figure 35. The total basin runoff of five LID scenarios and the CD scenario

As shown in Figure 35, compared to the CD scenario, all the five LID scenarios had significant effects on most peak runoffs. However for several large peaks happening in flood season (the last 100 days), all the five LID scenarios performed limited peak reduction ability. This is because the LID practices mainly influence the rainfall-runoff relationship of urban grey area. However these large peaks in flood season mainly generated from rural and urban green areas, since in flood season the water retention capacity of rural and urban green areas was almost exhausted. Another reason may be that in flood season the intensive rainfalls take up most space of LID practices and reduce the water retention capacity of LID practices when facing extreme peaks.

Secondly, it could be noticed that most peaks experience twice vertices as the magnified peak views in Figure 35. And the LID practices have more significant effect on the first vertex than the second vertex. It is also because the first peak vertex mainly generates from urban grey areas with rapid

hydrological reaction speed, which is also the domain of LID practices. However the second vertex mainly generates from large areas of urban green surface or rural areas, and therefore the LID practices have less influence on the second vertex.

And finally, the mixed LID scenario performed best on peak runoff reduction among these 5 LID scenarios. It may because in the mixed LID scenario 50% of the rainfall on urban grey areas is conveyed to LID practices and for other three single practice scenarios this number is only 15%.

The peak runoff happening on 29/03/2018 (the 351st modelling day) in dry season is selected as the typical peak runoff to show the LID performance on peak runoff reduction. The statistical results about total runoff volume and peak runoff reduction are shown in Table 15. The specific runoff reduction contribution by every hydrologic function of four LID practices is listed in Table 16.

Table 15. The statistical analysis of modelled runoff results for 5 LID scenarios

Scenarios	CD	Green roof	Vegetated swales	Bioretention	Permeable pavement	Mixed LID
Total volume of basin runoff [mm]	182	178	180	178	178	170
Decrease proportion of the total runoff [-]	-	2.3%	1.0%	2.4%	2.5%	6.9%
The first vertex of typical peak runoff [mm/d]	7.3	7.0	6.8	6.7	6.6	5.3
Decrease proportion of the first vertex [-]	-	4.4%	7.6%	8.8%	9.5%	28.3%
The second vertex of typical peak runoff [mm/d]	6.48	6.47	6.50	6.39	6.34	6.26
Decrease proportion of the second vertex [-]	-	0.2%	-0.2%	1.4%	2.2%	3.5%

Table 16. Specific runoff retention amount of 4 single LID scenarios in model results in 600 research days

		Prec.	Evap.	Infil.	Overflow	Storage
Bioretention cell	Amount (mm)	437	94.1	238.2	69.8	35.2
	Ratio	100%	21.5%	54.5%	16.0%	8.1%
Green roof	Amount (mm)	437	187.9	-	160.1	88.6
	Ratio	100%	43.0%	-	36.8%	20.3%
Vegetated swale	Amount (mm)	437	-	109.8	327.5	0
	Ratio	100%	-	25.1%	74.9%	0
Pervious pavement	Amount (mm)	437	-	383	37.8	16.1
	Ratio	100%	-	87.7%	8.6%	3.7%

Symbols: - the processes not in model structure (do not indicate non-exist process, but are neglected compared to other major functions)

7.3.1 The result of bioretention scenario

According to the statistical results in Table 15, the bioretention cells have large water retention capacity among these four test LID practices with less overflow volume. As might be expected, bioretention cells also have good performance on the peak runoff reduction with the removal proportion as 8.8% (the first vertex of the typical peak), second only to the pervious pavements.

The large water retention capacity and peak runoff reduction ability of bioretention cells could be ascribe to the thick soil layer and the rapid water infiltration ability of soil granules. According to the

specific runoff retention amount of each hydrologic function shown in Table 16, 54.5% of the collected rainwater infiltrated to the groundwater, 21.5% of the rainwater evaporated and the overflow from bioretention cells was only 16%.

7.3.2 The result of permeable pavement scenario

The permeable pavements show best hydrological performance on water retention among these four test LID practices. It is worth to mention that, permeable pavements generate the least overflow as only 8.6% of the total input rainwater in 600 research days as shown in Table 16.

The rainwater consumption method of permeable pavements depends on the infiltration. With additional interception space between the permeable pavers or in the porous asphalt pores, large volume of rainwater was captured for continuous infiltration.

Since the large water retention capacity and forceful peak runoff reduction ability, both of the bioretention cells and permeable pavements could be seen as the most effective LID practices from the view of urban flood control and pressure release of urban drainage system. Considering the multifunction of permeable pavements which do not need extra space, permeable pavements would be a more favourable LID practices for the areas without sufficient land resources.

7.3.3 The result of vegetated swales scenario

Vegetated swales could achieve a similar satisfactory effect on peak runoff reduction to bioretention cells and permeable pavements. As shown in Table 15, more than 7.5% peak runoff was reduced by these three LID measures.

As for the retention of total runoff volume in the long term, the performance of vegetated swales was not outstanding. It could be explained by the rapid water transportation of vegetated swales. Different from other volume-based control practices, the main function of vegetated swales is the water transportation. In the water conveyance process, part of the water could be consumed with favourable infiltration condition, and the last would be rapidly conveyed to urban stormwater drainage system. Without long water residence time, the infiltration process would just happen in a short period after precipitation. Therefore the total runoff retention volume of vegetated swales is the smallest one among these four test LID practices as shown in Table 15.

7.3.4 The result of extensive green roofs scenario

The extensive green roofs had the worst hydrologic performance on the peak runoff reduction among 4 test LID practices. It is because although shares the similar model structure to bioretention cells with both IR (vegetation) and UR (soil layer), the thickness of the soil layer for the modelled extensive green roofs is small and there is no infiltration ability on rooftops.

The small water retention capacity of green roof leads to a sensitive performance on peak runoff reduction to the predecessor rain condition as shown in Figure 36. If there was no or less predecessor rain, the green roof could still play the role of peak runoff reduction; However when it came to rain seasons, the green roof would be easily filled up by the dense predecessor rains and it would not reduce the peak runoff at all.

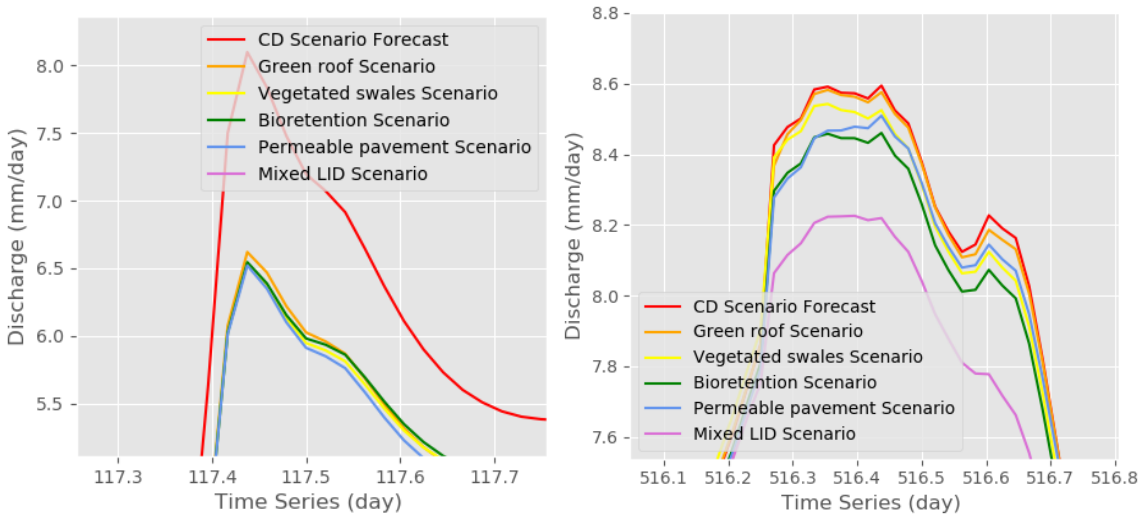

Figure 36. The different peak runoff reduction performance of green roofs: The left one shows a less predecessor rains situation and the right one shows one peak in flood period

7.3.5 The result of mixed LID scenario

The mixed LID scenario was the most forceful LID scenario to decrease both the peak runoff and the total runoff volume among the 5 test LID scenario. Except the reason of larger contribution area, another strength of the mixed LID scenario is because of the cascade connection design which regulates the unbalanced water capture capacity between different LID practices, and maximizes the hydrologic functions of LID practices, and increases the robustness of the LID system. For example, as the result analysis of the four single LID practice scenarios, when it came to rain seasons the green roof was quite easy to generate overflow, and at the same time the bioretention cell had larger retention capacity because of the thick soil layer. Under this circumstances, conveying the outflow of green roofs to bioretention cells could take more advantage of the large capacity of bioretention cells and increase the robustness of the whole LID system.

Table 17 shows the specific retention amounts of 4 LID practices in mixed LID scenario. The two columns, “Prec.” and “Inflow”, indicate the stormwater collected by the LID practices and the recharge from other LID practices respectively, both of which constitute the total water input for the LID practices; the last four columns, “Evap.” (evaporation), “Infil.” (infiltration), “Overflow”, show the water consumption approaches.

Table 17. Specific retention amounts of 4 LID practices in mixed LID scenario in 600 research days

		Prec.	Inflow	Evap.	Infil.	Overflow	Storage
Green roof	Amount (mm)	437	-	255	-	180	2.52
	Ratio	-	-	58.3%	-	41.1%	0.6%
Bioretention	Amount (mm)	437	59.9	257	133.3	82.0	24.9
cell	Ratio	87.9%	12.1%	51.7%	26.8%	16.5%	5.0%
Vegetated	Amount (mm)	437	82.0	-	43.4	476	0
swale	Ratio	84.2%	15.8%	-	8.4%	91.6%	0
Pervious	Amount (mm)	437	-	-	383.4	37.8	16.1
pavement	Ratio	-	-	-	87.7%	8.6%	3.7%

Symbol “-“: related to the processes not in model structure; The shaded numbers indicate the water route;

It is worth to mentioned that the drainage areas of bioretention cells, vegetated swales and pervious pavements were the same, but the construction areas of the bioretention cells and vegetated swales just took 2/3 and 1/3 of the drainage areas according to scenario design. According to the water routes of the mixed scenario, the bioretention cells received another 12% water input from green roofs and then the overflow from bioretention finally discharge to vegetated swales.

Comparing the performances of bioretention cells in mixed scenario and single bioretention scenario as shown in Table 18, with more input water and less construction area, the water retention ability of bioretention cells was better developed with almost the same proportion of overflow, especially the evaporation function.

Table 18 Performance comparison of bioretention cells in mixed LID scenario and single bioretention scenario

Scenarios		Prec.	Inflow	Evap.	Infil.	Overflow	Storage
Mixed	Amount (mm)	437	59.9	257	133.3	82.0	24.9
Scenario	Ratio	87.9%	12.1%	51.7%	26.8%	16.5%	5.0%
Bioretention	Amount (mm)	437	-	94.1	238.2	69.8	35.2
scenario	Ratio	100%	-	21.5%	54.5%	16.0%	8.1%

From the runoff comparison figure of the mixed LID scenario, the current CD scenario and the CD scenario forecast in 2040 in Figure 37, it could be found that the mixed LID scenario could control most peak runoffs effectively and for several large peaks happening in flood season the peak reduction ability was restrained significantly.

It is worth to mention that the CD scenario forecast selected here is based on a half-infill and half-expansion strategy of urban development scenario C. If the urban development in San Antonio City could follow the infill strategy more strictly, it is possible to keep the level of peak runoffs in 2040 as the same as current situation with the design mixed LID scenario.

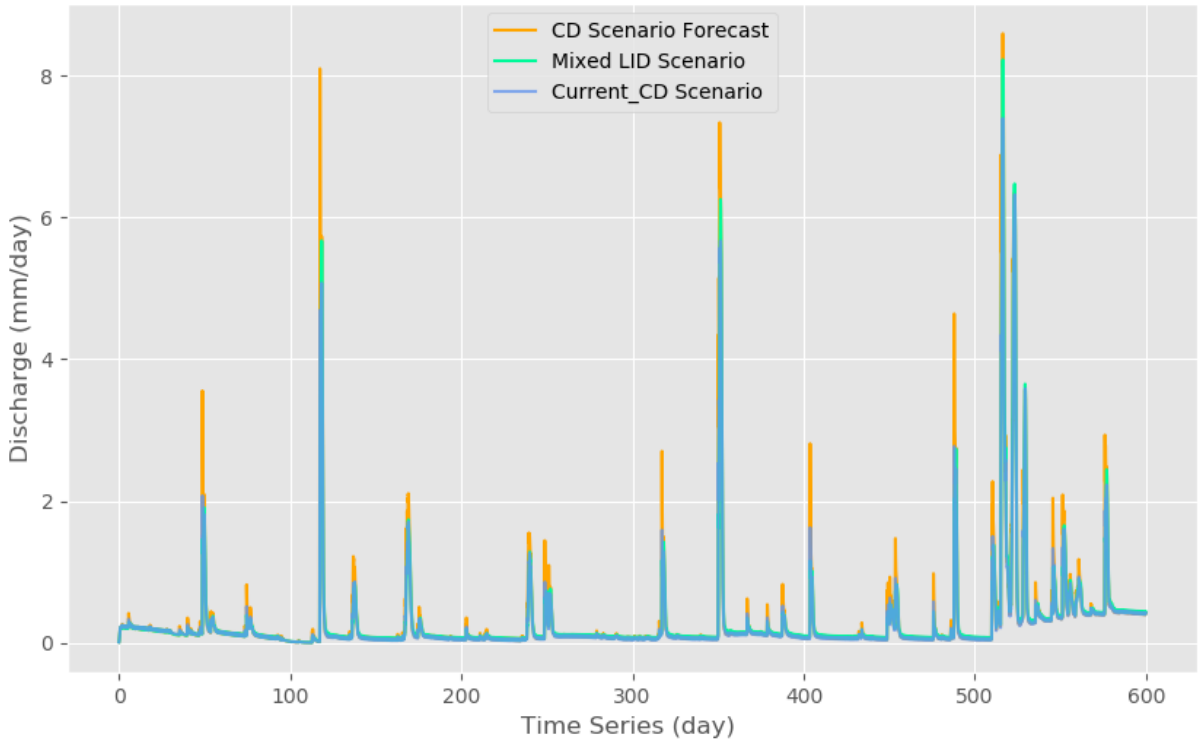

Figure 37. Model results of the total basin runoff in mixed LID scenario, the current CD scenario and the CD scenario in 2040

7.4 The time approaching and stacking of urban and rural peaks due to LID implementation

7.4.1 Four scenarios with single LID practice

According to the model result, the time lags between rural peaks and CD urban peaks varies from 6.5 to 15.5 hours. Since the covered areas by LID practices are small as 15% of urban grey areas in four

LID scenarios with single LID practices, these four scenarios only delayed part of urban peaks from 0.5 to 2.5 hours, which only slightly shorten the time difference of rural and urban peaks. And with large peak runoff reduction ability, the time approaching of constrained urban peaks and rural peaks would not increase the total basin peak.

One example is shown in Figure 38, in which the permeable pavements delayed the urban peak runoff time for 30 minutes compared to CD scenario. However since the forceful decrease of urban peak runoff value, the overlap of constrained urban peak runoff and rural peak runoff would not cause obvious negative effect on the basin peak runoff.

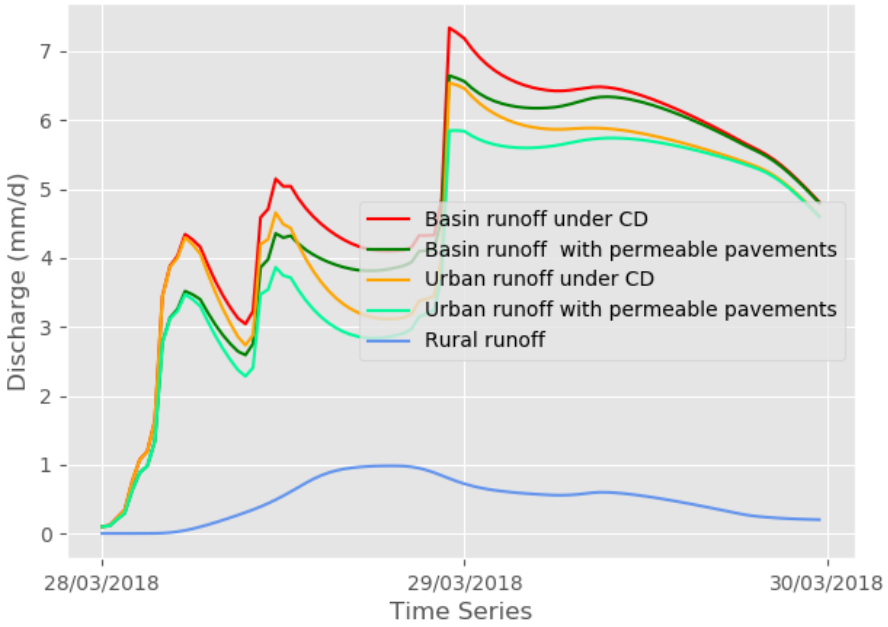

Figure 38. The peak runoffs from rural, urban, and basin areas in vegetated swales scenario and CD scenario

7.4.2 The mixed LID practices scenario

As for the mixed LID practices scenario, 50% of the precipitation on urban grey areas would be conveyed to LID practices, which will cause a time lag of urban runoff from 0.5 to 6.5 hours. And with large peak runoff reduction ability in non-flood period, the time approaching of constrained urban peaks and rural peaks would not cause negative problem. However in flood season, the peak runoff reduction of LID practices is not significant, and therefore the time approaching of urban and rural peak time will cause more stack of urban and rural peak runoffs and increase the total basin runoff.

The peak runoff happening on the 529th modelling day in flood season is selected as an example as shown in the left figure of Figure 39. The orange and light green lines indicate the urban runoffs under CD and LID scenarios respectively. Comparing these two lines, it could be found that the first vertex of CD urban runoff is successfully erased by LID practices but the decreased runoff volume of the first vertex was delayed and partly superimposed on the second vertex, which increase the second vertex by 0.06 mm/d, from 1.62 to 1.68mm/d.

The blue line indicates the rural runoff and the red and dark green lines show the total basin runoff under CD and LID scenarios respectively. If considering the overlap of rural and urban peak runoffs, the delayed urban peak by LID practices will have more overlap with the rural peak and lead to larger difference on basin peak values. According to the modelling result, the total basin rural is increased by 0.08 mm/d, from 3.57 to 3.65 mm/d.

The similar situation also happened on another large peak in flood season, which is shown in the right figure of Figure 39. In this case, the urban peak was indeed decreased by LID practices, but since the approaching of rural and urban peaks the total basin runoff increase by 0.12 mm/d, from 6.35 to 6.47 mm/d.

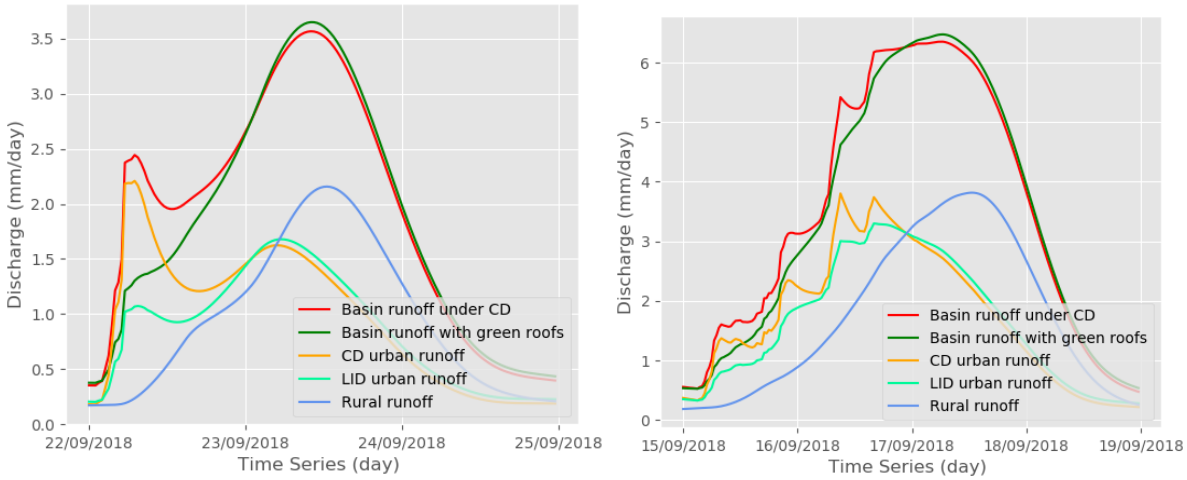

Figure 39. The peak runoffs from rural, urban, and basin areas in mixed LID practices scenario and CD scenario

These examples show that the implementation of LID practices will delay the peak runoff and the extent of time delay depends on the extent of LID implementation. Usually the more areas LID practices cover, the larger peak runoff is delayed and also decreased. But in flood seasons, the large or extreme large peak runoffs are always contributed by rural, urban green, and urban grey areas together, and the LID practices only adjust the rainfall-runoff relationship of urban grey areas. Therefore the peak runoff reduction function of LID practices on total basin runoff is restrained significantly in flood season.

Under these circumstances, some large or extreme large peaks in flood season will not be reduced by LID practices. And since the delay function of LID practices on urban runoff, the time approaching of rural and urban peaks brings more stack of rural and urban peaks and increases total basin peak runoff.

8

Discussion

This research aims to provide some insights about the impact of LID implementation with regard to peak runoff values and also the total runoff volume on the catchment scale. But since the specific conditions of study catchment, including the ratio of urban areas to catchment areas, the position of urban areas in study catchment, and local urban water management conditions, the results of this research are also limited in a restricted region.

Besides, the confidence space and reliability degree of this research are further discussed from the aspects of model uncertainty, scenario limitation, and the comparability of this research and literatures.

8.1 Model uncertainty

8.1.1 Low complexity of conceptual model structure

To decrease the equifinality and over-parameterization problems caused by complex physical-based model and avoid the high data requirement of distributed model, this research exploited SUPERFEX conceptual framework to build a tailor-made semi-distributed model for study catchment. In the relatively simple semi-distributed model, the rural and urban areas in study catchment are distinguished, however the heterogeneity within the rural or urban areas is not represented.

Besides, although many important artificial water processes in research area such as urban stormwater drainage, water pumping and groundwater recharge are quantified with simple conceptual expressions, the reliability and accuracy of these expressions are arguable.

8.1.2 Non-linearity in model

The non-linear hydrological processes in models of this research are mainly out of two reasons. Firstly, some constitutive functions are non-linear. For example, the discharge from HR (human impact reservoir) is expressed with a power function in which the exponent is larger than 1. It demonstrates that the discharge coefficient of HR is inconstant and the discharge coefficient will become leading to faster water discharge when there is more water storage in HR, and vice versa.

Secondly, the threshold behaviour leads to non-linear hydrological processes. For example, all the interception processes in this research are designed as threshold process in models; Besides, the threshold behaviour had been tested on the overflow from UR with a threshold parameter. But since the threshold function is not smooth enough, the performance of models is not satisfactory and finally the non-linear overflow from UR was described with more smooth non-linear constitutive function; The threshold behaviour of the rainfall-runoff relationship could be reflected from the model calibration results. At first, the runoff data of rural sub-catchment in the whole research period are exploited for model calibration. Since the rural runoff is base flow in most of the time, the peak runoff could not be modelled well. After that, the peak runoff data in flood season were extracted for model

calibration, and the model performance on peak runoff improved. It indicates that the rainfall-runoff relationship also has the threshold behaviour, which performs differently in dry and flood seasons.

8.1.3 The model components inheritance from lumped to semi-distributed model

In this research, the model started from two simple lumped models for the rural and urban sub-catchments respectively. After that, several model components and relevant parameter ranges in two lumped models would be inherited by semi-distributed model. Although this method reduced the uncertainty problem caused by starting from a complex semi-distributed model directly, part of information may be lost by this inheritance process from lumped models.

As shown in Figure 40, the rural sub-catchment covers the northwest of study catchment. When converting the rural lumped model to rural part of semi-distributed model, the information from the last small part of rural area may be lost or underestimated. But since the rural sub-catchment takes most of the rural areas in study catchment and the semi-distributed model is calibrated with total basin runoff after that, this neglected or underestimated information may be not significant.

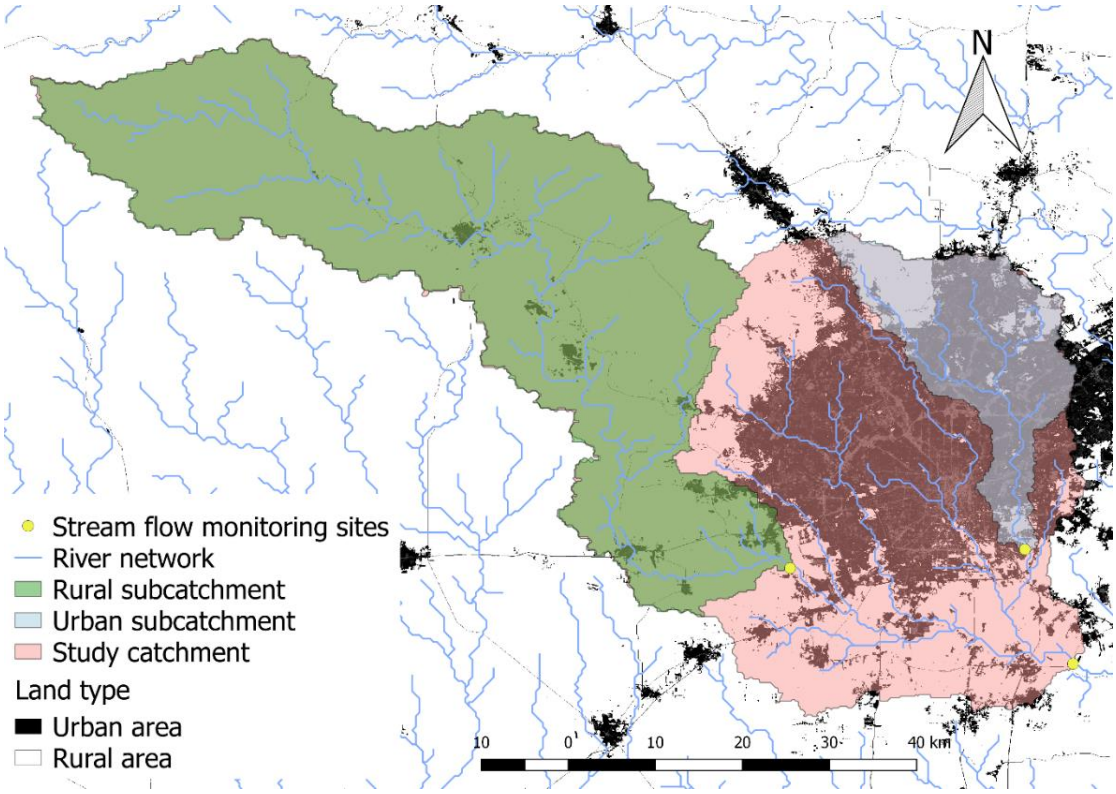

Figure 40. The location of study catchment and two sub-catchments with the stream network

8.1.4 Favourable LID parameter setups

For the LID parameter setups, a favourable LID implementation condition is presumed. For example, according to "*SARA LID Guidance Manual"*, 10 to 15 cm (4 to 6 inches) media depths are recommended for extensive green roofs. And based on this range, 12 cm is surmised as media depth for extensive green roofs in this research. However if the real LID construction condition can meet this size is doubtful.

Besides, many other factors may also influence the operation of LID practices such as the damage of LID practices, lack of daily maintenance or blockage problems of soil media. These possible negative events are also neglected by the LID parameter setups.

8.2 Scenario limitation

In this research, 3 urban development and 5 LID implementation scenarios are designed to deal with the prediction uncertainty. But these limited scenarios are built on certain assumptions; Although they aim to provide a meaningful and practical plan with great likelihood, they cannot cover all the possible future forecast. The limitation of urban development and LID implementation scenarios are stated below.

8.2.1 The limitation of urban development scenarios

The urban development scenarios are designed based on two important assumptions from "*City of San Antonio: Comprehensive Plan"* of local government: There will be 1.1 million new residents between 2010 and 2040, and the development strategy of San Antonio City would be less expansion and higher density.

The first assumption about resident growth provides a specific number to quantify the urban development degree. And this number was used in all the three urban development scenarios. But the reliability of this prediction is limited. For the second assumption, three urban development scenarios were designed to describe the different degree of urban expansion.

And then when expressing these scenarios in model, two premises are assumed: The urban construction density level and water drainage system are assumed to be roughly consistent in the whole urban areas; Since the infill development strategy may bring the compact of people living space, larger number of per capita urban grey areas is given for more expansion scenarios.

The first premise restricts the scenarios to an equal development situation. But in really the construction density level of core urban area is always higher than the new developed sub-urban area. This unequal development may cause some subtle differences on the hydrologic performance of urban areas. And the second premise was quantitatively expressed with 3 rough estimate ratios for the compaction degree of living space in model. The real compaction degree may have certain discrepancy with the estimate ratio numbers.

8.2.2 The limitation of LID implementation scenarios

There are 5 LID implementation scenarios in this research. The first four scenarios with single LID practice are designed to compare the different hydrologic performances of different LID practices. And the last mixed LID scenario is aimed to provide a potentially realistic LID implementation plan.

Firstly, the same assumption of equal LID implementation is presumed here as urban development scenarios. Secondly, for the last mixed LID scenario, as an optimistic LID implementation scenario, 50% of the precipitation on urban impervious surface is collected by LID practices, and besides, cascade connections among 4 LID practices are assumed. However if the real LID construction condition can realize this optimistic estimation is questionable.

8.3 The comparability of research results and literatures about LID

8.3.1 The comparability of model result

In this part, the simulated runoff reduction proportions of 4 test LID practices are compared with literatures. And the comparison result shows a high comparability.

Firstly, the forceful runoff reduction ability of bioretention cells is well documented. For example, bioretention cells were shown to reduce total runoff volume from 48% to 97% (Chapman and Horner, 2010; DeBusk and Wynn, 2011). And the number in this research is 84%.

Secondly for green roofs, the runoff reduction proportion varies even larger according to previous research between 23% and 100% (VanWoert, 2005; Hathaway, 2008; Carpenter and Kaluvakolanu, 2011). In this research, the runoff reduction of green roofs is 63%.

Thirdly, the runoff reduction proportion of permeable pavements were shown between 50% and 93% (Rushton, 2001; Hunt, 2002; Dreelin, 2006). And this runoff reduction proportion of permeable pavements in this research is 91%.

Finally, for vegetated swales, the runoff reduction proportion has significant difference between small storm events and large storm events. For small storms, 85% of the runoff volume can be retained; however for the large storms, this proportion ranges from 35% to 66% (Hunt, 2010). And the simulated runoff reduction proportion in this research is smaller than this range, as 25% for all the storms in 600 modelling days. This underestimation could lead to a slight overestimation of fast urban runoff and hence have a limited influence on calculated peak flows.

8.3.2 Analysis comparability

Except the model result shows a high comparability with literatures, some arguments in this research are also supported by former studies.

Firstly, the permeable pavements is considered as the most hydrologically effective LID practices among the four test LID practices with the most forceful runoff reduction ability according to model results. And this argument is supported by Ahiablame's research (2012), in which the flood mitigation ability of three LID practices (porous pavement, rain barrel, and rain garden) were compared.

Secondly, the ineffective runoff reduction performance of vegetated swales is ascribe to its fast rainwater transportation and short residence time in this research. Huang used the same reason to explain the less effective performance of infiltration trenches and vegetated swales than bioretention cells, porous pavements, green roofs and etc., regarding rainfalls in all return periods, in his research (2018).

Finally, compared to single LID practices, the mixed of various LID practices should be promoted with better robustness. The similar arguments are also mentioned by Qin, 2013; Askarizadeh, 2015; Fang, 2017; Huang, 2018. Especially Qin put forward this argument from another aspect; Different LID practices perform better during the different storm events with different peak time (2013).

9

Conclusions and recommendations

The study results of the four sub-problems are summarized in order to answer the main research problem all together. And this is followed by several recommendation for the suitable LID implementation and urban development strategies.

9.1 Conclusions

It should be mentioned that since the specific conditions of study catchment, such as the ratio of urban areas to catchment areas, the position of urban areas in study catchment, and local urban water management conditions, these conclusions below are also limited in a restricted region.

9.1.1 The different hydrologic characters of urban and rural areas

For rural areas in the Medina River basin, with large water retention capacity and evaporation ability, runoff peak flows rarely happen in dry seasons. However when it comes to flood seasons, the water retention capacity is easily exhausted and the peak flows will happen with large magnitude. And then, the base stream flow from groundwater recharge took a considering proportion of total rural runoff and the rural peak runoffs were always accompanied by the increase of base flow since large groundwater stock.

As for the urban areas in San Antonio City, the recharge capacity from groundwater to streamflow was extreme small, and most of the base flow values in urban sub-catchment were close to zero. Without large water retention capacity or forceful evaporation ability, the character of the urban rainfall-runoff relationship tended to swing between extreme flood and extreme drought.

9.1.2 The influence of urbanization on rainfall-runoff relationship

Urban development would always bring growth of total runoff volume. But different urban development strategies would bring different growth rates. For the scenario C which follows a half-infill and half-sprawl strategy, the total runoff would rise by 14.3% compared to current situation. And for a 70%-infill and 30%-sprawl development strategy, the total runoff would rise by 8.7% in scenarios B. As for a full infill development scenario A, this growth rate is only 2.7%.

Fortunately, differently from total runoff volume, the urban development would not always lead to a larger extreme peak runoff. By adjusting the ratio of grey and green urban areas and by designing the time difference of peak runoffs from grey and green urban areas, the extreme peak runoff could be reduced even with a higher level of urbanization. For scenario C and scenario B, the peak runoff of a typical extreme peak increased by 16.1% and 7,5% than current situation, however scenario A even decreased the peak runoff by 4.3%.

This odd peak runoff decrease situation is ascribed to the redistribution of urban green and grey areas in scenario A. Although small to medium peaks are mostly generated from the rapid runoffs from urban grey areas, the extreme peak flows are always contributed by the large runoff volume from

broad urban green surface. Therefore, with less urban green areas, the scenario A diminishes the value of extreme peak runoff.

9.1.3 The influence of LID implementation on rainfall-runoff relationship

Based on the urban development Scenario C, five LID implementation scenarios were formulated and tested. According to the model results, the rainfall-runoff relationships of all the five LID implementation scenarios had two characteristics: Firstly, most peak runoffs experienced twice vertices, as the first one generated from urban grey areas and the last one from urban green surface or rural areas. The LID practices have more significant effect on the first vertex than the second vertex. Secondly, for the large or extreme large peaks in flood season, all the five LID scenarios performed limited peak reduction ability, since large proportion of these peaks in flood season was generated from rural and urban green areas, and the LID practices were almost saturated and lost the water retention function.

a. The influence of Bioretention cells

Bioretention cells could be one of the most effective practices among the four test LID practices for both the total runoff volume reduction and peak runoff reduction. According to model result of bioretention cells scenario, the bioretention cells with favourable implementation condition could retain 84% of the total collected rainwater in 600 modelling days with only 16% overflow. As for the peak runoff reduction, the removal proportion by bioretention cells took 8.8% of the basin peak runoff.

And with larger drainage area and less construction area, the water retention ability of bioretention cells could be better developed, especially the evaporation function. According to model result, after increasing the ratio of drainage area to construction area from 1 to 1.5, the proportion of overflow from bioretention cells almost kept at the same level.

b. The influence of Permeable pavements

The most effective and efficient LID practice among 4 tested LID practices is permeable pavements. The rainwater consumption of permeable pavements mainly depended on the water infiltration process. Without additional construction space, permeable pavements have outstanding hydrological performance: According to the model result of permeable pavements scenario, more than 92% of the total rainwater on permeable pavement was retained in 600 modelling days and 9.5% of the typical basin peak runoff was reduced. Overall, permeable pavements could be a favourable LID practice for the land limited areas which is also suffering from urban flood problem.

c. The influence of Vegetated swales

Vegetated swales could achieve a similar satisfactory effect on peak runoff reduction to bioretention cells and permeable pavements as the peak removal proportion of 7.6%. However because of the rapid water transportation character, the performance of vegetated swales is not outstanding on the retention of total runoff volume. Only 25% of the rainwater collected by the vegetated swales was retained according to the model result for vegetated swales scenario, which is the least one among 4 tested LID practices.

d. The influence of Extensive green roof

The extensive green roof however had the worst hydrologic performance on the peak runoff reduction among 4 test LID practices. According to model result of green roof scenario, the green roofs only reduce 4.4% typical peak runoff. As for the total runoff reduction, the performance of green roofs is more favourable, as 63% of the total rainwater on green roofs in 600 modelling days was retained.

Since the small thickness of the soil layer, the green roofs showed a sensitive performance to the preceding rains. When it came to rain seasons, the green roof would be easily filled up by the dense precipitations and will lose its peak reduction ability.

9.1.4 The time approaching and stacking of urban and rural peak runoffs due to LID implementation

Based on the urban development Scenario C, five LID implementation scenarios were formulated and tested. Different LID implementation scenarios brought different time lags of peak runoff. According to the model results, the time lags between rural peaks and CD urban peaks varies from 6.5 to 15.5 hours. However, for the four LID scenarios with single LID practices, since the covered areas by LID practices are small as 15% of urban grey areas, the urban peaks were only delayed from 0.5 to 2.5 hours. And with more forceful peak runoff reduction ability of LID practices, the staggering of constrained urban peaks and rural peaks would not cause obvious effects on the total basin peak values.

But, for the mixed LID practiced scenarios, 50% of the precipitation on urban grey areas would be conveyed to LID practices, which will cause a significant time lag of urban runoff from 0.5 to 6.5 hours. And the peak runoff reduction ability of LID practices is restrained significant in flood season. Therefore the delay function of LID practices leads to time approaching of rural and urban peaks and brings larger stack of rural and urban peaks, which increases total basin peak runoff. According to model result, two basin peak runoffs were increased from 3.57 to 3.65 mm/d and from 6.35 to 6.47 mm/d respectively for this reason.

9.2 Recommendations

Several suggestions are provided for better urban development and LID implementation *in 9.2.1 Recommendations for the suitable LID implementation* which is also the fourth sub-problems of this research. And few directions are recommended here for future research *in 9.2.2 Recommendations and suggestions for future research.*

9.2.1 Recommendations for the suitable LID implementation

a. Compared to the LID implementation plan with single practice, a combination of various LID practices is advised to increase the robustness of the LID system.
b. Cascade connections among different LID practices are suggested for regulating the unbalanced water retention capacity to maximize the hydrologic function of LID practices. To offset the drawbacks of green roof performance, cascading LID systems are especially recommended.
c. Compared to the sprawl urban development strategy, the infill development strategy is more helpful to reduce both the total runoff volume and the peak runoff.
d. When designing urban development and LID implementation plans, extreme peak runoff could be controlled by adjusting the area ratio of urban and rural areas or urban grey and green areas and creating the time differences between the peak runoffs from these sub-areas.

9.2.2 Recommendations and suggestions for future research

a. According to this research result, the infill and sprawl urban development strategy brought different influences on the extreme peak runoffs. These different hydrological influences of infill and sprawl urban development strategies could be further analysed considering the heterogeneity among urban, sub-urban and rural areas with finer model like distributed model. And based on this analysis, a long time urban development plan could be designed for one pilot city from the view of urban flood control by reducing extreme peak runoffs.
b. According to this research result, the basin peak runoff is controllable by designing the time stagger among the peak flows from different sub-areas in one catchment to avoid stacking of high flows. (The sub-areas could be classified by land type such as rural and urban areas or grey and green areas; or by topography such as plateau, hillslope, and wetland areas; or by soil type such as clay and sand areas; or by vegetation condition, bare, grasses, bushes and trees.) The different runoff response time of these sub-areas could be studied. And by

designing the time difference of the peak flows from the sub-areas, the total basin runoff peaks could be restrained.

c. This research assumes a homogeneous urban hydrological condition, urban development status, and LID implementation situation, which is limited in a restricted homogeneous condition. Future research could go into this topic deeply by considering the heterogeneous urban condition caused by urban drainage system, regional water police, partial construction degree and etc. And other distributed models could be exploited for the regional differences research with more precise modelling and more data input.

Reference

A. Newman; K. Sampson; M. P. Clark; A. Bock; R. J. Viger; D. Blodgett, 2014. A large-sample watershed-scale hydrometeorological dataset for the contiguous USA. Boulder, CO: UCAR/NCAR. https://dx.doi.org/10.5065/D6MW2F4D

Ahiablame, L. M., Engel, B. A., & Chaubey, I. (2012). Effectiveness of Low Impact Development Practices: Literature Review and Suggestions for Future Research. *Water, Air, & Soil Pollution, 223*(7), 4253-4273. doi:10.1007/s11270-012-1189-2

Ahiablame, L. M., Engel, B. A., & Chaubey, I. (2012). Effectiveness of Low Impact Development Practices: Literature Review and Suggestions for Future Research. *Water, Air, & Soil Pollution,223*(7), 4253-4273. doi:10.1007/s11270-012-1189-2

Ahiablame, L., & Shakya, R. (2016). Modeling flood reduction effects of low impact development at a watershed scale. *Journal of Environmental Management, 171*, 81-91. doi:10.1016/j.jenvman.2016.01.036

Askarizadeh, A., Rippy, M. A., Fletcher, T. D., Feldman, D. L., Peng, J., Bowler, P., . . . Grant, S. B. (2015). From Rain Tanks to Catchments: Use of Low-Impact Development To Address Hydrologic Symptoms of the Urban Stream Syndrome. *Environmental Science & Technology, 49*(19), 11264-11280. doi:10.1021/acs.est.5b01635

Atchley, A. L., Painter, S. L., Harp, D. R., Coon, E. T., Wilson, C. J., Liljedahl, A. K., & Romanovsky, V. E. (2015). Using field observations to inform thermal hydrology models of permafrost dynamics with ATS (v0.83). *Geoscientific Model Development Discussions, 8*(4), 3235-3292. doi:10.5194/gmdd-8-3235-2015

Beck, H. E., Albert I. J. M. Van Dijk, Roo, A. D., Dutra, E., Fink, G., Orth, R., & Schellekens, J. (2017). Global evaluation of runoff from 10 state-of-the-art hydrological models. *Hydrology and Earth System Sciences, 21*(6), 2881-2903. doi:10.5194/hess-21-2881-2017sist

Bedan, E. S., & Clausen, J. C. (2009). Stormwater Runoff Quality and Quantity From Traditional and Low Impact Development Watersheds. *JAWRA Journal of the American Water Resources Association, 45*(4), 998-1008. doi:10.1111/j.1752-1688.2009.00342.

Berndtsson, J. C. (2010). Green roof performance towards management of runoff water quantity and quality: A review. *Ecological Engineering, 36*(4), 351-360. doi:10.1016/j.ecoleng.2009.12.014

Beven, K. (1997), *TOPMODEL: A critique, Hydrol. Processes*, *11*, 1069– 1085.

Beven, K., Kirkby, M., Schofield, N., & Tagg, A. (1984). Testing a physically-based flood forecasting model (TOPMODEL) for three U.K. catchments. *Journal of Hydrology*, 69(1-4), 119-143. doi:10.1016/0022-1694(84)90159-8

Bianchini, F., & Hewage, K. (2012). How “green” are the green roofs? Lifecycle analysis of green roof materials. *Building and Environment, 48*, 57-65. doi:10.1016/j.buildenv.2011.08.019

Broderick, C., Matthews, T., Wilby, R. L., Bastola, S., & Murphy, C. (2016). Transferability of hydrological models and ensemble averaging methods between contrasting climatic periods. *Water Resources Research*, 52(10), 8343-8373. doi:10.1002/2016wr018850

Caine, I., Walter, R., & Foote, N. (2017). San Antonio 360: The Rise and Decline of the Concentric City 1890–2010. *Sustainability, 9*(4), 649. doi:10.3390/su9040649

Carter, T. L., & Rasmussen, T. C. (2006). Hydrologic Behavior Of Vegetated Roofs. *Journal of the American Water Resources Association, 42*(5), 1261-1274. doi:10.1111/j.1752-1688.2006.tb05611.x

Carter, T., & Jackson, C. R. (2007). Vegetated roofs for stormwater management at multiple spatial scales. *Landscape and Urban Planning, 80*(1-2), 84-94. doi:10.1016/j.landurbplan.2006.06.005

Chapman, C., & Horner, R. R. (2010). Performance Assessment of a Street-Drainage Bioretention System. *Water Environment Research, 82*(2), 109-119. doi:10.2175/106143009x426112

City of San Antonio. (2016). *Storm Water Design Criteria Manual*. San Antonio, TX, USA.

Clark, M. P., A. G. Slater, D. E. Rupp, R. A. Woods, J. A. Vrugt, H. V. Gupta, T. Wagener, and L. E. Hay (2008), Framework for Understanding Structural Errors (FUSE): A modular framework to diagnose differences between hydrological models, *Water Resour. Res.*, 44, W00B02, doi:10.1029/2007WR006735.

Clark, M. P., Nijssen, B., Lundquist, J. D., Kavetski, D., Rupp, D. E., Woods, R. A., . . . Rasmussen, R. M. (2015). A unified approach for process-based hydrologic modeling: 1. Modeling concept. *Water Resources Research*, 51(4), 2498-2514. doi:10.1002/2015wr017198

County of Bexar. (2016). *Water Quality and Maintenance Manual.* Bexar, TX, USA.

Debusk, K. M., & Wynn, T. M. (2011). Storm-Water Bioretention for Runoff Quality and Quantity Mitigation. *Journal of Environmental Engineering, 137*(9), 800-808. doi:10.1061/(asce)ee.1943-7870.0000388

Dessie, M., Verhoest, N. E., Pauwels, V. R., Admasu, T., Poesen, J., Adgo, E., . . . Nyssen, J. (2014). Analyzing runoff processes through conceptual hydrological modeling in the Upper Blue Nile Basin, Ethiopia. *Hydrology and Earth System Sciences*, 18(12), 5149-5167. doi:10.5194/hess-18-5149-2014

Dietz, M. E. (2007). Low Impact Development Practices: A Review of Current Research and Recommendations for Future Directions. *Water, Air, and Soil Pollution, 186*(1-4), 351-363. doi:10.1007/s11270-007-9484-z

Dreelin, E. A., Fowler, L., & Carroll, C. R. (2006). A test of porous pavement effectiveness on clay soils during natural storm events. *Water Research, 40*(4), 799-805. doi:10.1016/j.watres.2005.12.002

Dvorak, B., & Volder, A. (2010). Green roof vegetation for North American ecoregions: A literature review. *Landscape and Urban Planning, 96*(4), 197-213. doi:10.1016/j.landurbplan.2010.04.009

Environmental Protection Agency. (1993). *Guidance Manual for Developing Best Management Practices (BMP),* USA.

Esse, W. R., Perrin, C., Booij, M. J., Augustijn, D. C., Fenicia, F., & Lobligeois, F. (2013). The influence of conceptual model structure on model performance: A comparative study for 237 French catchments. *Hydrology and Earth System Sciences Discussions*, 10(4), 5457-5490. doi:10.5194/hessd-10-5457-2013

Fang, X., Li, J., Gong, Y., & Li, X. (2017). Zero increase in peak discharge for sustainable development. *Frontiers of Environmental Science & Engineering, 11*(4). doi:10.1007/s11783-017-0935-5

Fenicia, F., Kavetski, D., & Savenije, H. H. (2011). Elements of a flexible approach for conceptual hydrological modeling: 1. Motivation and theoretical development. *Water Resources Research, 47*(11). doi:10.1029/2010wr010174

Fenicia, F., Kavetski, D., & Savenije, H. H. (2011). Elements of a flexible approach for conceptual hydrological modeling: 1. Motivation and theoretical development. *Water Resources Research*, 47(11). doi:10.1029/2010wr010174

Fenicia, F., Kavetski, D., Savenije, H. H., Clark, M. P., Schoups, G., Pfister, L., & Freer, J. (2013). Catchment properties, function, and conceptual model representation: Is there a correspondence? *Hydrological Processes*, 28(4), 2451-2467. doi:10.1002/hyp.9726

Fenicia, F., Savenije, H. H., Matgen, P., & Pfister, L. (2005). Is the groundwater reservoir linear? Learning from data in hydrological modelling. *Hydrology and Earth System Sciences Discussions*, 2(4), 1717-1755. doi:10.5194/hessd-2-1717-2005

Futter, M. N., Erlandsson, M. A., Butterfield, D., Whitehead, P. G., Oni, S. K., & Wade, A. J. (2014). PERSiST: A flexible rainfall-runoff modelling toolkit for use with the INCA family of models. *Hydrology and Earth System Sciences*, 18(2), 855-873. doi:10.5194/hess-18-855-2014

Gao, H., Ding, Y., Zhao, Q., Hrachowitz, M., & Savenije, H. H. (2017). The importance of aspect for modelling the hydrological response in a glacier catchment in Central Asia. *Hydrological Processes*, 31(16), 2842-2859. doi:10.1002/hyp.11224

Gao, H., Hrachowitz, M., Fenicia, F., Gharari, S., & Savenije, H. H. (2013). Testing the realism of a topography driven model (FLEX-Topo) in the nested catchments of the Upper Heihe, China. *Hydrology and Earth System Sciences Discussions*, 10(10), 12663-12716. doi:10.5194/hessd-10-12663-2013

Getter, K. L., Rowe, D. B., & Andresen, J. A. (2007). Quantifying the effect of slope on extensive green roof stormwater retention. *Ecological Engineering, 31*(4), 225-231. doi:10.1016/j.ecoleng.2007.06.004

Gharari, S., Hrachowitz, M., Fenicia, F., Gao, H., & Savenije, H. H. (2013). Using expert knowledge to increase realism in environmental system models can dramatically reduce the need for calibration. *Hydrology and Earth System Sciences Discussions, 10*(12), 14801-14855. doi:10.5194/hessd-10-14801-2013

Gilroy, K. L., & Mccuen, R. H. (2009). Spatio-temporal effects of low impact development practices. *Journal of Hydrology, 367*(3-4), 228-236. doi:10.1016/j.jhydrol.2009.01.008

Hathaway, A. M., Hunt,W. F., & Jennings, G. D. (2008). A field study of green roof hydrologic and water quality performance. *Transactions of the ASABE, 51*(1), 37–44.

Hostache, R., Chini, M., Giustarini, L., Neal, J., Kavetski, D., Wood, M., . . . Matgen, P. (2018). Near-Real-Time Assimilation of SAR-Derived Flood Maps for Improving Flood Forecasts. *Water Resources Research*. doi:10.1029/2017wr022205

Hrachowitz, M., Fovet, O., Ruiz, L., Euser, T., Gharari, S., Nijzink, R., . . . Gascuel-Odoux, C. (2014). Process consistency in models: The importance of system signatures, expert knowledge, and process complexity. *Water Resources Research*, 50(9), 7445-7469. doi:10.1002/2014wr015484

Hrachowitz, M., Savenije, H., Bogaard, T. A., Tetzlaff, D., & Soulsby, C. (2013). What can flux tracking teach us about water age distribution patterns and their temporal dynamics? *Hydrology and Earth System Sciences*, 17(2), 533-564. doi:10.5194/hess-17-533-2013

Huang, C., Hsu, N., Liu, H., & Huang, Y. (2018). Optimization of low impact development layout designs for megacity flood mitigation. *Journal of Hydrology, 564*, 542-558. doi:10.1016/j.jhydrol.2018.07.044

Hunt, W. F., Hathaway, J. M., Winston, R. J., & Jadlocki, S. J. (2010). Runoff Volume Reduction by a Level Spreader–Vegetated Filter Strip System in Suburban Charlotte, N.C. *Journal of Hydrologic Engineering, 15*(6), 499-503. doi:10.1061/(asce)he.1943-5584.0000160

Hunt, W. F., Smith, J. T., Jadlocki, S. J., Hathaway, J. M., & Eubanks, P. R. (2008). Pollutant Removal and Peak Flow Mitigation by a Bioretention Cell in Urban Charlotte, N.C. *Journal of Environmental Engineering, 134*(5), 403-408. doi:10.1061/(asce)0733-9372(2008)134:5(403)

Hunt, W. F., Stephens, S., & Mayes, D. (2002). *Permeable pavement effectiveness in Eastern North Carolina*. In Proceedings of 9th International Conference on Urban Drainage. ASCE. Portland, OR.

Kavetski, D., & Fenicia, F. (2011). Elements of a flexible approach for conceptual hydrological modeling: 2. Application and experimental insights. *Water Resources Research*, 47(11). doi:10.1029/2011wr010748

Kavetski, D., G. Kuczera, and S. W. Franks (2003), Semidistributed hydrological modeling: A ''saturation path'' perspective on TOPMODEL and VIC, *WaterResour.Res.*, 39(9), 1246, doi:10.1029/2003WR002122.

Ley, R., Hellebrand, H., Casper, M. C., & Fenicia, F. (2015). Comparing classical performance measures with signature indices derived from flow duration curves to assess model structures as tools for catchment classification. *Hydrology Research*. doi:10.2166/nh.2015.221

Li, H., Sharkey, L. J., Hunt, W. F., & Davis, A. P. (2009). Mitigation of Impervious Surface Hydrology Using Bioretention in North Carolina and Maryland. *Journal of Hydrologic Engineering, 14*(4), 407-415. doi:10.1061/(asce)1084-0699(2009)14:4(407)

Lindström, G., Johansson, B., Persson, M., Gardelin, M., & Bergström, S. (1997). Development and test of the distributed HBV-96 hydrological model. *Journal of Hydrology*, 201(1-4), 272-288. doi:10.1016/s0022-1694(97)00041-3

MIG in Association with Economic & Planning Systems, Inc.; WSP; Parsons Brinkerhoff; Ximenes & Associates, Inc. (2016). *City of San Antonio: Comprehensive Plan*. San Antonio, TX, USA.

Perrin, C., C. Michel, and V. Andre´assian (2003), Improvement of a parsimonious model for stream flow simulation, *J.Hydrol.*,279,275–289.

Perrin, C., Michel, C., & Andréassian, V. (2003). Improvement of a parsimonious model for streamflow simulation. *Journal of Hydrology*, 279(1-4), 275-289. doi:10.1016/s0022-1694(03)00225-7

Qin, H., Li, Z., & Fu, G. (2013). The effects of low impact development on urban flooding under different rainfall characteristics. *Journal of Environmental Management, 129*, 577-585. doi:10.1016/j.jenvman.2013.08.026

Qin, H., Li, Z., & Fu, G. (2013). The effects of low impact development on urban flooding under different rainfall characteristics. *Journal of Environmental Management, 129*, 577-585. doi:10.1016/j.jenvman.2013.08.026

Roehr, D., & Kong, Y. (2010). Runoff reduction effects of green roofs in Vancouver, BC, Kelowna, BC, and Shanghai, P.R. China. *Canadian Water Resources Journal, 35*(1), 53–67.

Rushton, B. T. (2001). Low-Impact Parking Lot Design Reduces Runoff and Pollutant Loads. *Journal of Water Resources Planning and Management, 127*(3), 172-179. doi:10.1061/(asce)0733-9496(2001)127:3(172)

San Antonio River Authority; Bexar Regional Watershed Management's Low Impact Development Manual Technical Subcommittee. (2015). *San Antonio River Basin Low Impact Development Technical Design Guidance Manual*. San Antonio, TX, USA.

San Antonio Water System. (2019). SAWS Water Recycling Facts. Retrieved from https://www.saws.org/

Savenije, H. H. (2010). HESS Opinions "Topography driven conceptual modelling (FLEX-Topo)". *Hydrology and Earth System Sciences Discussions*, 7(4), 4635-4656. doi:10.5194/hessd-7-4635-2010

Smith, T., Marshall, L., Mcglynn, B., & Jencso, K. (2013). Using field data to inform and evaluate a new model of catchment hydrologic connectivity. *Water Resources Research*, 49(10), 6834-6846. doi:10.1002/wrcr.20546

Texas Commission on Environmental Quality. (2005). *Technical Guidance on Best Management Practices*. TX, USA.

Van Seters, T., Smith, D., MacMillan, G. (2006). PERFORMANCE EVALUATION OF PERMEABLE PAVEMENT AND A BIORETENTION SWALE.

VanWoert, N. D., Rowe, D. B., Andresen, J. A., Rugh, C. L., Fernandez, R. T., & Xiao, L. (2005). Green roof stormwater retention: effects of roof surface, slope, and media depth. *Journal of Environmental Engineering, 34*, 1036–1044.

Vanwoert, N. D., Rowe, D. B., Andresen, J. A., Rugh, C. L., Fernandez, R. T., & Xiao, L. (2005). Green Roof Stormwater Retention. *Journal of Environment Quality, 34*(3), 1036. doi:10.2134/jeq2004.0364

Wagener, T., Boyle, D. P., Lees, M. J., Wheater, H. S., Gupta, H. V., and Sorooshian, S.: A framework for development and application of hydrological models, *Hydrol. Earth Syst. Sci.*, 5, 13-26, https://doi.org/10.5194/hess-5-13-2001, 2001.

Wagener, T., D. P. Boyle, M. J. Lees, H. S. Wheater, H. V. Gupta, and S. Sorooshian (2001), A framework for development and application of hydrological models, *Hydrol.EarthSyst.Sci.*,5,13–26.

Weiler, M., & Beven, K. (2015). Do we need a Community Hydrological Model? *Water Resources Research*, 51(9), 7777-7784. doi:10.1002/2014wr016731

Westhoff, M. C., & Zehe, E. (2012). Maximum entropy production: Can it be used to constrain conceptual hydrological models? *Hydrology and Earth System Sciences Discussions*, 9(10), 11551-11581. doi:10.5194/hessd-9-11551-2012

Westra, S., Thyer, M., Leonard, M., Kavetski, D., & Lambert, M. (2014). A strategy for diagnosing and interpreting hydrological model nonstationarity. *Water Resources Research*, 50(6), 5090-5113. doi:10.1002/2013wr014719

Wikipedia contributors. (2019, February 07). Edwards Aquifer. In Wikipedia, The Free Encyclopedia. Retrieved 12:09, March 06, 2019, from https://en.wikipedia.org/wiki/Edwards_Aquifer

Zhang, R., Liu, J., Gao, H., & Mao, G. (2018). Can multi-objective calibration of streamflow guarantee better hydrological model accuracy? *Journal of Hydroinformatics*, 20(3), 687-698. doi:10.2166/hydro.2018.13

Appendices

Appendix A General soil map of Bexar County

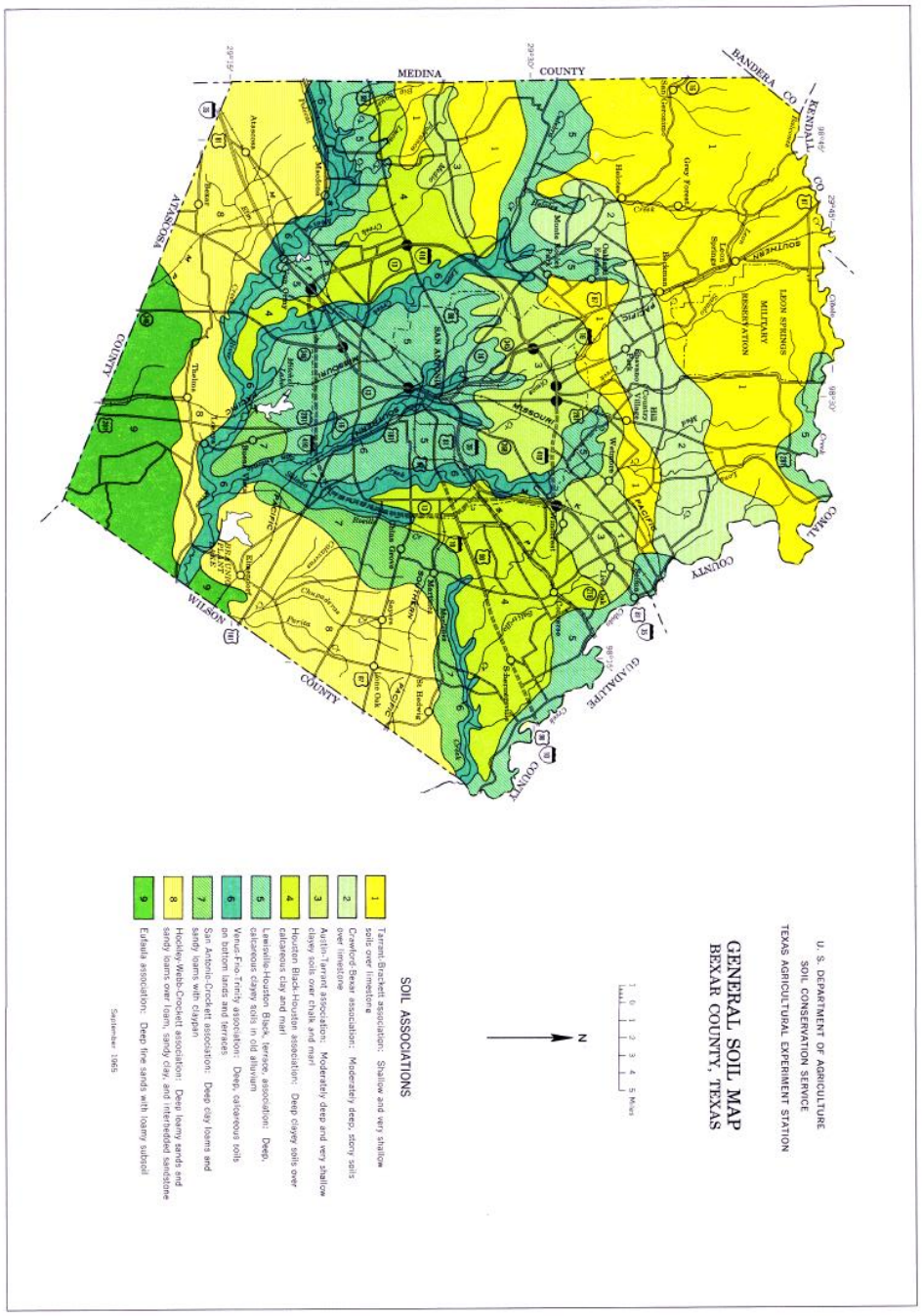

Figure 41. General soil map of Bexar County (Resources: United States Department of Agriculture)

Appendix B The Composition of SUPERFLEX framework

The following information was retrieved from the "*Elements of a flexible approach for conceptual hydrological modeling: 1. Motivation and theoretical development" of* Fenicia et al. (2010).

A SUPERFLEX model can be implemented by adding several kinds generic elements such as overall model architecture, process connectivity, reservoir element, lag function element and constitutive element.

B.1 Overall model architecture

The overall model architecture determines the basic frame of SUPERFLEX model, defining and coupling the dominant systems process (Fenicia et al., 2010). The overall model architecture is built based on how modeler's perceive the system processes of real world and which common control factors are seized to hackle the multivarious characteristics of the perceptual world.

The common control factors are key hypotheses of a hydrological model which should be reflected in model architecture. For example in TOPMODEL (Beven, 1997), topography is a key common control determining the overall model architecture and coupling the dominant water processes. In this research the land type (rural and urban areas) would be the key control factor to hackle the overall semi-distributed model architecture.

B.2 Process Connectivity

With the confirmed common control factor, the dominant water processes could be recognized (or assumed) and reflected as the process connectivity of conceptual model under the frame of overall model architecture.

Several connection elements of hydrologic process are exploited: 1) Union element can describe the import from different sources (Figure 2a). 2) Splitter element represents the separation of flux, which is used to describe many important water processes such as the separation of outflow from unsaturated reservoir to fast and slow response reservoir (Figure 2b), subtraction of evaporation from rainfall (Figure 2c), and the threshold-type subtraction of Horton overland flow from effective precipitation (Figure 2d).

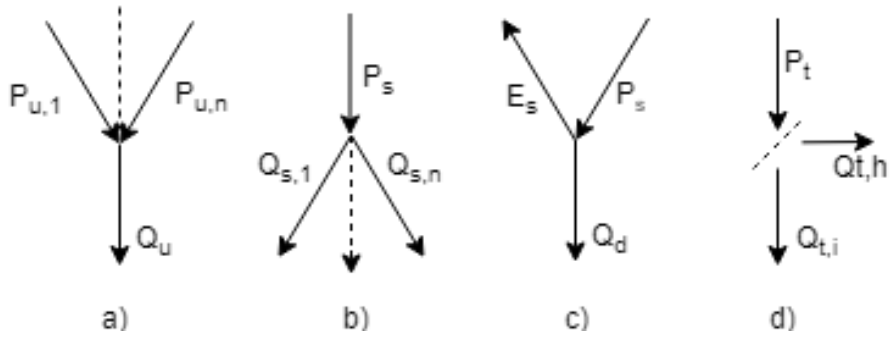

Figure 42. Four process connectivity elements

B.3 The Generic Reservoir Element: Storage-Release Process

The Generic Reservoir Element is used to describe the water accumulation and release processes in hydrological system such as interception, soil retention, groundwater aquifer store and snow accumulation.

In SUPERFLEX framework, 7 Generic Reservoir Elements for typical rural areas are provided, Interception Reservoir IR; Snow Reservoir WR; Unsaturated soil Reservoir UR; Combined Reservoir CR; Riparian zone Reservoir RR; Fast reacting Reservoir RR; and Slow reacting Reservoir SR.

Mathematically the Generic Reservoir Element can be described using ordinary differential equations(ODEs):

$\frac{dS(t)}{dt} = g_s[S(t), X(t)|\vartheta],$ (1)

$Q(t) = g_Q[S(t), X(t)|\vartheta],$ (2)

S(t): conceptual storage value at time t,

X(t): the time-dependent forcing

Q(t): outflow from reservoir

g(): the input-output fluxes associated with the component

ϑ: parameters

B.4 Lag Function Element: Transmission Delay

In principle the reservoir element and lag function element achieve the same function of describing the delay of water transmission progress. The difference is that the physical storage concept plays a key role on water release mode in reservoir element, but the lag function element is only a mathematical convolution operator to describe the delay of flow routing without water storage process. Two typical lag functions are listed below:

a. Gamma function (Press et al., 1992) is used in FUSE (Clark et al., 2010) and HYMOD (Wagener et al., 2001).
b. Triangular lag function is used in HBV (Lindström et al., 1997) and GR4J (Perrin et al., 2003) with curvature.

In this project, a simple half triangle lag function is exploited as shown in Figure 43.

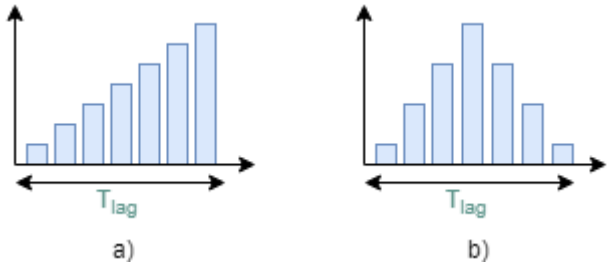

Figure 43. Half triangle (a) and Symmetric triangle (b) lag function

B.5 Constitutive Function Element

The constitutive functions could be used to quantitatively describe every model element such as storage-release relations, shapes of time lag functions and characteristics of junction elements (Fenicia et al., 2010). The selection of constitutive function is based on the empirical knowledge or data analysis. Some typical options are listed in Table 19.

Table 19. Typical constitutive function options

Function	Name
$f_p(x\|m) = x^m$	Power function
$f_r(x\|m) = 1 - (1 - x^m)$	Reflected power function [Moore, 1985]
$f_m(x\|m) = (1 + m)\frac{x}{x + m}$	Monod-type kinetics, adjusted so that $f_m(1\|m) = 1$

$f_h(x\|m) = 1 - \frac{(1-\mathrm{x})(1+\mathrm{m})}{1-\mathrm{x}+\mathrm{m}}$	Reflected hyperbolic function, scaled to the unit square
$f_e(x\|m) = 1 - e^{-x/m}$	Tessier function (note that $f_e(x\|m)\rightarrow 1$ as x→□)
$f_\lambda(x\|m,\lambda) = \frac{(1+e^{-m(1-\lambda)})(e^{-mx}-1)}{(1+e^{-m(1-\lambda)})(e^{-m}-1)}$	Modified logistic curve, scaled to the unit square

Appendix C Data processing and checking

C.1 Data processing

The research period is determined as 600 days between 2017-04-12 00:00:00 and 2018-12-02 23:30:00. There should be 28800 time-series data for both calibration and verification period.

C.1.1 Reference evaporation

On USGS websites, the provisional evaporation is provided for every 30 minutes with the unit of millimetres per day. Because the evaporation data is labelled with "Provisional data subject to revision", the evaporation data is further checked by comparing with the evaporation data of nearby CAMELS catchments. Figure 44 shows the distribution of CAMELS catchments and study catchment.

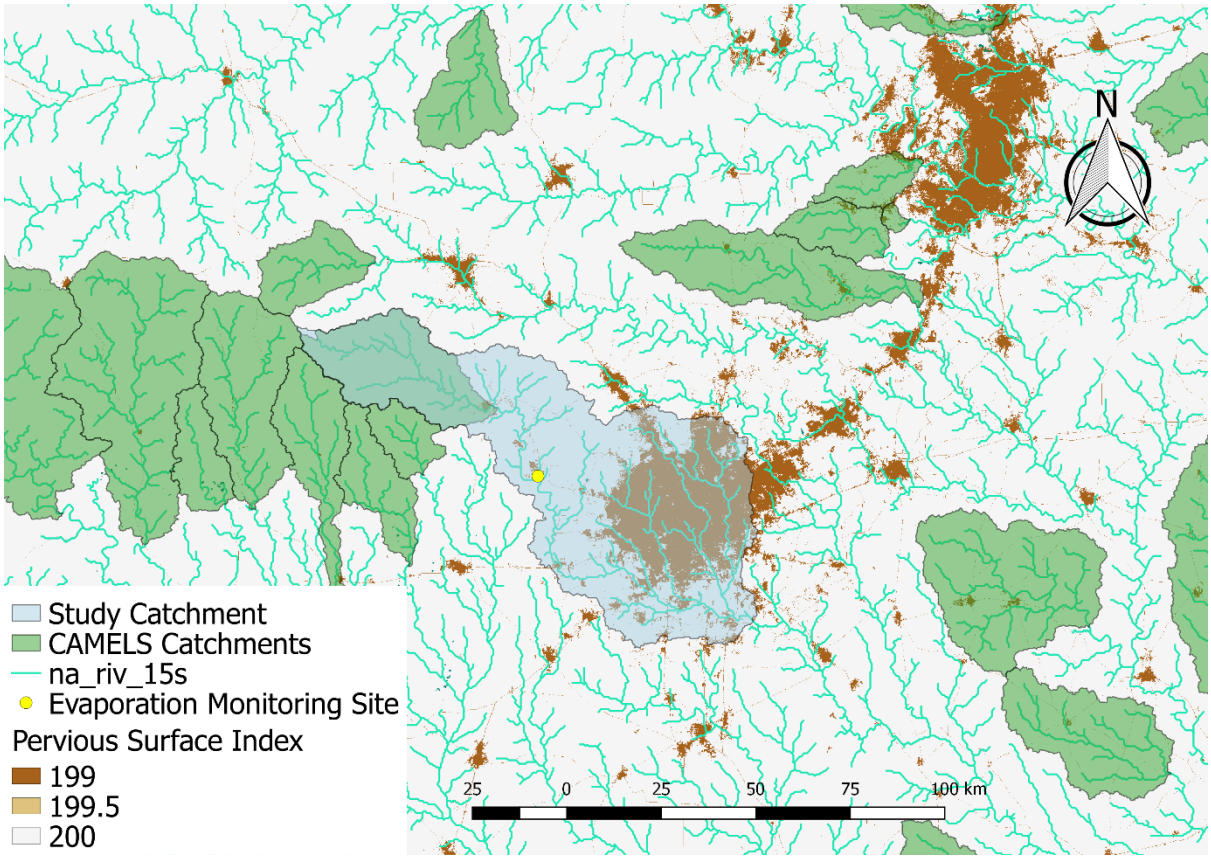

Figure 44. The relationship of CAMELS and Study catchment position

It is obvious that there is an overlap of CAMELS database and study catchment. The actual evaporation data of the overlap catchment and several nearby CAMELS catchments are analysed. It is found that the long-time average daily actual evaporation of CAMELS catchment is around 1.8 mm. However the "evapotranspiration" data of study area provided by USGS websites shows a mean value of 0.075mm/day which is far less than empirical value.

One hypothesis could be the error of USGS data unit, which should be mm/hour rather than mm/day. After unit transfer, the evaporation data shows a normal level with an average value of 1.75 mm/day. In addition, water balance of precipitation, discharge and evaporation of study catchment is also checked in data checking process, which also supports the hypothesis. Therefore the evaporation data after unit transfer is exploited in this research as reference evaporation.

And after the unit conversion, according to a preliminary data check, there are 5% evaporation data missing in research period with 1478 blank point in time. In addition, two data perform irregular with far more and less than others. After cleaning the irregular data, all blank evaporation data are interpolated obeying the regulations below: For the numbers of continuously missing data points which are less than 5 (3 hours), linear interpolation is exploited; For the missing data series which is longer than 3 hours, the average value of the evaporation data on the same time in one day before and one day after will be used. Finally for the 2406 data which are negative, zeros are used as reference evaporation.

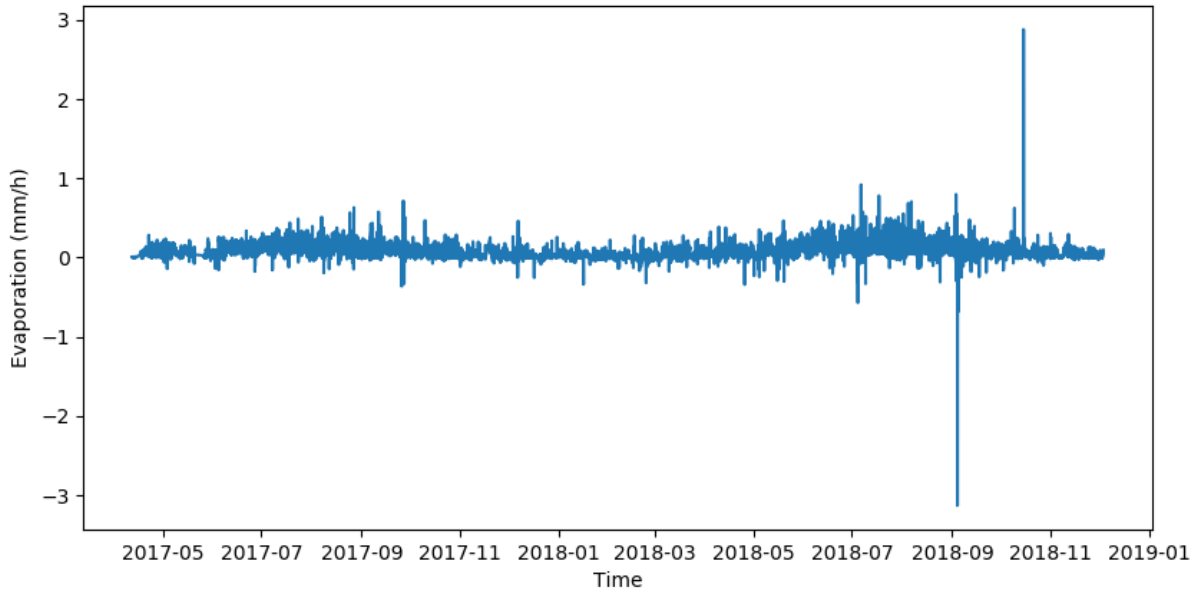

Figure 45. The raw evaporation time-series data

C.1.2 Discharge

For the discharge data of study catchment, the missing discharge data are only 96 and the longest time interval of missing data is 14 hours with 27 missing data happening on flood period. Linear interpolation method is exploited to get all the 96 missing values. The interpolation result and raw data of study catchment are shown in Figure 46. Finally, the discharge data in cubic feet per second are converted to millimetre per day by divided the area of research catchment.

The same discharge data processing method is exploited for the other two stations of sub-catchments.

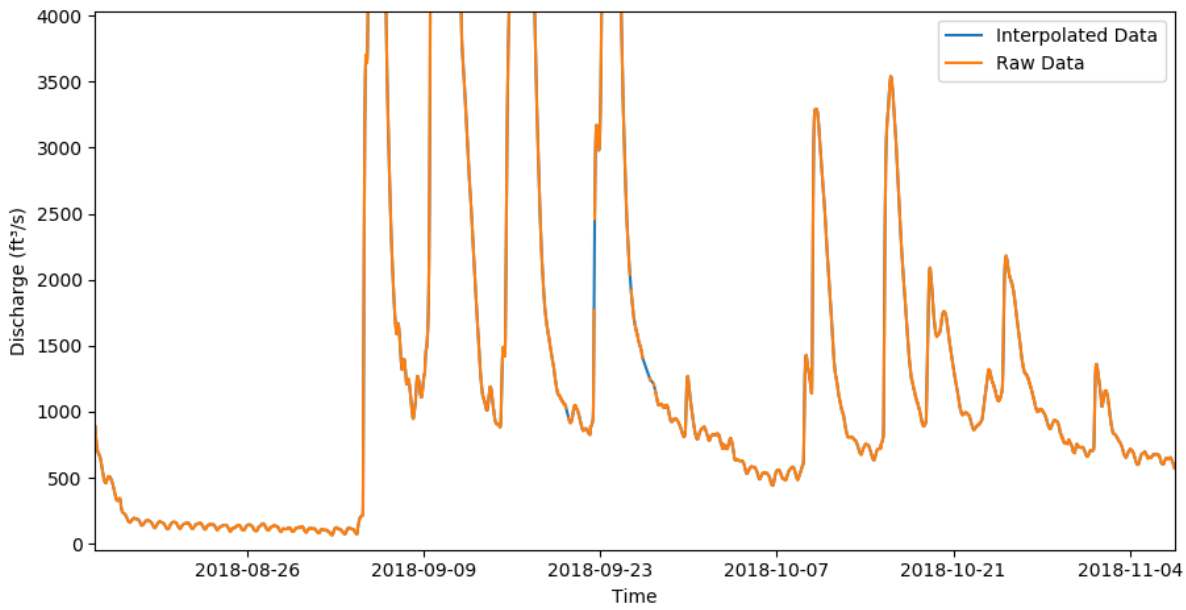

Figure 46. Raw discharge data from STN 08181800 and its interpolation result

C.1.3 Precipitation

The precipitation data of all the three catchments are processed according to the same procedures: Since all of the ten precipitation monitoring stations have complete cumulative precipitation time-series records with different time scale (smaller than 30 minutes), the first procedure of data processing is cumulated the precipitation to half an hour. And then the total precipitation value would be calculated with the weight of each monitoring stations according to the area ratios of Thiessen polygons. Finally the unit of data should be converted from inches per 30 minutes to millimetre per day.

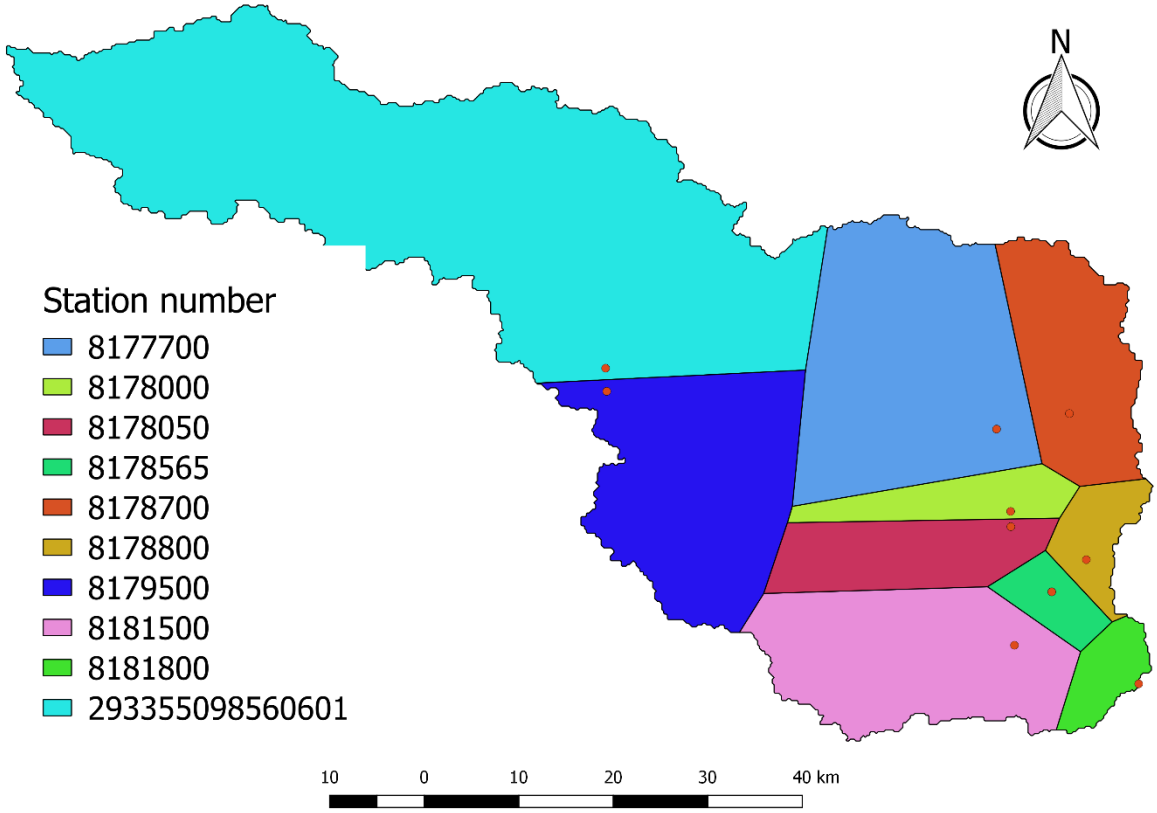

Figure 47. Thiessen polygons of available precipitation sites

C.2 Data checking

C.2.1 The Statistical Analysis of Data

a1. Average

The annual and daily average numbers of processed precipitation, reference evaporation and discharge data of three catchments are calculated and compared with the background information. Especially the evaporation data is the same for the three catchments. The calculated results are shown in the Table 20.

Table 20. Annual and Daily Average Data of three catchments

Study catchment	Precipitation	Reference Evaporation	Discharge (total)
Annual average (mm/y)	812.0	641.3	101.1
Daily average (mm/d)	2.225	1.757	0.277
Rural sub-catchment	Precipitation	Reference Evaporation	Discharge (total)
Annual average (mm/y)	724.9	641.3	15.1
Daily average (mm/d)	1.986	1.757	0.069
Urban sub-catchment	Precipitation	Reference Evaporation	Discharge (total)
Annual average (mm/y)	865.8	641.3	10.1
Daily average (mm/d)	2.372	1.757	0.027

a2. Histogram

The histograms of processed precipitation, evaporation and discharge data also have normal performances, which are shown in the Table 21.

Table 21. Histograms of daily data

	Histogram
Discharge	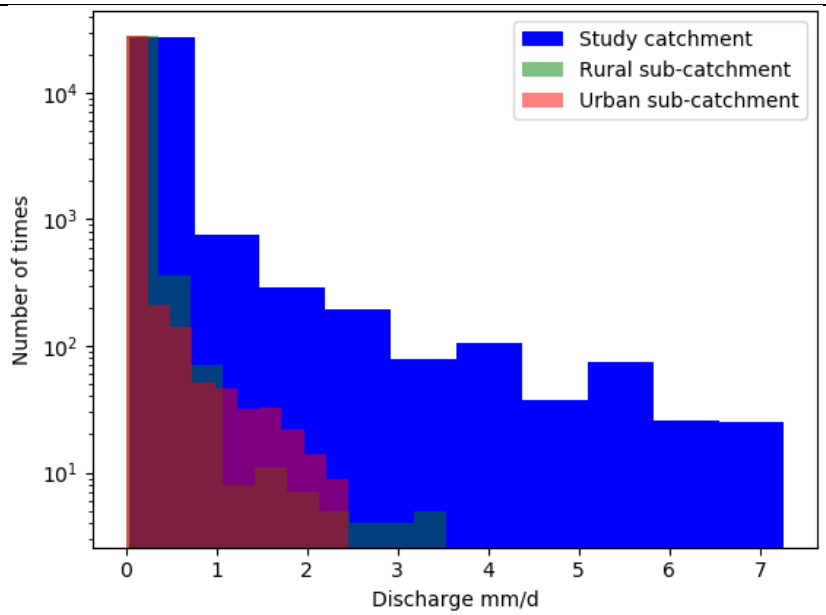
Precipitation	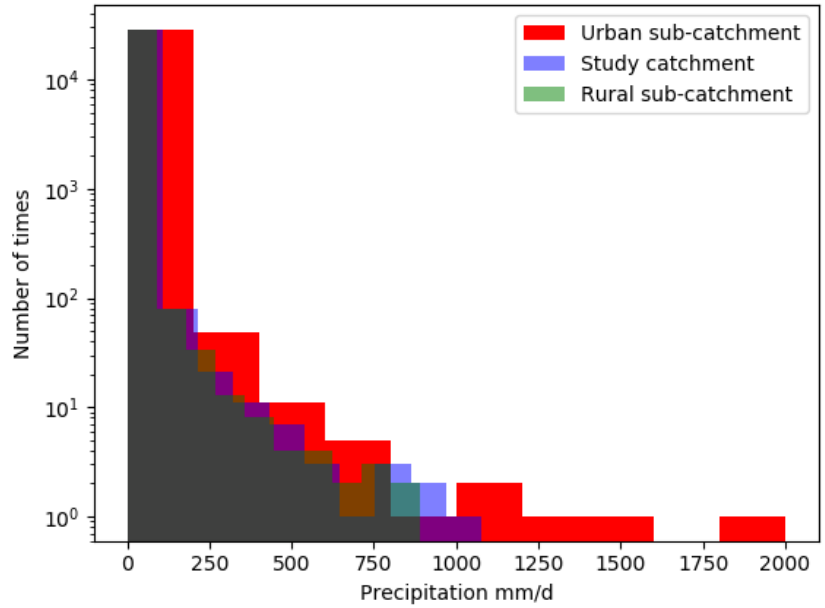

Evaporation	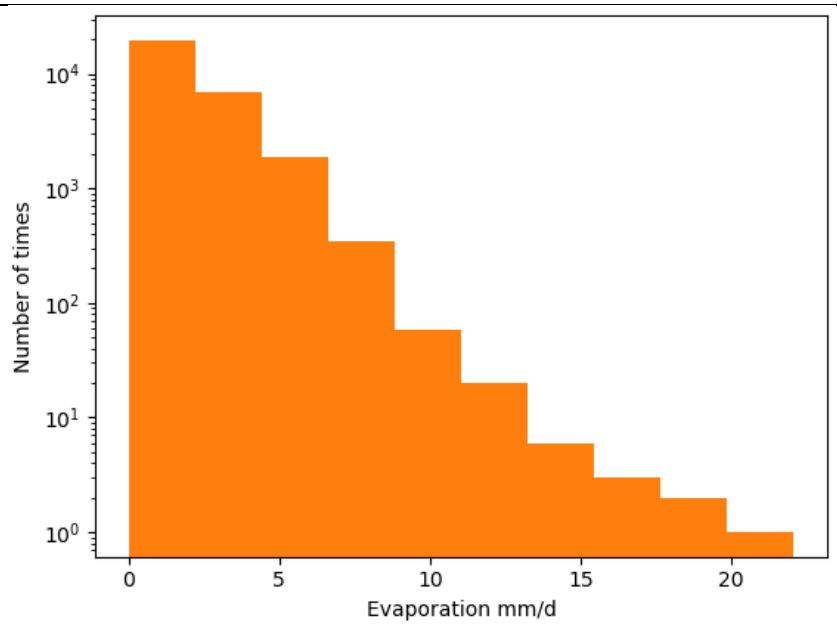

C.2.2 Water balance

Finally, the data is checked with water balance equation which means that the sum of precipitation in one year should be roughly equal to the sum of evaporation and discharge of the catchment. Because the research period is not two civil year, the yearly water balance is checked twice from 2017-04-12 00:00:00 to 2018-04-11 23:30:00 and from 2017-12-03 00:00:00 to 2018-12-02 23:30:00 respectively. The calculation results of the gap between water input and output are shown in Table 22.

Table 22. Water Balance Check Result

Study catchment		Precipitation	Evaporation	Discharge	Gap
From 2017-04-12 to 2018-04-11	Sum (mm/year)	632.24	551.43	66.54	14.27
	Daily Mean value (mm/day)	1.73	1.51	0.18	
From 2017-12-03 to 2018-12-02	Sum (mm/year)	961.10	594.22	128.07	238.81
	Daily Mean value (mm/day)	2.63	1.63	0.35	
Rural sub-catchment		Precipitation	Evaporation	Discharge	Gap
From 2017-04-12 to 2018-04-11	Sum (mm/year)	604.71	551.43	15.80	37.49
	Daily Mean value (mm/day)	1.66	1.51	0.04	
	Sum (mm/year)	843.74	594.60	31.47	217.67

From 2017-12-03 to 2018-12-02	Daily Mean value (mm/day)	2.31	1.63	0.09	
Urban sub-catchment		Precipitation	Evaporation	Discharge	Gap
From 2017-04-12 to 2018-04-11	Sum (mm/year)	729.38	551.43	7.19	170.76
	Daily Mean value (mm/day)	2.00	1.51	0.02	
From 2017-12-03 to 2018-12-02	Sum (mm/year)	1014.96	594.60	13.67	406.69
	Daily Mean value (mm/day)	2.78	1.63	0.04	

It is obvious that the second period has more rainwater and discharge than the first year. To the contrary, there is no significant difference of evaporation between the two years. And there are gaps between water recharge and discharge of study and rural catchment in both two period, which are in an acceptable error range. However the gap of urban catchment is far more than rural and study catchment.

One explanation of the gap of rural catchment could be the recharge to local groundwater aquifer, Edwards Aquifer. As for the larger water volume gap in urban sub-catchment, the urban water system may be the reason:

Therefore, when building the hydrologic model, the groundwater storage and convey and the water exchange between different hydrologic catchments due to urban water connection system should be considered.

Appendix D Rainfall-runoff rural and urban lumped models

D.1 Rural lumped model test

D.1.1 Rural lumped Model 01

The first lumped model for rural areas is a simple one bucket model which could also be the starting point of model generation. Three different constitutive functions are used to test different storage-outflow relationship in Model 01 (Qs, Qq, and Pc as shown in Table 23).

In rural lumped Model 01A (M01A), a Slow reacting Reservoir (SR) is used to simulate the relatively slow hydrological character of rural area. And the mathematical expression of discharge (Qs) describes the stable and slow groundwater flow. For Model 01B (M01B), the model structure focuses on the unsaturated zone and the mathematical expression of discharge (Qq) exploits an exponential equation of storage scaled to describe a quicker and more variable overflow mode. And in Model 01C (M01C), this overflow from unsaturated zone in M01B is combined with an additional percolation process, which also represents the core soil moisture accounting component of TOPMODEL and VIC (Kavetski et al., 2010).

The comparison of model structure and model performance of M01 are shown in Table 23.

Table 23. The comparison of model structure and model performance of Rural Lumped M01

Model (Par. Num.)	Schematic figure of model structure	Mathematical expression of water process	NSE	Relative error
Model 01A (3)	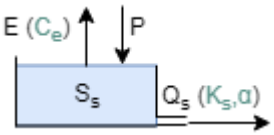	$E = C_e E_r$ $Q_s = K_s S_s^{\alpha}$	0.40	0.070
Model 01B (3)	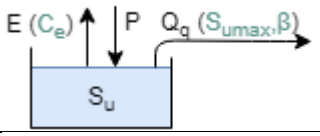	$E = C_e E_r$ $Q_q = P * \left(\frac{S_u}{S_{umax}}\right)^{\beta}$	-0.48	0.95
Model 01C (4)	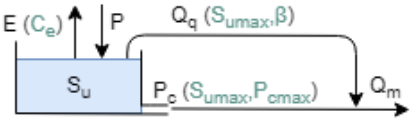	$E = C_e E_r$ $Q_q = P * \left(\frac{S_u}{S_{umax}}\right)^{\beta}$ $P_c = P_{cmax} \frac{S_u}{S_{umax}}$	0.36	0.050

"Relative error": Relative error of total outflow; "Par. Num.": Parameter Number

In which:

Parameter	Description	Model Components	Description
Ce [-]	Evaporation correction coefficient	Ss (mm)	Storage in SR
Ks [1/mmα*d]	Slow reservoir coefficient	Su (mm)	Storage in UR
α [-]	Discharge exponent	P (mm/d)	Precipitation
Pcmax [mm/d]	Maximum percolation velocity	E (mm/d)	Actual Evaporation
Sumax [mm]	Maximum unsaturated storage	Er (mm/d)	Reference Evaporation
β [-]	Unsaturated discharge exponent	Qs (mm/d)	Discharge from SR
		Qq (mm/d)	Overflow from UR
		Pc (mm/d)	Percolation from UR

There are 3 parameters in both M01A and M01B to quantify evaporation and discharge processes, and there are 4 parameters in M01C. The model starts from bare buckets condition. But the zero initial

storage leads to the unstable discharge result of the first several days. Therefore an initial storage value in reservoir is given as 5 mm to realize a stable discharge beginning.

3000 and 4000 sets of parameters are sampled for calibration process for M01A, M01B and M01C. The model performances of M01 are bad as shown from Figure 56 to Figure 61. It may because these over-simple one bucket models of M01 cannot reproduce the complex hydrologic processes in research rural sub-catchment.

D.1.2 Rural lumped Model 02

One additional Slow reacting Reservoir (SR) is added in rural lumped Model 02 to divide the saturated groundwater from unsaturated zone. A "Unsaturated Reservoir - Slow response Reservoir(UR-SR)" two buckets parallel model structure is created as Model 02. The model structure comparison of M02A and M02B is shown in Table 24.

Table 24. The comparison of model structure and model performance of Rural Lumped M02

Model (Par. Num.)	Schematic figure of model structure	Mathematical expression of water process	NSE	Relative error
Model 02A (5)	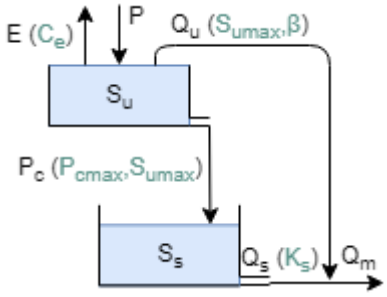	$E = C_e E_r$ $Q_u = P * \left(\frac{S_u}{S_{umax}}\right)^{\beta}$ $P_c = P_{cmax}\frac{S_u}{S_{umax}}$ $Q_s = K_s S_s$	0.18	-0.035
Model 02B (5)	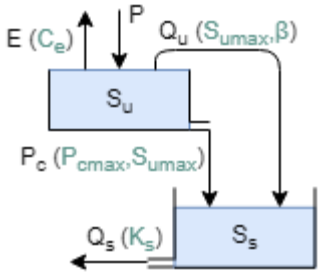	$E = C_e E_r$ $Q_u = P * \left(\frac{S_u}{S_{umax}}\right)^{\beta}$ $P_c = P_{cmax}\frac{S_u}{S_{umax}}$ $Q_s = K_s S_s$	0.22	0.067

"Relative error": Relative error of total outflow; "Par. Num.": Parameter Number

In which:

Parameter	Description	Model Components	Description
Ce [-]	Evaporation correction coefficient	Su (mm)	Storage in UR
Sumax [mm]	Maximum unsaturated storage	Ss (mm)	Storage in SR
β [-]	Unsaturated discharge exponent	Er (mm/d)	Reference Evaporation
Pcmax [mm/d]	Maximum percolation velocity	Pc (mm/d)	Percolation
Ks [1/mmα*d]	Slow reservoir coefficient	Qu (mm/d)	Overflow from UR
		Qs (mm/d)	Discharge from SR

There are 2 buckets and 5 parameters in M02 and accordingly 5000 sets of parameters are sampled for parameter calibration. The initial storage value in SR is given as 20 mm to realize a stable discharge beginning. The model result and parameter calibration result of M02 are shown from Figure 62 to Figure 65.

The model performances of M02A and M02B are still not good as shown in Figure 62 and Figure 64. However the defects of M02A and M02B are different: For M02A, in which the overflow (Qu) from

UR discharges directly, the modelled total runoff (Qm) swings between rapid peak and no peak. The moderate fast peak mode cannot be simulated in M02A; And for M02B, since all runoff discharges from SR, which follows the stable and slow characters of groundwater base flow, there is not peaks at all.

These defects of M02A and M02B could be also ascribed to the over-simple model structures which restrain the diversity of outflow pattern. Therefore, one additional Fast reacting Reservoir (FR) will be added in next generation to simulate the moderate fast peaks.

D.1.3 Rural lumped Model 03

Fast reacting Reservoir (FR) is added to increase the diversity of outflow pattern and a "UR-SR-FR" three buckets model structure is created in Model 03. And based on the "UR-SR-FR" three buckets model structure, a time lag function is exploited on the overflow from UR to FR (Qu) to simulate the delay function of unsaturated zone. The most simple version of Model 03 is built in M03A with 7 parameters. The schematic figures of model structures are shown in Table 25.

Table 25. The comparison of model structure and model performance of Rural Lumped M03

Model (Par. Num.)	Schematic figure of model structure	Mathematical expression of water process	NSE	Relative error
Model 03A (7)	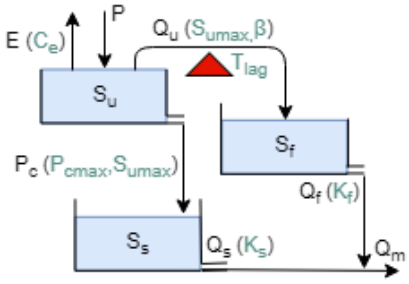	$E = C_e E_r$ $Q_u = P * \left(\frac{S_u}{S_{umax}}\right)^{\beta}$ $P_c = P_{cmax}\frac{S_u}{S_{umax}}$ $Q_f = K_f S_f$ $Q_s = K_s S_s$	0.662	0.019
Model 03B (8)	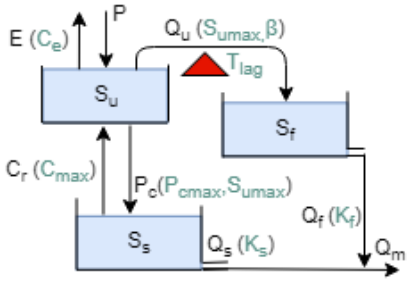	$E = C_e E_r$ $Q_u = P * \left(\frac{S_u}{S_{umax}}\right)^{\beta}$ $P_c = P_{cmax}\frac{S_u}{S_{umax}}$ $C_r = C_{max}(1 - \frac{S_u}{S_{umax}})$ $Q_f = K_f S_f$ $Q_s = K_s S_s$	0.668	0.085
Model 03C (8)	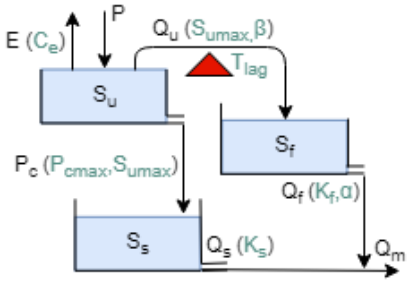	$E = C_e E_r$ $Q_u = P * \left(\frac{S_u}{S_{umax}}\right)^{\beta}$ $P_c = P_{cmax}\frac{S_u}{S_{umax}}$ $Q_s = K_s S_s$ $Q_f = K_f {S_f}^{\alpha}$	0.683	-0.050

Model 03D (9)	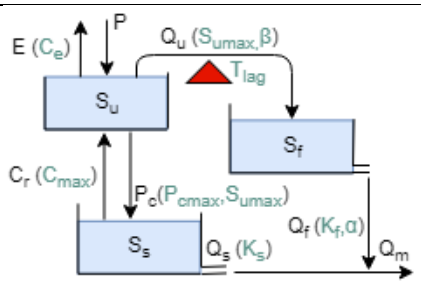	$E = C_e E_r$ $Q_u = P * \left(\frac{S_u}{S_{umax}}\right)^{\beta}$ $P_c = P_{cmax}\frac{S_u}{S_{umax}}$ $C_r = C_{max}(1 - \frac{S_u}{S_{umax}})$ $Q_s = K_s S_s$ $Q_f = K_f {S_f}^{\alpha}$	0.690	-0.023
Model 03E (9)	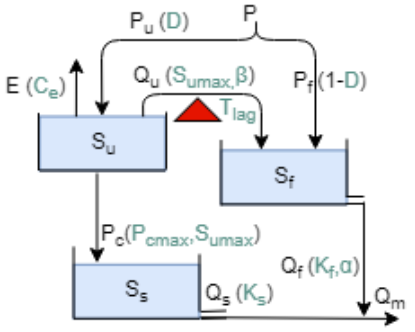	$P_u = D * P$ $P_f = (1 - D) * P$ $E = C_e E_r$ $Q_u = P_u * \left(\frac{S_u}{S_{umax}}\right)^{\beta}$ $P_c = P_{cmax}\frac{S_u}{S_{umax}}$ $Q_s = K_s S_s$ $Q_f = K_f {S_f}^{\alpha}$	0.713	-0.069
Model 03F (10)	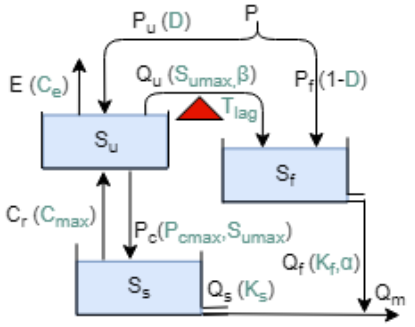	$P_u = D * P$ $P_f = (1 - D) * P$ $E = C_e E_r$ $Q_u = P_u * \left(\frac{S_u}{S_{umax}}\right)^{\beta}$ $P_c = P_{cmax}\frac{S_u}{S_{umax}}$ $C_r = C_{max}(1 - \frac{S_u}{S_{umax}})$ $Q_s = K_s S_s$ $Q_f = K_f {S_f}^{\alpha}$	0.723	-0.026

"Relative error": Relative error of total outflow; "Par. Num.": Parameter Number

In which:

Parameter	Description	Model Components	Description
D [-]	Precipitation distribution factor	Su (mm)	Storage in UR
Ce [-]	Evaporation correction coefficient	Ss (mm)	Storage in SR
Sumax [mm]	Maximum unsaturated storage	Sf (mm)	Storage in FR
β [-]	Unsaturated discharge exponent	Pu (mm/d)	Precipitation on UR
Pcmax [mm/d]	Maximum percolation velocity	Pf (mm/d)	Precipitation on FR
Cmax [mm/d]	Maximum capillary rise velocity	Pc (mm/d)	Percolation
Ks [1/mmα*d]	Slow reservoir coefficient	Cr (mm/d)	Capillary rise
Kf [1/mmα*d]	Fast reservoir coefficient	Qu (mm/d)	Overflow from UR
α [-]	Fast reservoir discharge exponent	Qf (mm/d)	Discharge from FR
Tlag [-]	Time lag coefficient	Qs (mm/d)	Discharge from SR

There are 7 parameters in M03A and accordingly 7000 sets of parameters were sampled for parameter calibration. The initial storage value in SR was given as 20 mm to realize a stable discharge beginning. The model result and parameter calibration result of M03A are shown in Figure 48.

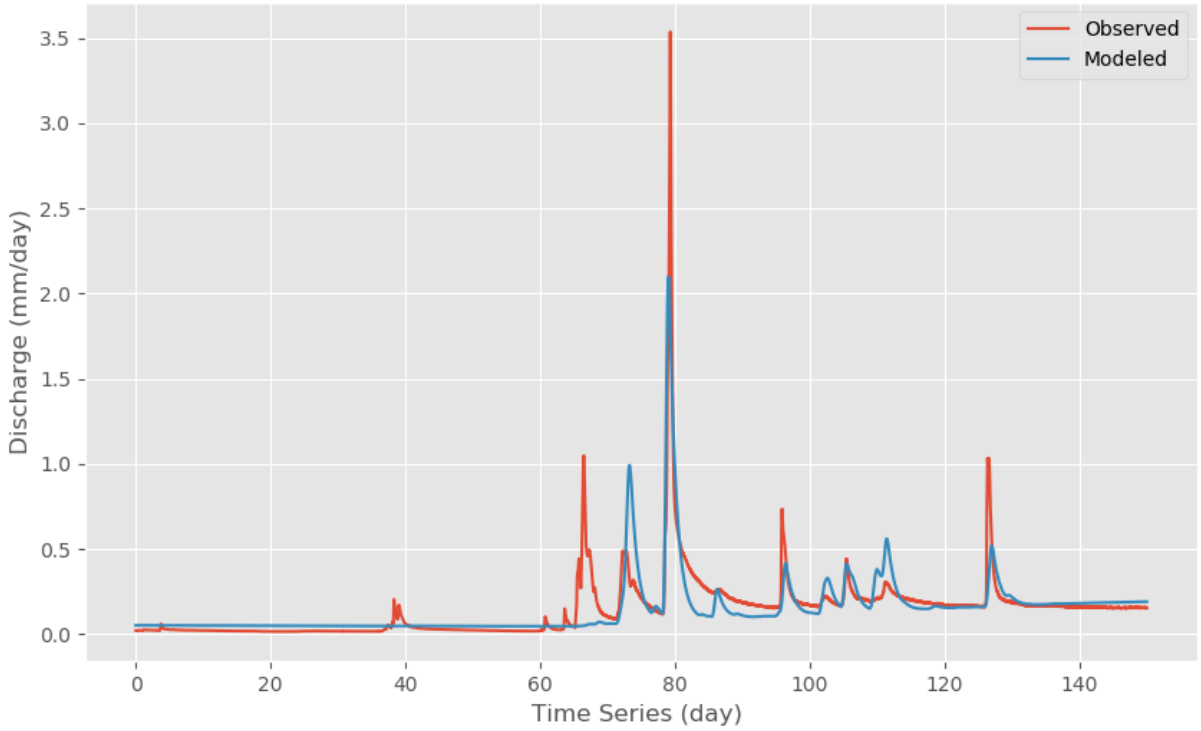

Figure 48. Model Result of M03A

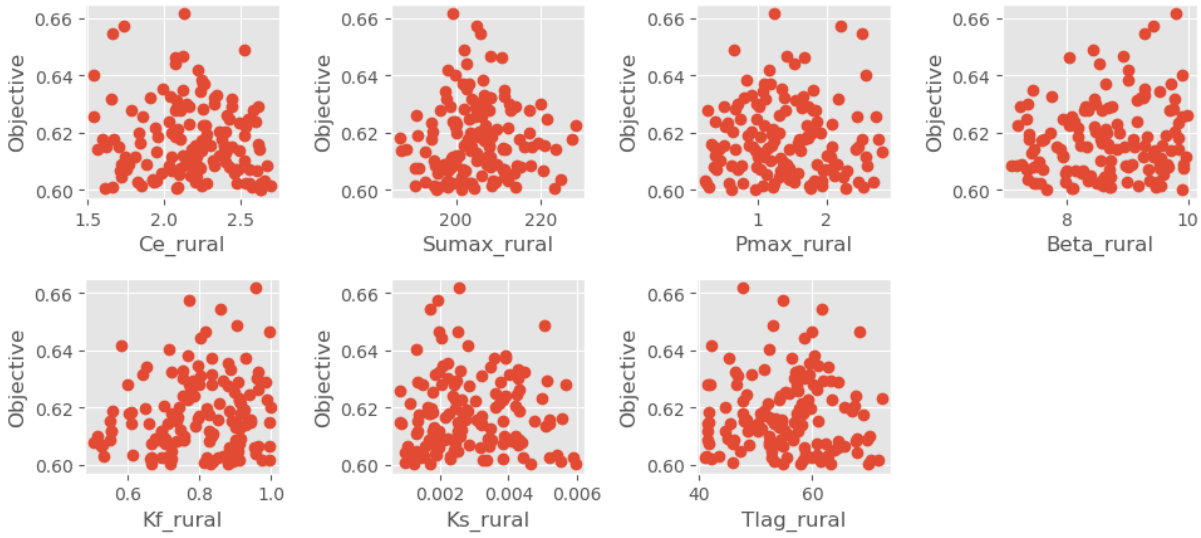

Figure 49. Parameter Calibration Result of M03A

It could be found from Figure 48 and Figure 49 that the model performance of M03A improved significantly compared to M02 with an additional FR especially on peak flow simulation. It may prove that the fast groundwater flow is one essential process to generate peak flows. But for the extreme peak flow (the largest peak runoff within the 150 simulating period, which is at around the 80th day), the model performance of M03A is still dissatisfactory.

To improve the model performance on extreme peak flow, three model components, capillary rise Cr (M03B, M03D and M03F), discharge exponent α (M03C, M03D, M03E and M03F), and precipitation distribution factor D (M03E and M03F) were added and tested based on the model structure of M03A.

There are 8-10 parameters in M03B-M03F and accordingly 8000 to 10000 sets of parameters were sampled for parameter calibration. And the initial storage value in SR is given as 20 mm to realize a stable discharge beginning. The model result and parameter calibration result of M03B-M03F are shown from Figure 66 to Figure 73.

As Table 25 shows, all of the three model components (discharge exponent, capillary rise, and precipitation distribution factor) contributed to the model performance on peak flow simulation and all of the five models had higher NSE than M03A. Especially, M03F with all the three additional model components achieved the highest NSE among six M03s as 0.723.

These model results may endorse the hydrological meaning of capillary rise in rural sub-catchment. And then in M03E and M03F, part of rainwater is conveyed to FR directly, which makes the FR also undertake the function of Riparian Reservoir (RR) rather than limited in a complete groundwater meaning.

D.1.4 Rural lumped Model 04

Based on the "UR-SR-FR" three buckets model structure of M03, one Riparian Reservoir (RR) is added and tested in Model 04. And the capillary rise process (Cr) and the position of discharge exponent (α) are further tested among M04A-M04D. The comparison of model structure and model performance of M04 are shown in Table 26.

Table 26. The comparison of model structure and model performance of Rural Lumped M04

Model (Par. Num.)	Schematic figure of model structure	Mathematical expression of water process	NSE	Relative error
Model 04A (10)	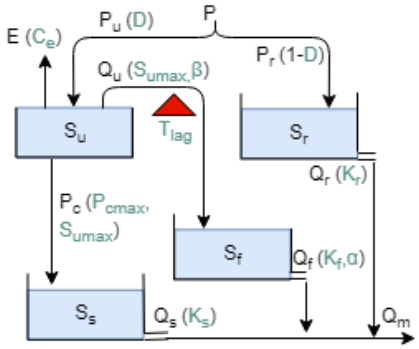	$P_u = D * P$ $P_r = (1 - D) * P$ $E = C_e E_r$ $Q_u = P_u * \left(\frac{S_u}{S_{umax}}\right)^{\beta}$ $P_c = P_{cmax}\frac{S_u}{S_{umax}}$ $Q_s = K_s S_s$ $Q_f = K_f {S_f}^{\alpha}$ $Q_r = K_r S_r$	0.770	0.126
Model 04B (11)	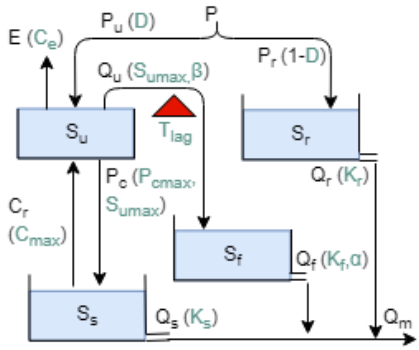	$P_u = D * P$ $P_r = (1 - D) * P$ $E = C_e E_r$ $Q_u = P_u * \left(\frac{S_u}{S_{umax}}\right)^{\beta}$ $P_c = P_{cmax}\frac{S_u}{S_{umax}}$ $C_r = C_{max}(1 - \frac{S_u}{S_{umax}})$ $Q_s = K_s S_s$ $Q_f = K_f {S_f}^{\alpha}$ $Q_r = K_r S_r$	0.802	0.002

Model 04C (10)	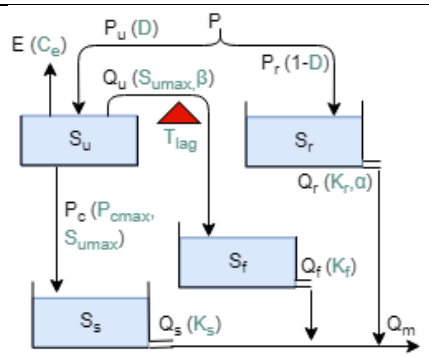	$P_u = D * P$ $P_r = (1 - D) * P$ $E = C_e E_r$ $Q_u = P_u * \left(\frac{S_u}{S_{umax}}\right)^{\beta}$ $P_c = P_{cmax} \frac{S_u}{S_{umax}}$ $Q_f = K_f S_f$ $Q_r = K_r {S_r}^{\alpha}$ $Q_s = K_s S_s$	0.685	-0.053
Model 04D (11)	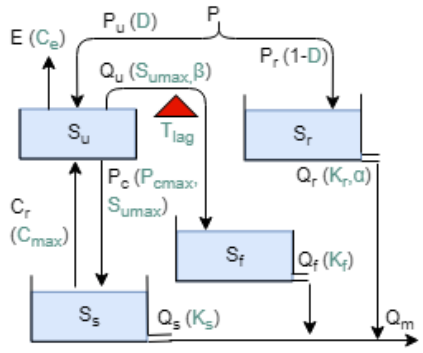	$E = C_e E_r$ $Q_u = P_u * \left(\frac{S_u}{S_{umax}}\right)^{\beta}$ $P_c = P_{cmax} \frac{S_u}{S_{umax}}$ $C_r = C_{max}(1 - \frac{S_u}{S_{umax}})$ $Q_f = K_f S_f$ $Q_r = K_r {S_r}^{\alpha}$ $Q_s = K_s S_s$	0.706	0.180

"Relative error": Relative error of total outflow; "Par. Num.": Parameter Number

In which:

Parameter	Description	Model Components	Description
D [-]	Precipitation distribution factor	Su (mm)	Storage in UR
Ce [-]	Evaporation correction coefficient	Ss (mm)	Storage in SR
Sumax [mm]	Maximum unsaturated storage	Sf (mm)	Storage in FR
β [-]	Unsaturated discharge exponent	Sr (mm)	Storage in RR
Pcmax [mm/d]	Maximum percolation velocity	Er (mm/d)	Reference Evaporation
Cmax [mm/d]	Maximum capillary rise velocity	Pc (mm/d)	Percolation
Ks [1/mmα*d]	Slow reservoir coefficient	Cr (mm/d)	Capillary rise
Kf [1/mmα*d]	Fast reservoir coefficient	Qu (mm/d)	Overflow from UR
Kr [1/mmα*d]	Riparian reservoir coefficient	Qf (mm/d)	Discharge from FR
α [-]	Discharge exponent	Qs (mm/d)	Discharge from SR
Tlag [-]	Time lag coefficient	Qr (mm/d)	Discharge from RR

There are 10 or 11 parameters in M04. The initial storage value of SR was given as 20 mm and 10000 and 11000 sets of parameters were sampled for parameter calibration. The model result and parameter calibration result of M04 are shown from Figure 74 to Figure 81.

The position of discharge exponent is tested between M04A, M04B and M04C, M04D. It could be found compared to the overflow from RR (Qr), the exponent discharge on overflow from FR (Qf) could bring better model performance on peak flow simulation as NSE_{M04A}>NSE_{M04C} and NSE_{M04B}>NSE_{M04D}. Secondly, capillary rise also improve the NSE significant as NSE_{M04B}>NSE_{M04A} and NSE_{M04D}>NSE_{M04C}.

Compared to M03E and M03F, with one more RR, the NSEs of M04A and M04B are improved obviously. It is reasonable that since the intensive expansion of river network in study rural sub-catchment, the riparian environment should be an important part in rural lumped model. And although in Model 04 most of the precipitation falls on the UR rather than RR (the precipitation distribution factor D is close to 1 as the parameter calibration result shown in Figure 75), the effect of riparian

reservoir on peak flow generation is obvious especially for the small peaks. Therefore the additional RR improved the NSE from 0.713 (M03E) to 0.770 (M04A) and from 0.723 (M03F) to 0.802 (M04B).

D.1.5 Rural lumped Model 05

Interception Reservoir (IR) is tested in Model 05, based on the "UR-SR-FR" three buckets model framework of M03. Since the contributions of discharge exponent (α) and capillary rise has been proved twice in M03 and M04, these two parameters will be contained in M05. And two distribution methods of effective precipitation (Pe) are tested between Model 05A and M05B. The schematic figure of model structures are shown in Table 27.

Table 27. The comparison of model structure and model performance of Rural Lumped M05

Model (Par. Num.)	Schematic figure of model structure	Mathematical expression of water process	NSE	Relative error
Model 05A (10)	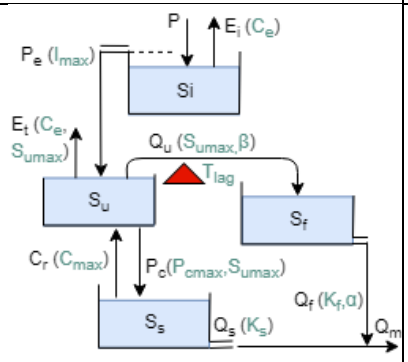	$E_i = C_e E_r$ $P_e = S_i - I_{max}$ $E_t = (C_e E_r - E_i) * (\frac{S_u}{S_{umax}})$ $Q_u = P_e * \left(\frac{S_u}{S_{umax}}\right)^{\beta}$ $P_c = P_{cmax} \frac{S_u}{S_{umax}}$ $C_r = C_{max}(1 - \frac{S_u}{S_{umax}})$ $Q_s = K_s S_s$ $Q_f = K_f {S_f}^{\alpha}$	0.672	0.116
Model 05B (11)	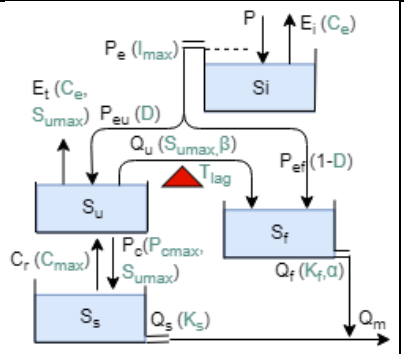	$E_i = C_e E_r$ $P_e = S_i - I_{max}$ $P_{eu} = D * P_e$ $P_{ef} = (1 - D) * P_e$ $E_t = (C_e E_r - E_i) * (\frac{S_u}{S_{umax}})$ $Q_u = P_{eu} * \left(\frac{S_u}{S_{umax}}\right)^{\beta}$ $P_c = P_{cmax} \frac{S_u}{S_{umax}}$ $C_r = C_{max}(1 - \frac{S_u}{S_{umax}})$ $Q_s = K_s S_s$ $Q_f = K_f {S_f}^{\alpha}$	0.727	0.167

"Relative error": Relative error of total outflow; "Par. Num.": Parameter Number

In which:

Parameter	Description	Model Components	Description
Imax [mm]	Maximum interception thickness	Si (mm)	Storage in IR
D [-]	Precipitation distribution factor	Su (mm)	Storage in UR
Ce [-]	Evaporation correction coefficient	Ss (mm)	Storage in SR
Sumax [mm]	Maximum unsaturated storage	Sf (mm)	Storage in FR
β [-]	Unsaturated discharge exponent	Pe (mm/d)	Effective Precipitation
Pcmax [mm/d]	Maximum percolation velocity	Ei (mm/d)	Interception

Cmax [mm/d]	Maximum capillary rise velocity	Et (mm/d)	Transpiration
Ks [1/mmα*d]	Slow reservoir coefficient	Pc (mm/d)	Percolation
Kf [1/mmα*d]	Fast reservoir coefficient	Cr (mm/d)	Capillary rise
α [-]	Discharge exponent	Qu (mm/d)	Overflow from UR
Tlag [-]	Time lag coefficient	Qf (mm/d)	Discharge from FR
		Qs (mm/d)	Discharge from SR

There are 10 or 11 parameters in M05A and M05B respectively. 10000 and 11000 sets of parameters are sampled for parameter calibration. The initial storage value of SR is given as 20 mm. The model results and parameter calibration results of M05 are shown from Figure 82 to Figure 85.

As the model result shown in Table 27, the additional IR does not have obvious positive effect on the NSEs of M05A and M05B compared to original M03D and M03F. Besides the model performance on extreme peaks simulation are not improved neither. It may because that the interception process is not one dominant water process in rural sub-catchment.

As for the precipitation distribution method tested between Model 05A and M05B, as similar as the results of M03, conveying part of precipitation to FR with an additional distribution factor D in M05B will bring higher NSE than it of M05A.

D.1.6 Rural lumped Model 06

Interception Reservoir (IR) is added and tested again in rural lumped Model 06 based on the model structure of M04B. The schematic figure of model structure is shown in Figure 50.

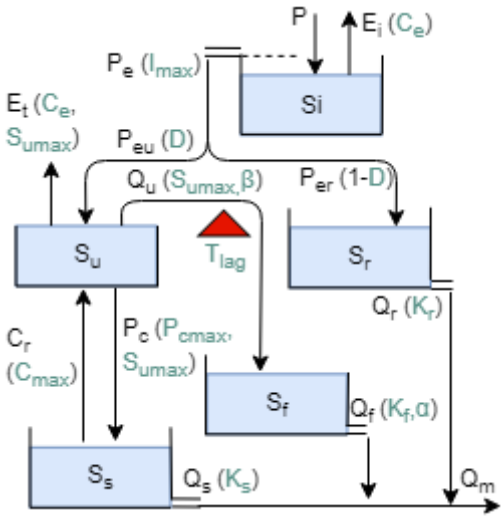

Figure 50. The schematic figure of model structure of rural lumped M06

There are 12 parameters in M06. The mathematical expressions of water processes in M06 are:

Evaporation from interception reservoir (mm/d): $E_i = C_e E_r$

Effective Precipitation (mm/d): $P_e = S_i - I_{max}$

The effective precipitation on UR (mm/d): $P_{eu} = D * P_e$

The effective precipitation on RR (mm/d): $P_{er} = (1 - D) * P_e$

Transpiration from unsaturated reservoir (mm/d): $E_t = (C_e E_r - E_i) * (\frac{S_u}{S_{umax}})$

Percolation from UR to SR: $P_c = P_{cmax} \frac{S_u}{S_{umax}}$

Capillary rise from SR to UR: $C_r = C_{max}(1 - \frac{S_u}{S_{umax}})$

Overflow from UR (mm/d): $Q_u = P_{eu} * \left(\frac{S_u}{S_{umax}}\right)^{\beta}$

Discharge from RR (mm/d): $Q_r = K_r S_r$

Discharge from FR (mm/d): $Q_f = K_f {S_f}^{\alpha}$

Discharge from SR (mm/d): $Q_s = K_s S_s$

With the parameters:

Parameter	Description	Model Components	Description
Imax [mm]	Maximum interception thickness	Si (mm)	Storage in IR
D [-]	Precipitation distribution factor	Su (mm)	Storage in UR
Ce [-]	Evaporation correction coefficient	Ss (mm)	Storage in SR
Sumax [mm]	Maximum unsaturated storage	Sf (mm)	Storage in FR
β [-]	Unsaturated discharge exponent	Sr (mm)	Storage in RR
Pcmax [mm/d]	Maximum percolation velocity	Pe (mm/d)	Effective Precipitation
Cmax [mm/d]	Maximum capillary rise velocity	Et (mm/d)	Transpiration
Ks [1/mmα*d]	Slow reservoir coefficient	Pc (mm/d)	Percolation
Kf [1/mmα*d]	Fast reservoir coefficient	Cr (mm/d)	Capillary rise
Kr [1/mmα*d]	Riparian reservoir coefficient	Qu (mm/d)	Overflow from UR
α [-]	Discharge exponent	Qf (mm/d)	Discharge from FR
Tlag [-]	Time lag coefficient	Qs (mm/d)	Discharge from SR
		Qr (mm/d)	Discharge from RR

There are 12 parameters in M06, and 12000 sets of parameters are sampled for parameter calibration. The initial storage value in SR is given as 20 mm. The model result and parameter calibration result are shown in Figure 51 and Figure 52 respectively.

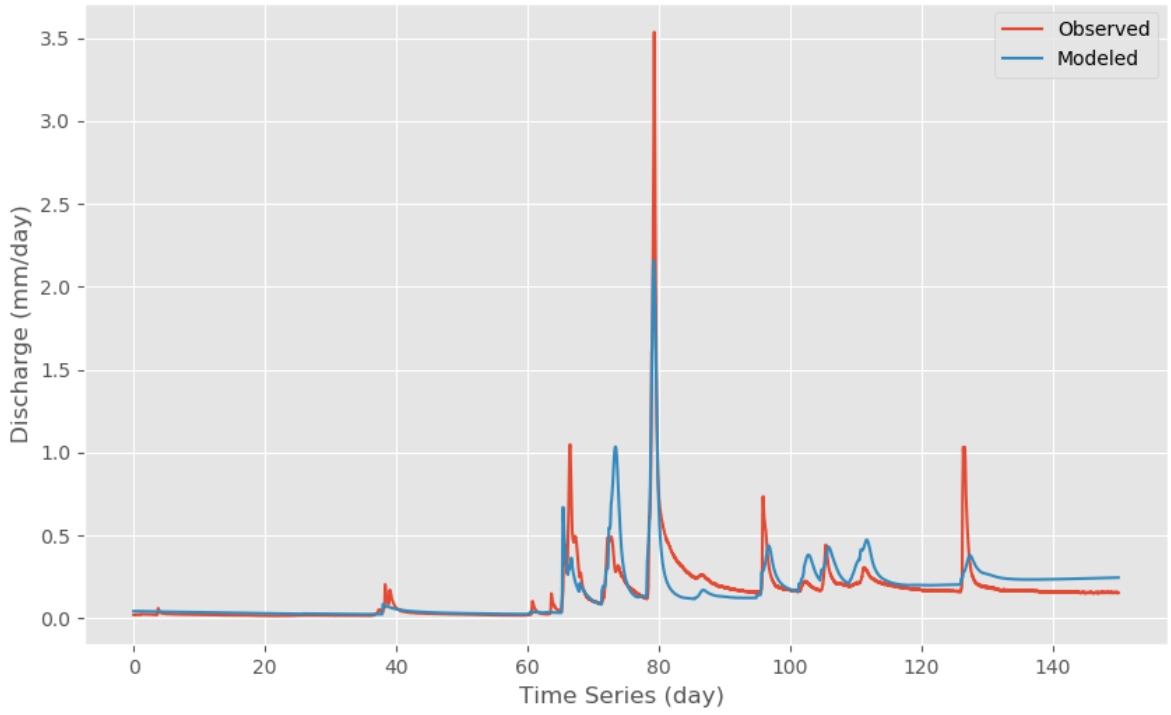

Figure 51. Model Result of M06

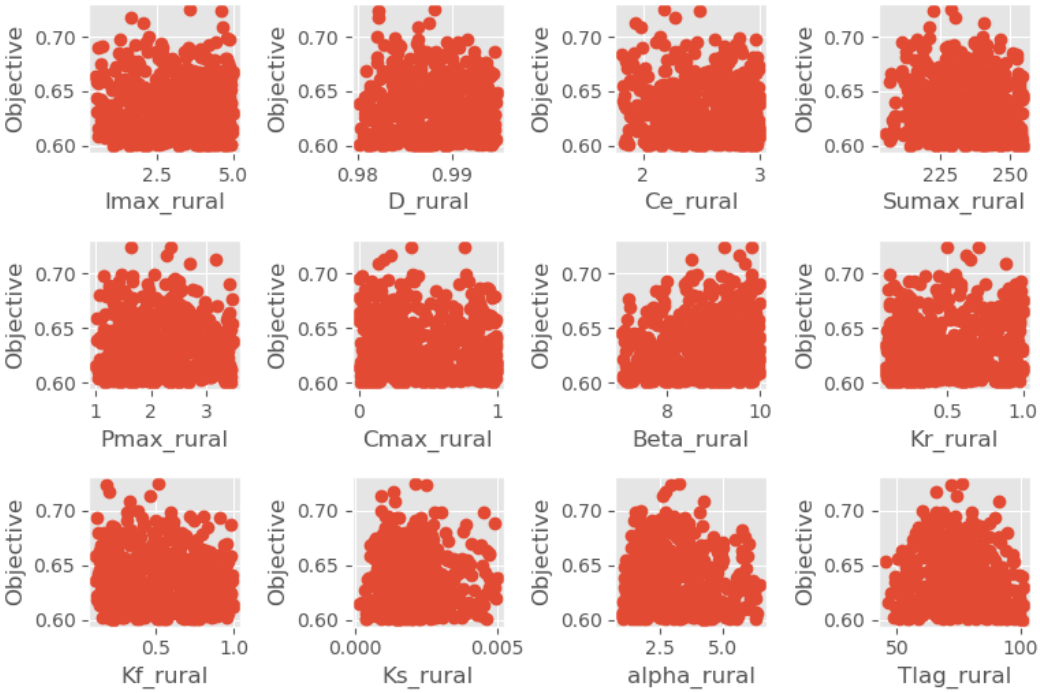

Figure 52. Parameter Calibration Result of M06

Model 06 describes a relative full hydrological picture with the IR, RR and capillary rise process, but surprisingly it does not achieve the highest NSE among the 6 generations of rural lumped model. The NSE of M06 is 0.725 and the relative error of total outflow is -0.073.

Comparing the NSE of M06 (with IR) and M04B (without IR), the additional IR decreases the NSE from 0.802 in M04B to 0.725 in M06 and at the same time the M06 performed worse than M04B on extreme peak simulation, which may prove again that the interception process is not one dominant water process in rural sub-catchment and the IR is not an effective generic element in this case.

D.2 Urban lumped model test

D.2.1 Urban lumped Model 01

The first generation of urban lumped model is as the same as the first generation of rural lumped model. The schematic figure of model structure and model performance of urban lumped Model 01 are shown in Table 28.

Table 28. The comparison of model structure and model performance of Urban Lumped M01

Model (Par. Num.)	Schematic figure of model structure	Mathematical expression of water process	NSE	Relative error
Model 01A (3)	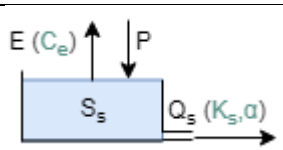	$E = C_e E_r$ $Q_s = K_s S_s^{\alpha}$	0.016	0.017
Model 01B (3)	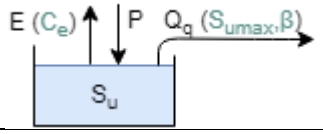	$E = C_e E_r$ $Q_q = P * \left(\frac{S_u}{S_{umax}}\right)^{\beta}$	-0.66	0.61

Model 01C (4)	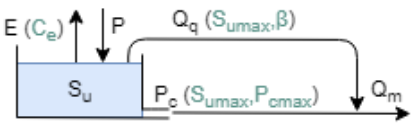	$E = C_e E_r$ $Q_q = P * \left(\frac{S_u}{S_{umax}}\right)^{\beta}$ $P_c = P_{cmax} \frac{S_u}{S_{umax}}$	-0.51	-0.21

"Relative error": Relative error of total outflow; "Par. Num.": Parameter Number

In which:

Parameter	Description	Model Components	Description
Ce [-]	Evaporation correction coefficient	Ss (mm)	Storage in SR
Ks [1/mmα*d]	Slow reservoir coefficient	Su (mm)	Storage in UR
α [-]	Discharge exponent	P (mm/d)	Precipitation
Sumax [mm]	Maximum unsaturated storage	E (mm/d)	Actual Evaporation
β [-]	Unsaturated discharge exponent	Er (mm/d)	Reference Evaporation
		Qs (mm/d)	Discharge from SR
		Qq (mm/d)	Overflow from UR
		Pc (mm/d)	Percolation from UR

There are 3 parameters in urban lumped M01A and M01B to quantify evaporation and discharge process and there are 4 parameters in M01C. 3000 or 4000 sets of parameters are sampled for parameter calibration. The model result and parameter calibration result of M01 are shown from Figure 86 to Figure 91. As the figures shows, none of M01 have acceptable model performance since the over-simple one-bucket model structure cannot reproduce the complex hydrologic processes in urban sub-catchment.

D.2.2 Urban lumped Model 02

As similarly as the rural lumped model, one additional Slow reacting Reservoir (SR) is added in urban lumped Model 02 to divide the saturated groundwater from unsaturated zone. A "Unsaturated Reservoir - Slow response Reservoir(UR-SR)" two buckets parallel model structure is created as Model 02. The model structure comparison of M02A and M02B is shown in Table 29.

Table 29. The comparison of model structure and model performance of Urban Lumped M02

Model (Par. Num.)	Schematic figure of model structure	Mathematical expression of water process	NSE	Relative error
Model 02A (5)	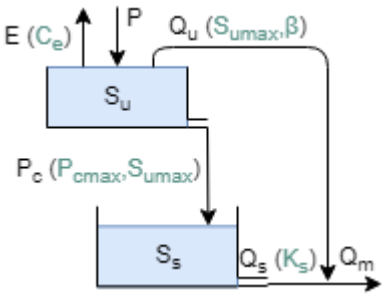	$E = C_e E_r$ $Q_u = P * \left(\frac{S_u}{S_{umax}}\right)^{\beta}$ $P_c = P_{cmax} \frac{S_u}{S_{umax}}$ $Q_s = K_s S_s$	0.049	-0.13
Model 02B (5)	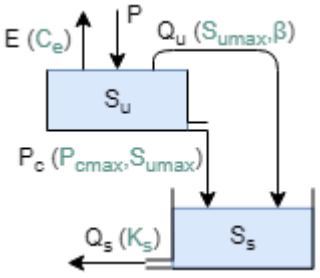	$E = C_e E_r$ $Q_u = P * \left(\frac{S_u}{S_{umax}}\right)^{\beta}$ $P_c = P_{cmax} \frac{S_u}{S_{umax}}$ $Q_s = K_s S_s$	0.016	-0.007

"Relative error": Relative error of total outflow; "Par. Num.": Parameter Number

In which:

Parameter	Description	Model Components	Description
Ce [-]	Evaporation correction coefficient	Su (mm)	Storage in UR
Sumax [mm]	Maximum unsaturated storage	Ss (mm)	Storage in SR
β [-]	Unsaturated discharge exponent	Er (mm/d)	Reference Evaporation
Pcmax [mm/d]	Maximum percolation velocity	Pc (mm/d)	Percolation
Ks [1/mmα*d]	Slow reservoir coefficient	Qu (mm/d)	Overflow from UR
		Qs (mm/d)	Discharge from SR

There are 5 parameters in M02 and accordingly 5000 sets of parameters are sampled for parameter calibration. The model result and parameter calibration result of M02 are shown from Figure 92 to Figure 95.

The model performances of M02 are still not good. It suffered the same problem as rural lumped M02: most fast peak flows cannot be captured by M02A; And for M02B, since all runoff discharges from SR, which follows the stable and slow characters of groundwater base flow, there is not peaks at all.

These bad model performance could be also ascribed to the over-simple model structures which restrain the diversity of outflow pattern. Therefore, one additional Fast reacting Reservoir (FR) will be added in next generation to better simulate the peak flows.

D.2.3 Urban lumped Model 03

Urban lumped Model 03 is developed with one additional Fast reacting Reservoir (FR) based on the "UR-SR" two buckets model framework of M02. And a time lag function is exploited on the overflow from UR to FR (Qu) to simulate the delay function of unsaturated zone. The schematic figure of model structure is shown in Figure 53.

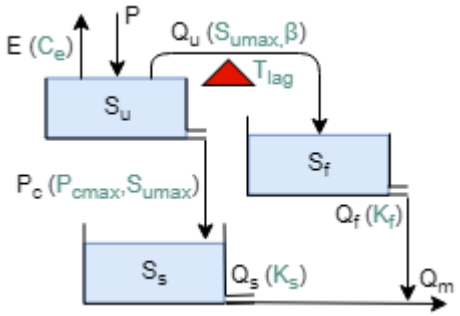

Figure 53. The schematic figure of model structure of urban lumped M03

There are 7 parameters in M03. The mathematical expression are:

Evaporation from Unsaturated Reservoir (mm/d): $E = C_e E_r$

Percolation from UR to SR: $P_c = P_{cmax} \frac{S_u}{S_{umax}}$

Overflow from UR (mm/d): $Q_u = P * \left(\frac{S_u}{S_{umax}}\right)^{\beta}$

Discharge from FR (mm/d): $Q_f = K_f S_f$

Discharge from SR (mm/d): $Q_s = K_s S_s$

In which:

Parameter	Description	Model Components	Description

Ce [-]	Evaporation correction coefficient	Su (mm)	Storage in UR
Sumax [mm]	Maximum unsaturated storage	Ss (mm)	Storage in SR
β [-]	Unsaturated discharge exponent	Sf (mm)	Storage in FR
Pcmax [mm/d]	Maximum percolation velocity	Er (mm/d)	Reference Evaporation
Ks [1/mmα*d]	Slow reservoir coefficient	Pc (mm/d)	Percolation
Kf [1/mmα*d]	Fast reservoir coefficient	Qu (mm/d)	Overflow from UR
Tlag [-]	Time lag coefficient	Qf (mm/d)	Discharge from FR
		Qs (mm/d)	Discharge from SR

7000 sets of parameters are sampled for parameter calibration. Since the base flow of urban sub-catchment is quite small, bare bucket is adopt as the initial storage condition. The model result and parameter calibration result are shown in Figure 54 and Figure 55 respectively.

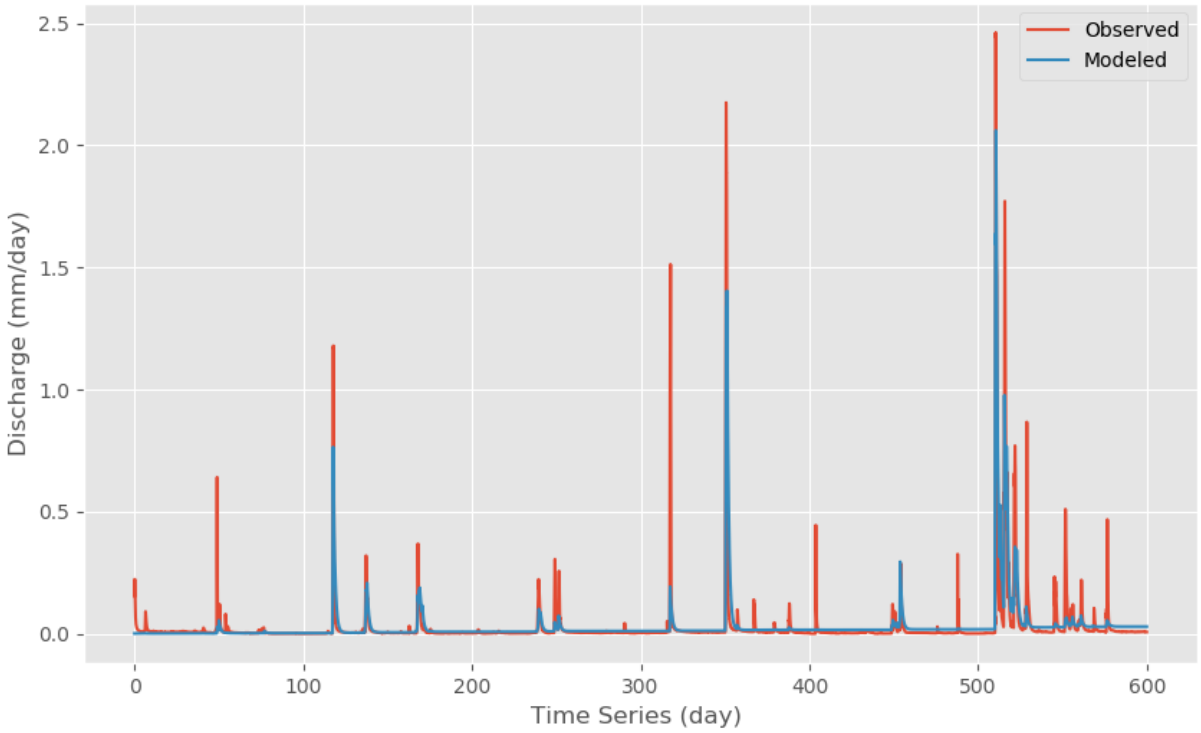

Figure 54. Model Result of Urban Lumped M03

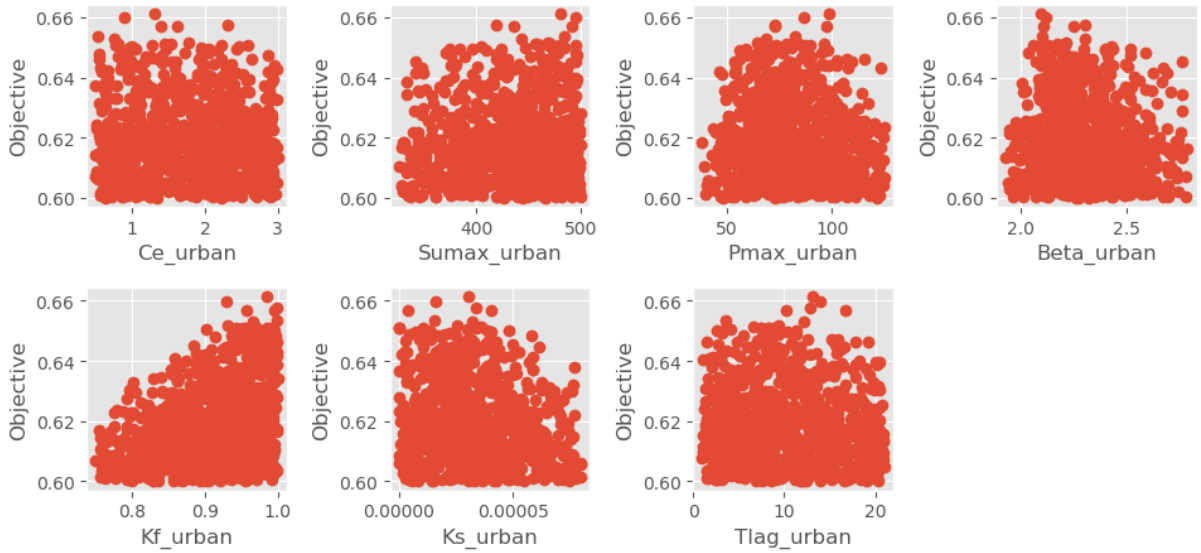

Figure 55. Parameter Calibration Result of Urban Lumped M03

With an additional FR, the model performance of M03 improves significantly compared to M02 with an additional FR. But the model performance on extreme peak flow simulation are still dissatisfactory and many peaks are neglected by M03.

In addtion, according to the parameter calibration result of M03 as shown in Figure 55, a remarkable percolation process happens in research urban sub-catchment as the calibrated maximum percolation velocity (Pmax) could be larger than 120 mm/d, which is far more than natural percolation level. This significant rainwater infiltration phenomenon could be ascribed to a local groundwater recharge program. Therefore one Human impact Reservoir (HR) with an artificial groundwater recharge process (Re) will be designed to describe the artificial hydrological activities in next generation.

D.2.4 Urban lumped Model 04

Urban lumped Model 04 is developed with one additional Human impact Reservoir (HR) based on the "UR-SR" two buckets model of M02. The most simple version of Model 04 is built in M04A with 8 parameters. Based on the basic model framework of M04A, three model components, precipitation distribution factor D (M04B), discharge exponent α (M04C), and capillary rise Cr (M04D), are further added and tested successfully. The schematic figures of model structures are shown in Table 30.

Table 30. The comparison of model structure and model performance of Urban Lumped M04

Model (Par. Num.)	Schematic figure of model structure	Mathematical expression of water process	NSE	Relative error
Model 04A (8)	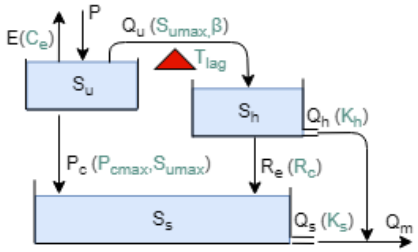	$E = C_e E_r$ $Q_u = P * \left(\frac{S_u}{S_{umax}}\right)^{\beta}$ $P_c = P_{cmax}\frac{S_u}{S_{umax}}$ $R_e = R_c S_h$ $Q_h = K_h S_h$ $Q_s = K_s S_s$	0.794	-0.195
Model 04B (9)	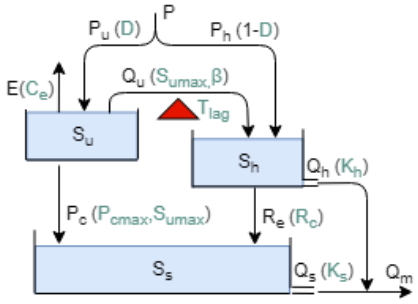	$P_u = D * P$ $P_h = (1 - D) * P$ $E = C_e E_r$ $Q_u = P_u * \left(\frac{S_u}{S_{umax}}\right)^{\beta}$ $P_c = P_{cmax}\frac{S_u}{S_{umax}}$ $R_e = R_c S_h$ $Q_s = K_s S_s$ $Q_h = K_h S_h$	0.810	-0.063
Model 04C (10)	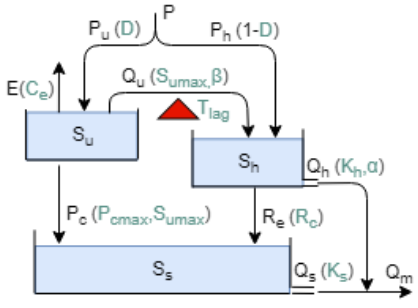	$P_u = D * P$ $P_h = (1 - D) * P$ $E = C_e E_r$ $Q_u = P_u * \left(\frac{S_u}{S_{umax}}\right)^{\beta}$ $P_c = P_{cmax}\frac{S_u}{S_{umax}}$ $R_e = R_c S_h$ $Q_s = K_s S_s$	0.816	0.286

		$Q_h = K_h S_h{}^{\alpha}$		
Model 04D (11)	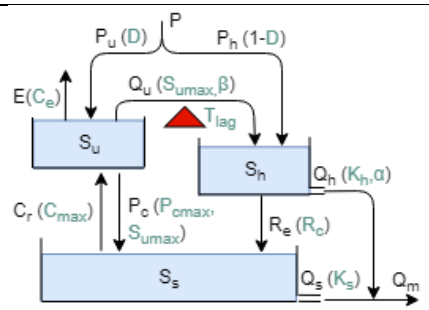	$P_u = D * P$ $P_h = (1 - D) * P$ $E = C_e E_r$ $Q_u = P_u * \left(\frac{S_u}{S_{umax}}\right)^{\beta}$ $P_c = P_{cmax} \frac{S_u}{S_{umax}}$ $C_r = C_{max}(1 - \frac{S_u}{S_{umax}})$ $R_e = R_c S_h$ $Q_s = K_s S_s$ $Q_h = K_h S_h{}^{\alpha}$	0.842	-0.150

"Relative error": Relative error of total outflow; "Par. Num.": Parameter Number

In which:

Parameter	Description	Model Components	Description
D [-]	Precipitation distribution factor	Su (mm)	Storage in UR
Ce [-]	Evaporation correction coefficient	Ss (mm)	Storage in SR
Sumax [mm]	Maximum unsaturated storage	Sh (mm)	Storage in HR
β [-]	Unsaturated discharge exponent	Er (mm/d)	Reference Evaporation
Pcmax [mm/d]	Maximum percolation velocity	Pc (mm/d)	Percolation
Cmax [mm/d]	Maximum capillary rise velocity	Cr (mm/d)	Capillary rise
Rc [1/mm*d]	Recharge coefficient	Re (mm/d)	Groundwater recharge
Ks [1/mmα*d]	Slow reservoir coefficient	Qu (mm/d)	Overflow from UR
Kh [1/mmα*d]	Human impact reservoir coefficient	Qh (mm/d)	Discharge from HR
α [-]	Fast reservoir discharge exponent	Qs (mm/d)	Discharge from SR
Tlag [-]	Time lag coefficient	Pu (mm/d)	Precipitation on UR
		Ph (mm/d)	Precipitation on HR

There are 8-11 parameters in M04, and correspondingly 8000-11000 sets of parameters are sampled for parameter calibration. Since the base flow of urban sub-catchment is quite small, bare bucket is adopt as the initial storage condition. The model result and parameter calibration result of M04s are shown from Figure 96 to Figure 103.

As Table 30 shows, the NSE of Model 04A, with additional HR and groundwater recharge process (Re), increased obviously from 0.661 of M03 to 0.794. And all the three test model components (precipitation distribution factor, discharge exponent, and capillary rise) are able to improve the model performance on peak flow simulation and could bring higher NSE than M04A. And M04D with all the three additional model components achieve the highest NSE among 4 generations of urban lumped model as 0.842.

D.2.5 Urban lumped Model 05

Based on the "UR-SR-HR" three buckets model structure of M04D, one additional Interception Reservoir (IR) is added in Model 05. And three connection methods of IR are tested among Model 05A, M05B and M05C.The comparison of model structure and model performance of M05 are shown in Table 31.

Table 31. The comparison of model structure and model performance of Urban Lumped M05

Model	Schematic figure of model structure	Mathematical expression of water process	NSE	Relativ e error

(Par. Num.)				
Model 05A (12)	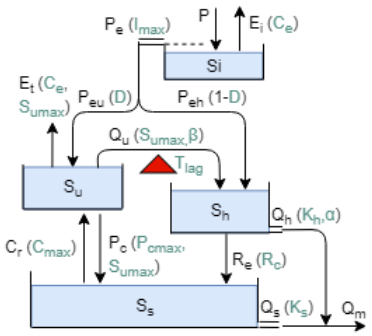	$E_i = C_e E_r$ $P_e = S_i - I_{max}$ $P_{eu} = D * P_e$ $P_{eh} = (1 - D) * P_e$ $E_t = (C_e E_r - E_i) * (\frac{S_u}{S_{umax}})$ $Q_u = P_{eu} * \left(\frac{S_u}{S_{umax}}\right)^{\beta}$ $P_c = P_{cmax} \frac{S_u}{S_{umax}}$ $C_r = C_{max}(1 - \frac{S_u}{S_{umax}})$ $R_e = R_c S_h$ $Q_s = K_s S_s$ $Q_h = K_h {S_h}^{\alpha}$	0.813	-0.049
Model 05B (12)	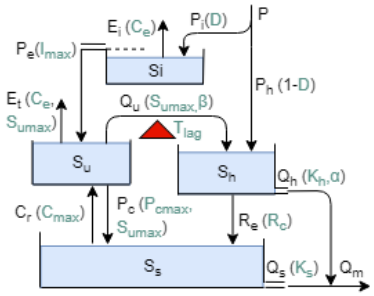	$P_i = D * P$ $P_h = (1 - D) * P$ $E_i = C_e E_r$ $P_e = S_i - I_{max}$ $E_t = (C_e E_r - E_i) * (\frac{S_u}{S_{umax}})$ $Q_u = P_e * \left(\frac{S_u}{S_{umax}}\right)^{\beta}$ $P_c = P_{cmax} \frac{S_u}{S_{umax}}$ $C_r = C_{max}(1 - \frac{S_u}{S_{umax}})$ $R_e = R_c S_h$ $Q_s = K_s S_s$ $Q_h = K_h {S_h}^{\alpha}$	0.802	0.381
Model 05C (11)	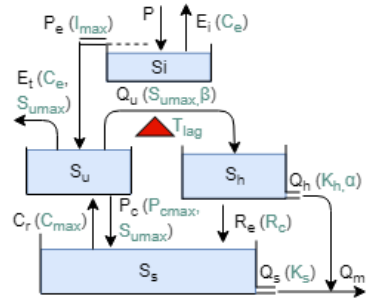	$E_i = C_e E_r$ $P_e = S_i - I_{max}$ $E_t = (C_e E_r - E_i) * (\frac{S_u}{S_{umax}})$ $Q_u = P_e * \left(\frac{S_u}{S_{umax}}\right)^{\beta}$ $P_c = P_{cmax} \frac{S_u}{S_{umax}}$ $C_r = C_{max}(1 - \frac{S_u}{S_{umax}})$ $R_e = R_c S_h$ $Q_s = K_s S_s$ $Q_h = K_h {S_h}^{\alpha}$	0.809	0.174

"Relative error": Relative error of total outflow; "Par. Num.": Parameter Number

In which:

Parameter	Description	Model Component	Description
Imax [mm]	Maximum interception thickness	Si (mm)	Storage in IR
D [-]	Precipitation distribution factor	Su (mm)	Storage in UR

Ce [-]	Evaporation correction coefficient	Ss (mm)	Storage in SR
Sumax [mm]	Maximum unsaturated storage	Sh (mm)	Storage in HR
β [-]	Unsaturated discharge exponent	Pe (mm/d)	Effective Precipitation
Pcmax [mm/d]	Maximum percolation velocity	Et (mm/d)	Transpiration
Cmax [mm/d]	Maximum capillary rise velocity	Ei (mm/d)	Interception
Rc [1/mm*d]	Recharge coefficient	Pc (mm/d)	Percolation
Ks [1/mmα*d]	Slow reservoir coefficient	Cr (mm/d)	Capillary rise
Kh [1/mmα*d]	Human impact reservoir coefficient	Re (mm/d)	Groundwater recharge
α [-]	Discharge exponent	Qu (mm/d)	Overflow from UR
Tlag [-]	Time lag coefficient	Qh (mm/d)	Discharge from HR
		Qf (mm/d)	Discharge from FR
		Qs (mm/d)	Discharge from SR

There are 11 or 12 parameters in M05, and accordingly 11000 or 12000 sets of parameters are sampled for parameter calibration. Besides bare bucket is adopt as the initial storage condition. The model result and parameter calibration result of M05 are shown from Figure 104 to Figure 109.

Compared to M04D, M05 with additional IR do not make obvious improvement on NSE. However as Figure 106 shown, the model performances of M05 on extreme peak runoff simulation are improved. Therefore the interception process in urban area cannot be abandoned, which would be further tested in semi-distributed models.

D.3 Semi-distributed model test

D.3.1 Semi-distributed Model 01

The semi-distributed Model 01 (M01) has six buckets, which is the simplest model among the 4 generations of semi-distributed models.

The urban module of M01 is composed of the "UR-SR-HR" three buckets which indicate urban green surface, grey surface and underground zone respectively. And the rural module of M01 is composed of the "UR-SR-FR" three buckets. In the rural module of M01A, all the rain falls into the UR, and in M01B most of the rain falls into the UR and the last small part of rain will fall into the FR. The schematic figures of model structures are shown in Table 32.

Table 32. The comparison of model structure and verification performance of Semi-distributed M01

		Schematic figure of model structure
Model Num.	M01A	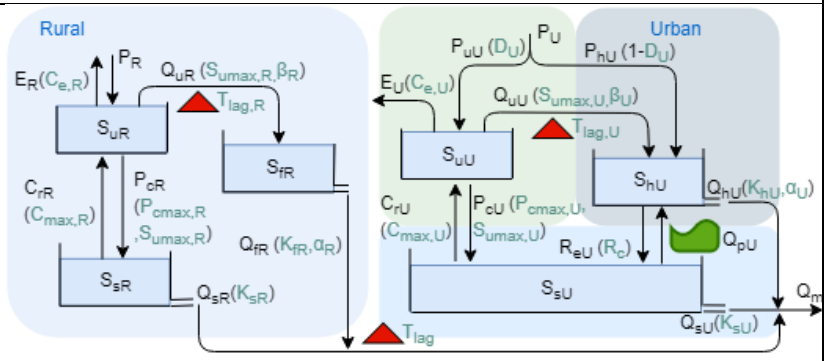
Parameter Num.	21	
Optimal NSE of verification	0.735	
Optimal R^2 of verification	0.865	
Mean NSE for verification	0.117	
Variance of NSE for verification	0.399	
Model Num.	M01B	
Parameter Num.	22	
Optimal NSE of verification	0.748	

Optimal R^2 of verification	0.873
Mean NSE for verification	0.297
Variance of NSE for verification	0.240

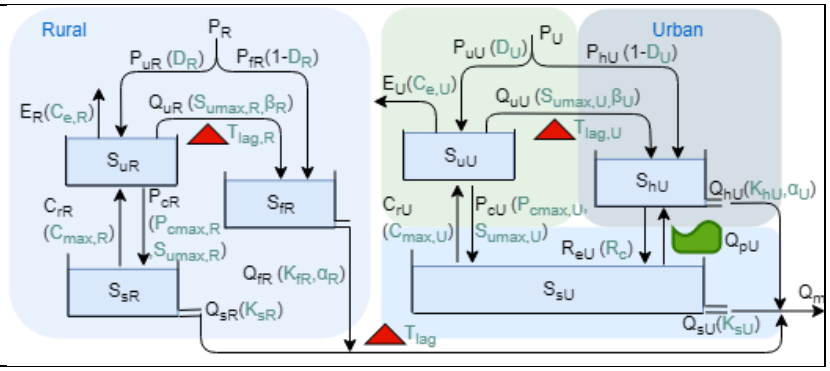

The capital letters R or U in subscript in model structure schematic figure indicate Rural or Urban area.

With the mathematical expressions of water processes:

Water process	Mathematical expression
Precipitation on UR	$P_u = D * P$
Precipitation on FR/HR	$P_f = (1-D) * P / P_h = (1-D) * P$
Evaporation	$E = C_e E_r$
Overflow from UR	$Q_u = P_u * \left(\frac{S_u}{S_{umax}}\right)^{\beta}$
Percolation	$P_c = P_{cmax} \frac{S_u}{S_{umax}}$
Capillary rise	$C_r = C_{max}\left(1 - \frac{S_u}{S_{umax}}\right)$
Groundwater recharge	$R_e = R_c S_h$
Discharge from FR/HR	$Q_f = K_f {S_f}^{\alpha} / Q_h = K_h {S_h}^{\alpha}$
Discharge from SR	$Q_s = K_s S_s$
Time lag of rural area	$f = \begin{cases} \frac{4t}{(T_{lag})^2}, 0 < t < \frac{T_{lag}}{2} \\ \frac{4(T_{lag}-t)}{(T_{lag})^2}, \frac{T_{lag}}{2} < t < T_{lag} \\ 0, t > T_{lag} \end{cases}$

In which:

Parameter	Description	Model Components	Description
D [-]	Precipitation distribution factor	Su (mm)	Storage in UR
Ce [-]	Evaporation correction coefficient	Sh (mm)	Storage in HR
Sumax [mm]	Maximum unsaturated storage	Ss (mm)	Storage in SR
β [-]	Discharge exponent	Sf (mm)	Storage in FR
Pmax [mm/d]	Maximum percolation velocity	Re (mm/d)	Groundwater recharge
Cmax [mm/d]	Maximum capillary rise velocity	Qu (mm/d)	Overflow from UR
Rc [1/mm*d]	Recharge coefficient	Pc (mm/d)	Percolation
Kh [1/mm*d]	Human impact reservoir coefficient	Cr (mm/d)	Capillary rise
Ks [1/mm*d]	Slow reservoir coefficient	Qs (mm/d)	Discharge from SR
Kf [1/mm*d]	Fast reservoir coefficient	Qh (mm/d)	Discharge from HR
α [-]	Discharge exponent	Qf (mm/d)	Discharge from FR
Tlag [-]	Time lag coefficient	t (1/48 d)	Time step

21000 or 22000 sets of parameters are sampled for parameter calibration. According to the calibration result, the parameter sets with the NSE smaller than 0.6 will be abandoned, and the parameter sets

with NSE larger than 0.6 will be remained. Among the remained parameter sets, the optimal verification result of NSE, R^2 and the mean verified NSE are used to show the accuracy of the model structure. And the precision of the model structure is indicated by the variance of the verified NSE of the remained parameter sets.

The NSE and R^2 results are shown in Table 32. It is obvious that, with one more parameter (precipitation distribution factor D), the accuracy and precision of M01B perform better than M01A as larger optimal NSE, R^2, mean NSE and smaller variance of NSE. It may endorse the precipitation distribution mode in rural module. This precipitation distribution mode in rural module would be further tested in semi-distributed M03.

The figures of model result and parameter calibration result of M01A and M01B are shown from Figure 110 to Figure 113. As the Figure 110 and Figure 112 shown, the model performances of M01A on peak flow simulation are not satisfactory especially for the verification period. More complex rural module will be test in M02 then.

D.3.2 Semi-distributed Model 02

Semi-distributed Model 02 is developed with one additional Riparian Reservoir (RR) in rural module based on the semi-distributed M01. And the urban module of M02 is as the same as it of M01. The schematic figure of model structure is shown in Table 33.

Table 33. The model structure and verification performance of Semi-distributed M02

		Schematic figure of model structure
Model Num.	M02	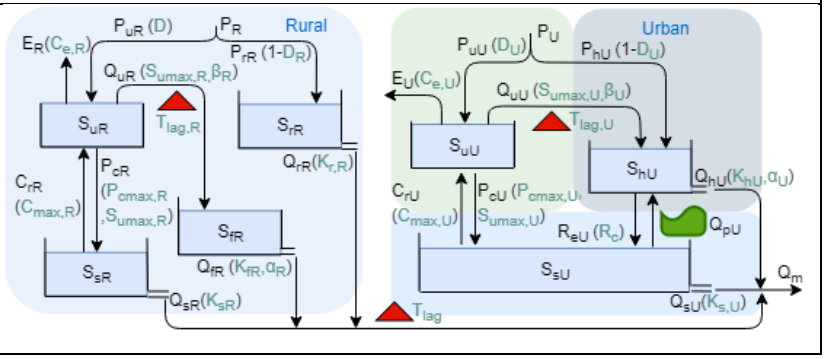
Parameter Num.	23	
Optimal NSE of verification	0.749	
Optimal R^2 of verification	0.871	
Mean NSE for verification	0.155	
Variance of NSE for verification	0.424	

The capital letters R or U in subscript in model structure schematic figure indicate Rural or Urban area.

With the mathematical expressions of water processes:

Water process	Mathematical expression
Precipitation on UR	$P_u = D * P$
Precipitation on RR	$P_r = (1 - D) * P$
Precipitation on HR	$P_h = (1 - D) * P$
Evaporation	$E = C_e E_r$
Overflow from UR	$Q_u = P_u * \left(\frac{S_u}{S_{umax}}\right)^{\beta}$
Percolation	$P_c = P_{cmax} \frac{S_u}{S_{umax}}$
Capillary rise	$C_r = C_{max}\left(1 - \frac{S_u}{S_{umax}}\right)$
Groundwater recharge	$R_e = R_c S_h$
Discharge from FR/HR	$Q_f = K_f {S_f}^{\alpha} / Q_h = K_h {S_h}^{\alpha}$
Discharge from RR/SR	$Q_r = K_r S_r / Q_s = K_s S_s$

Time lag of rural area	$f = \begin{cases} \frac{4t}{(T_{lag})^2}, 0 < t < \frac{T_{lag}}{2} \\ \frac{4(T_{lag}-t)}{(T_{lag})^2}, \frac{T_{lag}}{2} < t < T_{lag} \\ 0, t > T_{lag} \end{cases}$

In which:

Parameter	Description	Model Components	Description
D [-]	Precipitation distribution factor	Si (mm)	Storage in IR
Ce [-]	Evaporation correction coefficient	Su (mm)	Storage in UR
Sumax [mm]	Maximum unsaturated storage	Ss (mm)	Storage in SR
β [-]	Unsaturated discharge exponent	Sf (mm)	Storage in FR
Pcmax [mm/d]	Maximum percolation velocity	Sr (mm)	Storage in RR
Cmax [mm/d]	Maximum capillary rise velocity	Re (mm/d)	Groundwater recharge
Ks [1/mmα*d]	Slow reservoir coefficient	Pc (mm/d)	Percolation
Kf [1/mmα*d]	Fast reservoir coefficient	Cr (mm/d)	Capillary rise
Kh [1/mmα*d]	Human impact reservoir coefficient	Qu (mm/d)	Overflow from UR
Kr [1/mmα*d]	Riparian reservoir coefficient	Qf (mm/d)	Discharge from FR
α [-]	Discharge exponent	Qs (mm/d)	Discharge from SR
Tlag [-]	Time lag coefficient	Qr (mm/d)	Discharge from RR

There are 23 parameters in M02, and 23000 sets of parameters are sampled for parameter calibration. According to the calibration result, the parameter sets with the NSE smaller than 0.6 will be abandoned, and the parameter sets with NSE larger than 0.6 will be remained. Among the remained parameter sets, the optimal verification result of NSE, R^2 and the mean verified NSE are used to show the accuracy of the model structure. And the precision of the model structure is indicated by the variance of the verified NSE of the remained parameter sets.

The NSE and R^2 results are shown in Table 33. It could be found that, compared to M01B, the verification result of M02 does not improves on neither the accuracy nor precision. The model result and parameter calibration result are shown in Figure 114 and Figure 115. As the Figure 114 shown, the model performance of M02 on peak flow simulation is better than M01A and M01B.

D.3.3 Semi-distributed Model 03

There are 7 buckets in semi-distributed Model 03. In M03A and M03B, one additional IR is added for urban module based on the 6 buckets framework of M01A and M01B. Two different precipitation distribution modes in rural module between M01A and M01B are tested again between M03A and B. The model structures and model performances of Model 03 are shown in Table 34.

Table 34. The comparison of model structure and verification performance of Semi-distributed M03

		Schematic figure of model structure
Model Num.	M03 A	
Parameter Num.	22	
Optimal NSE of verification	0.706	
Optimal R^2 of verification	0.850	
Mean NSE for verification	-0.056	

Variance of NSE for verification	0.758
Model Num.	M03B
Parameter Num.	23
Optimal NSE of verification	0.730
Optimal R^2 of verification	0.855
Mean NSE for verification	0.039
Variance of NSE for verification	0.587

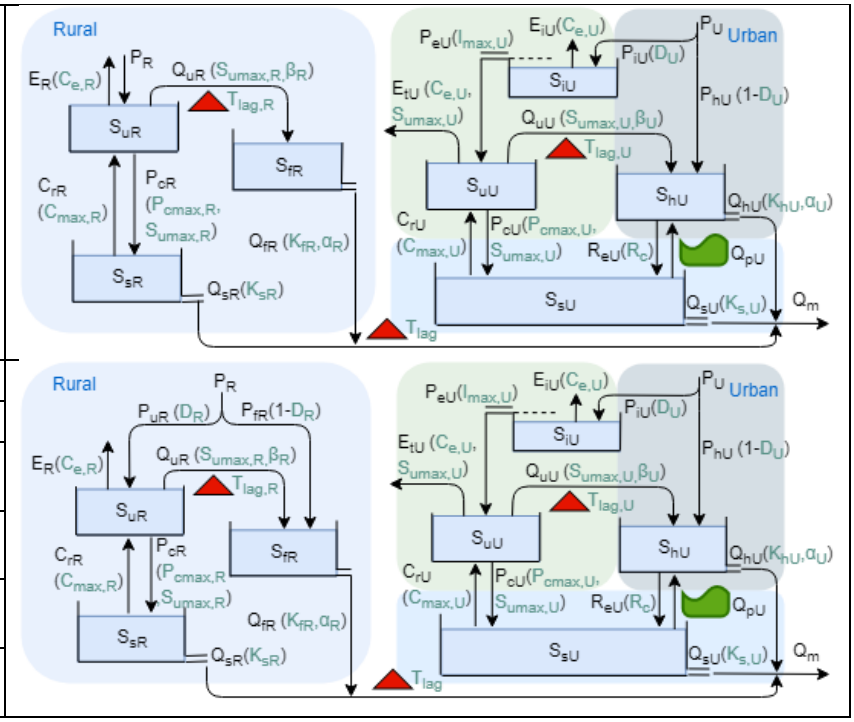

The capital letters R or U in subscript in model structure schematic figure indicate Rural or Urban area.

With the mathematical expressions of water processes:

Water process	Mathematical expression
Precipitation on UR	$P_u = D * P / P_{eu} = D * P_e / P_e = S_i - I_{max}$
Precipitation on FR	$P_f = (1 - D) * P$
Precipitation on HR	$P_h = (1 - D) * P / P_{eh} = (1 - D) * P_e$
Evaporation	$E = C_e E_r$
Interception	$E_i = C_e E_r$
Transpiration	$E_t = (C_e E_r - E_i) * (\frac{S_u}{S_{umax}})$
Overflow from UR	$Q_u = P * \left(\frac{S_u}{S_{umax}}\right)^{\beta} / Q_u = P_{eu} * \left(\frac{S_u}{S_{umax}}\right)^{\beta} / Q_u = P_u * \left(\frac{S_u}{S_{umax}}\right)^{\beta}$
Percolation	$P_c = P_{cmax} \frac{S_u}{S_{umax}}$
Capillary rise	$C_r = C_{max} \left(1 - \frac{S_u}{S_{umax}}\right)$
Groundwater recharge	$R_e = R_c S_h$
Discharge from FR/HR	$Q_f = K_f {S_f}^{\alpha} / Q_h = K_h {S_h}^{\alpha}$
Discharge from SR	$Q_s = K_s S_s$
Time lag	$f = \begin{cases} \frac{4t}{(T_{lag})^2}, 0 < t < \frac{T_{lag}}{2} \\ \frac{4(T_{lag} - t)}{(T_{lag})^2}, \frac{T_{lag}}{2} < t < T_{lag} \\ 0, t > T_{lag} \end{cases}$

In which:

Parameter	Description	Model Components	Description
Imax [mm]	Maximum interception thickness	Si (mm)	Storage in IR
D [-]	Precipitation distribution factor	Su (mm)	Storage in UR
Ce [-]	Evaporation correction coefficient	Sh (mm)	Storage in HR

Sumax [mm]	Maximum unsaturated storage	Ss (mm)	Storage in SR
Cmax [mm/d]	Maximum capillary rise velocity	Sf (mm)	Storage in FR
β [-]	Discharge exponent	E (mm/d)	Evaporation
Pmax [mm/d]	Maximum percolation velocity	Et (mm/d)	Transpiration
Rc [1/mm*d]	Recharge coefficient	Ei (mm/d)	Interception
Kh [1/mm*d]	Human impact reservoir coefficient	Pc (mm/d)	Percolation
Kr [1/mm*d]	Riparian reservoir coefficient	Cr (mm/d)	Capillary rise
Ks [1/mm*d]	Slow reservoir coefficient	Re (mm/d)	Groundwater recharge
Kf [1/mm*d]	Fast reservoir coefficient	Qu (mm/d)	Overflow from UR
α [-]	Discharge exponent		
Tlag [-]	Time lag coefficient		

22000 or 23000 sets of parameters are sampled for calibration process. According to the calibration result, the parameter sets with the NSE smaller than 0.6 will be abandoned, and the parameter sets with NSE larger than 0.6 will be remained. Among the remained parameter sets, the optimal verification result of NSE, R^2 and the mean verified NSE are used to show the accuracy of the model structure. And the precision of the model structure is indicated by the variance of the verified NSE of the remained parameter sets. The NSE and R^2 results are shown in Table 34.

The model result and parameter calibration result of M03 are shown from Figure 116 to Figure 119. As Figure 116 and Figure 118 shown, the simulation performance on extreme peaks is improved, especially the M03B.

Since M03A and M03B have the same urban module, the rural module of M03A and M03B can be compared and analysed. As similar as the test result of M01, with one more parameter (precipitation distribution factor D), the accuracy and precision of M03B perform better than M03A as larger optimal NSE, R^2. This result supports the same argument as the analysis in M01.

Then for the urban module, M03A, B could be compared with M01A, B. For M03, with additional interception bucket in urban module, both the accuracy and precision performance are worse than M01, which may because the interception process is not a dominant process for urban areas.

D.3.4 Semi-distributed Model 04

The Model 04 has the most complete model structure among the 4 generations of semi-distributed models with 8 buckets, which describes a relatively full hydrologic picture with various natural and artificial water processes such as interception, transpiration, percolation, slow groundwater slow, and water pumping, groundwater recharge, rapid urban stormwater collection and discharge.

The rural module of M04 is as the same as it of M02 and the urban module is as the same as it of M03. The model structure and model performance of Model 04 are shown in Table 35.

Table 35. The model structure and verification performance of Semi-distributed M04

		Schematic figure of model structure
Model Num.	M04	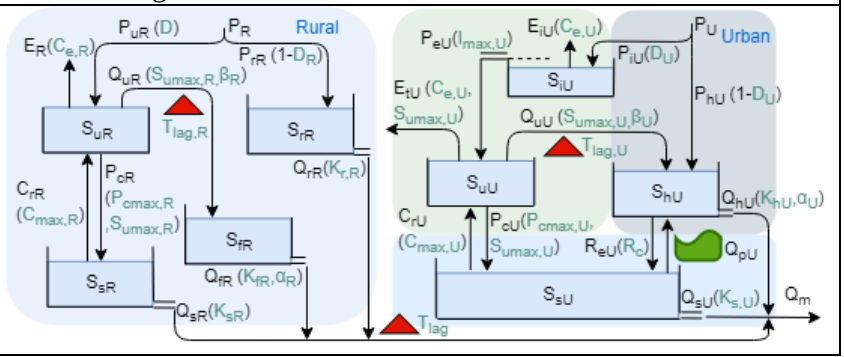
Parameter Num.	24	
Optimal NSE of verification	0.744	
Optimal R^2 of verification	0.883	
Mean NSE for verification	0.036	
Variance of NSE for verification	0.606	

The capital letters R or U in subscript in model structure schematic figure indicate Rural or Urban area.

With the mathematical expressions of water processes:

Water process	Mathematical expression
Precipitation on UR	$P_u = D * P / P_{eu} = D * P_e / P_e = S_i - I_{max}$
Precipitation on RR	$P_f = (1 - D) * P$
Precipitation on HR	$P_h = (1 - D) * P / P_{eh} = (1 - D) * P_e$
Evaporation	$\mathrm{E} = C_e E_r$
Interception	$E_i = C_e E_r$
Transpiration	$E_t = (C_e E_r - E_i) * (\frac{S_u}{S_{umax}})$
Overflow from UR	$Q_u = P * \left(\frac{S_u}{S_{umax}}\right)^{\beta} / Q_u = P_{eu} * \left(\frac{S_u}{S_{umax}}\right)^{\beta} / Q_u = P_u * \left(\frac{S_u}{S_{umax}}\right)^{\beta}$
Percolation	$P_c = P_{cmax} \frac{S_u}{S_{umax}}$
Capillary rise	$C_r = C_{max} \left(1 - \frac{S_u}{S_{umax}}\right)$
Groundwater recharge	$R_e = R_c S_h$
Discharge from FR/HR	$Q_f = K_f {S_f}^{\alpha} / Q_h = K_h {S_h}^{\alpha}$
Discharge from SR/RR	$Q_s = K_s S_s \,/\, Q_r = K_r S_r$
Time lag	$f = \begin{cases} \frac{4t}{(T_{lag})^2}, 0 < t < \frac{T_{lag}}{2} \\ \frac{4(T_{lag} - t)}{(T_{lag})^2}, \frac{T_{lag}}{2} < t < T_{lag} \\ 0, t > T_{lag} \end{cases}$

In which:

Parameter	Description	Model Components	Description
Imax [mm]	Maximum interception thickness	Si (mm)	Storage in IR
D [-]	Precipitation distribution factor	Su (mm)	Storage in UR
Ce [-]	Evaporation correction coefficient	Sh (mm)	Storage in HR
Sumax [mm]	Maximum unsaturated storage	Ss (mm)	Storage in SR
Cmax [mm/d]	Maximum capillary rise velocity	Sr (mm)	Storage in RR
β [-]	Discharge exponent	P (mm/d)	Precipitation
Pmax [mm/d]	Maximum percolation velocity	E (mm/d)	Evaporation
Rc [1/mm*d]	Recharge coefficient	Er (mm/d)	Reference Evaporation
Kh [1/mm*d]	Human impact reservoir coefficient	t (1/48 d)	Time step
Kr [1/mm*d]	Riparian reservoir coefficient		
Ks [1/mm*d]	Slow reservoir coefficient		
Kf [1/mm*d]	Fast reservoir coefficient		
α [-]	Discharge exponent		
Tlag [-]	Time lag coefficient		

24000 sets of parameters are sampled for calibration process. According to the calibration result, the parameter sets with the NSE smaller than 0.6 will be abandoned, and the parameter sets with NSE larger than 0.6 will be remained. Among the remained parameter sets, the optimal verification result of NSE, R^2 and the mean verified NSE are used to show the accuracy of the model structure. And the precision of the model structure is indicated by the variance of the verified NSE of the remained parameter sets.

The model result and parameter calibration result of M04 are shown in Figure 120 and Figure 121. As Figure 120 shown, the model performance on peak flow simulation is not satisfactory.

And the NSE and R^2 results are shown in Table 35. Since M02 and M04 share the same rural module, M04 could be compared to M02 for the urban module. It could be found that the optimal NSE and R^2 of M04 are similar as M02, but the mean and variance of NSE are significantly worse than M02, which means the additional IR in urban module would not improve the model accuracy yet weaken the model precision. For the rural module, M04 could be compared to M03. It could be revealed that, with one more RR bucket in M03, there is no obvious improvement on model performance of M04, which may prove that the RR is not an effective and efficient model component in rural module.

D.4 Figures of rural and urban lumped models

D.4.1 Rural lumped model

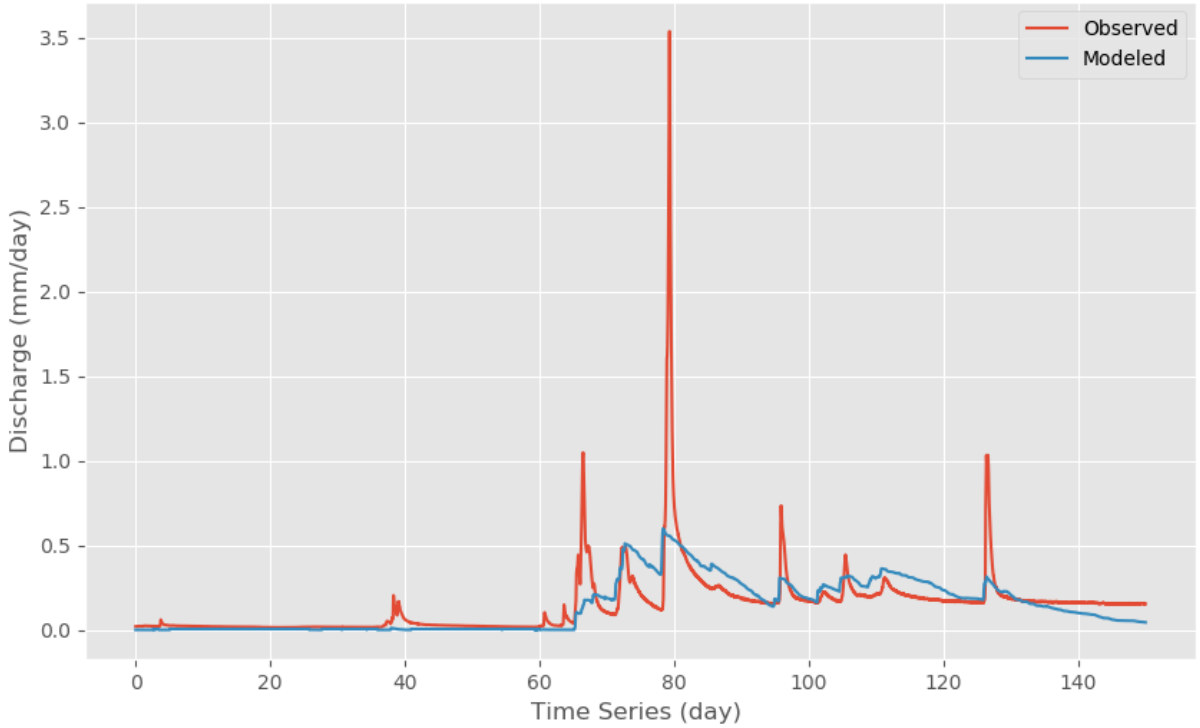

Figure 56. Model Result of M01A

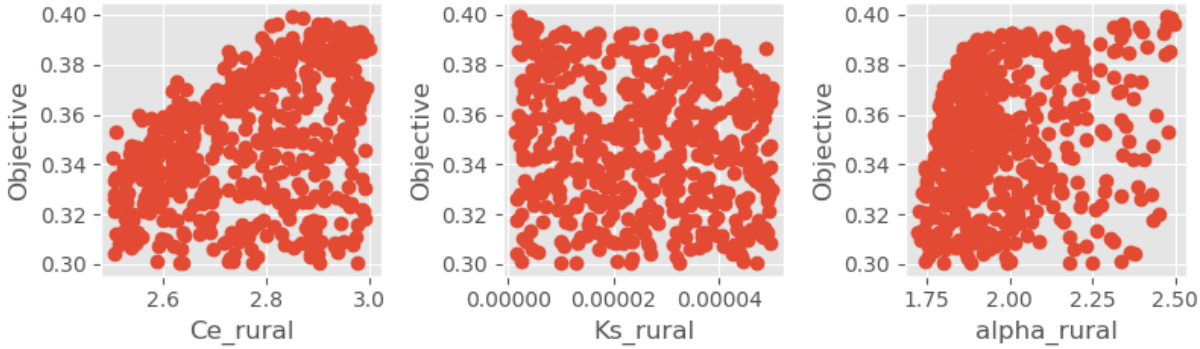

Figure 57. Parameter Calibration Result of M01A

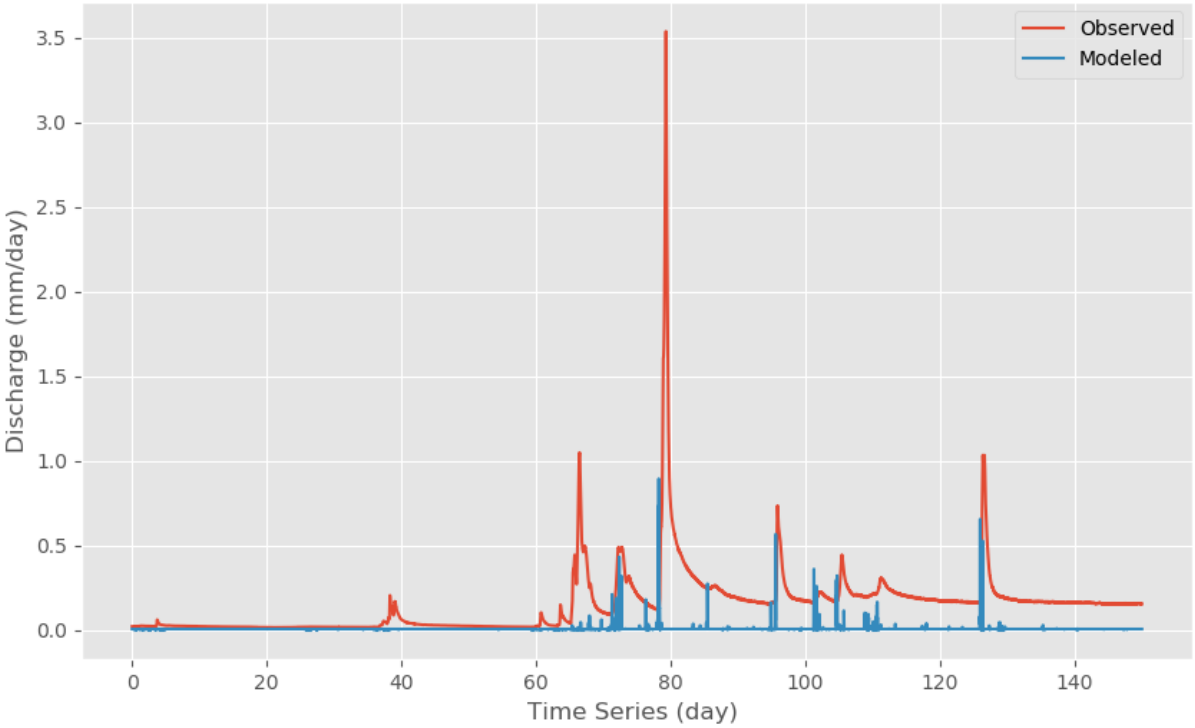

Figure 58. Model Result of M01B

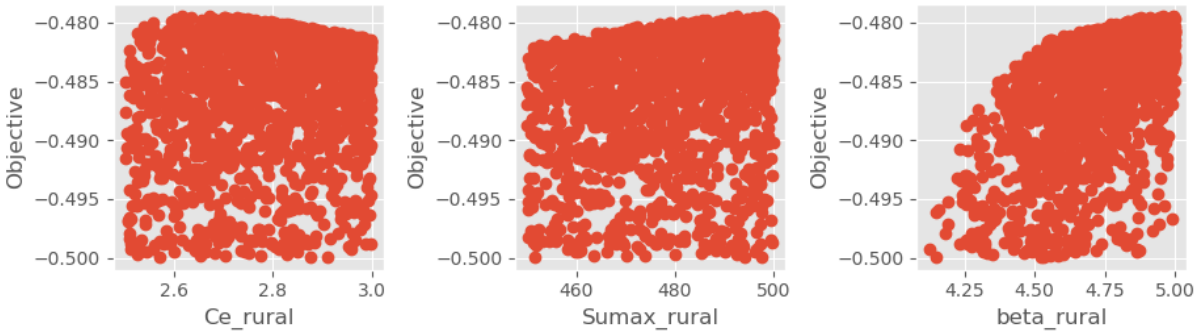

Figure 59. Parameter Calibration Result of M01B

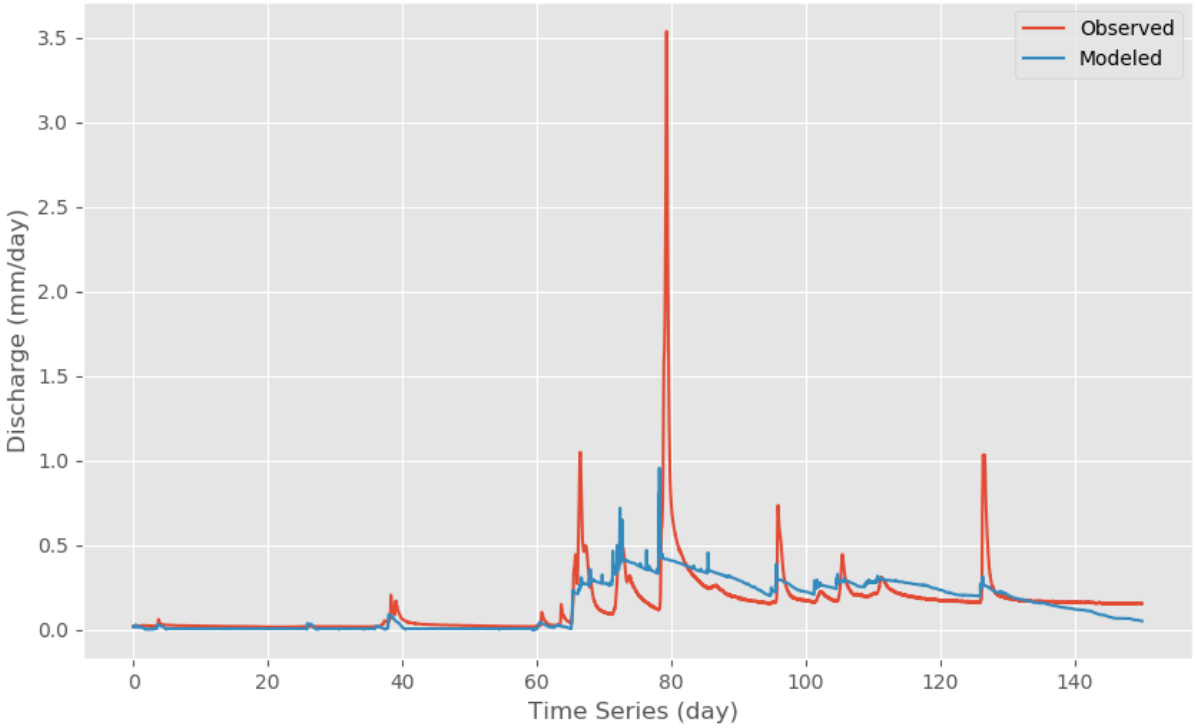

Figure 60. Model Result of M01C

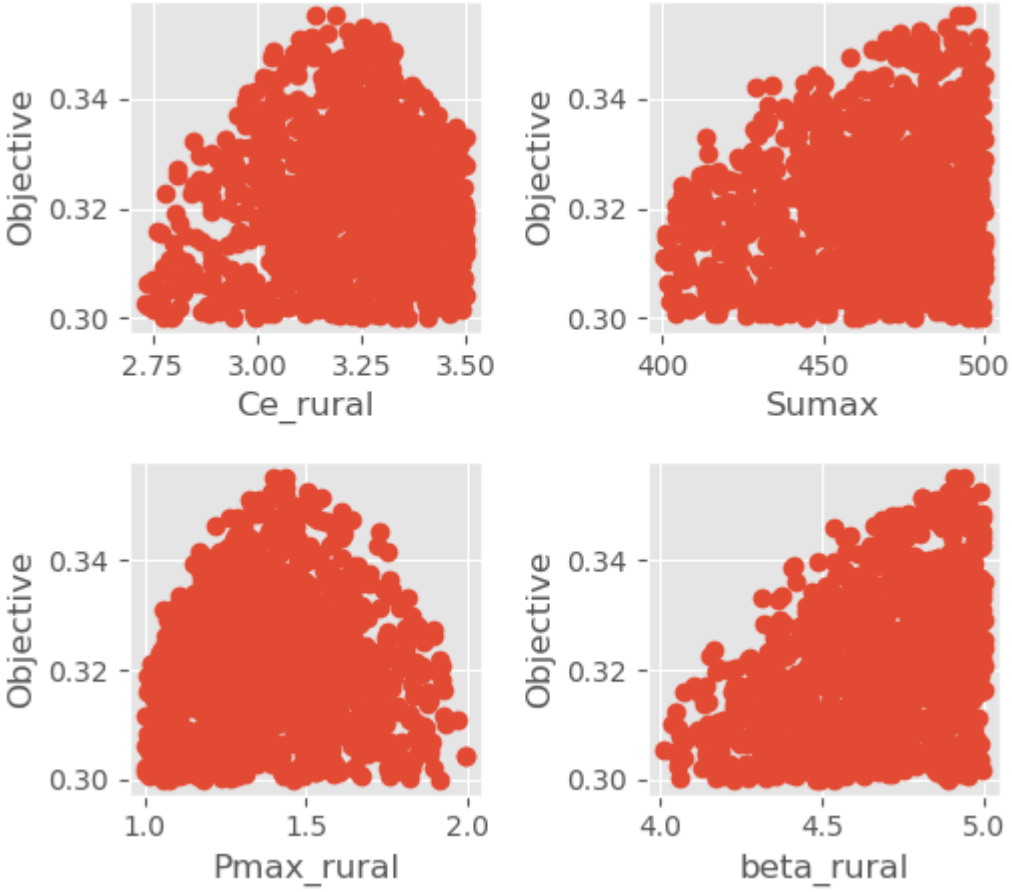

Figure 61. Parameter Calibration Result of M01C

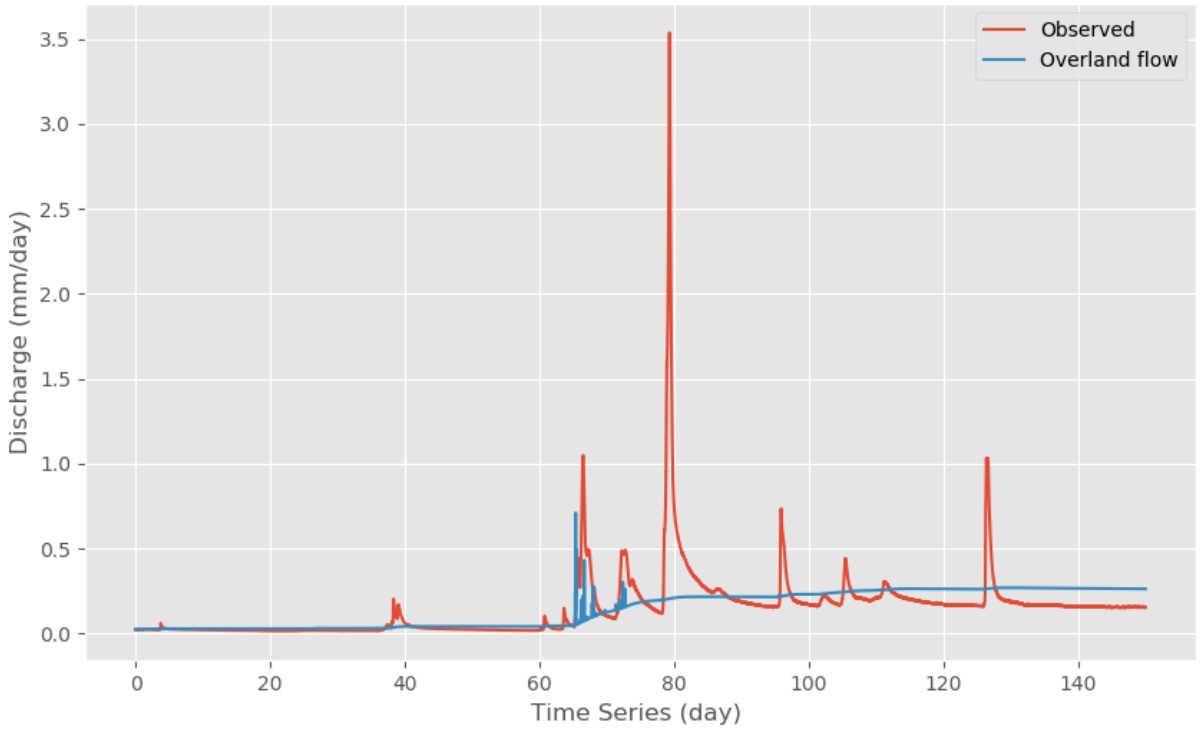

Figure 62. Model result of Rural Lumped M02A

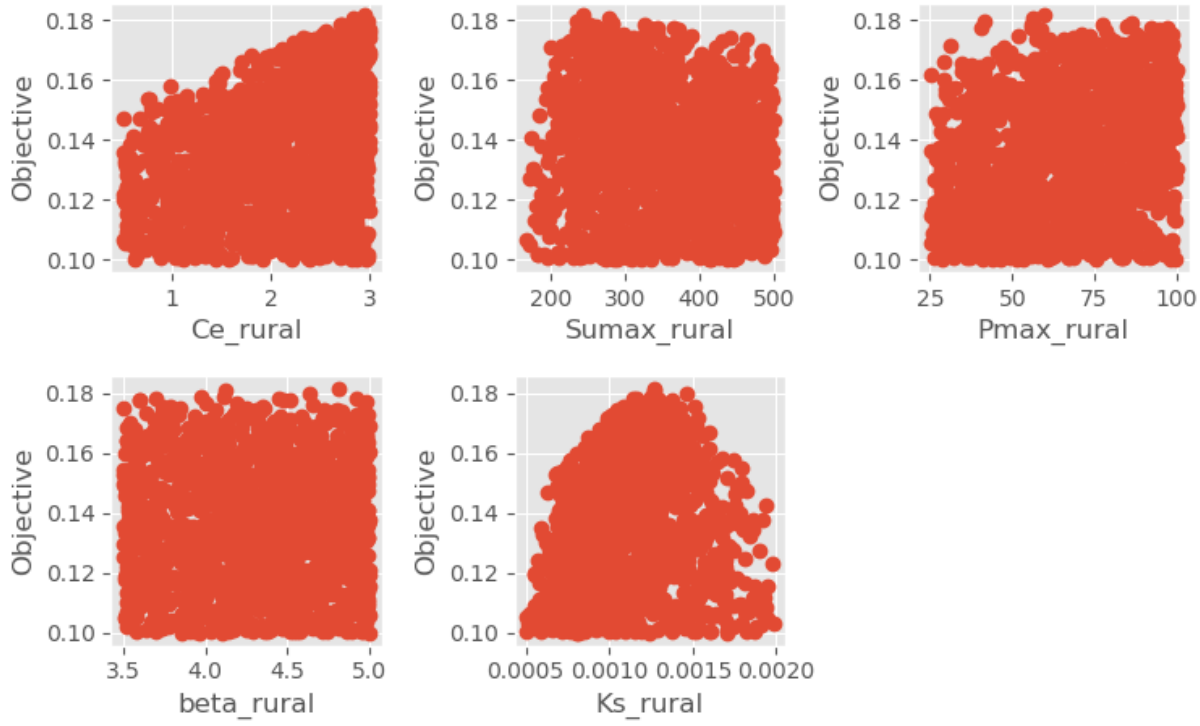

Figure 63. Parameter Calibration Result of Rural Lumped M02A

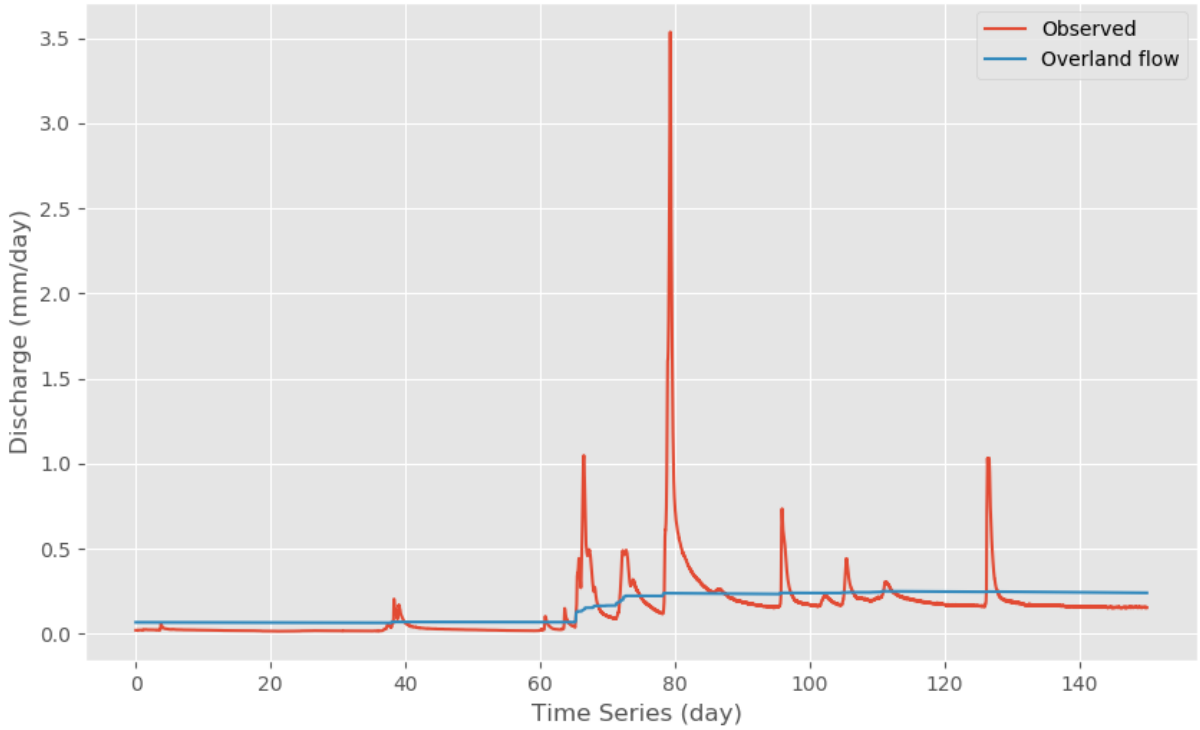

Figure 64. Model result of Rural Lumped M02B

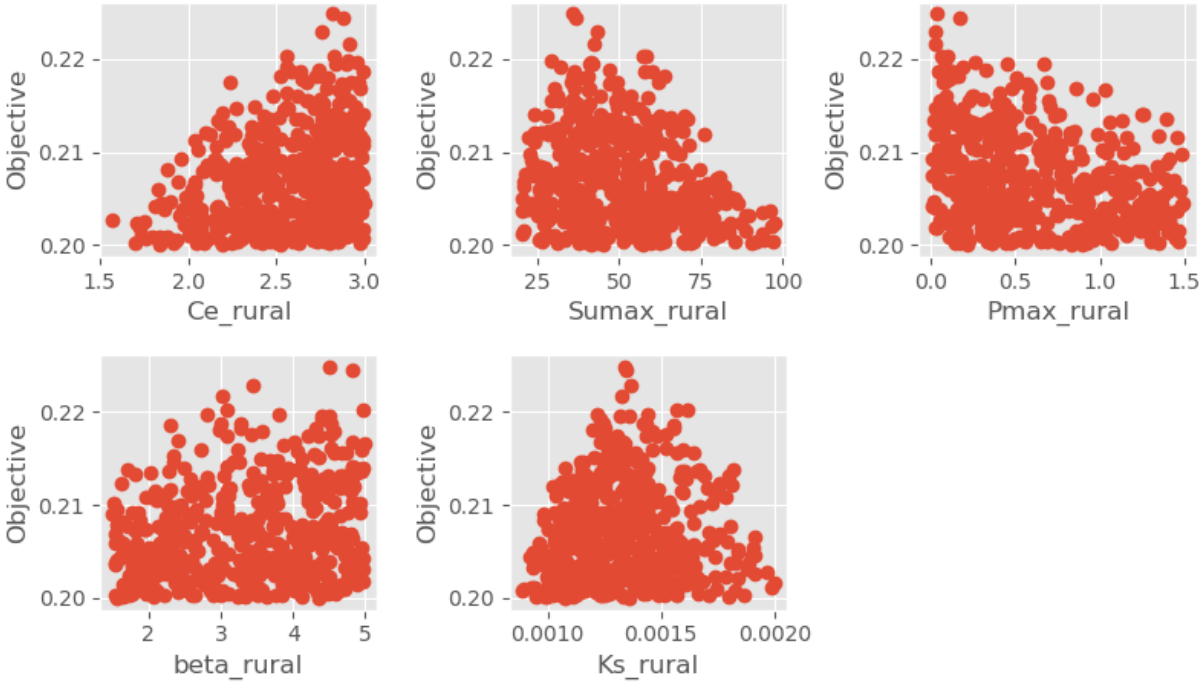

Figure 65. Parameter Calibration Result of Rural Lumped M02B

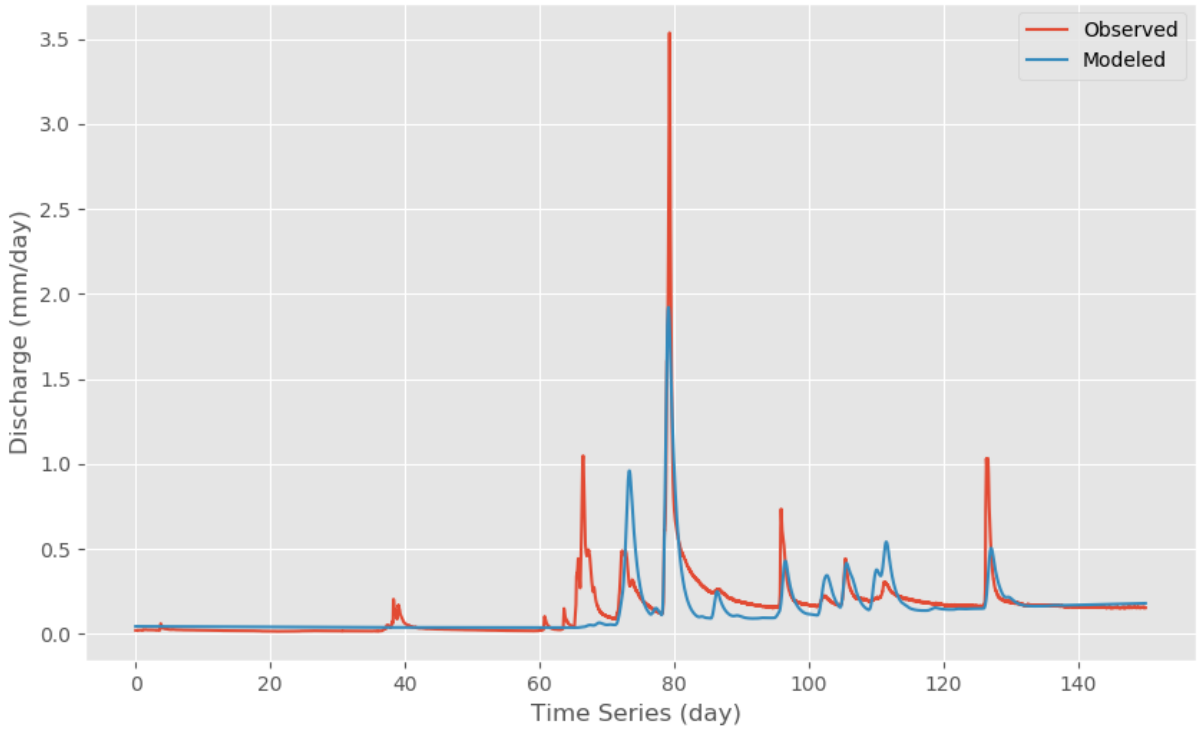

Figure 66. Model result of Rural Lumped M03B

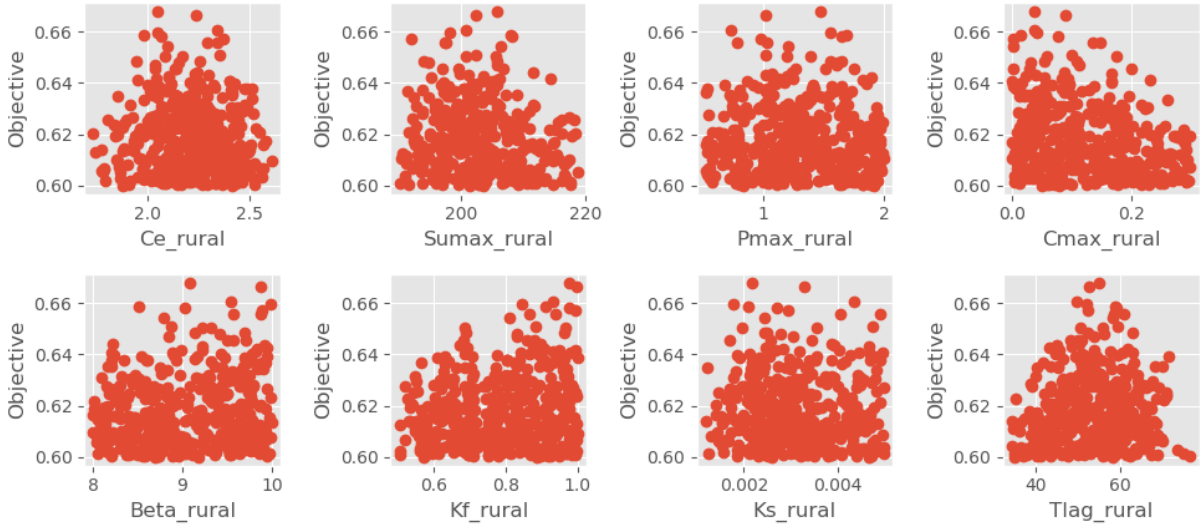

Figure 67. Parameter Calibration Result of Rural Lumped M03B

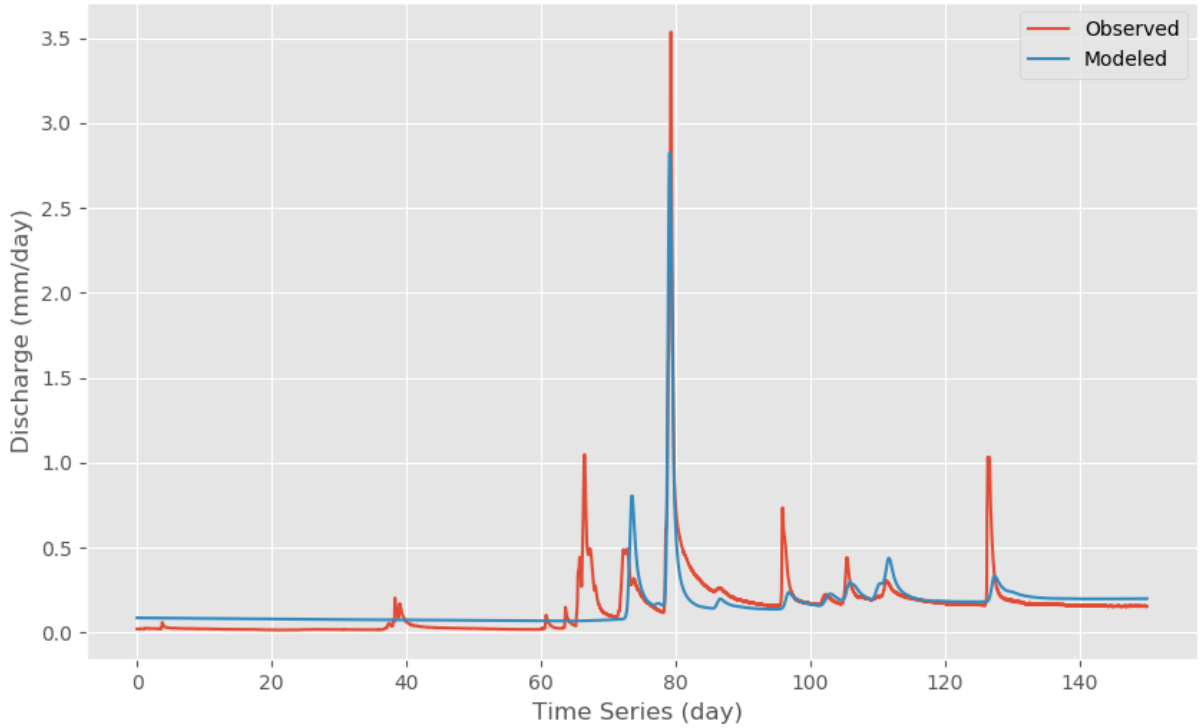

Figure 68. Model result of Rural Lumped M03C

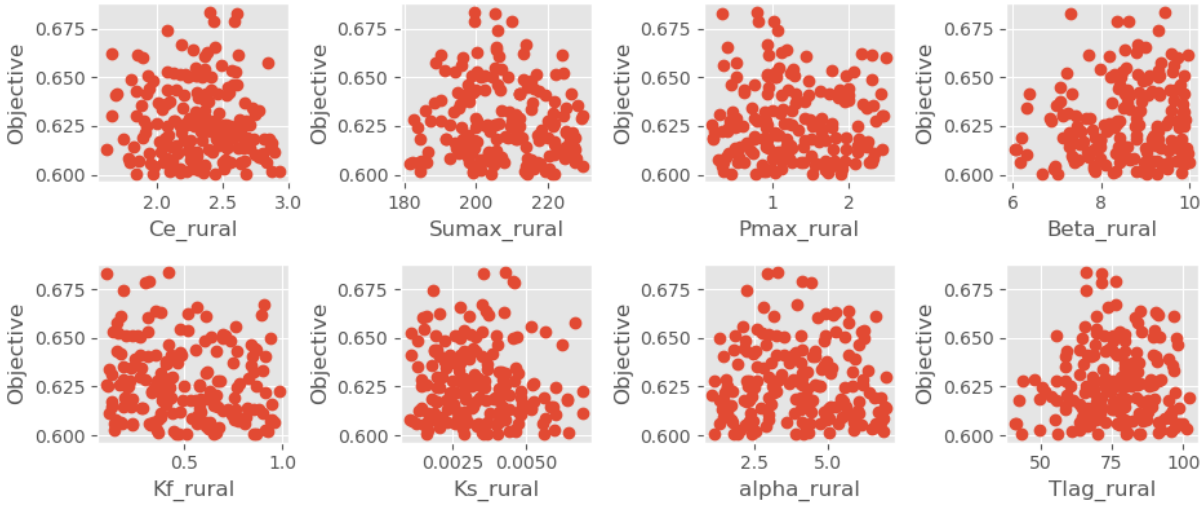

Figure 69. Parameter Calibration Result of Rural Lumped M03C

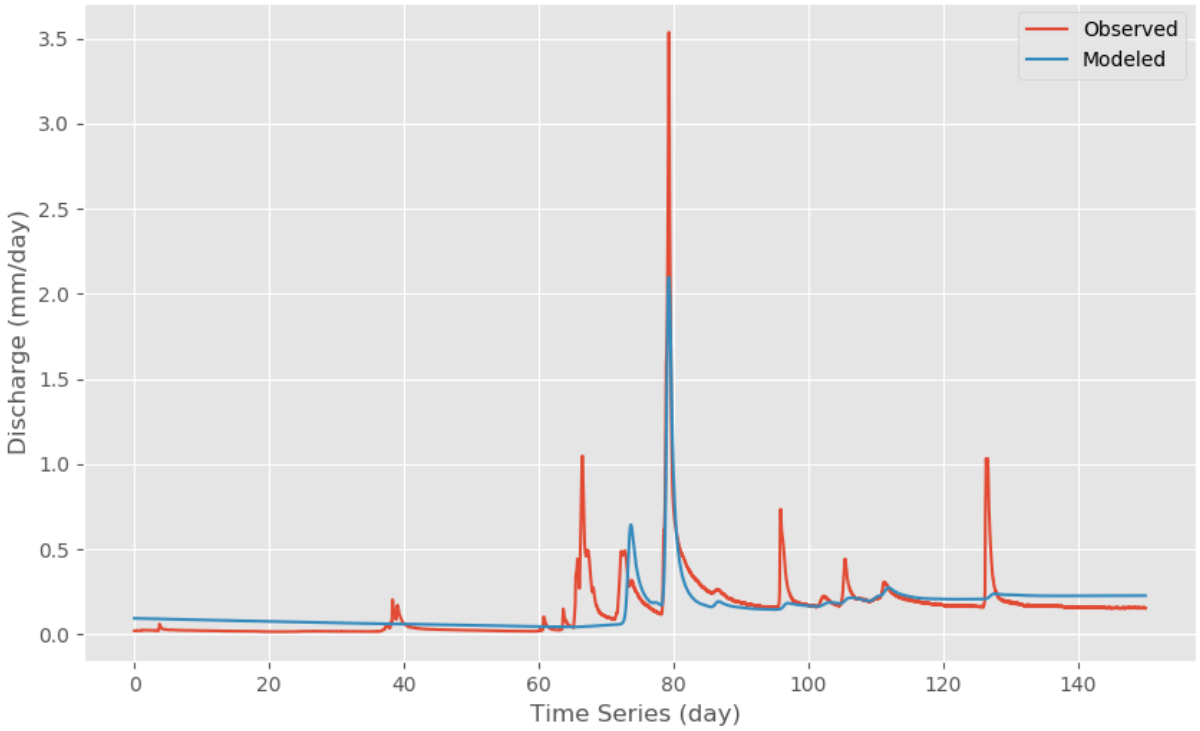

Figure 70. Model result of Rural Lumped M03D

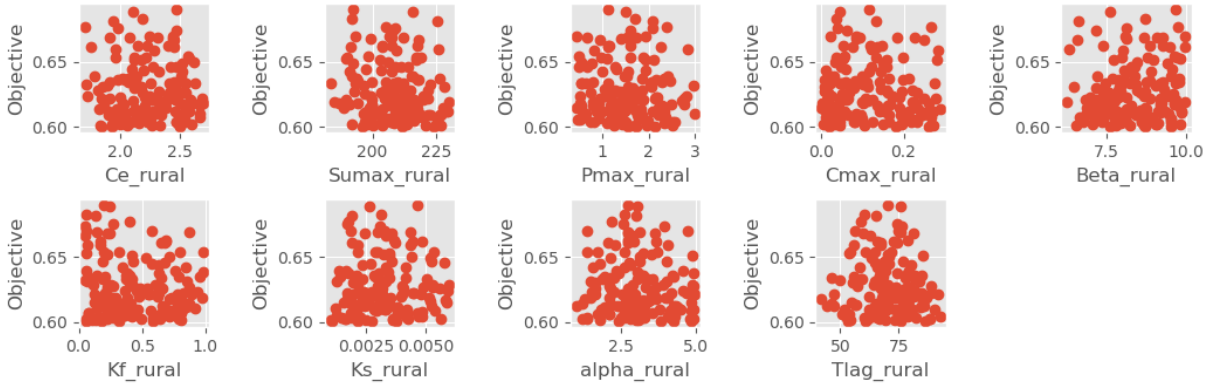

Figure 71. Parameter Calibration Result of Rural Lumped M03D

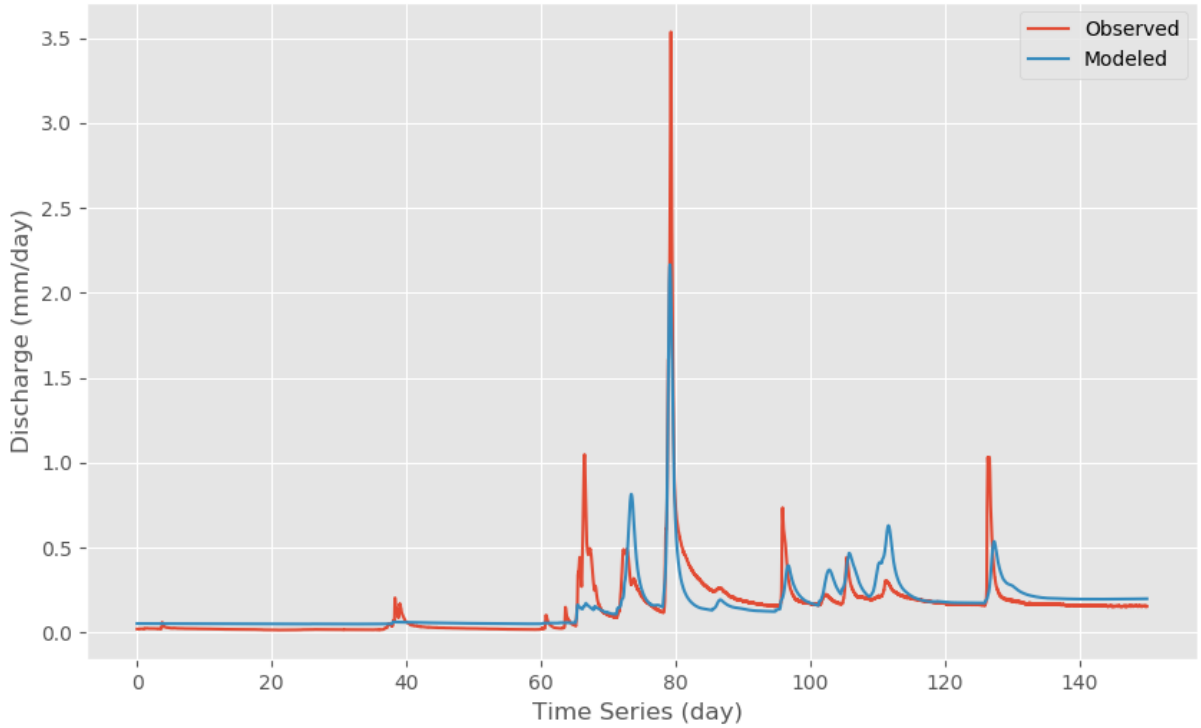

Figure 72. Model result of Rural Lumped M03E

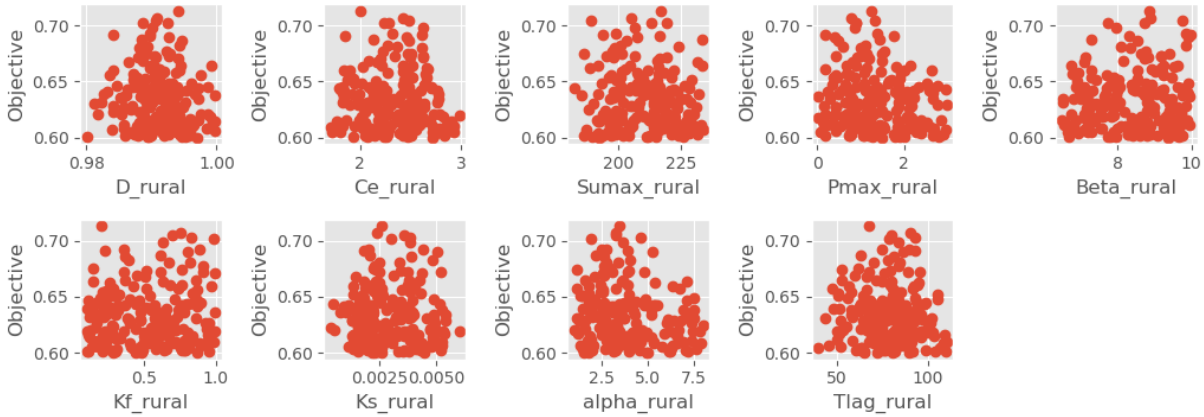

Figure 73. Parameter Calibration Result of Rural Lumped M03E

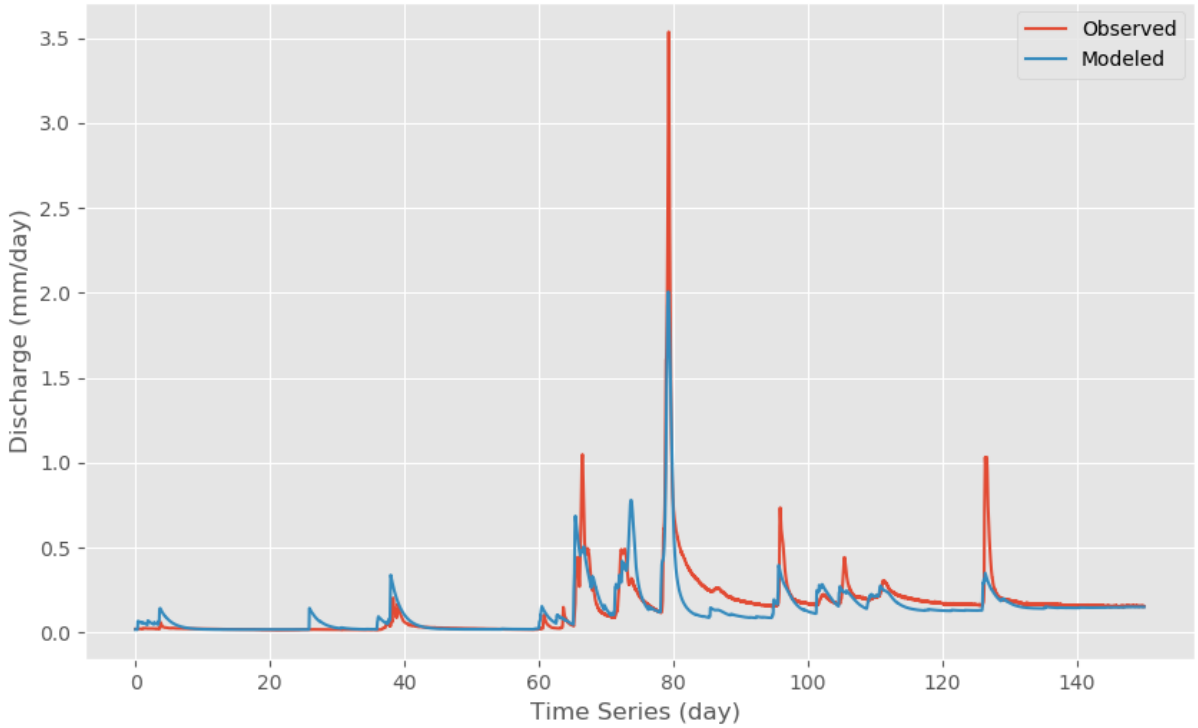

Figure 74. Model result of Rural Lumped M04A

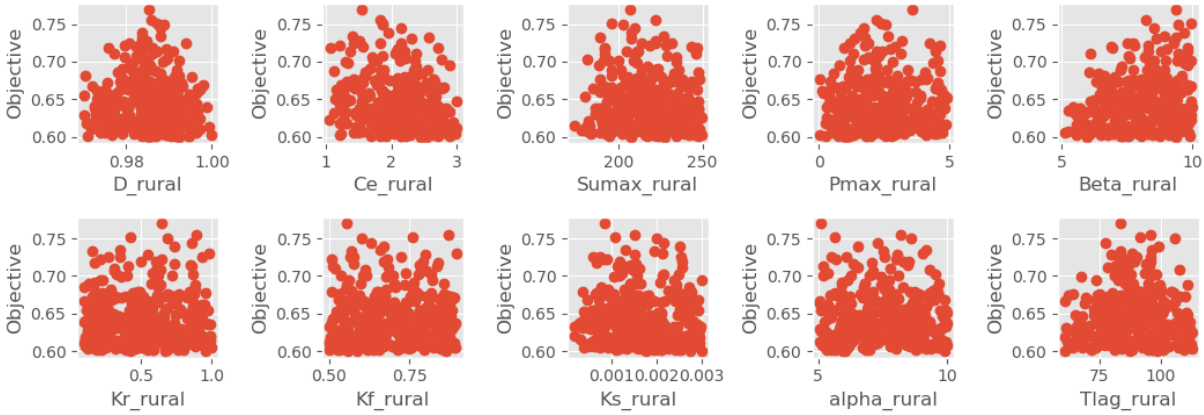

Figure 75. Parameter Calibration Result of Rural Lumped M04A

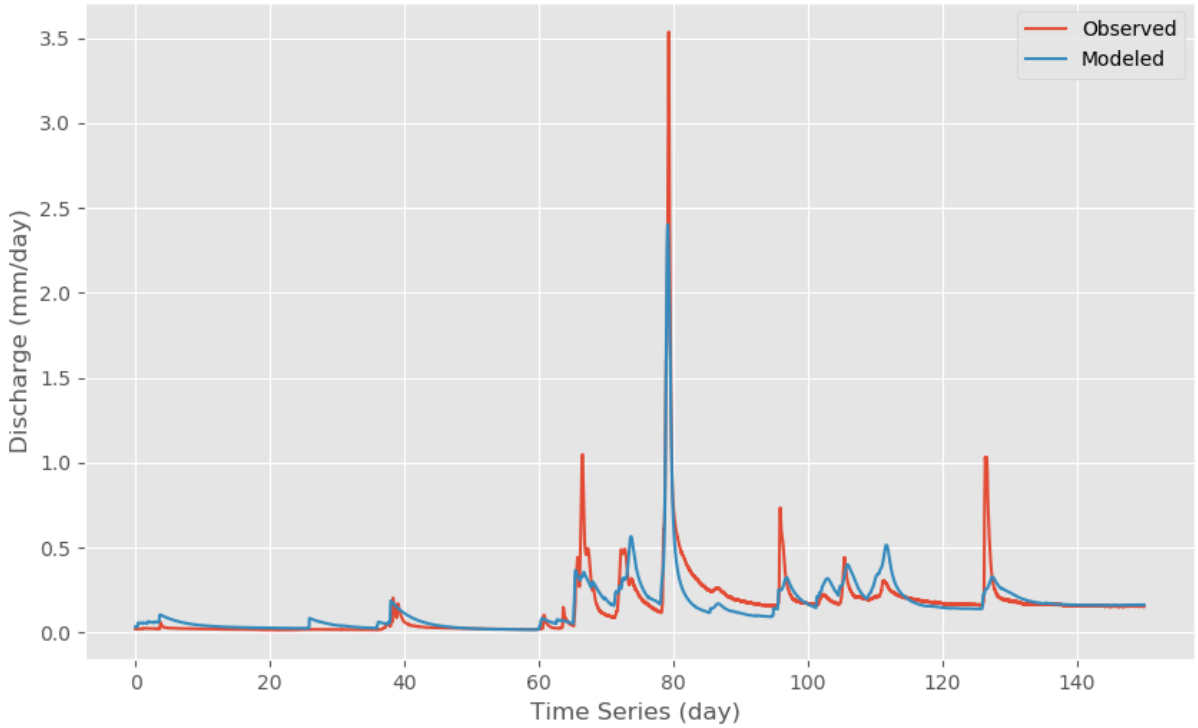

Figure 76. Model result of Rural Lumped M04B

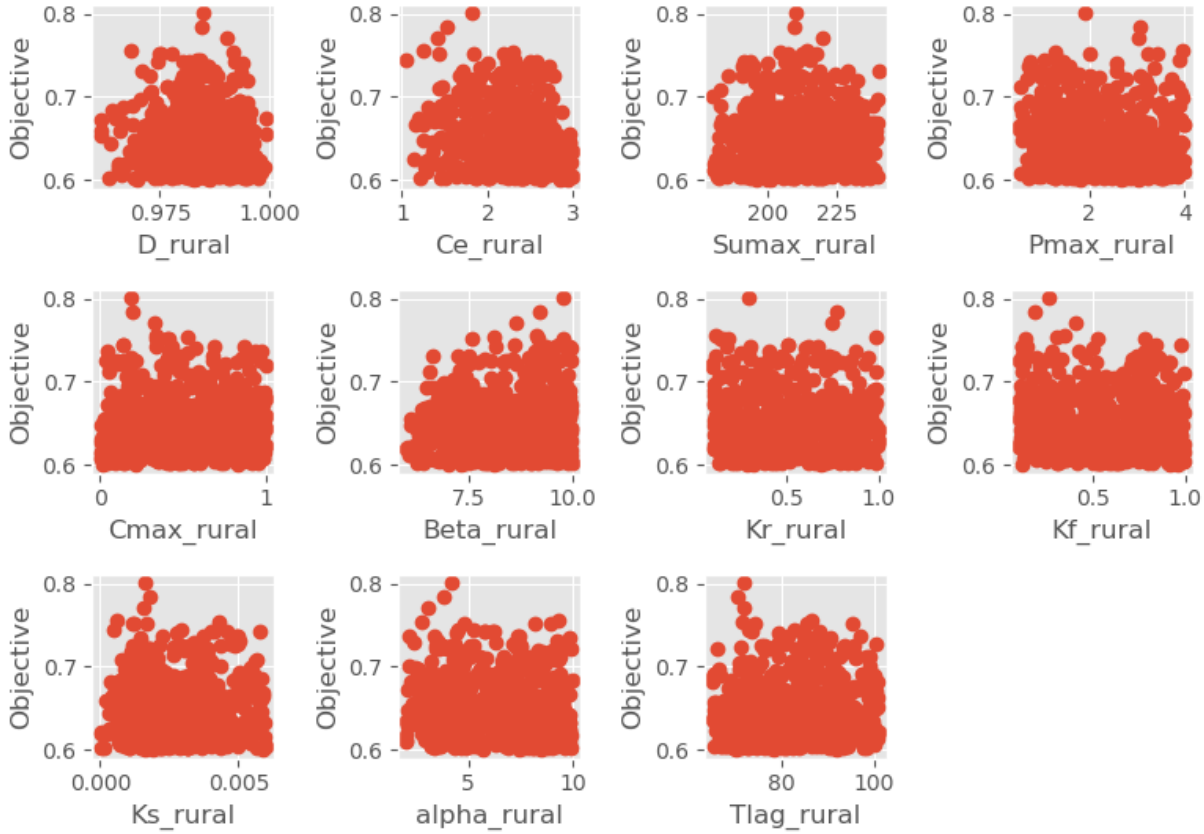

Figure 77. Parameter Calibration Result of Rural Lumped M04B

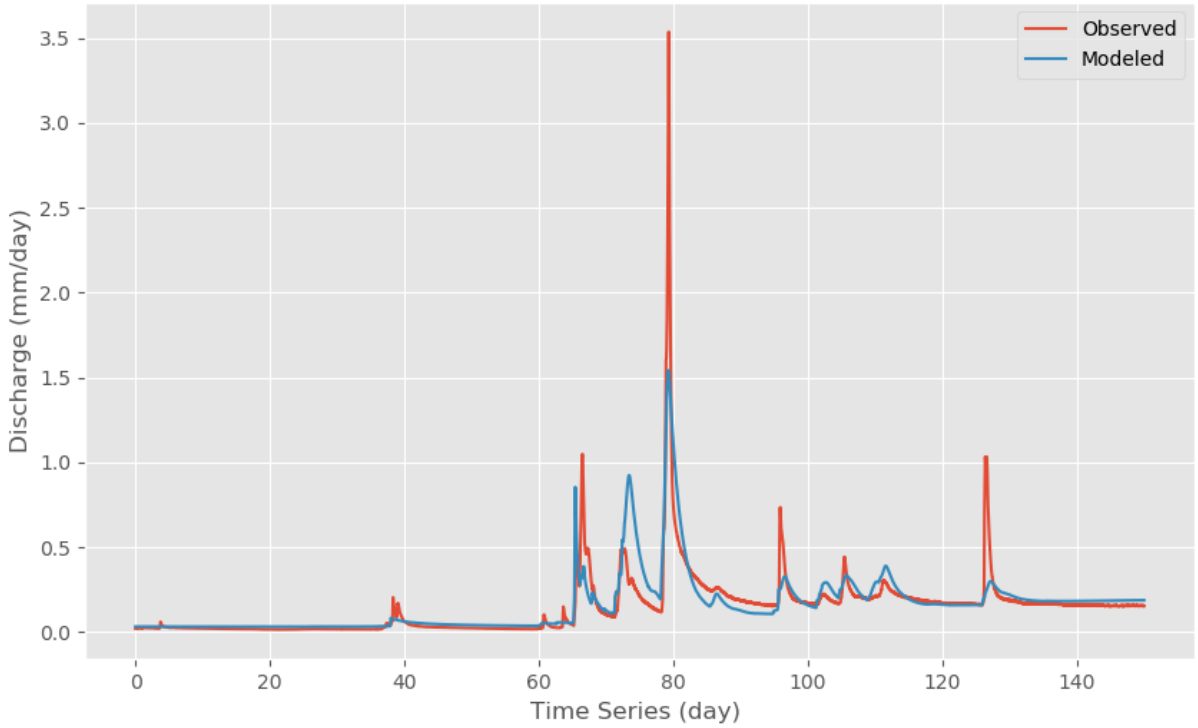

Figure 78. Model result of Rural Lumped M04C

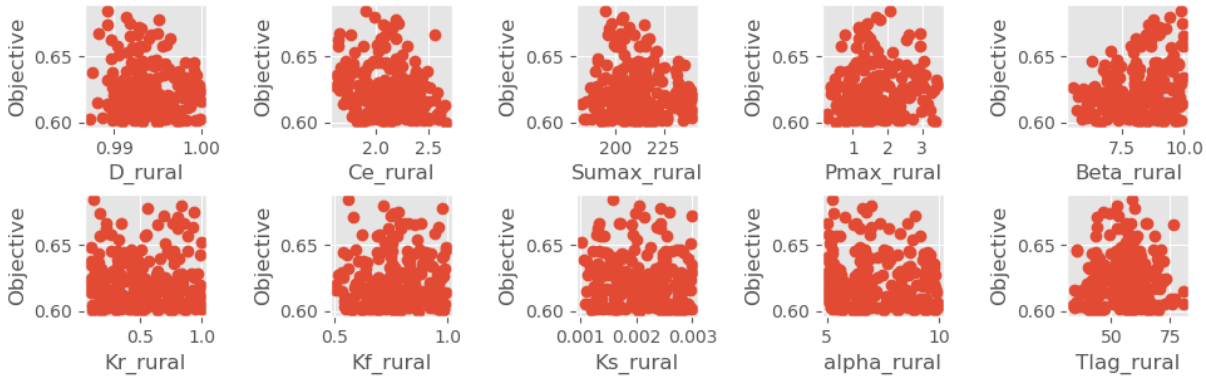

Figure 79. Parameter Calibration Result of Rural Lumped M04C

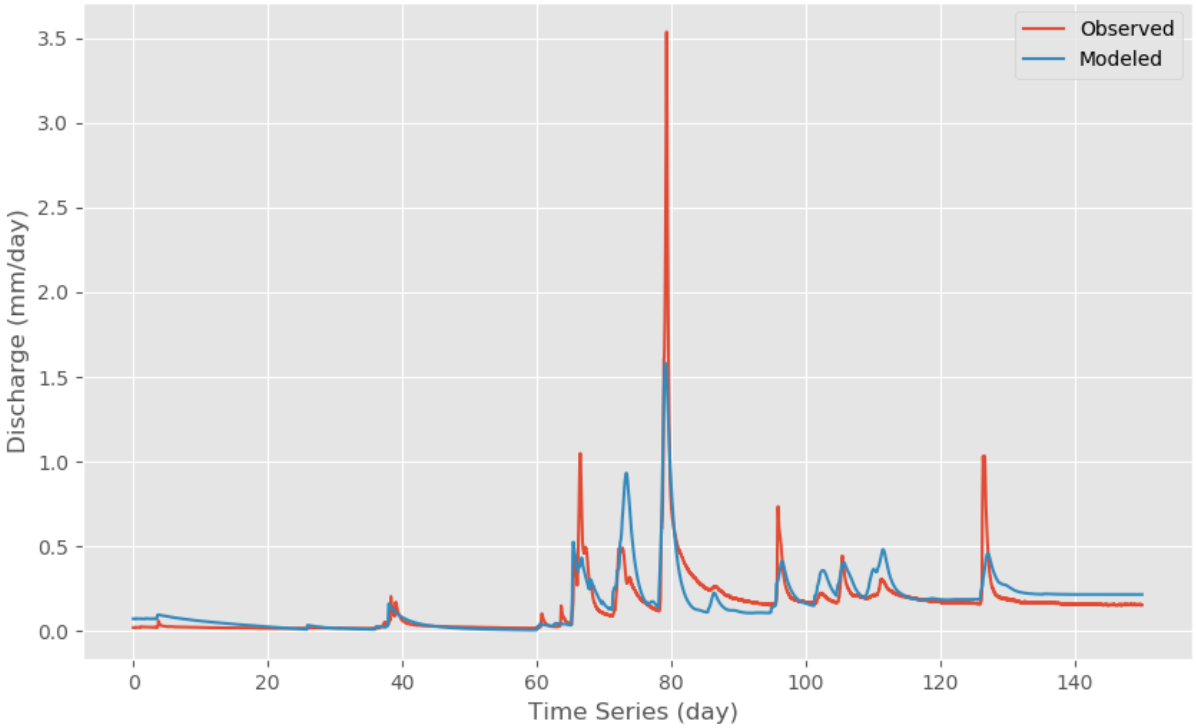

Figure 80. Model result of Rural Lumped M04D

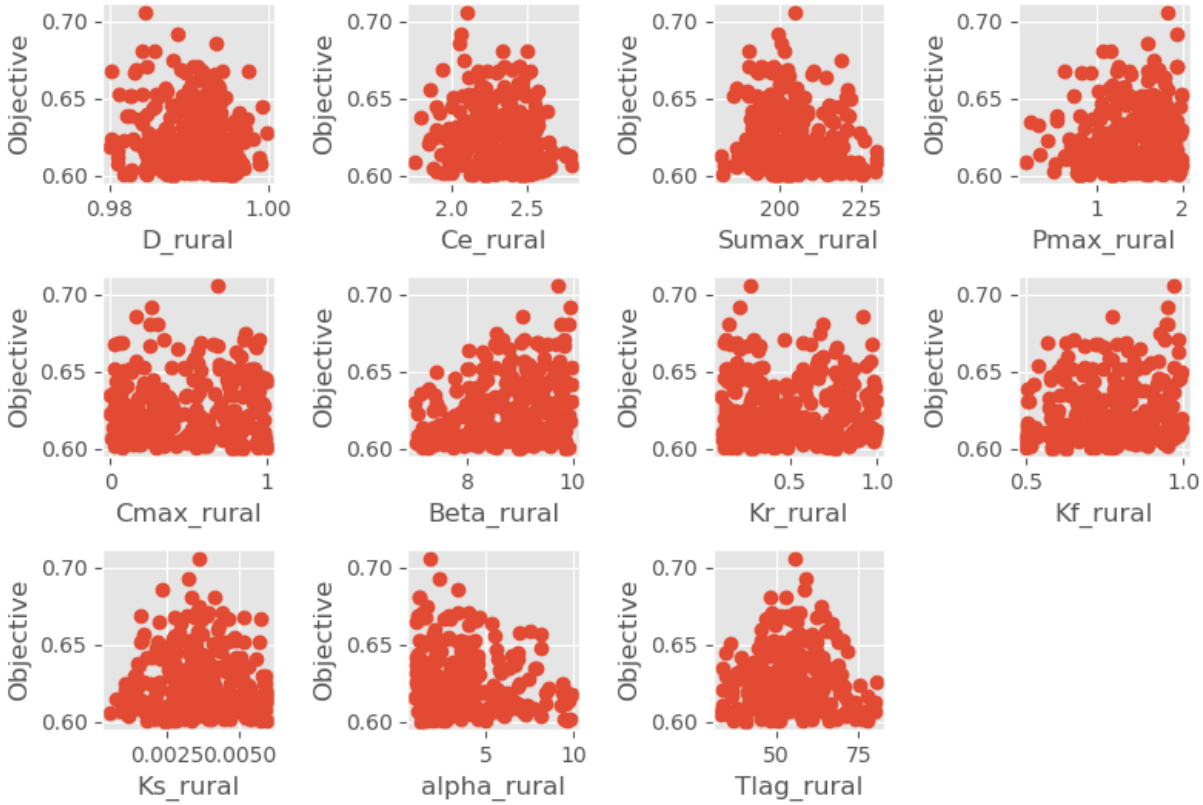

Figure 81. Parameter Calibration Result of Rural Lumped M04D

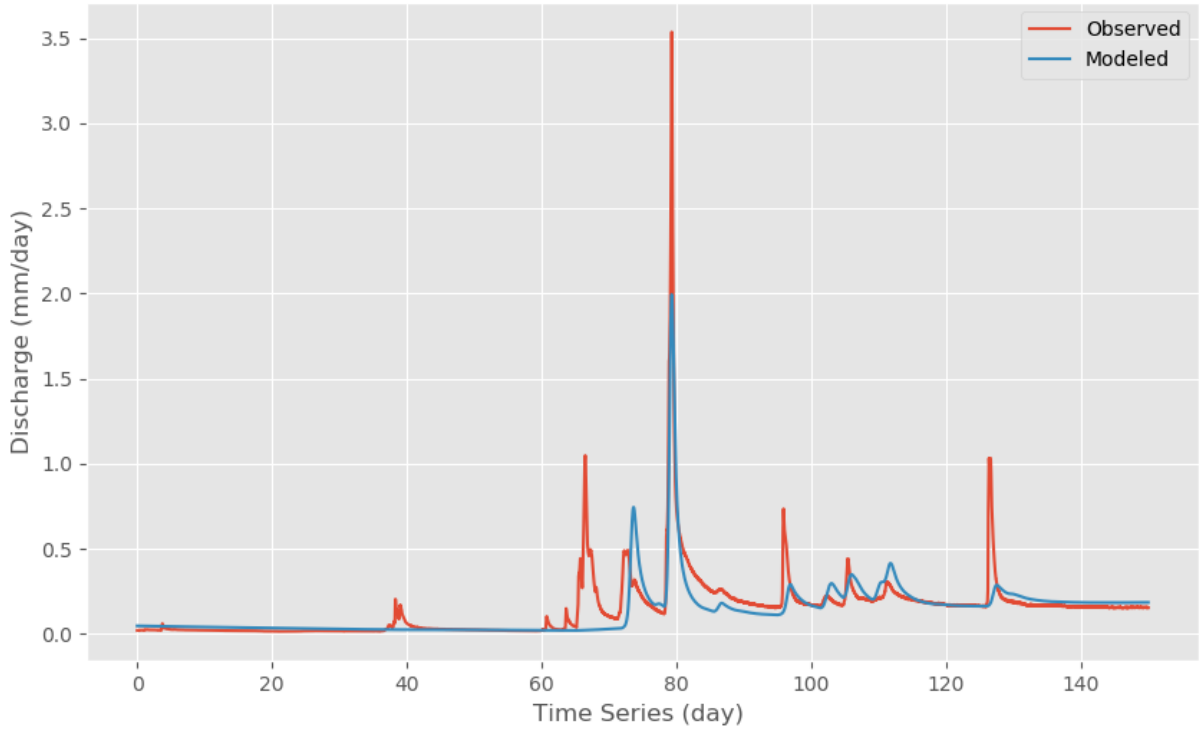

Figure 82. Model result of Rural Lumped M05A

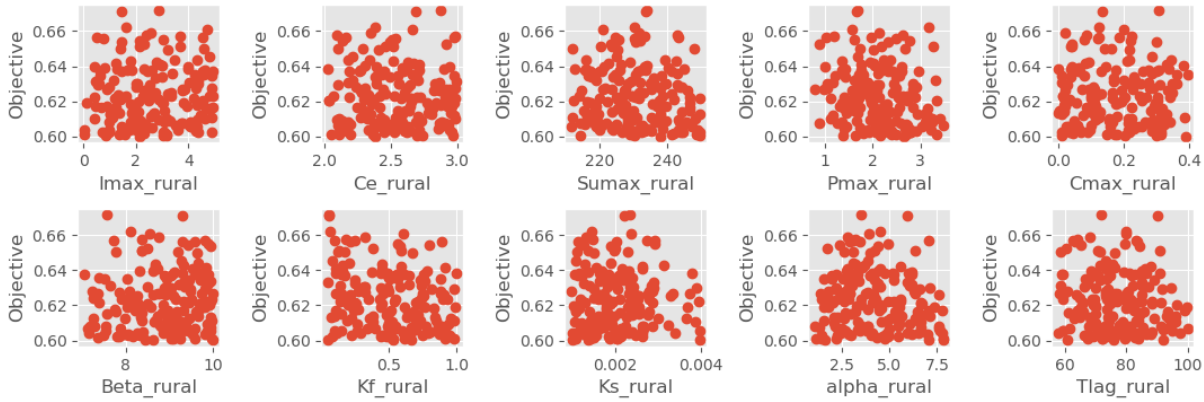

Figure 83. Parameter Calibration Result of Rural Lumped M05A

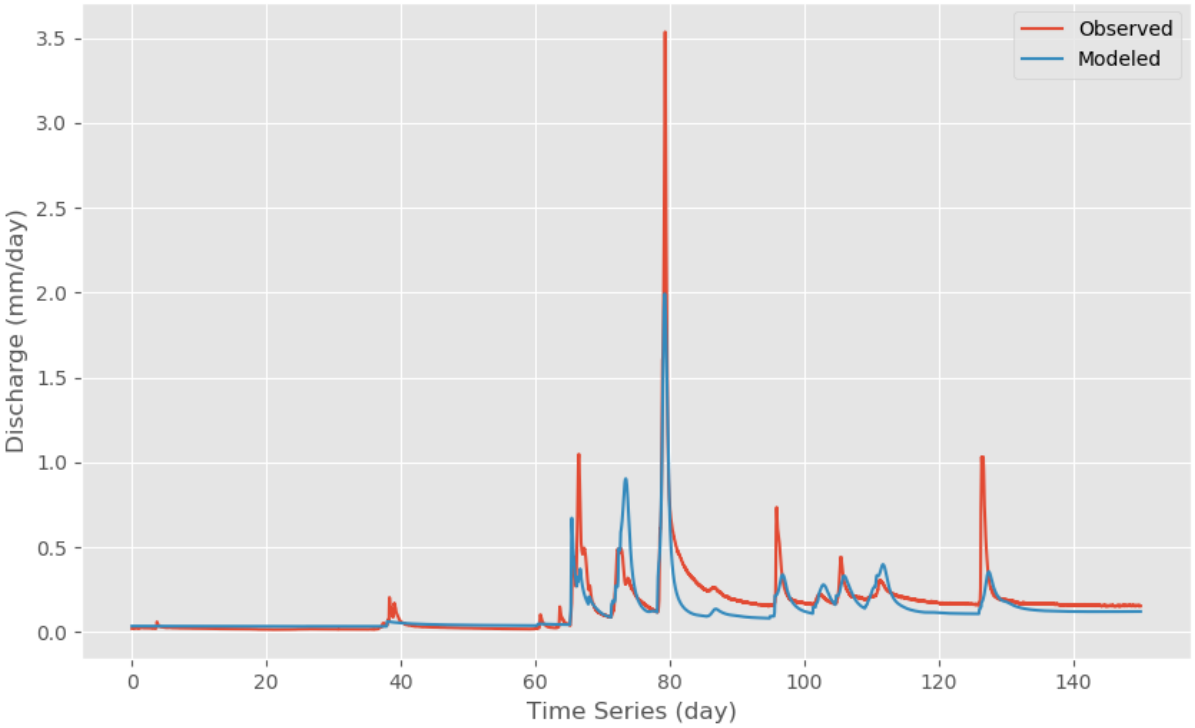

Figure 84. Model result of Rural Lumped M05B

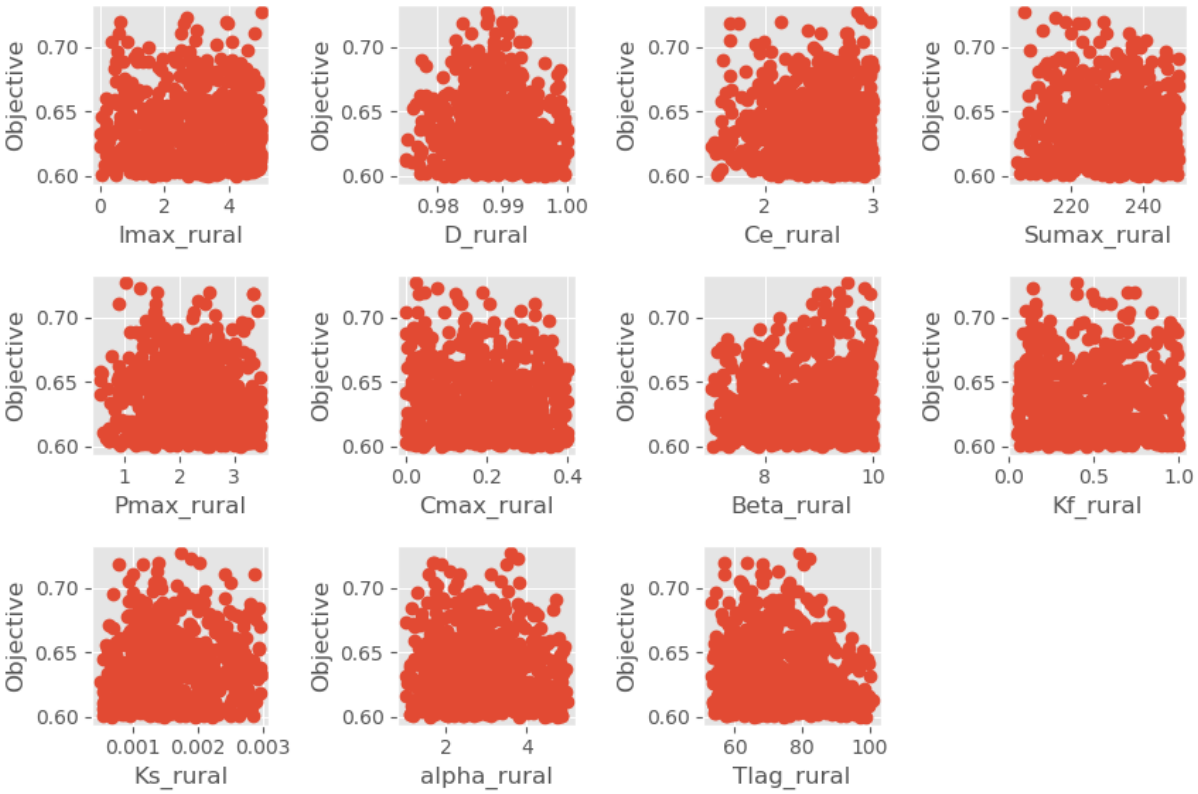

Figure 85. Parameter Calibration Result of Rural Lumped M05B

D.4.2 Urban lumped model

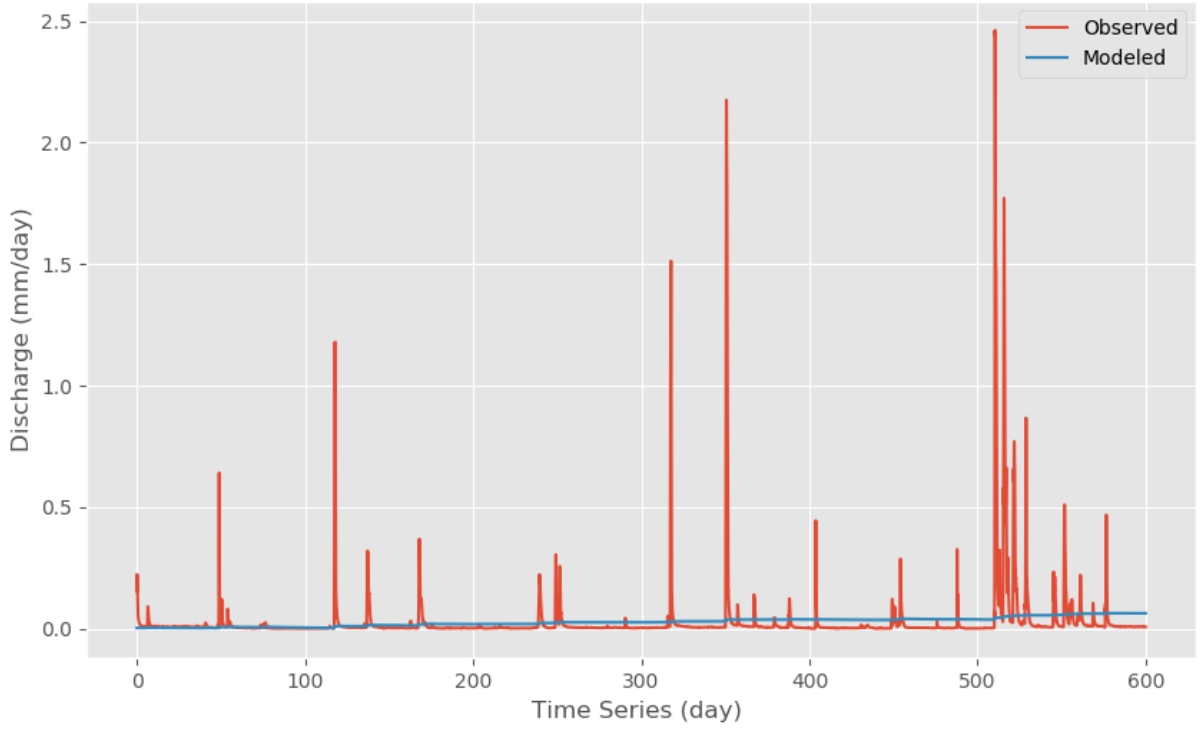

Figure 86. Model Result of Urban Lumped M01A

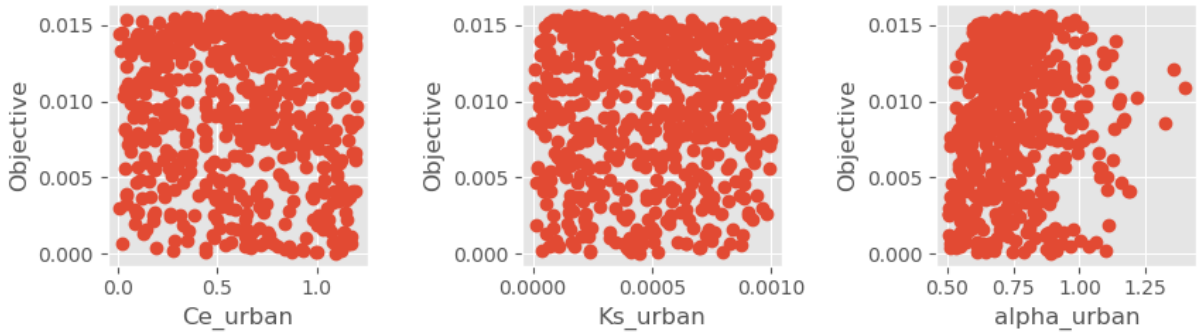

Figure 87. Parameter Calibration Result of Urban Lumped M01A

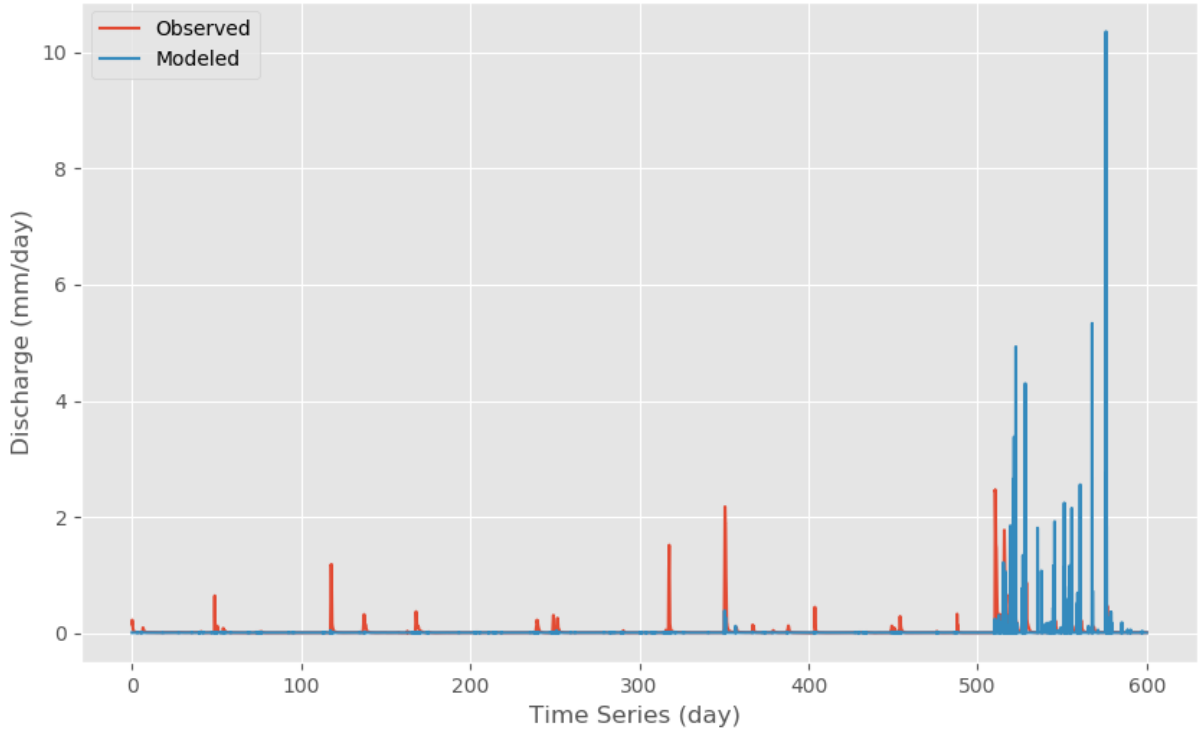

Figure 88. Model Result of Urban Lumped M01B

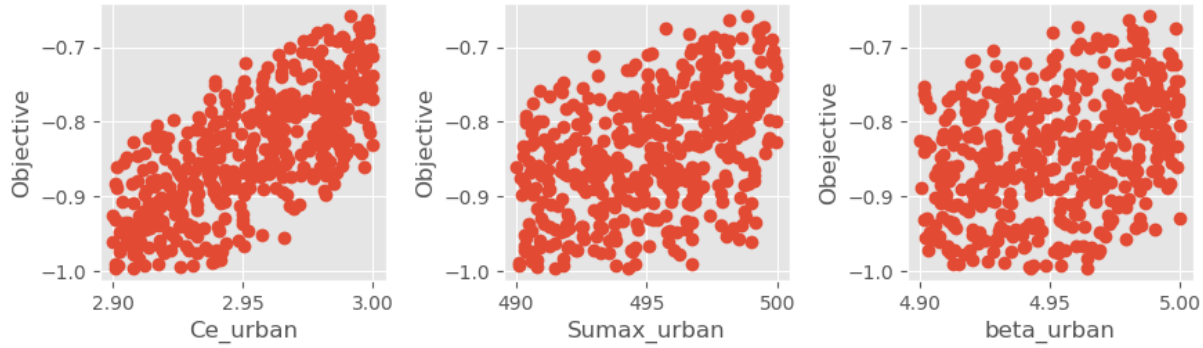

Figure 89. Parameter Calibration Result of Urban Lumped M01B

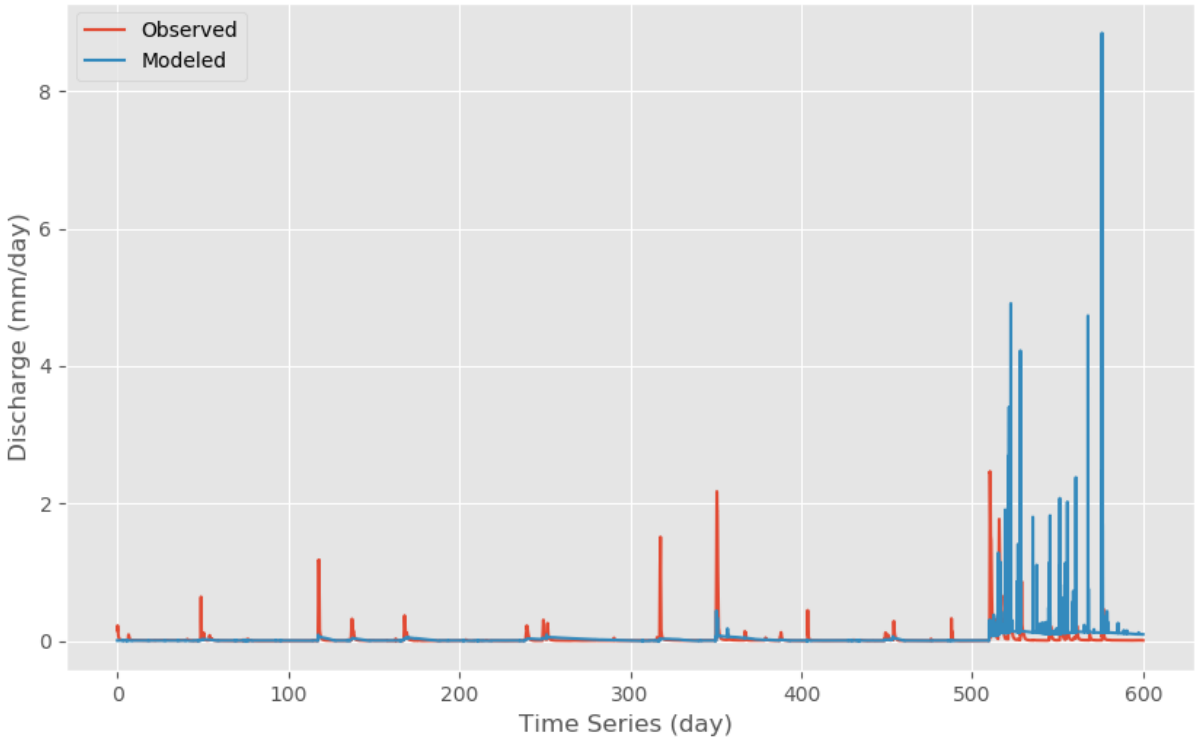

Figure 90. Model Result of Urban Lumped M01C

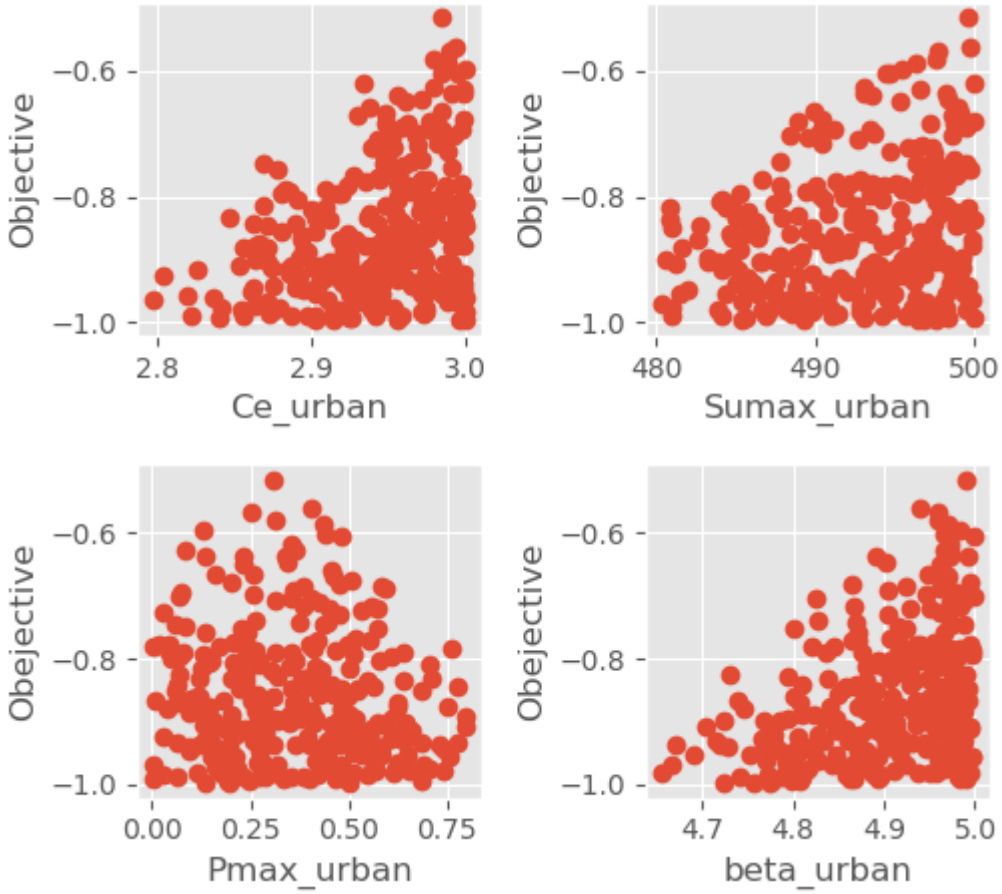

Figure 91. Parameter Calibration Result of Urban Lumped M01C

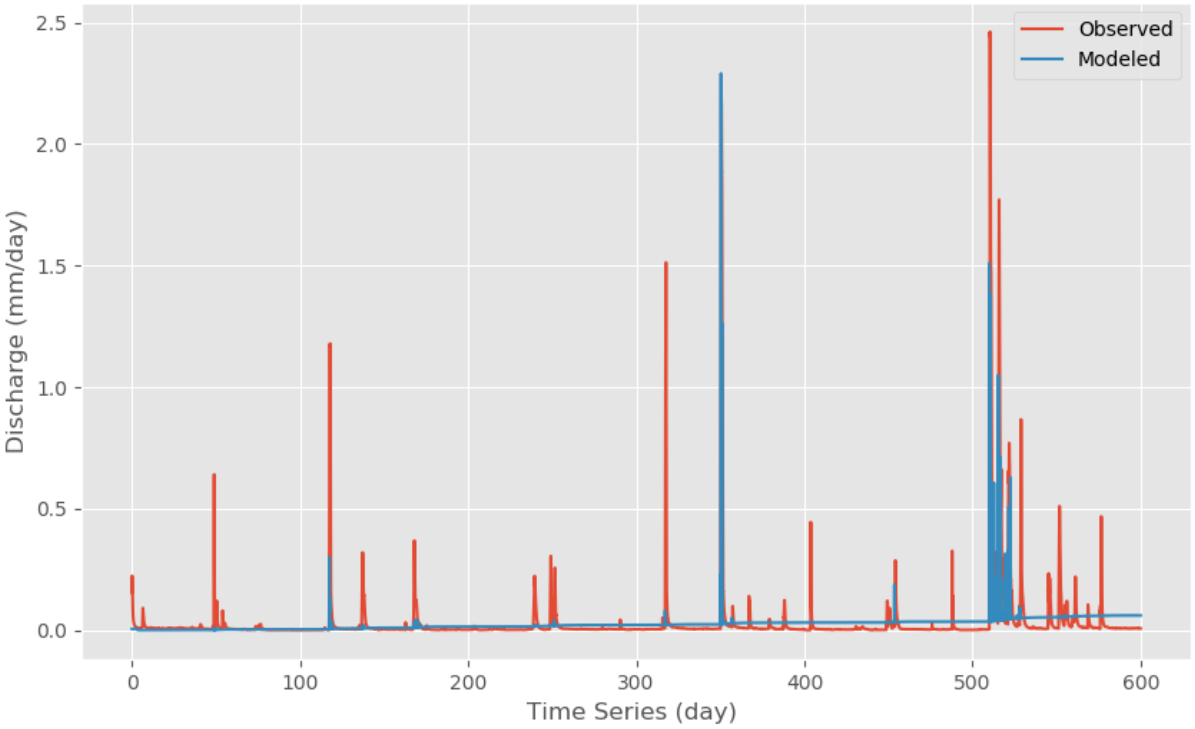

Figure 92. Model Result of Urban Lumped M02A

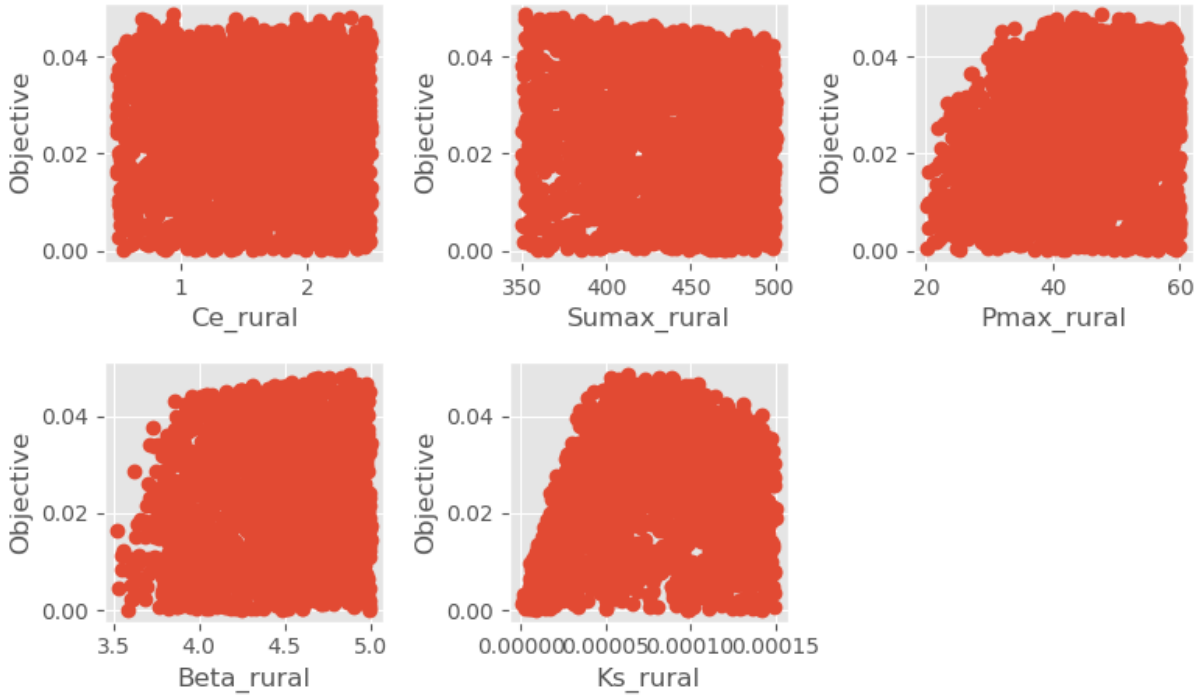

Figure 93. Parameter Calibration Result of Urban Lumped M02A

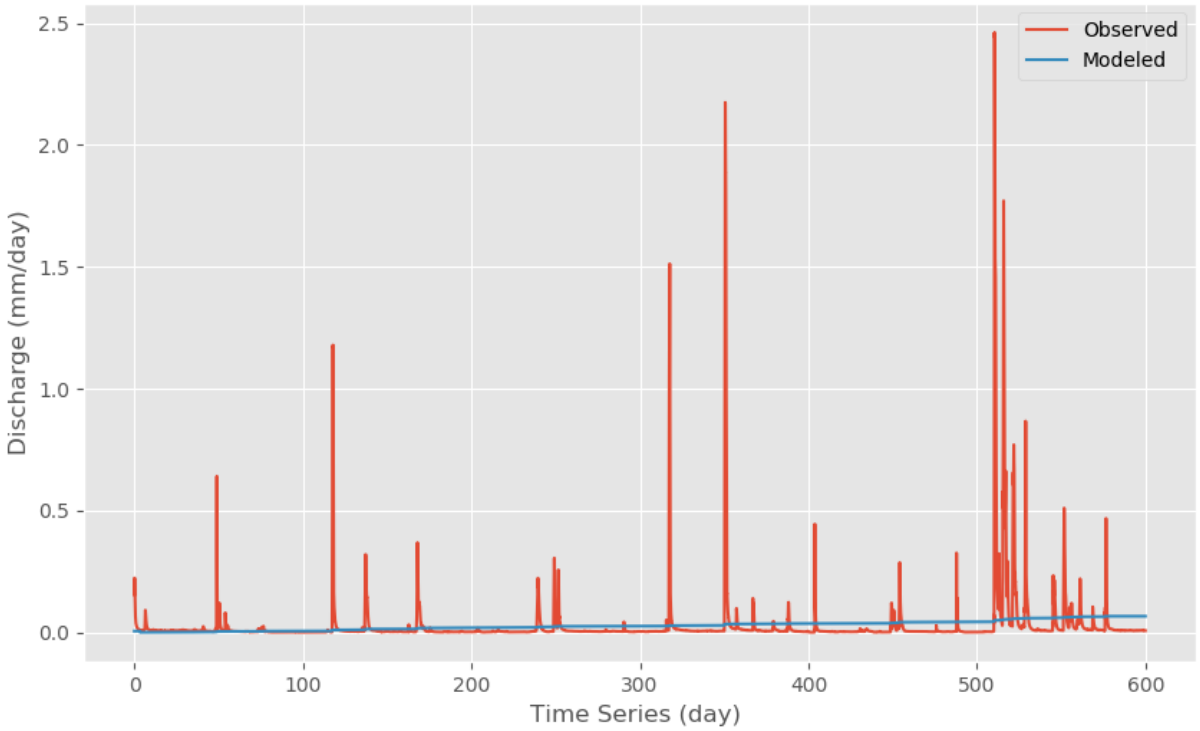

Figure 94. Model Result of Urban Lumped M02B

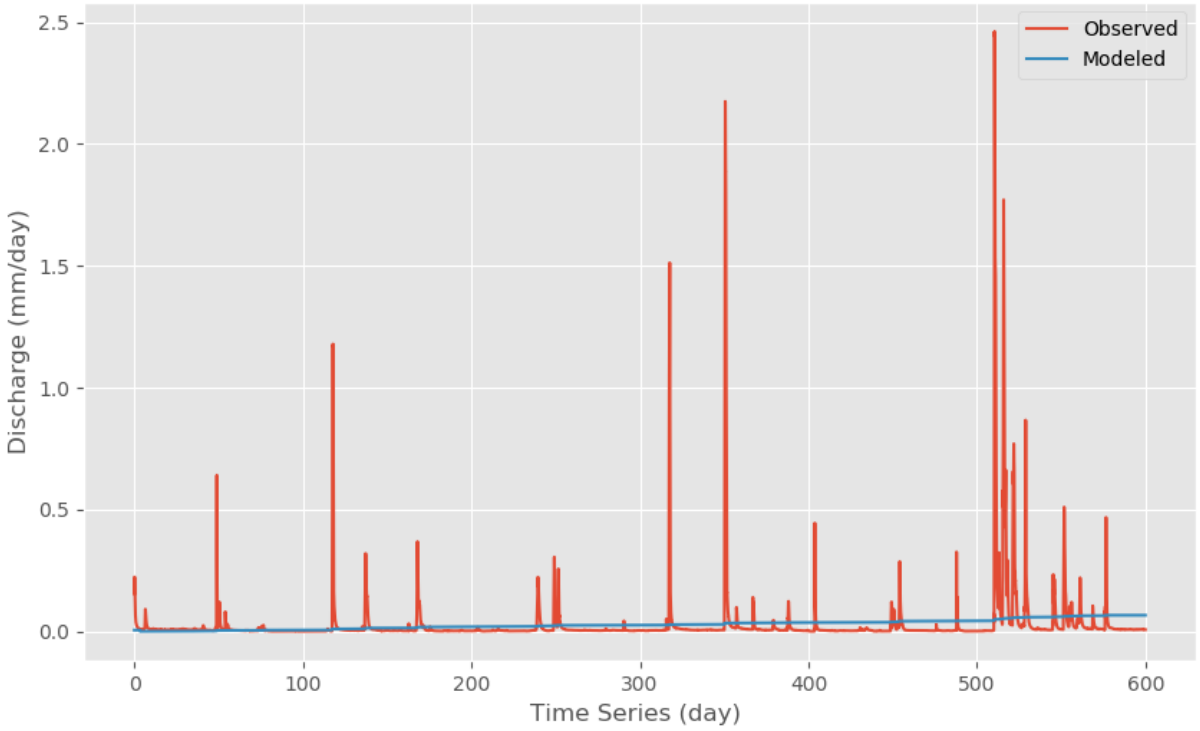

Figure 95. Parameter Calibration Result of Urban Lumped M02B

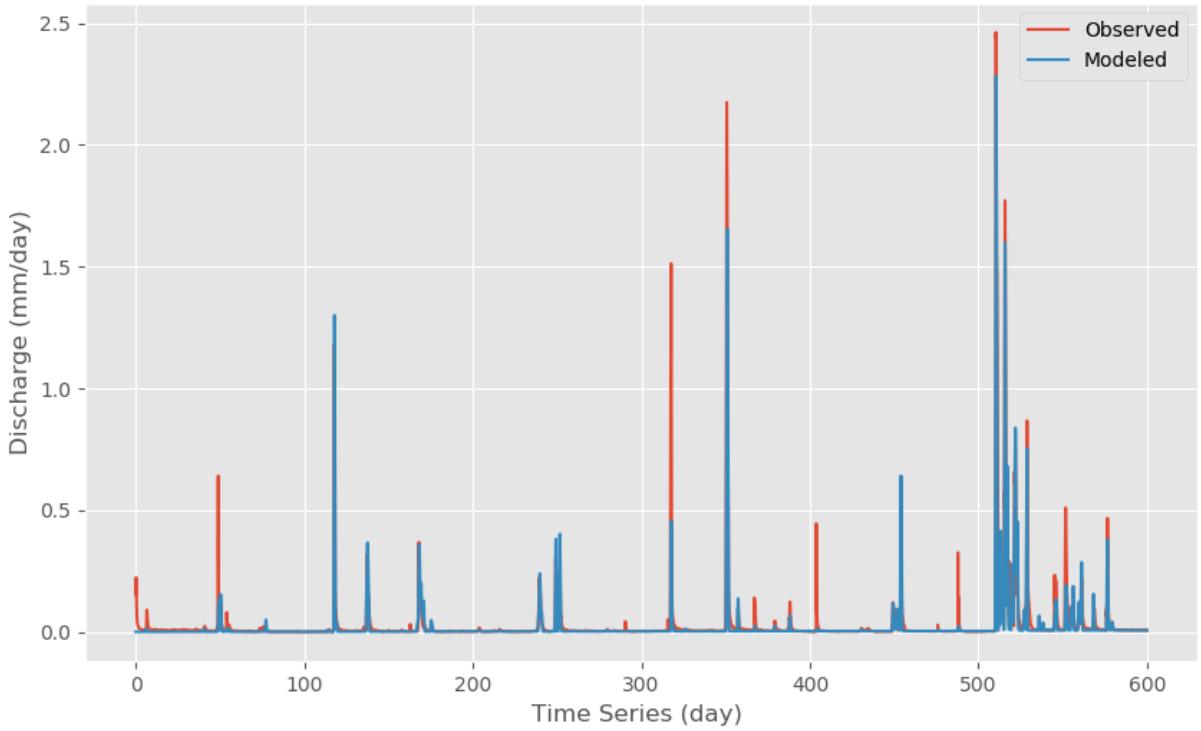

Figure 96. Model Result of Urban Lumped M04A

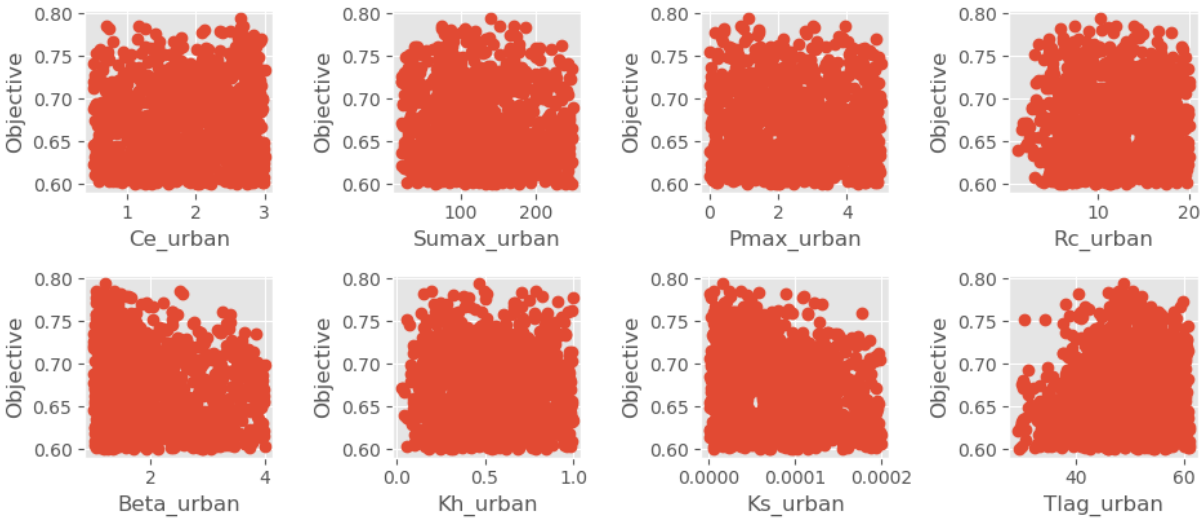

Figure 97. Parameter Calibration Result of Urban Lumped M04A

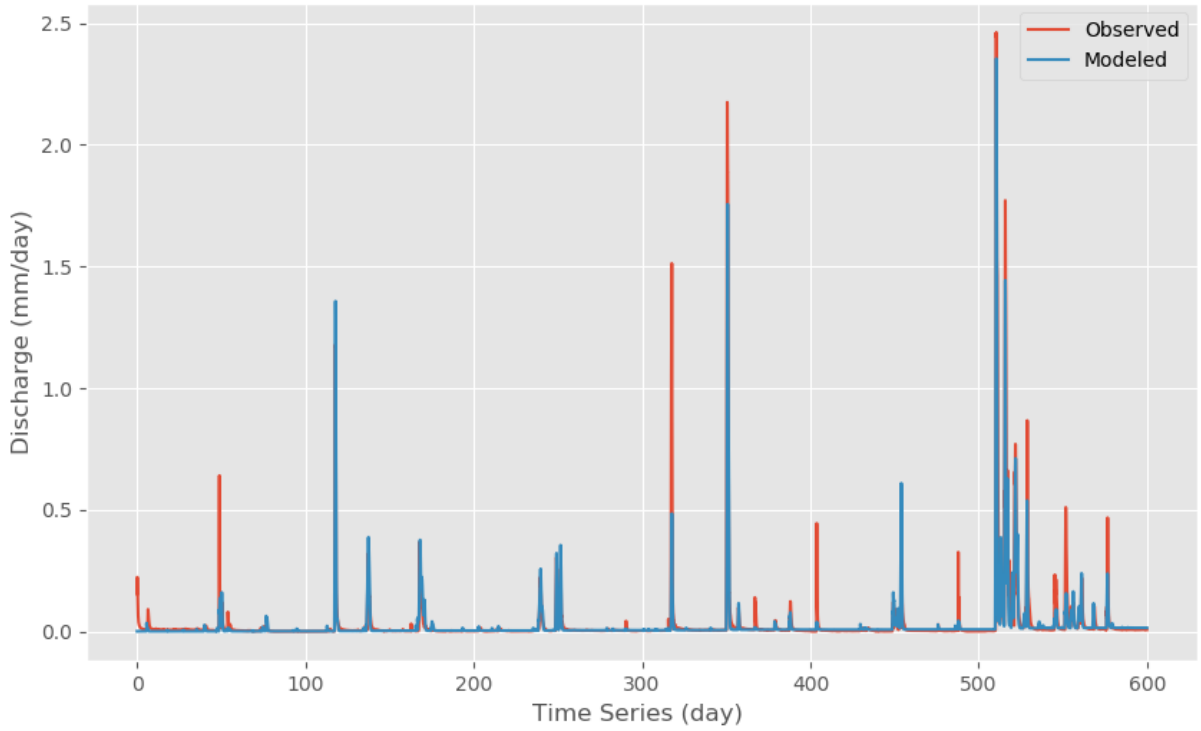

Figure 98. Model Result of Urban Lumped M04B

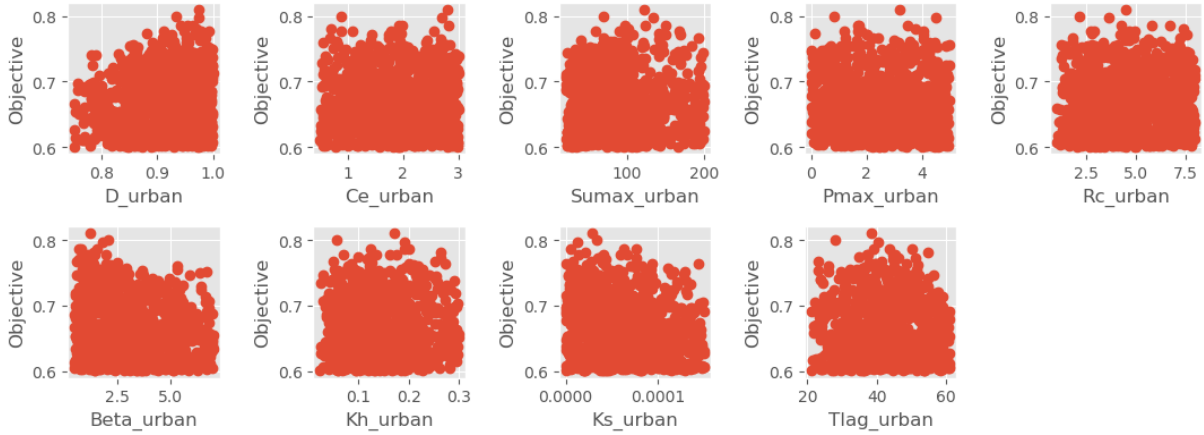

Figure 99. Parameter Calibration Result of Urban Lumped M04B

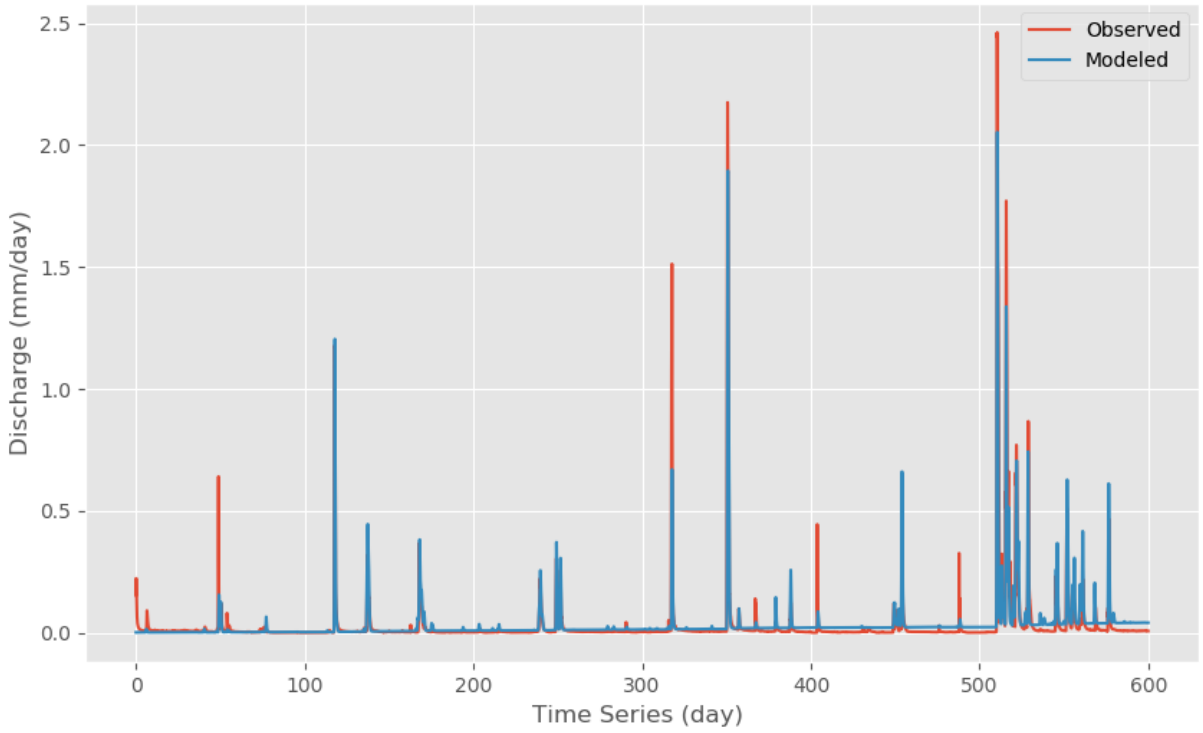

Figure 100. Model Result of Urban Lumped M04C

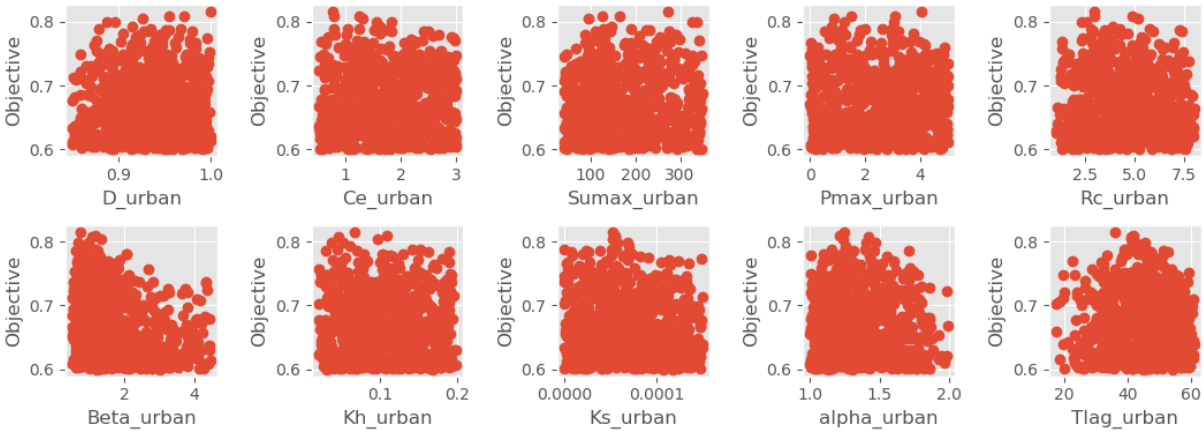

Figure 101. Parameter Calibration Result of Urban Lumped M04C

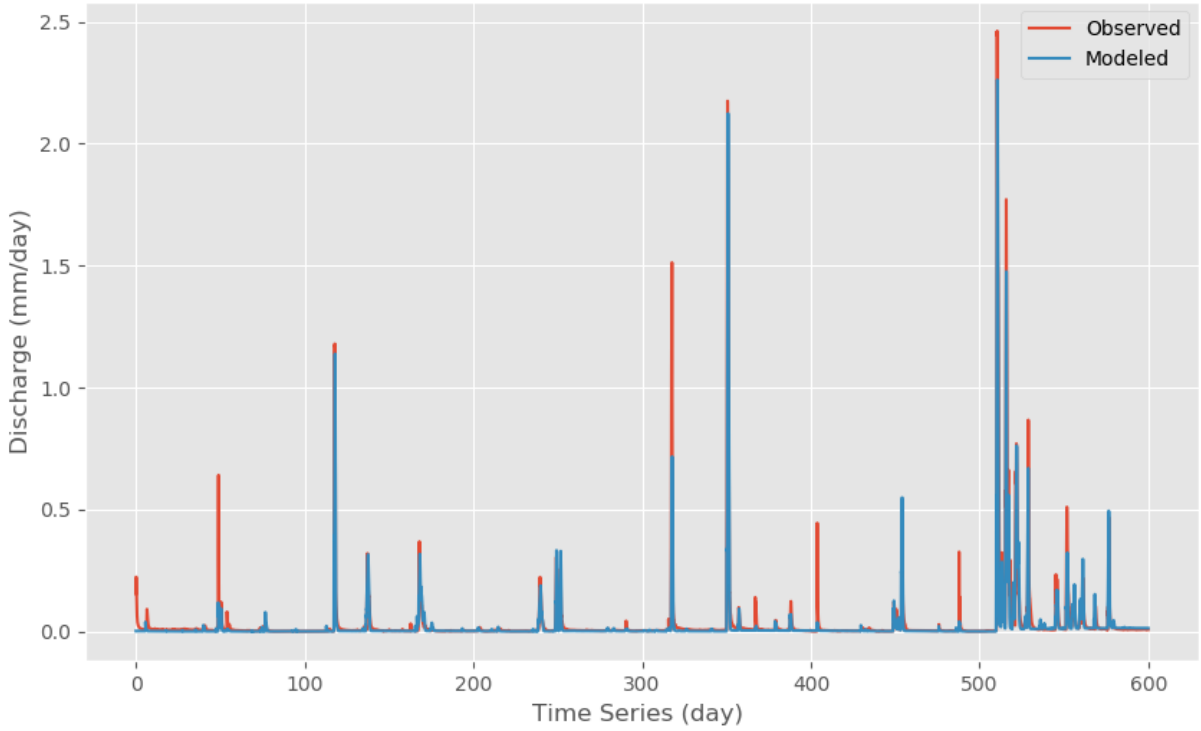

Figure 102. Model Result of Urban Lumped M04D

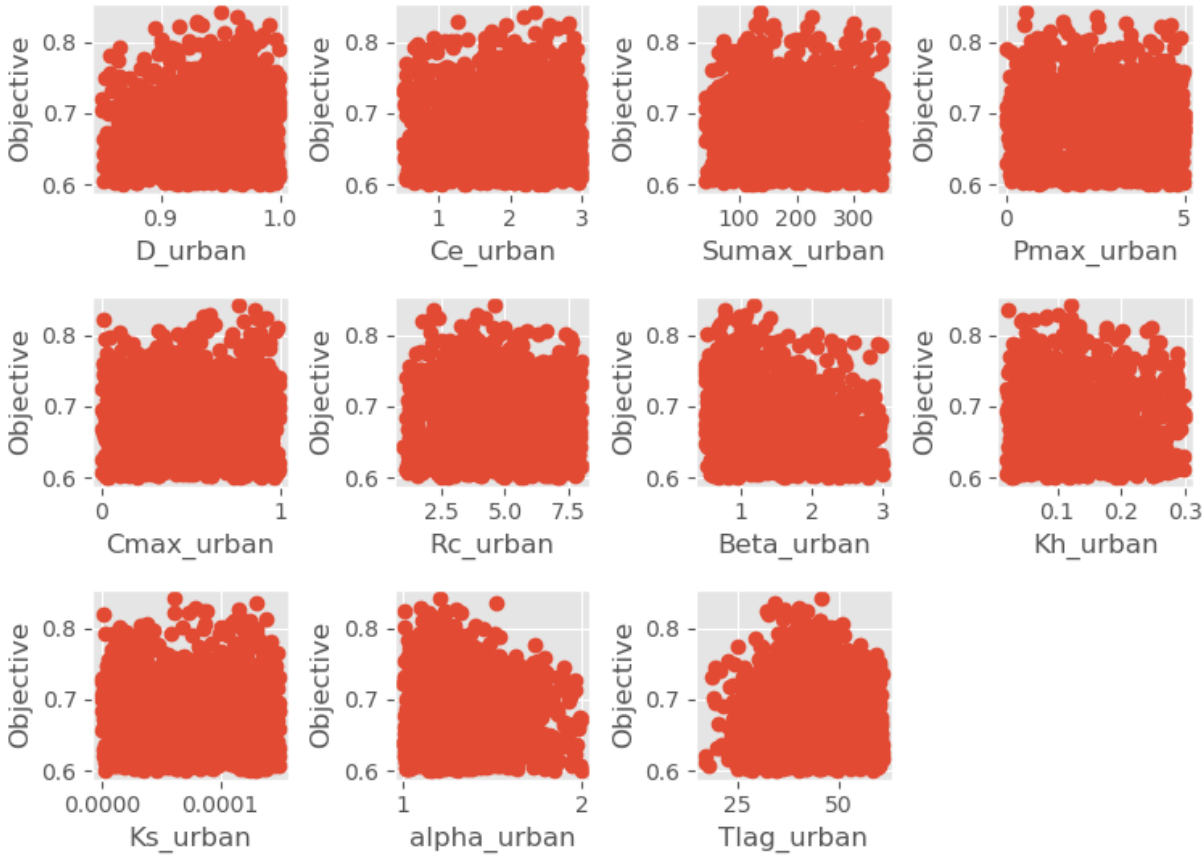

Figure 103. Parameter Calibration Result of Urban Lumped M04D

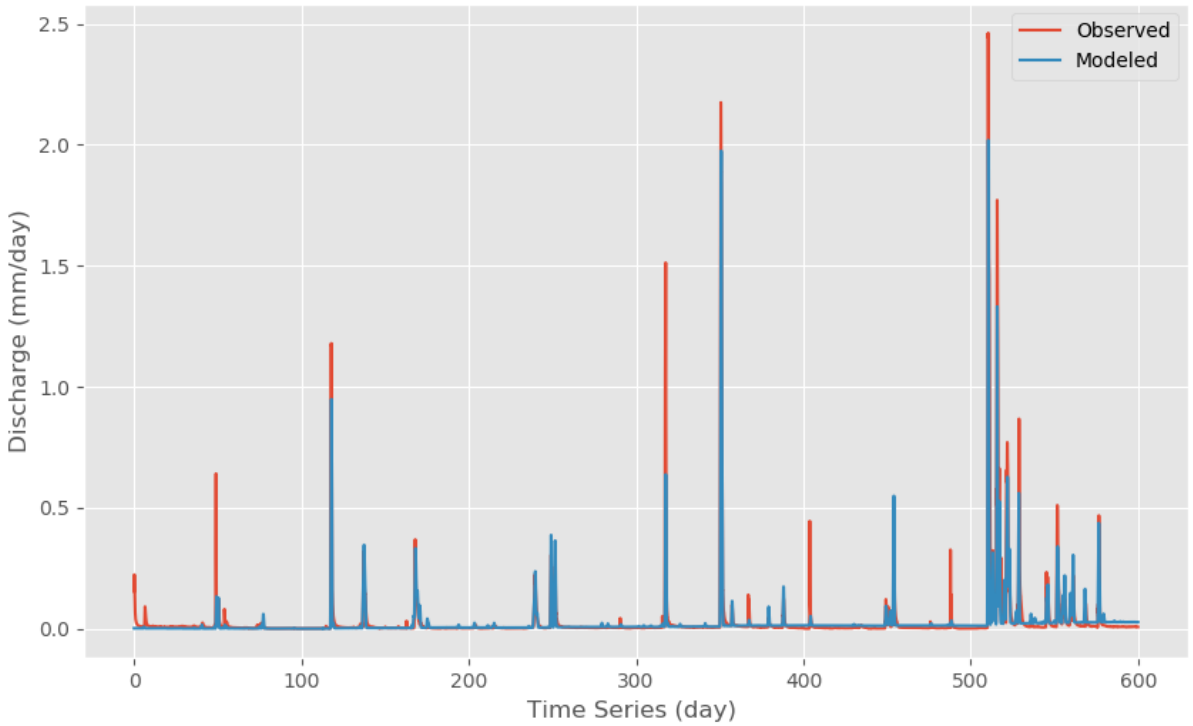

Figure 104. Model Result of Urban Lumped M05A

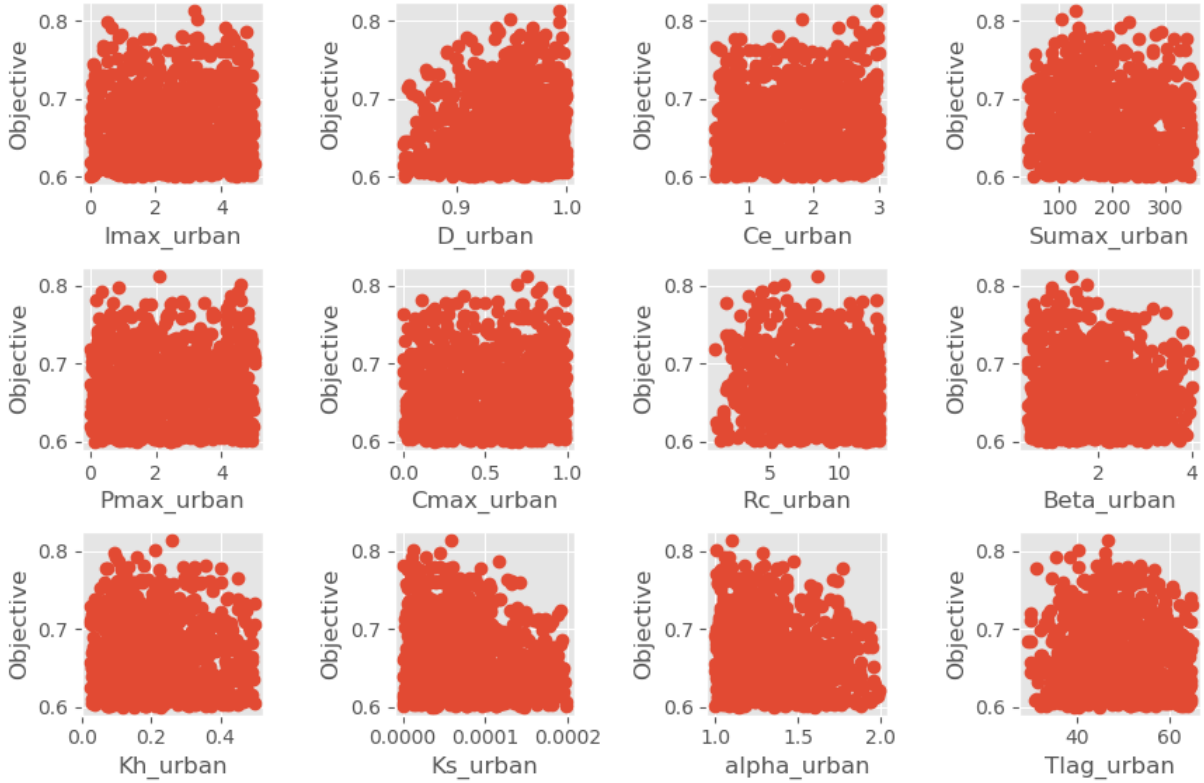

Figure 105. Parameter Calibration Result of Urban Lumped M05A

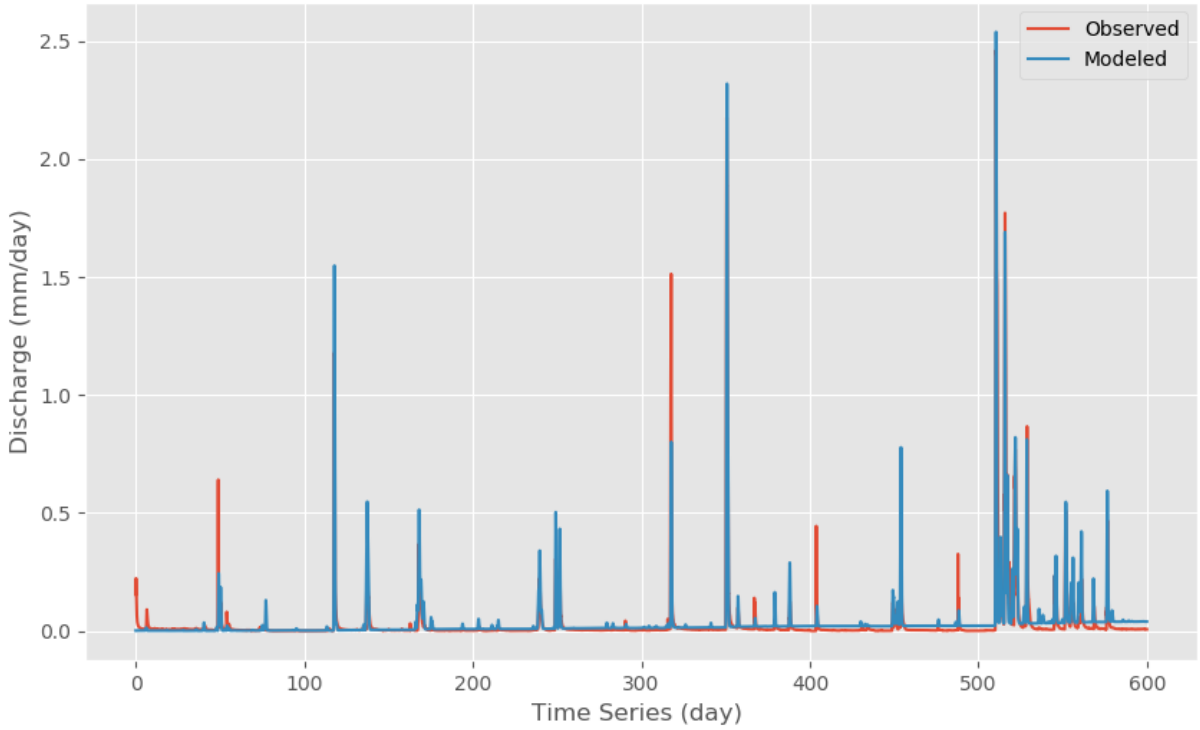

Figure 106. Model Result of Urban Lumped M05B

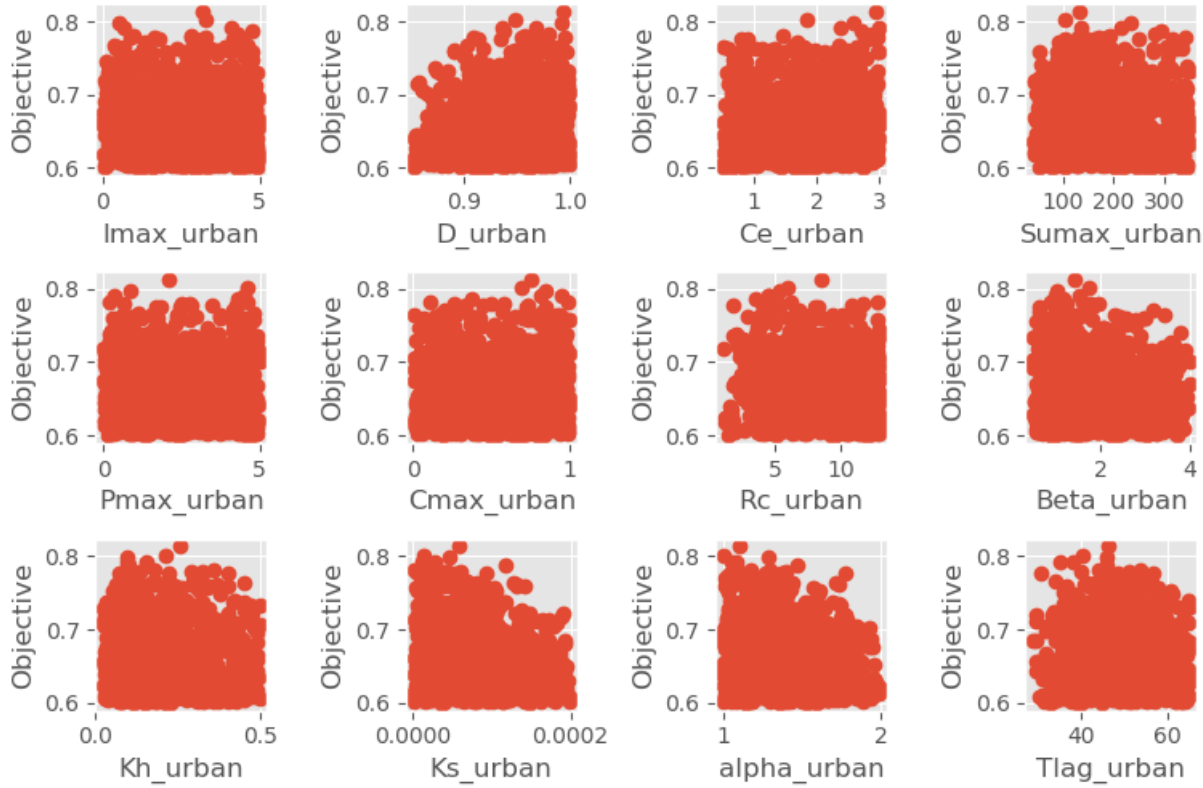

Figure 107. Parameter Calibration Result of Urban Lumped M05B

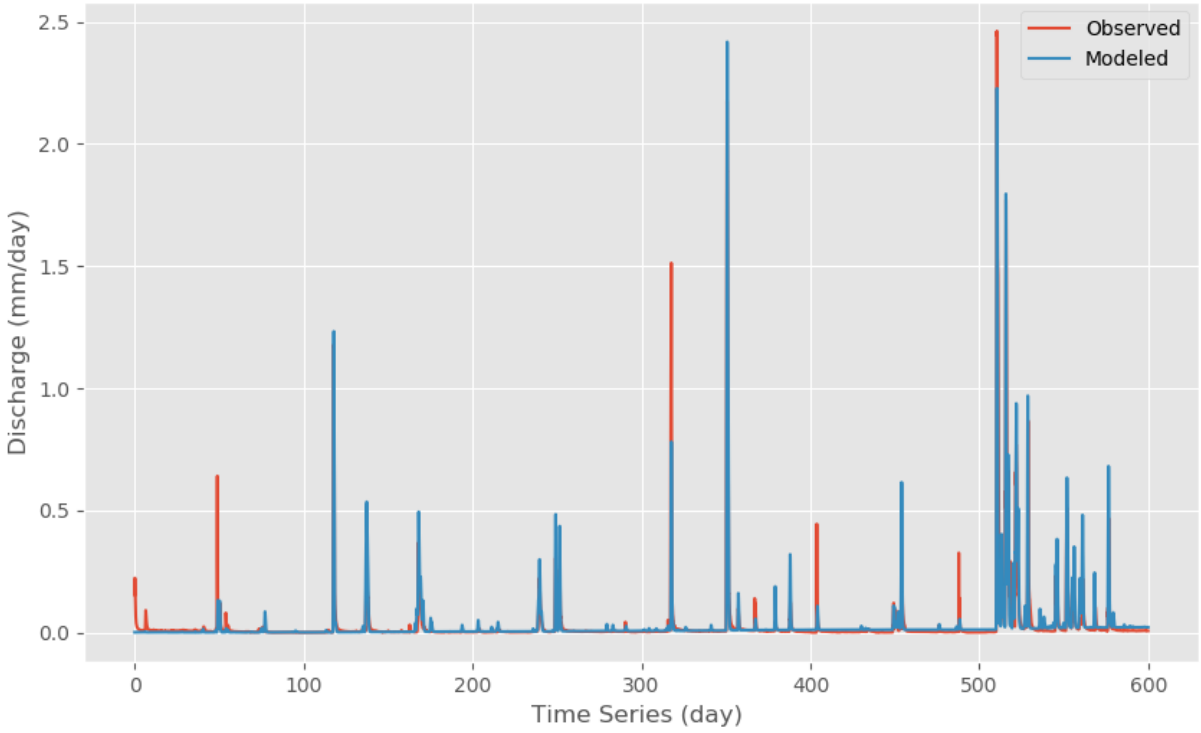

Figure 108. Model Result of Urban Lumped M05C

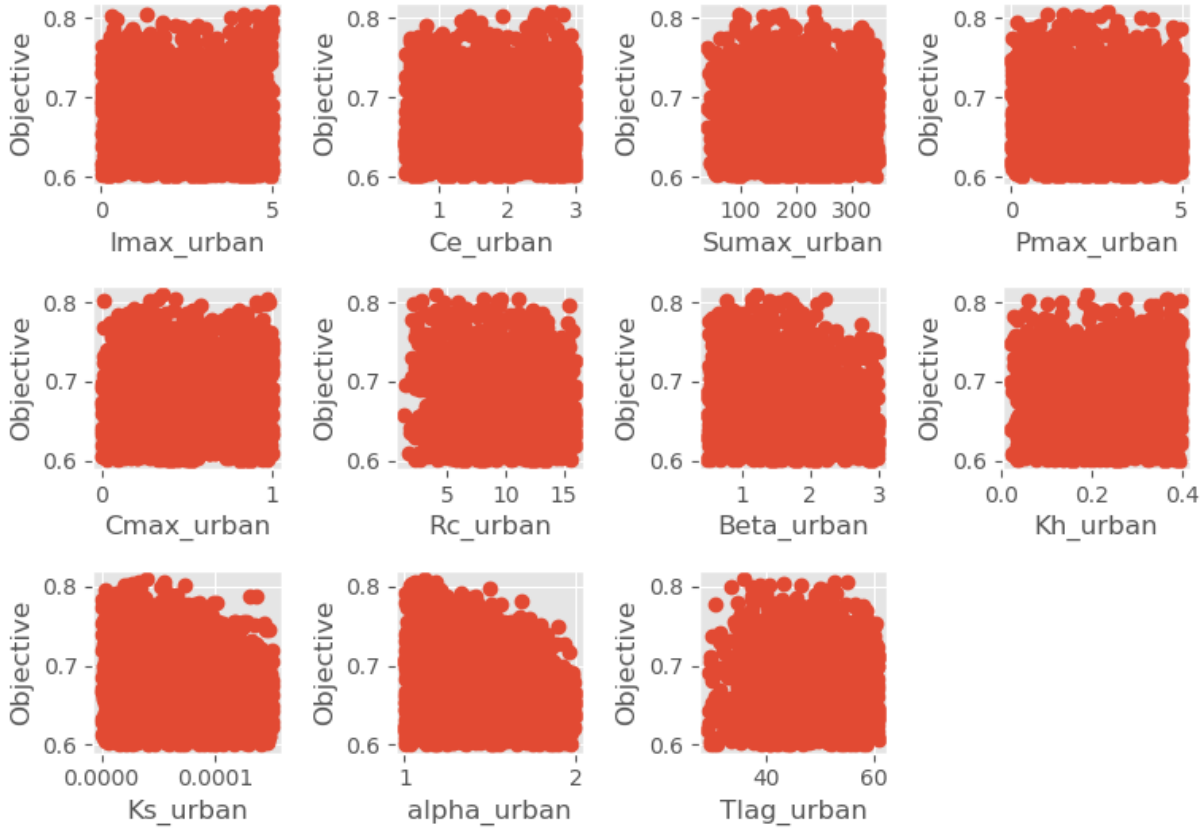

Figure 109. Parameter Calibration Result of Urban Lumped M05C

D.4.3 Semi-distributed model

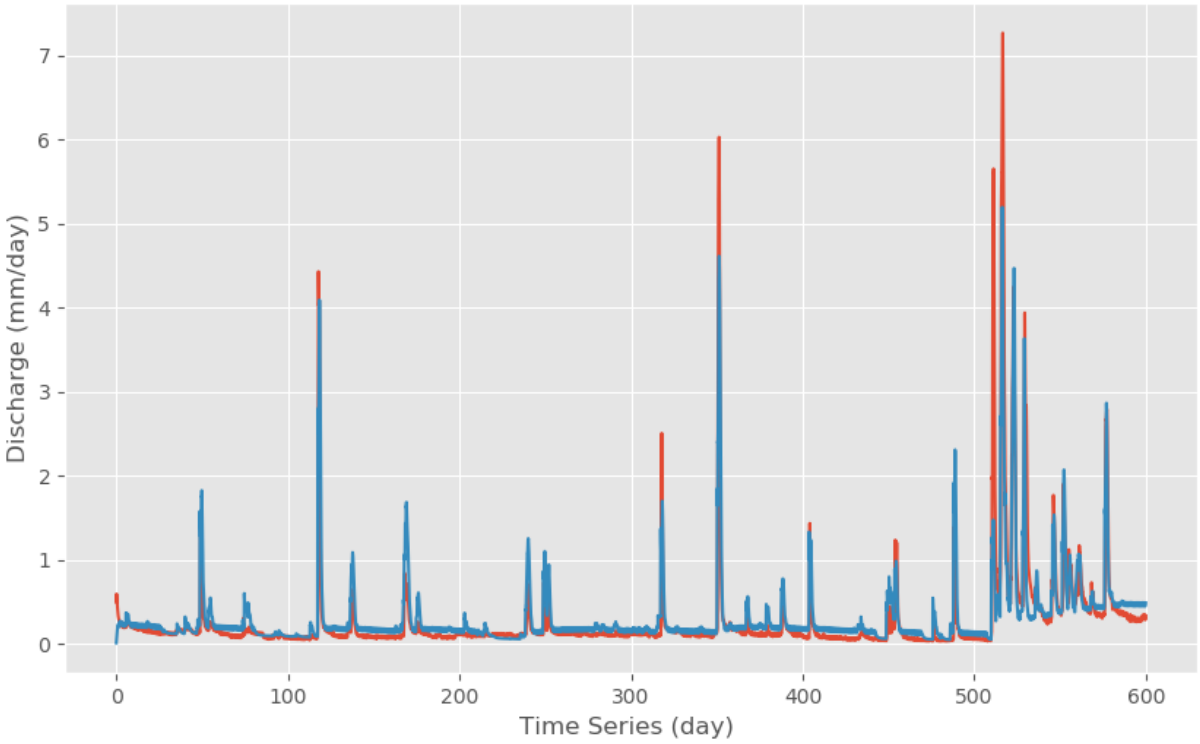

Figure 110. Model result of Semi-distributed M01A

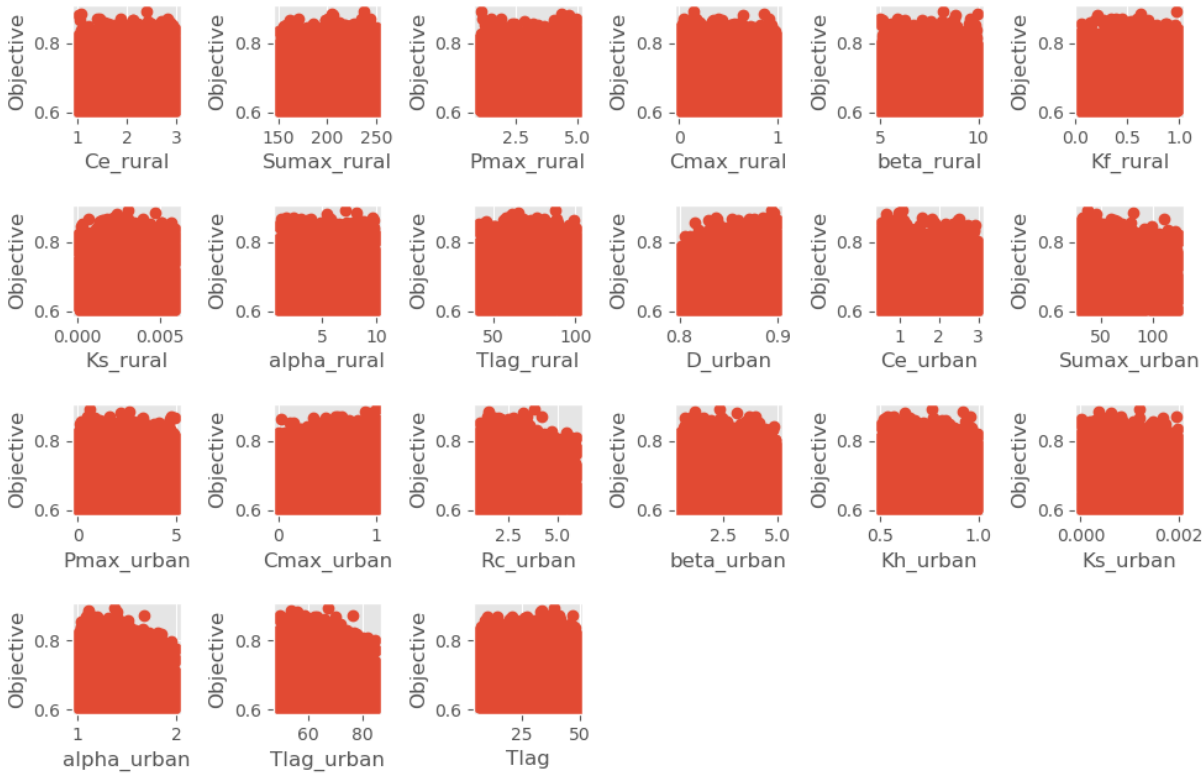

Figure 111. Parameter Calibration Result of Semi-distributed M01A

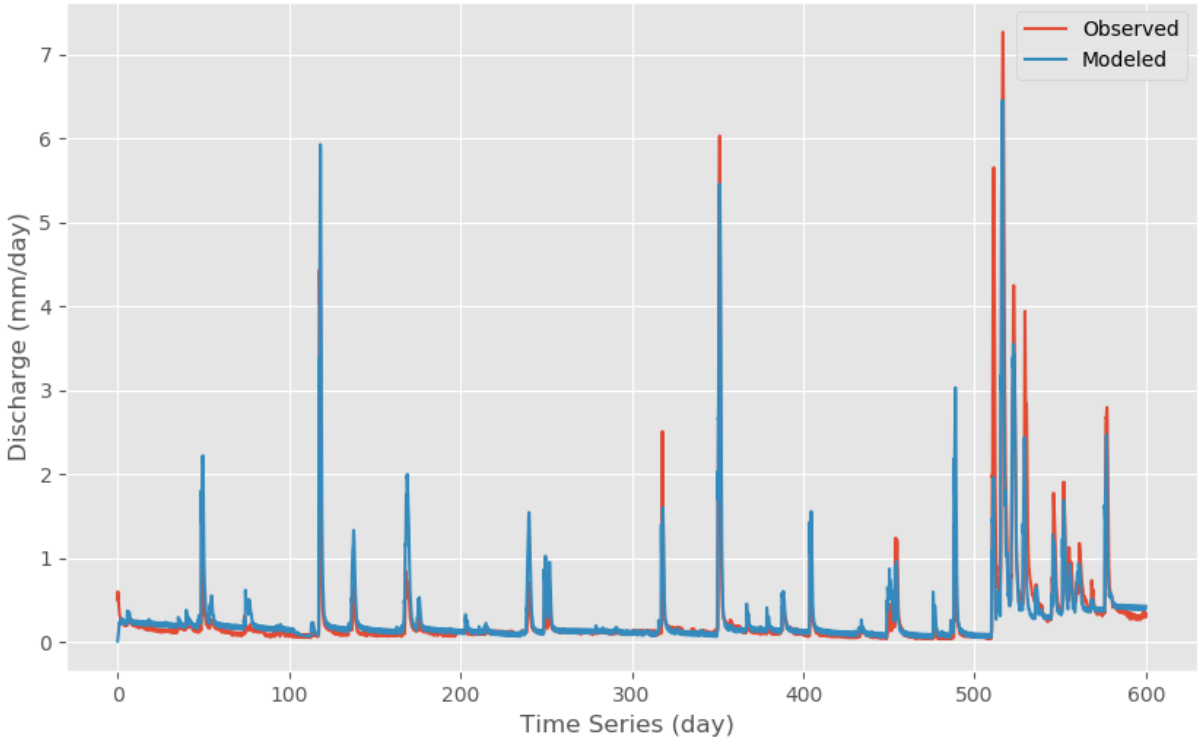

Figure 112. Model result of Semi-distributed M01B

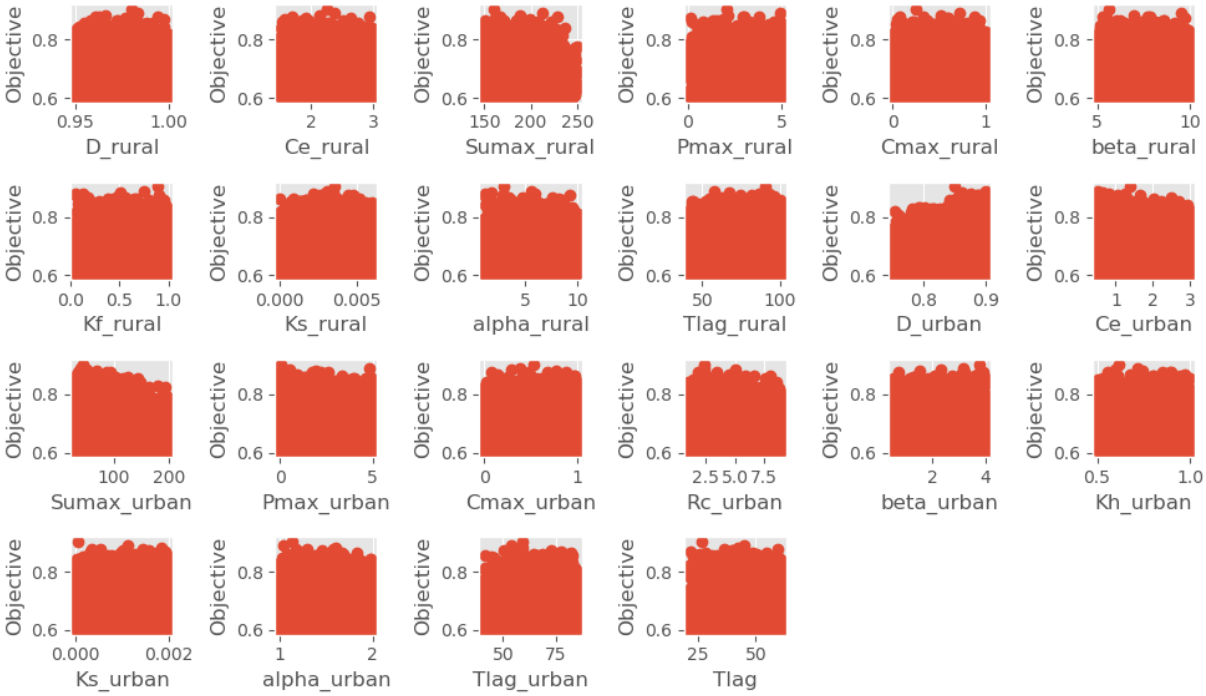

Figure 113. Parameter Calibration Result of Semi-distributed M01B

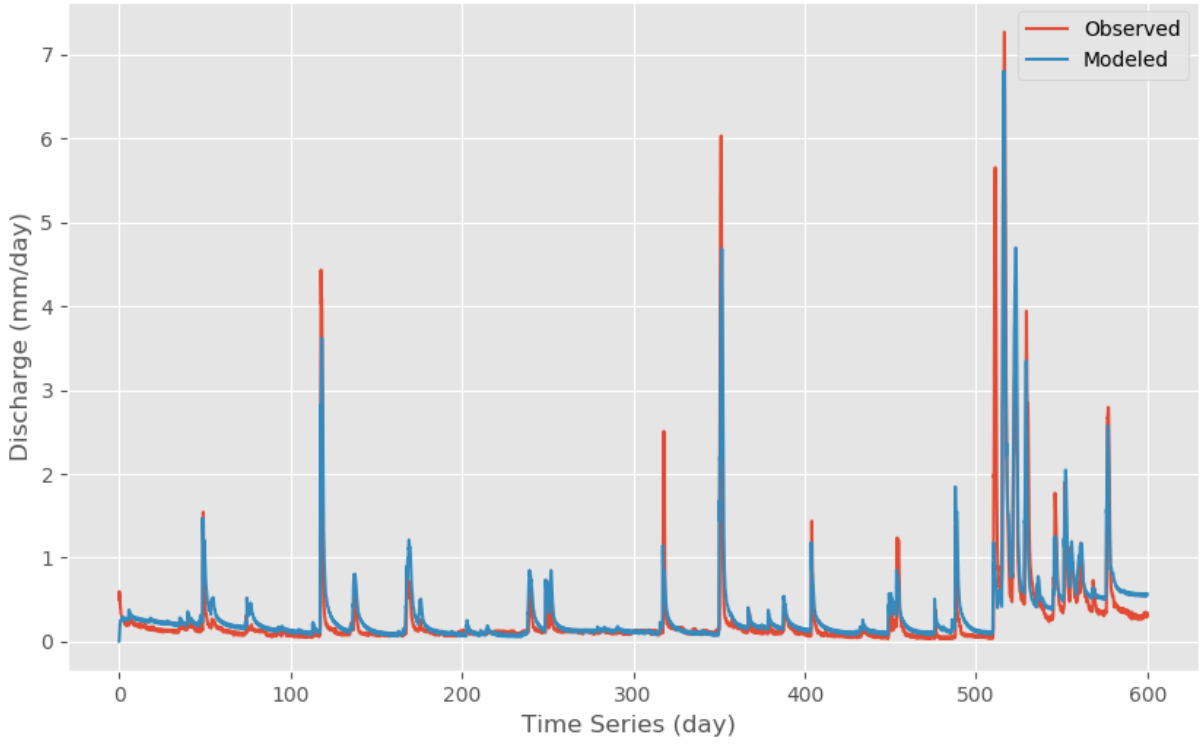

Figure 114. Model result of Semi-distributed M02

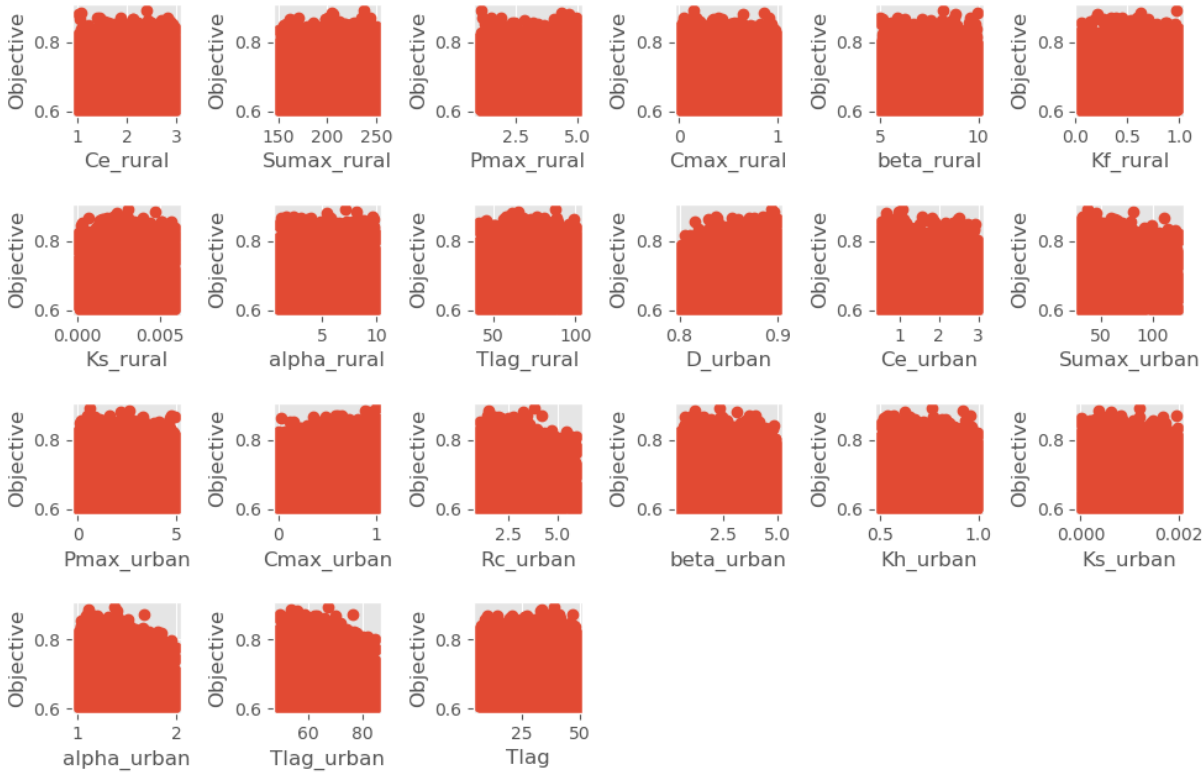

Figure 115. Parameter Calibration Result of Semi-distributed M02

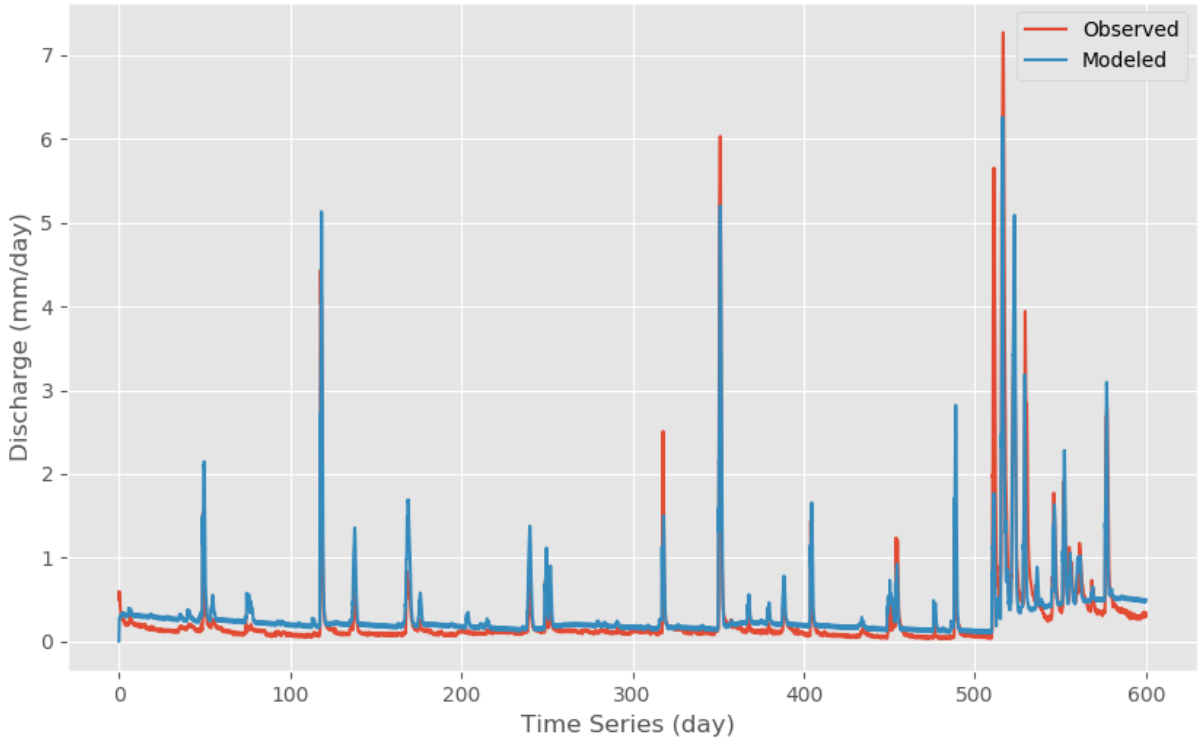

Figure 116. Model result of Semi-distributed M03A

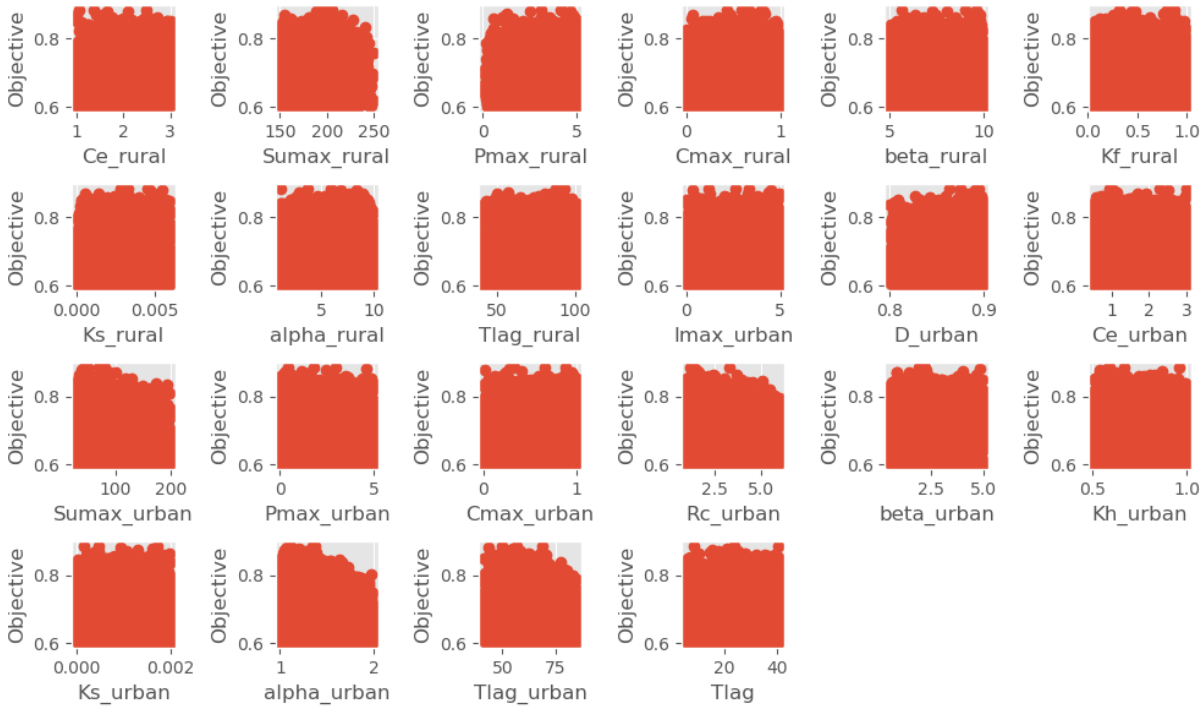

Figure 117. Parameter Calibration Result of Semi-distributed M03A

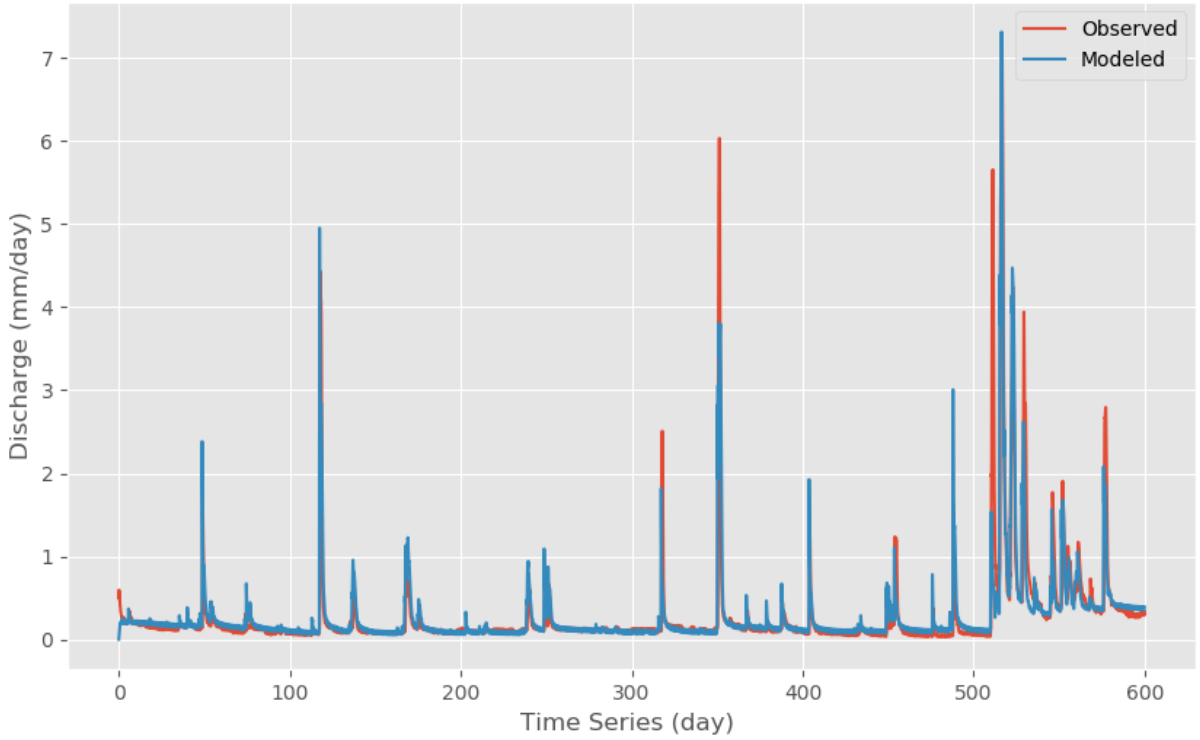

Figure 118. Model result of Semi-distributed M03B

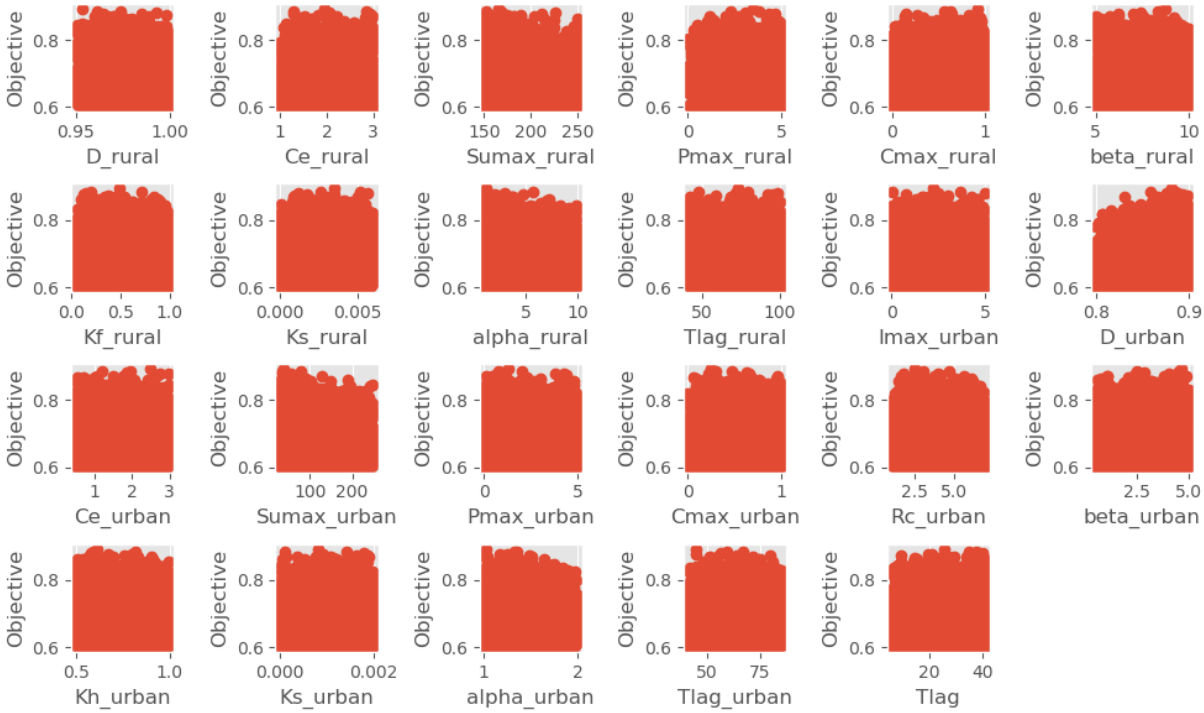

Figure 119. Parameter Calibration Result of Semi-distributed M03B

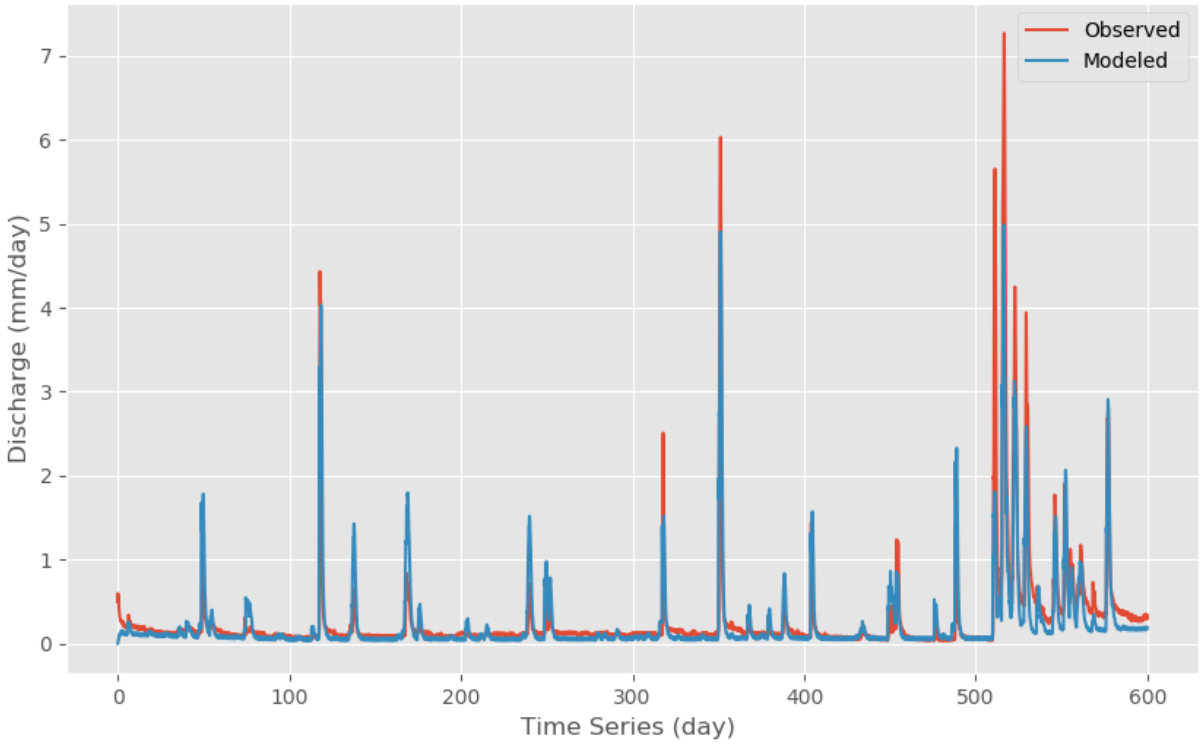

Figure 120. Model result of Semi-distributed M04

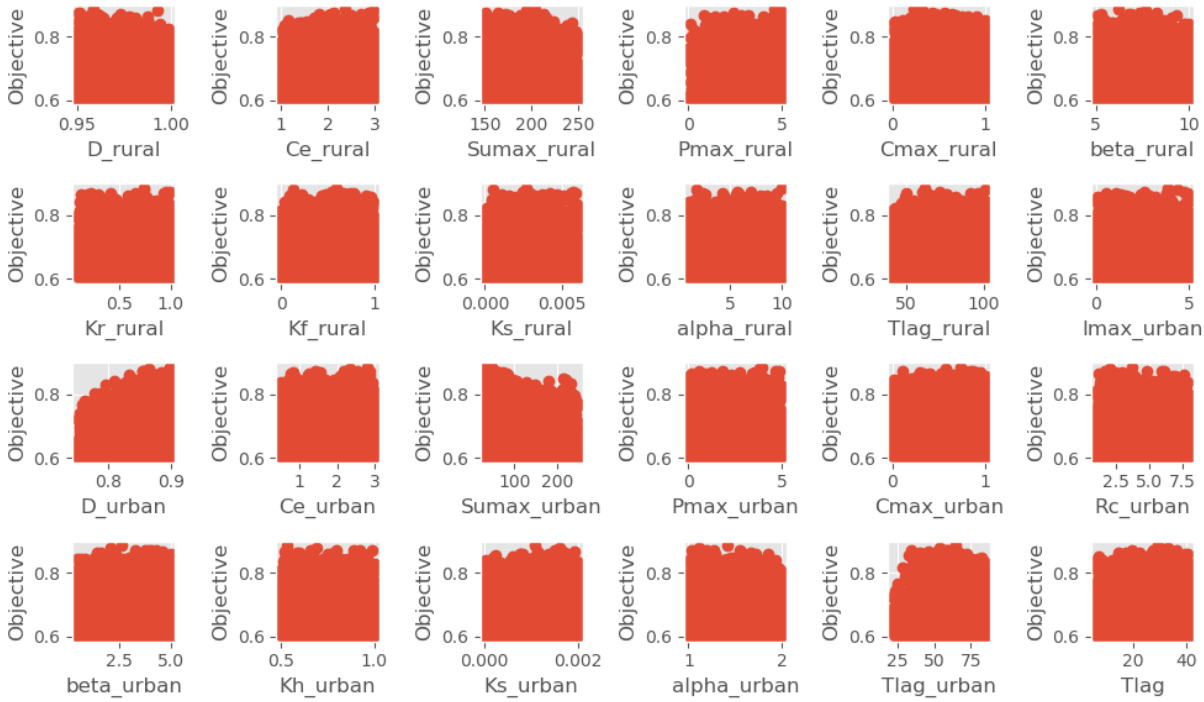

Figure 121. Parameter Calibration Result of Semi-distributed M04

Appendix E Relevant LID implementation criteria and assessment

In 1990, United States Environmental Protection Agency (EPA) promulgated rules establishing Phase I of the National Pollutant Discharge Elimination System (NPDES) storm water program for the "large" Municipal Separate Storm Sewer System (MS4) which serve populations of 100,000 or greater. In the beginning of 20th century, the Stormwater Phase II Rule was established and expanded to "small" MS4s. The term Best Management Practice (BMP) was established at that time to support NPDES program and MS4 implementation. EPA issued "*Guidance Manual for Developing Best Management Practices (BMP)"* to provide guidance to BMPs. The LID concept was put forward based on BMP later.

After that local governments successively introduced guidance manual relating to BMP and LID. Texas Commission on Environmental Quality (TCEQ) issued "*Technical Guidance on Best Management Practices*"; San Antonio River Authority (SARA) published "*San Antonio River Basin Low Impact Development Technical Design Guidance Manual*"; County of Bexar promulgated "*Water Quality and Maintenance Manual*"; And City of San Antonio released "*Storm Water Design Criteria Manual (SWDCM)*".

E.1 LID implementation guideline

The roughly LID implementation criteria and the LID practice management methods are provided as a reference in the "*San Antonio River Basin Low Impact Development Technical Design Guidance Manual"* (referred to as "*SARA LID Guidance Manual"*) developed by SARA collaboratively with Bexar Regional Watershed Management's Low Impact Development Manual Technical Subcommittee and issued by SARA in 2015. The following information was retrieved from the "*SARA LID Guidance Manual"*.

According to the "*SARA LID Guidance Manual"*, the design rainfall of LID should be the frequent small to medium storm which is typically around 25 to 50 mm over 24 hours (one to two inches over 24 hours) rather than the large storm with return period of 5-year to 100-year. Because the annual total runoff comes from the majority of storms that are smaller than the 90th percentile event, even with such a small design rainfall, LID practices could capture a large portion of annual total runoff by accumulating from those small but frequent rainfalls.

Two LID management methods are introduced for LID implementation: Volume-based control practices and flow-based control practices.

Volume-based control practices

Volume management is typically required for offsetting hydromodification effects and to extend water quality treatment times. For volume-based control practice, a specific annual pollutant should be reduced and the volume of runoff produced by a design storm (85th to 95th percentile storm event dependent on local condition) should be infiltrated, filtered or treated. And both of the water quantity and water quality goals need to be meet.

Flow-based control practices

Flow based designs are typically used for configuring inlets, sizing conveyance, or setting hydraulic controls. For flow-based control practice, the maximum flow rate produced by a design storm intensity (typically exceeds 50 mm per hour) should be infiltrated, filtered or treated.

E.2 LID implementation assessment

"Bexar County Post-Construction Storm Water Control Measures (PCSWCM)" Program regularizes all projects in Bexar County that constitute new development or significant redevelopment greater than or equal to 1 acre (4047 m2). And one corresponding document "*Water Quality and Maintenance Manual"* is issued by County of Bexar. The following information was retrieved from the "*Water Quality and Maintenance Manual"*.

In PCSWCM, the LID implementation is assessed as part of BMP following this procedure:

(1) One allowable Impervious Cover (IC) percentage of every project could be weighted calculated according to different land use type as Table 36.

Table 36. Allowable impervious cover (%) according to different land use

Land Use	Allowable Impervious Cover %
Single-Family Residential	30%
Multi-Family Residential	50%
Commercial/Industrial	65%
Transportation	85%

For example, if 80% the area of one project would be built into commercial areas and the last 20% areas would be used to transportation according to project proposal. The allowable IC of this project would be:

$$80\% * 65\% + 20\% * 85\% = 69\%$$

(2) The calculated allowable IC from procedure (1) should be compared with existing IC. The greater IC percentage would be determined as target IC for next step.

(3) The target Mitigation Point is calculated as the difference between the IC (%) in project proposal and target IC (%). For example if the IC in project proposal is 65%, the proposed IC is smaller than the allowable IC. Therefore the target Mitigation Point is negative (65% - 69% = -4%), and then no additional BMP practice is required; However if the IC in project proposal is 75%, target Mitigation Point would be 5 (75% - 69% = 5%). Under this circumstance, the 5 target Mitigation Points should be achieved with additional BMPs.

(4) For these projects with positive target Mitigation Points, additional BMP measures need to be designed. In "*Water Quality and Maintenance Manual",* several non-structural and structural BMPs are designated with different number of Mitigation Points. And the requirements for qualifying BMPs are mentioned. For example a general qualifying volume-based control LID practice must provide enough volume to capture 12.7 mm (0.5 inches) of runoff from its contributing watershed. According to the corresponding terms in "*Water Quality and Maintenance Manual"*, specific Mitigation Point of every designed BMP in project proposal could be accumulated as the total achieved Mitigation Point.

(5) The accumulated achieved Mitigation Point would be compared with the target Mitigation Point. If the achieved Mitigation Point is higher than the target Mitigation Point, the proposed development plan could be preliminary approved.

(6) The above procedure for Mitigation Point assessment would be verified by County Staff with Storm Water Quality Control Measures Worksheet (Mitigation worksheet). After verification, the

complete Mitigation worksheet should be submitted by project manager as one of materials for project application.

According to "*Water Quality and Maintenance Manual"*, the SARA approved LID features could obtain the maximum 15 mitigation points and the concrete mitigation point is computed by entering the percentage of the total areas that is covered by the LID measures or contributes to the LID measures. If the target mitigation point number is larger than 15, other non-structural and structural BMPs could be selected to earn the last mitigation points.

It is worth mentioning that as one part of the optional BMPs, the implementation of LID measures is not strictly mandatory for every development/redevelopment project. And there is a great flexibility of optional non-structural and structural BMPs for project manager. For example posting the Bexar County standardized public outreach flyer is also one of the non-structural BMPs and the project manager shall receive 2 mitigation points for this BMP. Besides, if other BMPs options are not feasible, project manager shall receive mitigation points by payment into the regional storm water quality program with the maximum relief of half of the required mitigation points.

Appendix F Figures of LID scenarios model results

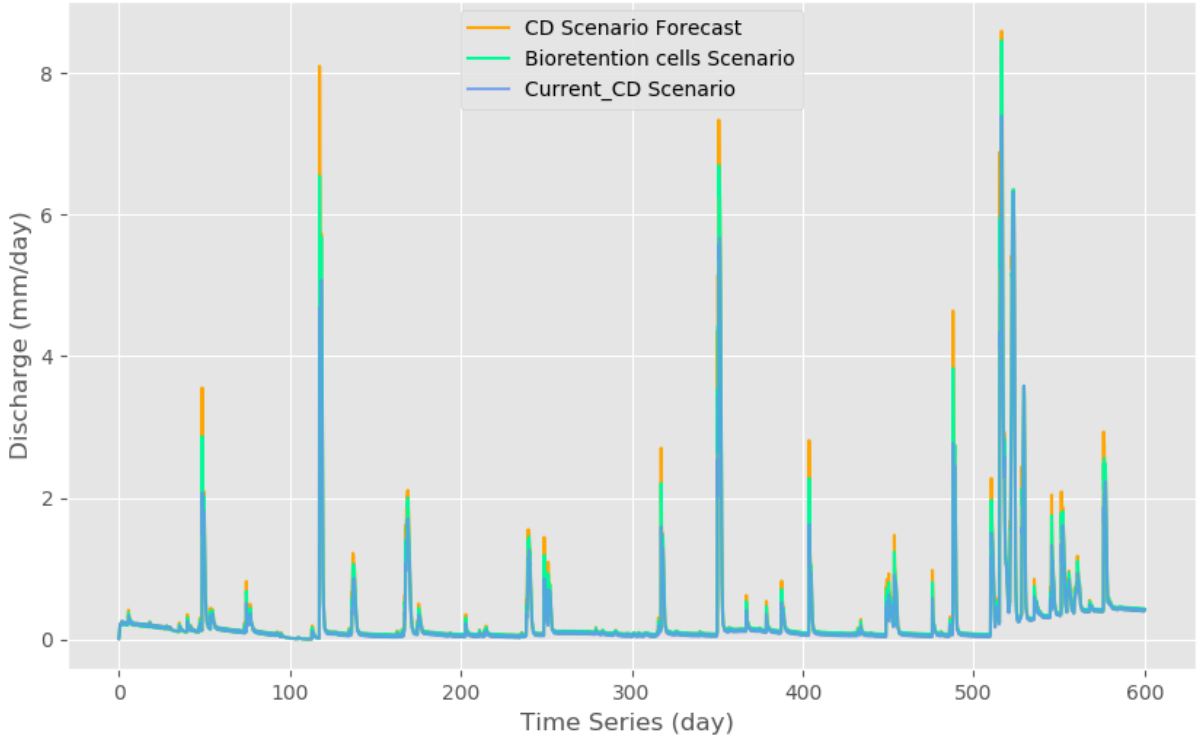

Figure 122. Model results of the Bioretention cells scenario, the current CD scenario and the CD scenario

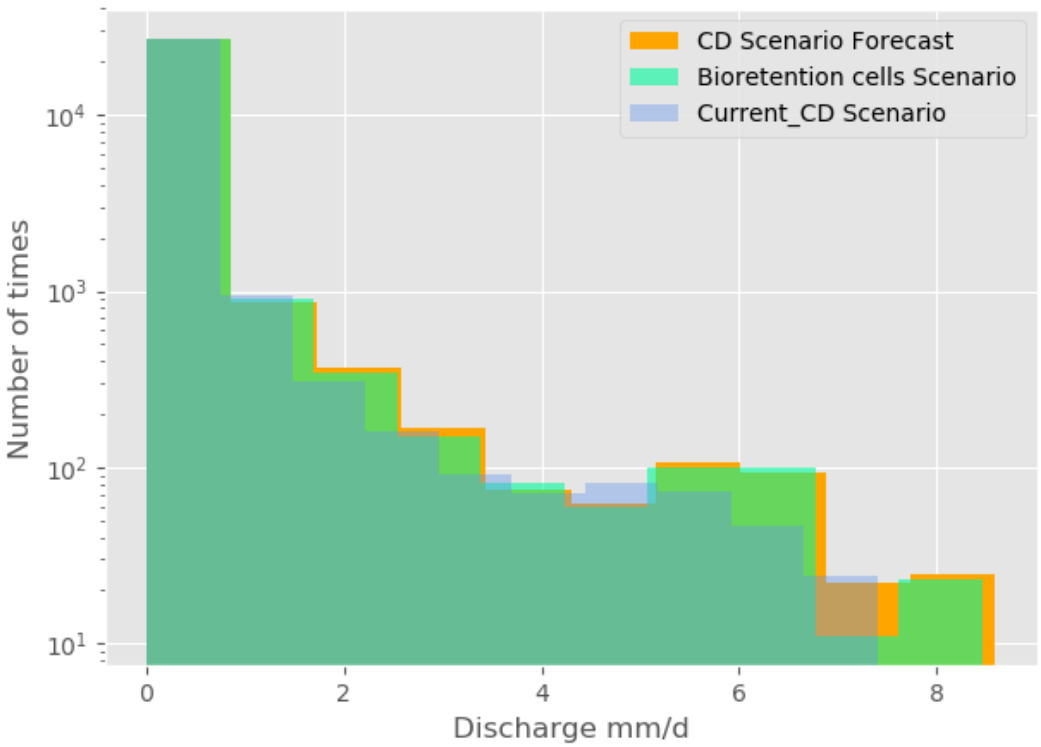

Figure 123. The histogram of discharge values of the Bioretention cells scenario, the current CD scenario and the CD scenario

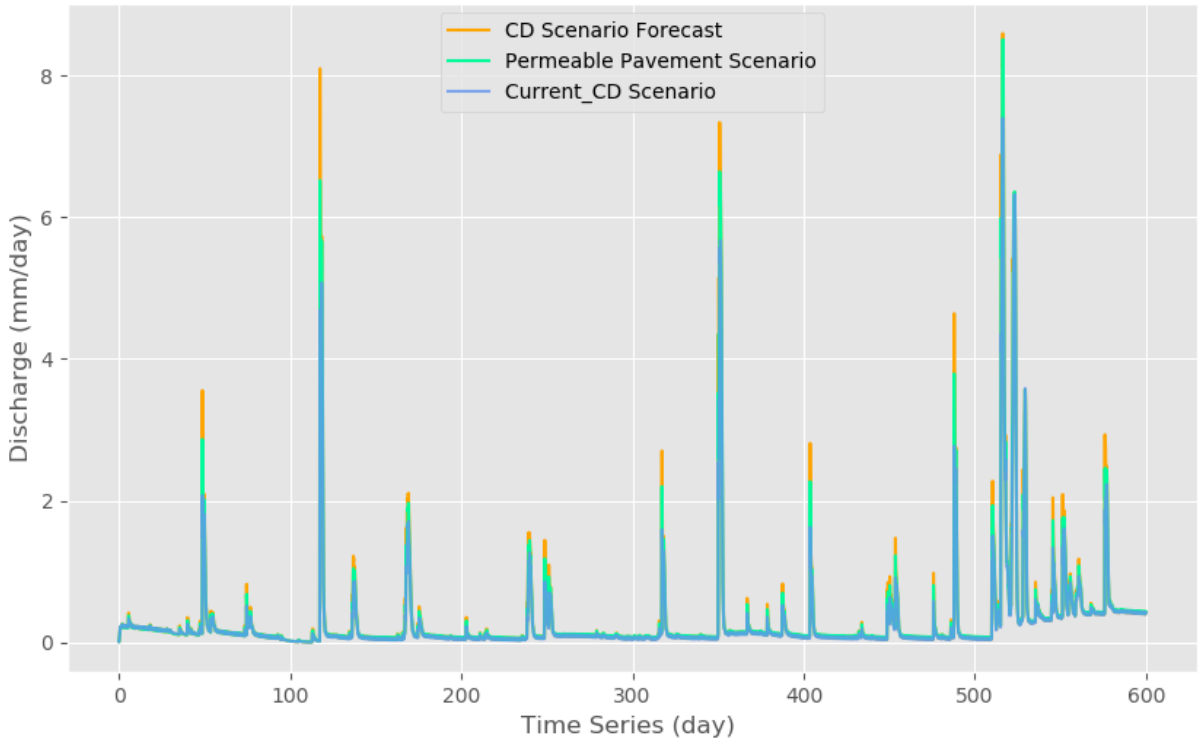

Figure 124. Model results of the Permeable Pavements scenario, the current CD scenario and the CD scenario

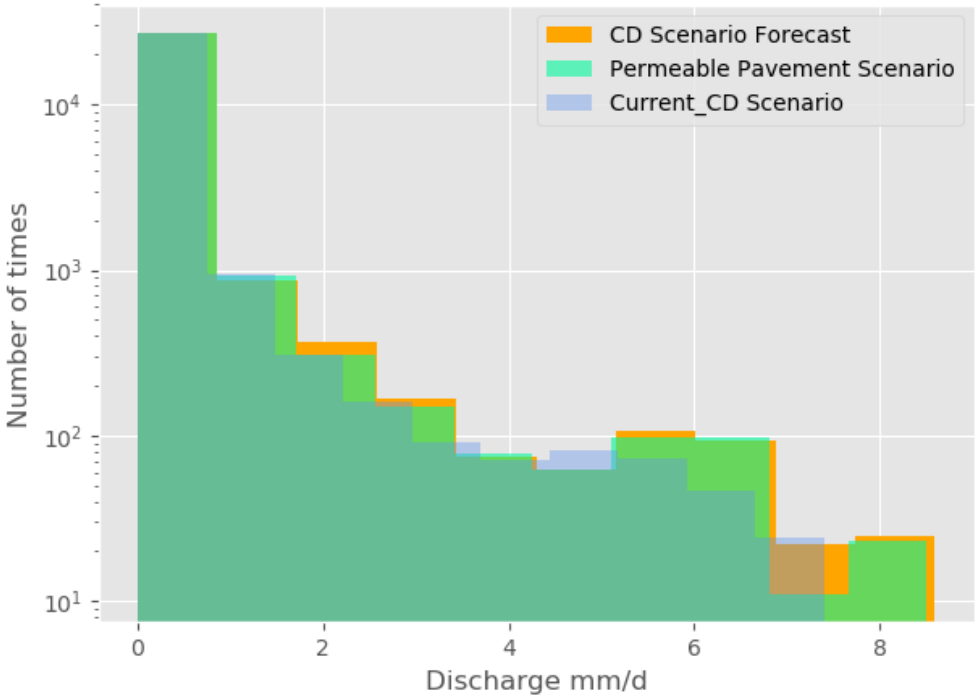

Figure 125. The histogram of discharge values of the Permeable Pavements scenario, the current CD scenario and the CD scenario

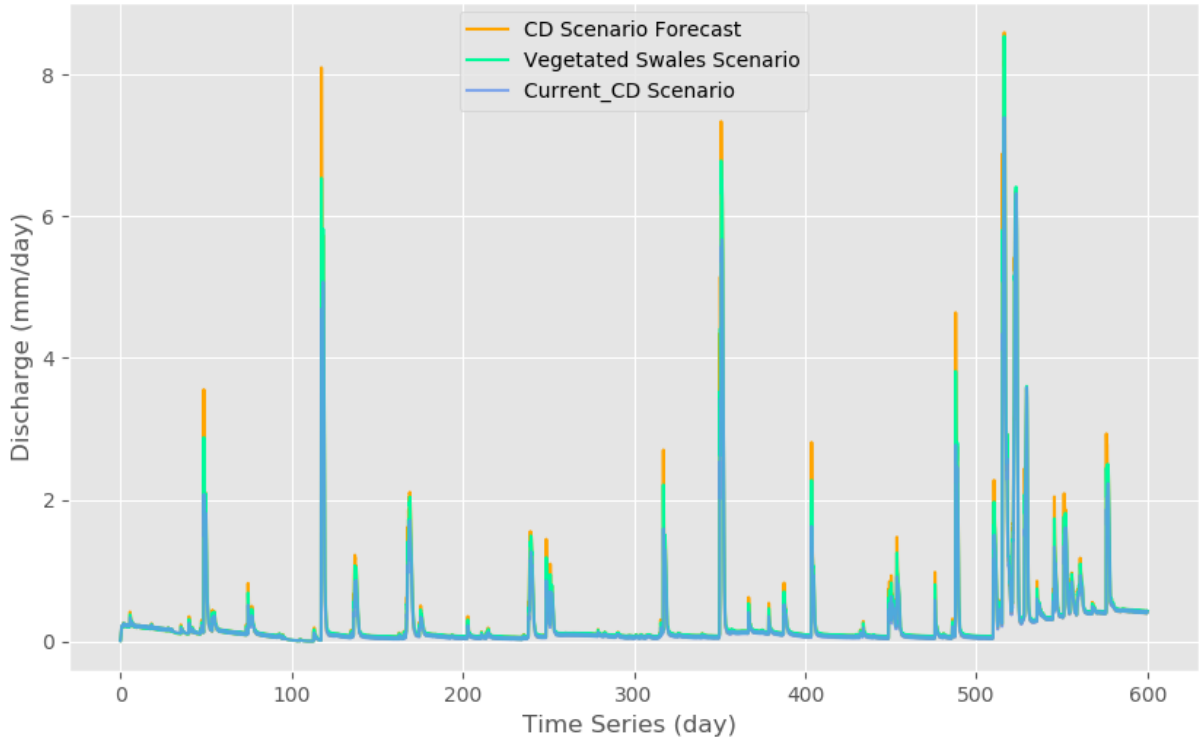

Figure 126. Model results of the Vegetated swales scenario, the current CD scenario and the CD scenario

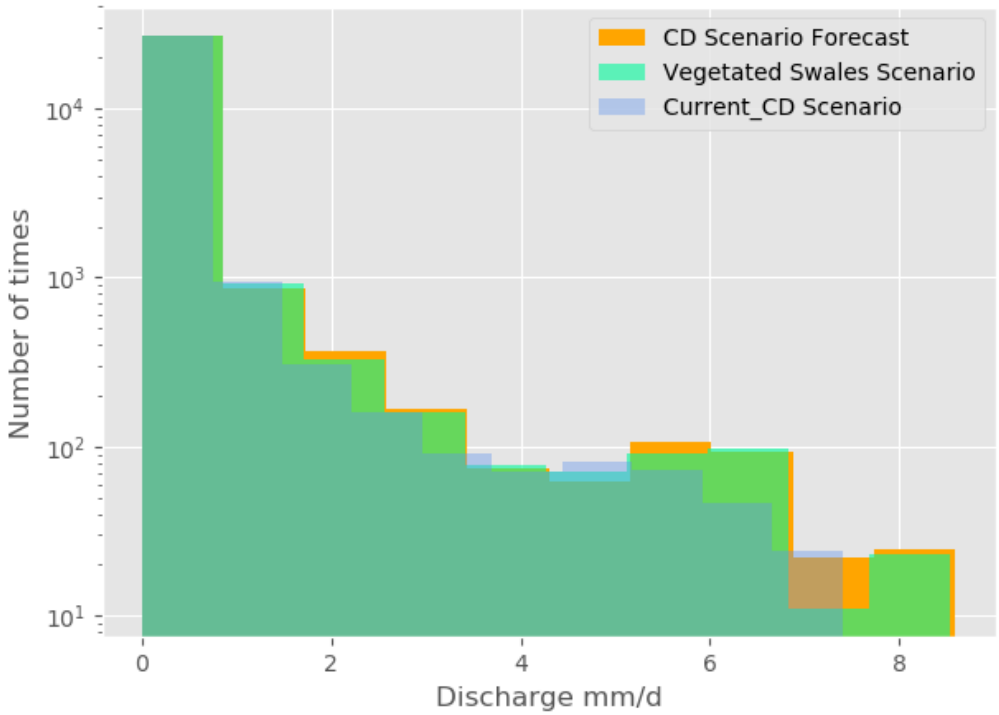

Figure 127. The histogram of discharge values of the Vegetated swales scenario, the current CD scenario and the CD scenario

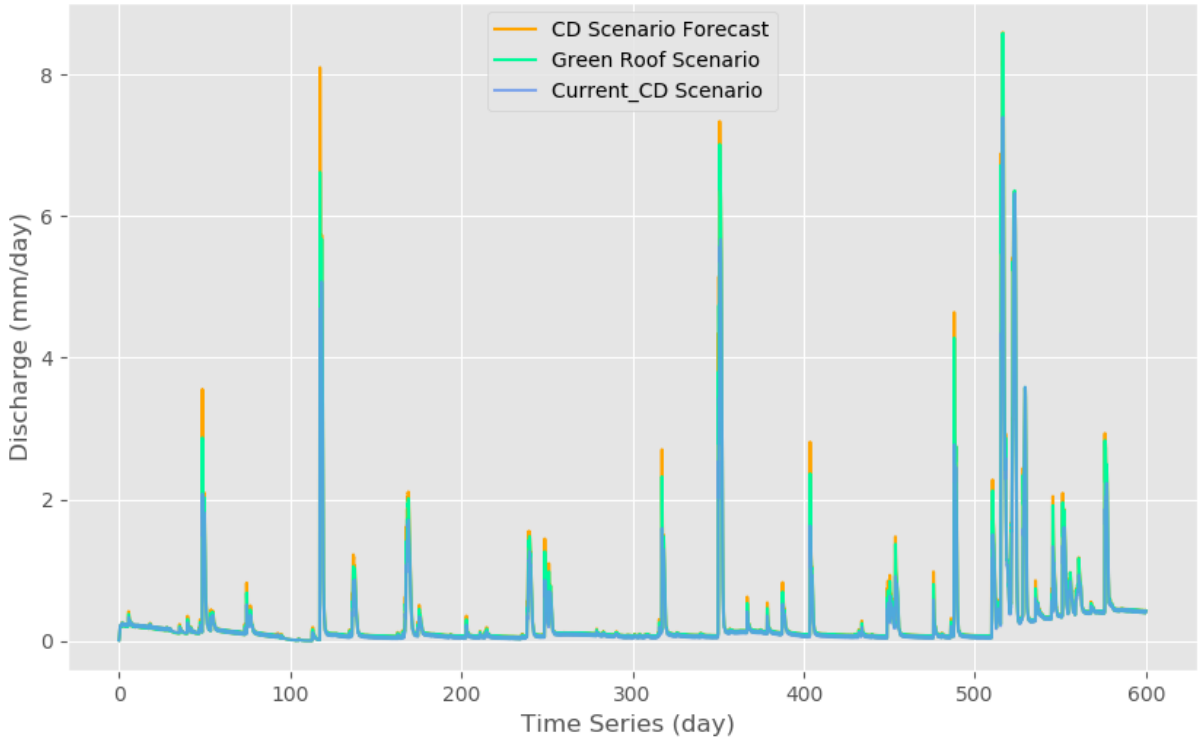

Figure 128. Model results of the Green roof scenario, the current CD scenario and the CD scenario

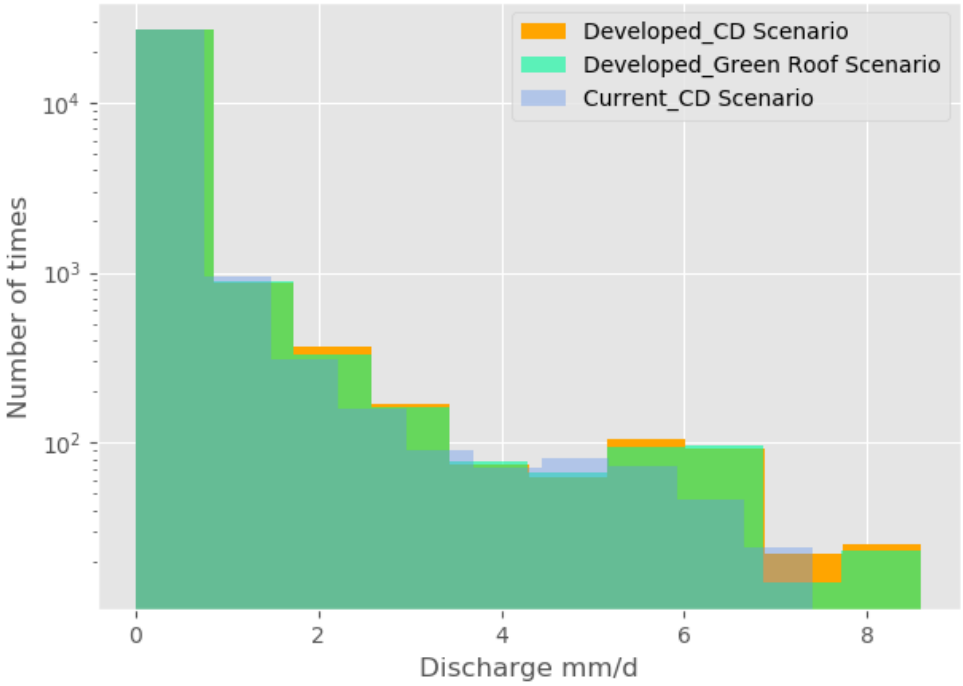

Figure 129. The histogram of discharge values of the Green roof scenario, the current CD scenario and the CD scenario